Oral Drug Delivery as an Alternative to Needle-Based Injection for Large Molecules: an Assessment of the Field & Evaluation of High-Priority Technologies

by

Kaitlyn Nealon

Bachelor of Science in Engineering as Recommended by the Mechanical Engineering Department (Course 2A), Minor in Biomedical Engineering, Massachusetts Institute of Technology (2014)

Submitted to the MIT Sloan School of Management and the Department of Mechanical Engineering in Partial Fulfillment of the Requirements for the Degrees of

Master of Business Administration

and

Master of Science in Mechanical Engineering

In conjunction with the Leaders for Global Operations (LGO) Program at the

MASSACHUSETTS INSTITUTE OF TECHNOLOGY

June 2018

Author Signature redacted

Department of Mechanical Engineering & MIT Sloan School of Management

May 11, 2018

Certified By Signature redacted

Roger Kamm, Thesis Advisor

Cecil and Ida Green Distinguished Professor of Biological and Mechanical Engineering

Certified By Signature redacted

Thomas Roemer, Thesis Advisor

Senior Lecturer in Operations Management and Executive Director of LGO

Accepted By Signature redacted

Rohan Abeyaratne

Chairman, Committee on Graduate Students, MIT Department of Mechanical Engineering

Accepted By Signature redacted

Maura Herson

Director of MIT Sloan MBA Program, MIT Sloan School of Management

This page was intentionally left blank.

Oral Drug Delivery as an Alternative to Needle-Based Injection for Large Molecules: an Assessment of the Field, Evaluation of High-Priority Technologies, and Considerations for Technology Evaluation Processes

by
Kaitlyn Nealon

Submitted to the MIT Sloan School of Management and the Department of Mechanical Engineering on May 11, 2018 in Partial Fulfillment of the Requirements for the Degrees of Master of Business Administration and Master of Science in Mechanical Engineering

Abstract

Oral delivery of large molecules is widely considered the "holy grail" of drug delivery, but attempts to achieve this within the past century have been met with a lack of success, confounded by low bioavailability. Novel mechanisms need to be assessed in order to deliver a clinically relevant amount of drug into systemic circulation, while protecting the drug from pH denaturation and the harsh enzymatic environment of the gut.

To assess the field, this thesis evaluates startup companies and academic labs focusing their efforts on the oral delivery of biologics. The holistic, phased analysis of the field includes the following items:

- Value proposition assessment as applicable to Amgen's pipeline
- Literature review into historical barriers
- Technology landscape of the current space
- Down-selection to highly valued technology prospects
- Risk assessment and mitigation planning activities

The approach outlined above led to the identification of two promising technologies (Tech A and Tech B) that use novel methods to deliver drug through the lining of the small intestine into systemic circulation. Both early stage technologies hold a significant amount of promise for Amgen if they enable both systemic and localized GI delivery successfully, but have multiple risks to address prior to use as a platform delivery option. Risks that have been prioritized for evaluation include: health concerns over long term damage and infection, low bioavailability, limited payload capabilities, and large final device size.

In Silico modeling in COMSOL Multiphysics of the mechanism of action of Technology A and the resultant spread of drug product into the lining of the small intestine was completed as a preliminary test of the risk of low bioavailability. Results from this model indicate that Technology A can be optimized via nozzle diameter and ejection threshold pressure to deliver liquid drug product into the desired locations within the small intestinal wall for optimal drug uptake into systemic circulation. If these technologies prove to be successful, the resultant product offering could prove highly disruptive in the industry and allow Amgen to revolutionize the manner in which patients interact with their medications.

Thesis Advisor: Roger Kamm
Title: Cecil and Ida Green Distinguished Professor of Biological and Mechanical Engineering

Thesis Advisor: Thomas Roemer
Title: Senior Lecturer in Operations Management and Executive Director of LGO

This page is intentionally left blank.

Acknowledgements

I'd like to thank the MIT Leaders for Global Operations program and Amgen Inc. for their support of this thesis. I am grateful for the support and wisdom imparted by my thesis advisors, Roger Kamm, Jeff Karp and Thomas Roemer both during my internship and in the writing of this thesis. It was a pleasure to work with and learn from my colleagues at Amgen. My Amgen supervisors, Jeff Schacherl and Scott Gibson, provided invaluable guidance and direction throughout my internship. I am also thankful for the support of the Advanced Device Technology and Innovation (ADT&I) group that provided helpful context, an amazing sounding board, and direction in the Novel Oral project. I am thankful that I had the opportunity to work with Fabrice Schlegel from the Digital Integration and Predictive Technologies (DIPT) team at Amgen, without whom the major findings of this thesis would not have been possible. Bill Rich, my project champion, and Aine Hanly, the first VP I met at Amgen, are major supporters of the LGO program, acted as personal champions for me, and were instrumental in removing any barriers to my success. Additionally, I'd like to thank Dollie Grajczak and Diana Ecker, the coordinators of the LGO program at Amgen, as well as the wider LGO community at Amgen, including but not limited to Kerry Weinberg, Matt Dumouchel, Leigh Hunnicut, and Jeff Schacherl for their guidance and support as well.

My classmates at LGO have inspired me time and again to become stronger both personally and professionally and I am grateful to have been among them in this program. Lastly, I would like to thank my family for their continuing support and encouragement. Without my parents I would not have had the opportunity to attend MIT the first time, when I first got exposed to the LGO program. I am in awe of their unwavering belief in my abilities and their encouragement to pursue further education – for that, I am truly grateful. Throughout these past two years Thomas Maxwell has been an amazing source of support throughout the classes, internship, and travel that the LGO program affords me. I am thankful for his patience and unwavering encouragement of me.

This page intentionally left blank.

Table of Contents

List of Figures

List of Tables

Glossary

ADT&I	Advanced Device Technology & Innovation; the group the LGO intern worked at within Amgen
Bioavailability	The proportion of active drug substance that enters into systemic circulation when introduced into the body in order to have an effect on the intended condition
Bolus	Administration of a discrete amount of medication, drug, or other compound within a specific time, generally within 1 - 30 minutes, in order to raise its concentration in blood to an effective level
Drug Product	Finished dosage form of therapeutic agent including pure drug substance and other formulation additives (see formulation and drug substance)
Drug Substance	Mostly pure active pharmaceutical ingredient
Formulation	Chemical additives to drug substance to form drug product; different additives or "excipients" can perform different functions
GRAS	Generally Recognized as Safe; FDA designation given to materials if considered safe by experts
Hydrogel	Network of polymer chains that are hydrophilic
Intramuscular	Administered into a muscle
New Molecular Entity	Drug that is without precedent among regulated and approved drug products, indicates drug is not a version or derivative of existing and previously investigated, trialed, and approved substance.
Parenteral	Administered or occurring elsewhere in the body than the mouth
Pharmacodynamics (PD)	The relationship between drug concentration at the site of action and the resulting effect, including the time course and intensity of therapeutic and adverse effects; study of how the drug affects the organism
Pharmacokinetics (PK)	The study of the time course of drug absorption, distribution, metabolism, and excretion; study of how the organism affects the drug
Subcutaneous	Administered under the skin

Chapter 1 Background and Introduction

This section details the history of the biotechnology industry, as well as one of its biggest players, Amgen. Chapter 1 further provides an explanation of large molecule therapeutics and how they differ from traditional pharmaceuticals. In particular, the delivery of large molecules to the patient is substantially different than that for small molecules, and this section further dives into the historical methods for large molecule delivery and emerging research on alternative methods. Finally, Chapter 1 concludes with a discussion on patient adherence to medication, and how alternative routes of drug delivery could potentially aid in the fight against the epidemic of nonadherence.

1.1 Large Molecule Therapeutics

The medical industry has been revolutionized by the introduction of various recombinant large molecule therapeutics over the past several decades - hundreds of these types of molecules have been approved by the FDA for use and thousands more are in the pipeline undergoing extensive research and development.

1.1.1 History of Biotechnology Industry

Historically, chemically-synthesized small molecule medications have been widely used for treatment of a wide range of diseases. Small molecules typically have a low molecular weight (<1000 Da) and are generally delivered in a pill form factor. While small molecule drugs still remain the first-line treatment for a variety of maladies, the need for more targeted and effective therapies led to the development of large molecule therapeutics.

Large molecule therapeutics, otherwise known as biologics, macromolecules, and biotherapeutics, first appeared as an FDA approved treatment in 1978, with the approval of the first recombinant human insulin (Diabetes.co.uk, 2018). Large molecule therapeutics can include protein therapies, vaccines, cell therapy, gene therapy, and others. The focus of this thesis will remain on protein therapeutics, many of which use recombinant DNA technology to target, modify, and produce the protein of interest to alter, lessen, or erase the effect of the targeted disease on the patient. As the knowledge and understanding of disease pathophysiology has increased in the past century, the research into and production of protein therapies has grown, leading to greater than 130 protein therapies on the market today (Leader, Baca, & Golan, 2008).

Among many differences, the most poignant to the industry may be that large molecule drugs are derived from living systems, in contrast to small molecule therapeutics that are chemically synthesized. The living system, whether bacteria, yeast, or Chinese hamster ovary (CHO) cells, are coded with the appropriate DNA sequence of interest that yields the designer protein. These cells grow and reproduce within a series of large bioreactors, where they express the protein of interest. This protein is then harvested, purified, and formulated to be used as treatment.

Despite this complicated manufacturing process, business incentives were put in place to drive companies towards the development of protein therapeutics. In comparison to small molecule therapies, protein therapeutics typically gain approval faster (Leader, Baca, & Golan, 2008) and have a higher probability to

gain approval in the earlier stages of R&D (Hay, Thomas, Craighead, Economides, & Rosentahl, 2014). Additionally, they often have longer market exclusivity and lack the same amount of competition from generics in comparison to small molecules, due to the complexity of developing a biosimilar exactly the same as the branded version. Given these business incentives, and the fact that there are multitudes of proteins that can be studied and developed as disease-modifying drugs, the biotech has grown into the $107 billion dollar industry it is today (Curran, 2017).

1.1.2 Amgen

Amgen is one of the world's leading biotechnology companies, deeply committed to developing therapeutics for patients who suffer from serious illnesses. Since 1980, Amgen has focused on areas of high unmet medical need and leveraged its expertise in R&D, process development, and manufacturing to deliver its therapeutics to patients in need. Amgen launched its first product, Epogen®, in 1989, 9 years after its incorporation in 1980 (Amgen, Inc., 2017). This was quickly followed by Neupogen® in 1991, and both became blockbuster drugs, enabling Amgen to become one of the world's leading biotechnology companies today.

Currently, the company has a presence in approximately 100 countries, and focuses on six therapeutic areas: cardiovascular disease, oncology, bone health, neuroscience, nephrology, and inflammation (Amgen, Inc., 2017). With 20,000 staff worldwide, the company expects to bring in nearly $23 billion in total revenue in 2017 (Amgen, Inc., 2017) and currently has a market cap of $135.8 billion (Yahoo Finance, 2017). There are 16 drugs on the market, detailed in Table 1-1, of which 12 are large molecule biologics.

Furthermore, Amgen has more than 33 products in the pipeline and approximately 70% of those are large molecule proteins or antibodies that are generally delivered via intravenous, subcutaneous, or intramuscular injection (Amgen, Inc., 2018). Given the prevalence of large molecule therapeutics in the commercial and pipeline offerings, Amgen has a vested interest to develop the best delivery methods to accompany large molecule products.

Table 1-1 Amgen's Commercial Products

Name	Initial U.S. Approval	Disease Area	Type	Molecular Weight (kDa)	Type
Epogen®	1989	Nephrology	Biologic	30.4 [1]	Therapeutic Protein
Neupogen®	1991	Oncology	Biologic	18.8 [2]	Therapeutic Protein
Enbrel®	1998	Inflammation	Biologic	150 [3]	Fusion Protein
Aranesp®	2001	Nephrology	Biologic	37 [4]	Therapeutic Protein
Neulasta®	2002	Oncology	Biologic	39 [5]	Therapeutic Protein
Sensipar®	2004	Bone Health	Small Molecule	0.39 [6]	Small Molecule
Vecitbix®	2006	Oncology	Biologic	147 [7]	Monoclonal Antibody
Nplate®	2008	Oncology	Biologic	60 [8]	Peptibody
Prolia®	2010	Bone Health	Biologic	147[9]	Monoclonal Antibody
Xgeva®	2010	Bone Health	Biologic	147 [10]	Monoclonal Antibody
Kyprolis®	2012	Oncology	Small Molecule	0.72 [11]	Peptide
Blincyto®	2014	Oncology	Biologic	54 [12]	Bispecific T-Cell Engager (BiTE)
Corlanor®	2015	Cardiovascular	Small Molecule	0.50 [13]	Small Molecule
Imlygic®	2015	Oncology	Biologic	N/A	Oncolytic Immunotherapy Virus
Repatha®	2015	Cardiovascular	Biologic	142 [14]	Monoclonal Antibody
Parsabiv®	2017	Nephrology	Small Molecule[15]	1 [16]	Peptide

[1] (Amgen, Inc., 2013)
[2] (Amgen, Inc., 2013)
[3] (Amgen, Inc., 2017)
[4] (Amgen, Inc., 2013)
[5] (Amgen Canada Inc., 2017)
[6] (Amgen, Inc., 2017)
[7] (Amgen, Inc., 2017)
[8] (Amgen, Inc., 2014)
[9] (Amgen, Inc., 2017)
[10] (Amgen, Inc., 2018)
[11] (Amgen, Inc., 2015)
[12] (Amgen, Inc., 2017)
[13] (Amgen, Inc., 2015)
[14] (Amgen, Inc., 2017)
[15] Parsabiv has a molecular weight of 1kDa (Amgen, Inc., 2017), meaning its on the line between small vs. large molecule. However, it is delivered via intravenous injection, which makes it a candidate for an oral form factor.
[16] (Amgen, Inc., 2017)

1.1.3 Differences between Large and Small Molecule Therapies

There are many differences between small and large molecule therapies, including but not limited to the molecular weight, mode of administration, manufacturing process, relative efficacy, side effects, and price. Some of these differences are detailed in Table 1-2.

Evidenced by Table 1-2, there are many differences between small molecule therapies and biologics that stem from the different sizes between the two types of drugs. The manufacturing process involves a living cell-line that produces proteins that are highly sensitive to heat, light, and contamination, making the process much more complex than the chemical synthesis of small molecules.

Most biologics are designed for and targeted to a specific disease pathway, and as such can often be more efficacious and have fewer side effects than small molecule drugs. Additionally, biologics tend to have a higher cost and longer timeline associated with development (Mestre-Ferrandiz, Sussex, & Towse, 2012). This, combined with the complex manufacturing processes and longer exclusivity rights associated with biologics, allow these drugs to command on average a price premium of 22x greater than that of small molecules (Opportunities for biosimilar development, 2011).

Table 1-2 Differences between Small Molecule Pharmaceuticals and Biologics[17]

	Small Molecule Pharmaceuticals	Biologics
Method of Synthesis	Chemical Synthesis	Genetically engineered via living cells
Molecular Size	<1000 Da	>1000 Da
Structure	Usually fully known	Complex, Frequently Partially Unknown
Susceptibility to Contamination during Manufacturing	Low	High
Molecular Structure	Relatively simple spatial structures, determined through analytical technology	Exhibit complex spatial structures, difficult to determine
Sensitivity to Physical Factors (heat, light)	Low	High
Clinical Behavior	Well understood mode of action	Complicated modes of action, not always well understood
Manufacturing Process	Straightforward, relatively simple	Highly Complex
Delivery Method	Most prevalent is oral form factor	Intravenous, subcutaneous, & intramuscular injection
Absorption	Good	Poor

[17] Adapted from (Lybecker, 2016) and (Zelikin, Ehrhardt, & Healy, 2016)

However, the most relevant difference between small and large molecule drugs to this thesis stems from the mode of administration. Although other options exist, the oral route of administration is by far the most prevalent for small molecule therapies, while biologics are administered via injection.

Although oral drug delivery of biologics is considered the "holy grail" of drug delivery, attempts at oral delivery have been largely unsuccessful over the past century. The main reason for this is due to the sheer size of large molecule therapies. For example, the molecular weight of aspirin, a widely used and known oral medication, is 180 Da (Sigma Aldrich, 2017). When compared to the biologics in Table 1-1, it is evident that biologics range in size from 100 to 830 times larger than aspirin. Due to this large difference in size, biologics are metabolized like food, while small molecules are treated as nutrients. As such, large molecule therapeutics are not viable by the time they reach their intended site of action if administered orally. This difference, among others, result in the inability to deliver biologics via an oral route of administration (ROA), and will be explored in greater detail in section 1.2.

1.2 Drug Delivery of Large Molecule Therapies

Drug delivery can be largely divided into two major categories: invasive and non-invasive methods. Invasive methods include intravenous (IV), intramuscular (IM), and subcutaneous (SC) injection. Non-invasive methods include delivery via oral, buccal (through the cheek), nasal, pulmonary, and transdermal routes of administration. The main difference between these two categories is the presence and use of a needle to deliver drug product.

1.2.1 Current Delivery methods for Large Molecule Drugs

Most large molecule drugs are formulated for invasive delivery due to their size and low absorption via non-invasive routes. IV injection (or infusion) is generally performed in-clinic over a longer period of time, with a low-concentration of drug product. IV injection allows for drug product to enter the bloodstream directly via the vein, resulting in rapid absorption. IV injection also allows for control over dosage, so the dose can be titrated to the appropriate amount for the patient's weight or condition (Healthline, n.d.). IV injection can be completed through standard IV lines, central venous catheters, implanted ports, or portable pumps (Figure 1-1).

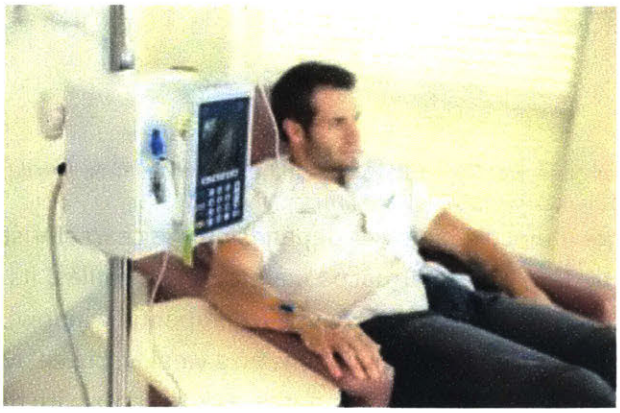

Figure 1-1 Typical setup for IV infusion (Intravenous (IV) Infusion Therapy, n.d.)

IM injection involves delivery deep into the muscle, allowing for quick absorption into the bloodstream, and are widely used for vaccine delivery (Healthline, n.d.). IM injections can either be administered by syringes or auto injectors (Figure 1-2 (a) and (b)), and are often more painful than subcutaneous injections with the same devices, due to the deeper level of penetration needed to reach the muscular layers. Drugs administered via IM injection are absorbed faster than SC injection, due to the greater blood supply in the muscular tissue. The muscle can also hold a larger volume of medication than SC tissue.

SC injection is administered via a short-needle as a small volume (1-2mL) bolus into the fatty tissue layer just under the skin, and can often be self-administered by the patient (HealthLine, n.d.). Medication is absorbed more slowly via this route, but is generally preferred over IV due to its low-cost and convenience, and over IM due to the pain associated with delivery into the muscular layer. Similar to IM injection, SC injection can be performed with a syringe, auto injector, or wearable injector/infusor Figure 1-2 (a), (b), and (c)).

A syringe administers drug product by manual insertion of the hypodermic needle under the skin, and manual depression of the plunger to eject liquid from the body of the device. The syringe is then manually retracted from the patient and disposed of. An auto injector, on the other hand, can include features such as automatic needle insertion and retraction and automatic depression of the plunger to pump the drug product into the patient. This limits the steps the patient or health care provider (HCP) needs to perform to inject the drug product and restricts the visibility of the needle. Wearable pumps allow for the injection of either large volume or time-sensitive (i.e. delayed delivery) drug product, and generally also includes automatic needle insertion and retraction and automatic pumping features.

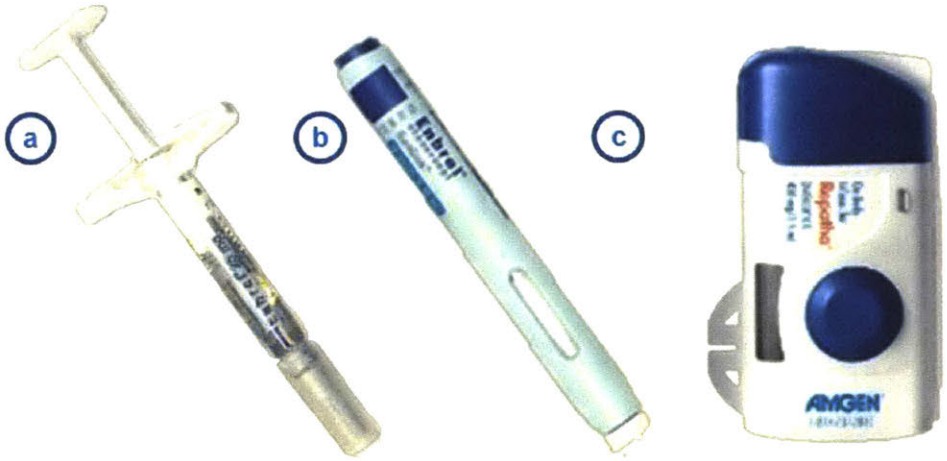

Figure 1-2 Examples of devices for IM and SC injection. (a) Syringe (MIMS, n.d.) (b) Auto injector (Amgen, Inc., n.d.) and (c) wearable infusor (Amgen, Inc., 2018)

The dosing frequency of large molecule biologics depends on the characteristics of the drug in question, including its pharmacokinetic (PK) and pharmacodynamics (PD) profiles, its half-life, and the range of concentrations over which it is considered therapeutic (therapeutic window). For the most part, SC, IV, and IM administration of Amgen's drugs either happens on a weekly, biweekly, or monthly basis. In some cases, injections can also be administered every 6 months, as is the case with the osteoporosis drug Prolia® (Amgen, Inc., 2017).

Bioavailability is defined as the proportion of active drug substance that enters into systemic circulation when introduced into the body in order to have an effect on the intended condition. This proportion is often compared across different delivery methods, and is defined at baseline as 100% for IV administration. Percent bioavailability is often used as a metric to compare different delivery methods, and will be used extensively as a metric in the remaining parts of this thesis. For example, subcutaneous and intramuscular injection often have a lower bioavailability than intravenous injection, although it can vary depending on the characteristics of the delivered drug product.

However, all of these delivery methods involve the use of a needle. Although auto injectors and wearable pumps limit the interactions patients have with the needle, 10% of the population can be needle-phobic to the extent that they will not take medications that involve delivery via needles (Dangi, 2015). This, among other factors, has led to the exploration of noninvasive routes of administration for biologics in recent years.

1.2.2 Emerging technologies for Drug Delivery of Biologics

Due to the challenges associated with parental delivery, noninvasive routes have been studied for delivery of large molecules. Figure 1-3 depicts some of the non-invasive routes studied for drug delivery. Buccal and oral delivery will be covered in more detail in Section 3.1, and so will not be covered in detail here.

Nasal delivery occurs through the highly vascularized layers of the nose. In order to increase permeability into the bloodstream, drug products are often combined with permeation enhancers, such as Nasulin, a

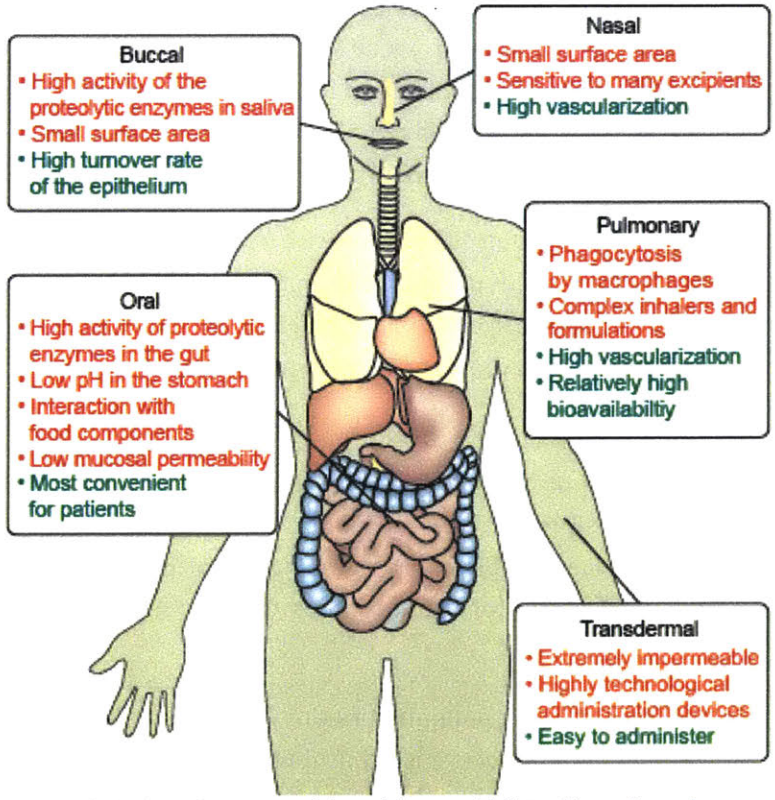

Figure 1-3 Noninvasive routes of drug delivery with lists of benefits and challenges (Zelikin, Ehrhardt, & Healy, 2016)

CPEX Pharmaceuticals insulin product for nasal delivery (Zelikin, Ehrhardt, & Healy, 2016). Insulin, with a molecular weight of 5800 Da (PubChem, n.d.), is considered a large molecule, but would be considered small compared to some of Amgen's product offerings detailed in Table 1-1. However, the nasal cavity has a small surface area to absorb drug product and can result in sensitivity to the excipients used in drug product formulation. These challenges, along with the relative discomfort a patient may experience while using nasal devices in comparison to other noninvasive routes, makes nasal delivery a less-appealing noninvasive route.

Pulmonary delivery via inhalation into the lungs can often result in rapid absorption and relative high bioavailability (Zelikin, Ehrhardt, & Healy, 2016). However, oral inhalation often requires the use of complex inhalers and formulations and leaves drug product susceptible to phagocytosis by macrophages (Zelikin, Ehrhardt, & Healy, 2016). Despite these challenges, two insulin products have been approved for systemic delivery via oral inhalation – *Exubera* from Nektar & Pfizer and *Afrezza* from Sanofi & MannKind. Due to poor sales and other economic reasons, both products discontinued sales after a short time (Zelikin, Ehrhardt, & Healy, 2016). Among others, reasons for the economic difficulties could be associated with the difficulty in manufacturing the appropriate sized molecules for absorption through the lung and the cumbersome patient experience with the complicated inhalers required for delivery.

Transdermal delivery through topical administration of drug product on the surface of the skin is challenging for large molecules. Although easy to administer over the large surface area of the skin, the outermost layer of the skin – the stratum corneum – is very impermeable to large molecules, and often requires co-administration with complicated devices to increase the permeability of this layer. Microneedles, ultrasound, iontophoresis, and electroporation have been used to increase the permeability of the skin. However, the complexity and inconvenience associated with the devices can cause poor adoption, and the bioavailability is still not high enough to make transdermal administration economically viable (Mitragotri, Burke, & Langer, 2014).

Even though pulmonary, nasal, and transdermal delivery are associated with their own challenges, the noninvasive route of administration remains preferable by many patients, not just those that are severely needle-phobic. Development of noninvasive routes of delivery for large molecules can possibly even increase patient adherence and persistence with prescribed medication regimens.

1.3 Patient Adherence Remains a Costly Challenge in the Pharmaceutical Industry

Development of noninvasive routes of delivery for large molecules can possibly even increase patient adherence and persistence with their medication regimens, which remains a costly challenge within the pharmaceutical industry. Adherence is defined as a combination of the patient's compliance with the prescribed timing, frequency, and dosing of medication as well as the persistence to the prescribed medical regimen.

Studies have shown that adherence among patients suffering from chronic diseases averages only about 50% (WHO, 2003). This lack of patient of adherence contributes to 33-69% of hospital admissions in the United States, at a cost of $100 billion annually (Osterberg & Blaschke, 2005). In addition to the human

pain and suffering caused by patient adherence, pharmaceutical companies lost upwards of $637 billion in revenue in 2015 due to patient non-adherence and non-persistence (Schull & Sackowitz, n.d.).

However, patient nonadherence is much easier to study for oral medication, due to the relatively straightforward and predictable administration for these types of therapies. Because of the complex dosing schedules and various delivery methods associated with biologics, methods to measure adherence to biologics are not as well established. As biologics continue to become increasingly prevalent in the medical world, studies continue to come out describing the effects of poor adherence to biologic therapies.

Given that biologics targeted towards management of autoimmune disease are among the top grossing biologics (Stone, 2017), most adherence studies focus around therapies used to treat such conditions. In a study comparing adherence rates to biologic therapies for rheumatoid arthritis (RA), persistence to the medication over 12 months ranged from 44-62.2% in the US (Blum, Koo, & Doshi, 2011). Another study reported that across populations using anti-TNF therapies (e.g. Enbrel among others), only 23-51% remained adherent to medication over the period of a year (Esposti, et al., 2014). The low adherence rates to biologic therapies indicate that they also have an adverse effect on patient outcomes, hospitalization rates, and revenue as with oral nonadherence.

The low adherence rates to biologics could be due to a number of factors, including but not limited to: the high cost of medication, cumbersome delivery methods, dosing frequency, needle-phobia, disease duration and severity, side-effects, beliefs about treatment necessity and efficacy, emotional well-being, relationship between patient and HCP, confidence in self-administration, and others (Vangeli, et al., 2015). The relationship between all of these factors and their interdependence makes it difficult to pinpoint a reason for patient nonadherence. However, remedies to alleviate any of the listed factors could potentially work to turn the tide of patient nonadherence.

1.4 Summary

Chapter 1 focused on providing the relevant background information to understand the basics about the biotechnology industry and the types of drugs that Amgen provides to the market. In addition, this section provided insights into the differences between the manufacturing methods, molecular size, complexity, and, in particular, the delivery methods between small and large molecules. The historical methods for delivery of large molecule therapeutics rely on the use of needle-based devices, such as syringes, auto injectors, and wearable infusers, which results a problem for the 10% of the population that is severely needle phobic. The benefits and challenges of novel noninvasive routes for the delivery of large molecule therapeutics, including transdermal, pulmonary, nasal, were also discussed. Finally, the costly epidemic of patient non-adherence was presented, revealing low adherence rates for a wide variety of biologic therapies. Potential influential factors of this problem, including the cost of medication, delivery methods, dosing frequency, and needle phobia, were discussed and serve as motivation to research delivery methods that can reduce the influence of such factors on patient adherence.

Chapter 2 Purpose of Project / Problem Statement

Given the preference for noninvasive routes of drug delivery in the face of the patient nonadherence epidemic gripping the healthcare system, the LGO internship was designed to further evaluate the field of novel oral drug delivery for biologics. Chapter 2 details the value proposition of novel orals, in terms of patient preference for noninvasive delivery, top-line growth for commercial products, and the launch-enabling abilities of an oral route for certain types of therapies. Next, this section details the goals of the project, including the milestones to be completed during the LGO internship, the scope of the project, and the approach taken by the LGO student to fully understand the field of novel oral drug delivery for biologics.

2.1 Value Proposition of Novel Orals

Novel Oral Drug Delivery of Biologics can revolutionize the ways in which patients interact with their drugs and potentially turn the tide on the patient nonadherence trends detailed in the previous section. However, gaining a competitive edge in the battle against patient nonadherence is not the only benefit from oral drug delivery. The value proposition of oral drug delivery of biologics can be segmented into three distinct categories. The first is that it can potentially increase adherence by meeting patient needs and preferences. The second is that novel orals can drive top-line growth within Amgen's six therapeutic areas and operational benefits within manufacturing. Finally, novel orals could potentially enable the launch of new molecules that require targeted delivery to the gut for efficacy.

2.1.1 Patient Preference

Oral drug delivery of biologics could increase patient adherence by minimizing pain, anxiety, and invasiveness associated with injection. As stated earlier, up to 10% of the population is severely needle-phobic to the extent that they avoid medication (Dangi, 2015), and an even greater population likely experiences discomfort with self-injection. Furthermore, adding an oral option to the suite of delivery options for large molecule therapies increases the flexibility of delivery options, allowing patients to select what is best for them to remain adherent to medication. Supposing that oral delivery of biologics would be analogous to taking an aspirin, this could also increase the ease of use and limit the disruption to daily activities in comparison to the typical preparation required for IV, IM, or SC injection.

An oral option is not always the more preferred option over injection, as many factors are considered when patients judge delivery routes. A literature review was conducted to search for studies in which a comparison between oral vs. injectable delivery routes was made to determine patient preference. Table 2-1details the finding of that literature review, where the oral option was preferred by patients in 6 of those studies, and the injectable in 2 studies. Reasons for preferring an oral medication included, but are not limited to, the dislike of needles and the convenience. However, injectable medications were preferred for reasons surrounding dosing frequency, side effects, and forgetfulness. From this literature review, it is evident that there is a tradeoff between dosing frequency and route of administration and that the patients preference are highly dependent upon the disease class and other factors associated with the route of administration (i.e. presence of certain side effects).

Table 2-1 Literature Review Patient Preference Oral vs. Injectable

	Oral Preferred	Injectable Preferred	No Preference
# of Studies	6	2	3
Reasons Cited	- Convenience[18,20] - Dislike of Needles[18]	- Forget to take daily oral[18] - High BMI[18] - Frequency of side effects[19] - Dosing Frequency[19,25]	- Patient adherence, not patient preference[25,26]
Disease Space	- Breast Cancer[18] - MS[19] - Type-2 Diabetes[20] - RA[21] - Migraine[22] - Cancer[23]	- Osteoporosis[24]	- MS[25] - Tuberculosis[26] - Anticoagulants[27]

The tradeoff between dosing frequency and route of administration is one that warrants further investigation. Oral medications have a payload limited by the size that is swallow-able by the human adult, which resides around a capsule size of 9mm in outer diameter by 15mm in length (Langer & Traverso, 2017). Therefore, medications that have larger doses – as is associated with many large molecule biologics – will have to be dosed more frequently to treat patients. One study conducted with multiple sclerosis patients analyzed this specific tradeoff. As seen in Figure 2-1, oral delivery is preferred in a multitude of cases. Most interestingly, a once daily pill is preferred 57% of the time vs. a monthly injection and 74% of the time vs. a weekly injection. This preference indicates that an oral option, even if it drastically increases the dosing frequency, could still ameliorate the patient experience.

[18] (Fallowfield, 2005)
[19] (Utz, 2014)
[20] (Dibonaventura, 2010)
[21] (Emadi, 2017)
[22] (Dahlöf, 2005)
[23] (Krohe, 2016)
[24] (Kendler, 2009)
[25] (Munsell, 2016)
[26] (Chum, 1995)
[27] (Benedetto, 2016)

Furthermore, the growing aging population would benefit from the limited pain and disruption incurred with injection via IV, SQ, and IM delivery routes (Dibonaventura, 2010). Given that many of Amgen's drug products treat the aging population and this population continues to grow as Baby Boomers enter into retirement age, the value of an option preferred by this population is high.

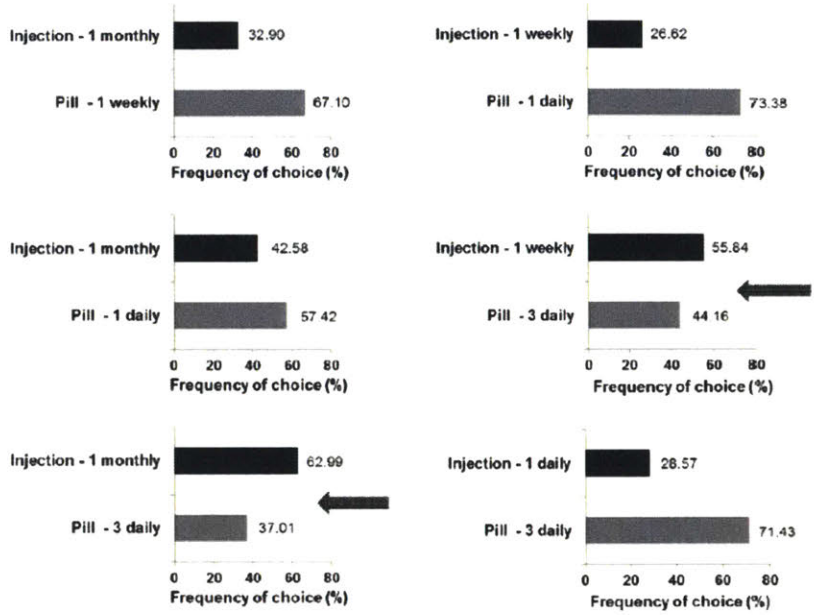

Figure 2-1 Preference judgements: frequency of choices for one route of administration in relation of treatment frequency with frequency of side-effects held constant. Adapted from (Utz, 2014).

Although Table 2-1 tabulates the patient preference, patient preference does not necessarily equal patient adherence. In fact, two of the studies concluded that patient adherence does not change between usage of an oral vs. injectable medication (Munsell, 2016) (Chum, 1995). Of note, there does not seem to be a consistent method to measure preference or adherence, and adherence studies outcomes are highly dependent upon the use-case within the disease space. This indicates that study of the patient preferences within a specific therapeutic area should be conducted prior to applying an oral delivery technology to ensure that the oral route could both increase patient preference and adherence. However, given that the oral route is preferred for patients in most cases, enabling an oral option for patients holds value.

2.1.2 Top-Line Growth

Top line growth would be expected if an oral route of administration were available as an alternative delivery route for Amgen's products for a multitude of reasons. Given the 10% of the population that refuses medication due to the presence of needles (Dangi, 2015), provision of a needle-free delivery method could result in an increase in the volume of sales for a given drug by that same amount. Similarly, an oral route could enable an increase in new patient starts and market share within established markets due to the decrease in anxiety around medication administration.

Second, an oral delivery route would make Amgen's products highly competitive within all therapy areas, regardless of whether or not an alternative oral medication is available. For example, within the highly competitive rheumatoid arthritis market, an oral option would entice patients with needle-phobia to

switch from Amgen's competitors to Enbrel. Furthermore, if there is IP generation potential around the drug-device combination, market exclusivity for Amgen's products can be expanded and prevent direct competitors from adopting the oral delivery route.

Additionally, in disease areas where therapies have pivoted from an injectable option to an oral one, the oral options experienced incredible growth. When the gold-standard injectable option was supplanted for an oral medication in the migraine market, the oral medication experienced year over year growth of 60% (EvaluatePharma). Similarly, in the MS market, the oral medication option has experienced a compounded annual growth rate (CAGR) of 75% over the past 5 years (EvaluatePharma). Additionally, studies have indicated that for Type-2 diabetes treatment, doctors have increased the prescription rates of the oral medication over the traditional injectable due concerns over patient adherence, even in the face of lower efficacy (Langer & Traverso, 2017).

Finally, if the solution to oral delivery of large molecules is a platform technology that can be applied across multiple assets, Amgen could experience operational benefits over time. The first medication paired with the oral delivery technology will likely undergo extensive research and development to ensure safety and efficacy, but the time and resources necessary for verification and validation will likely decrease with each subsequently paired medication.

2.1.3 Launch Enabling

Finally, for therapies that need to be delivered locally, an oral delivery route could be launch enabling for the medication. Local delivery to the gastrointestinal tract could increase the effectiveness of the drug and reduce side effects if delivered to the appropriate location for the drug target. However, if the oral delivery route is able to deliver medication into systemic circulation, rather than just locally in the gut, it could be applied as a delivery platform for a whole range of medications that target areas outside of the gastrointestinal tract.

2.2 Project Goals

Given the value of an oral delivery route for biologics, the objective of this internship was to develop a holistic strategy in the space of Novel Orals, identify high-priority technologies for advancement into further technical evaluation, and begin technical evaluation of high-priority technologies prioritized by risk. Given this objective, specific deliverables within the internship included:

- Description of the technology landscape of promising candidates for oral drug delivery of large molecules
- Identification of prioritized technologies via rigorous down-selection
- Risk assessment of prioritized technologies
- Initiation of technical feasibility testing and modeling

This thesis focuses on the method for determining the high-priority technologies and the technical evaluation via *in silico* simulation of one of those candidates.

2.3 Scope

For the purposes of the investigation, considered novel oral technologies included all technologies able to deliver large molecules via an oral route of administration via:

- the gastrointestinal (GI) tract
- the sublingual (under the tongue) route
- the buccal (through the cheek) route

Platform technologies that could be applied to a wide range of sizes and modalities of molecules were prioritized for consideration. Although this investigation was undertaken from the perspective of a device solution, formulation techniques that enabled absorption in the gut or mouth were considered as they could potentially aid device platforms for delivery. Modification directly to the drug substance which resulted in a new chemical entity were excluded. This would include the appendage or modification to the chemical structure of the active pharmaceutical ingredient.

2.4 Project Approach

An overall project approach for the assessment of the field of novel oral drug delivery of biologics was conceived, with the LGO internship activities embedded within the overall plan. Figure 2-2 is a graphical depiction of the steps taken to ensure a holistic evaluation of the novel oral space. In Phase 1, the value of the field of novel orals was assessed, a literature review was completed into the historical barriers to oral delivery of large molecules, and a landscape assessment of current technologies was completed. In Phase 2, the technologies identified in the landscape were down-selected to two high-priority candidates, a technical risk assessment was performed on those candidates, and a future testing strategy was identified. Both Phases 1 and 2 were completed by the LGO intern in coordination with the Advanced Device Technology & Innovation (ADT&I) group at Amgen. In phase 3, the LGO student completed *in silico* simulation of one of the high-priority technology candidates. The project was then transitioned for the continuation and completion of phase 3 to another Amgen employee with ADT&I.

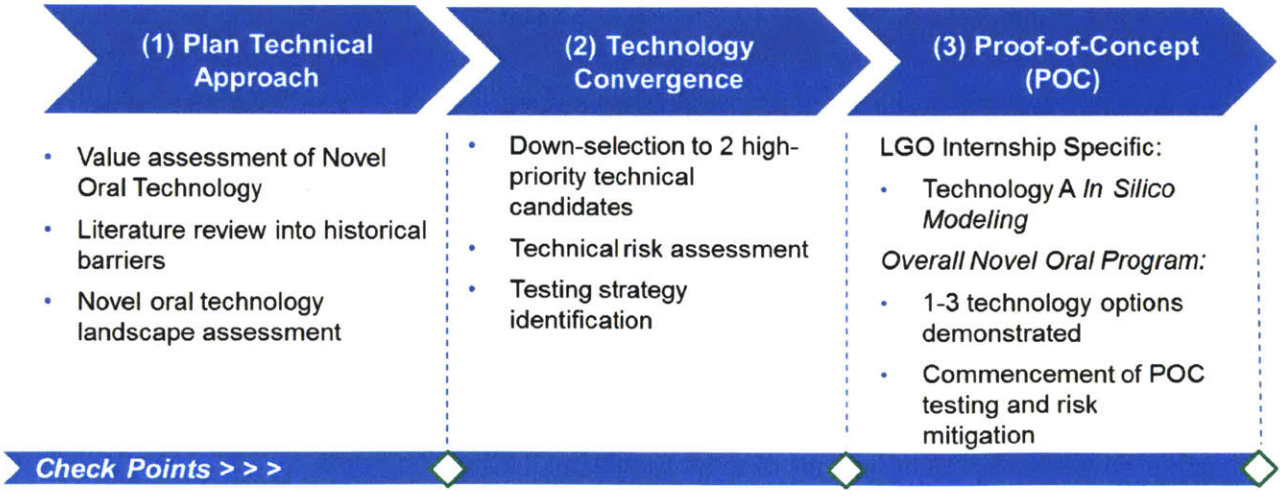

Figure 2-2 Project Approach for Novel Oral Program

In each of the checkpoints in Figure 2-2, the LGO intern conferred with the wider ADT&I group to ensure progress was made in the appropriate direction and that all were on board. The rest of this thesis coordinates to the different phases within this figure, and details the specifics of the work completed within each phase. The preliminary value assessment of Novel Oral technology was used as motivation for the project, and was detailed in section 2.1. The next section of the thesis will dive into the historical barriers to oral drug delivery of large molecules.

2.5 Summary

Chapter 2 explains the motivation for the LGO project investigating the field of novel oral drug delivery of biologics. Studies have shown that patients prefer an oral delivery option as opposed to needle-based delivery, largely due to the dislike of needles and the need for convenience. One study revealed that patients prefer the oral option even when they have to take a daily pill as opposed to a monthly injection. Furthermore, an oral delivery option could aid in the top-line growth for Amgen's commercial products, due to the increase in volume of sales by needle-phobic patients and the expected growth conveyed by past examples of therapies switching from an injectable to oral option. Finally, an oral delivery option could be launch enabling for therapies that need to be delivered locally to the gut, as opposed to systemically throughout the body, in order to limit side effects from medication.

The LGO project goals revolved around the completion of a technology landscape, prioritization of technologies, risk-assessment, and initiation of technical feasibility on high-priority candidates. The scope was limited to platform technologies enabling delivery through the GI, buccal, or sublingual routes, and would be able to be paired with multiple medications. The approach taken by the student is summarized in Figure 2-2, and follows three distinct phases: (1) plan technical approach, (2) technology convergence, and (3) proof-of-concept.

The following chapters follow the three different phases of the project, and will dive deeper into the scientific, biological, and technical aspects of oral drug delivery of large molecule therapeutics.

Chapter 3 Historical Barriers to Oral Drug Delivery of Large Molecules

Phase 1 of the project, as seen in Figure 2-2, included a literature review into the historical barriers to oral delivery of large molecules. Given the large value proposition of oral drug delivery of biologics, this route of delivery has been researched and attempted in the past with unsuccessful results. In order to understand the best way to evaluate current methodologies that claim to deliver biologics via an oral

route, a good understanding of the barriers, and the differences between the buccal, sublingual, and GI routes, needs to be understood.

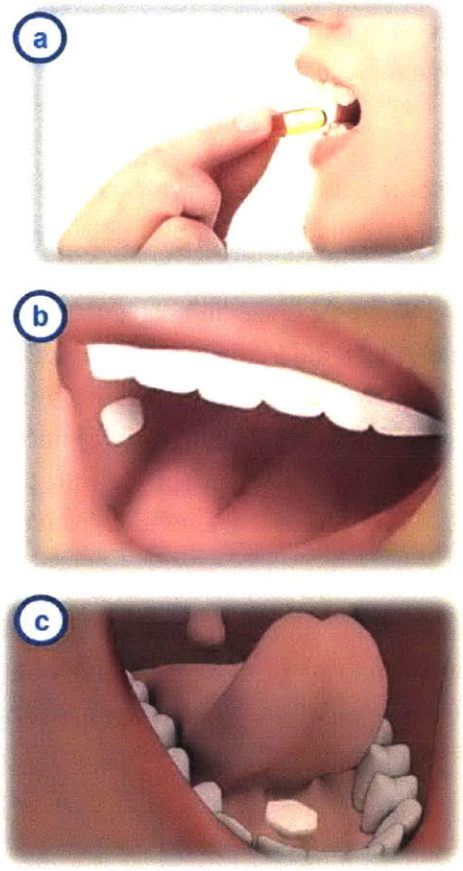

Figure 3-1 Oral drug delivery via (a) the GI tract (Benjamin, 2017), (b) the buccal route (IPEC Europe, 2013), (c) the sublingual route (Emaze, n.d.).

This chapter further discusses and compares the benefits and challenges of the buccal, sublingual, and GI routes for oral drug delivery. This section then explains the historical attempts made over the past century to enable oral delivery of large molecule therapeutics, through formulation, drug modification, and device strategies. The chapter concludes with a summary of the three main challenges for oral delivery of biologics: (1) lack of bioavailability, (2) clinical challenges of oral delivery, and (3) safety challenges.

3.1 Routes of Oral Drug Absorption

As indicated in Section 2.3, there are three routes of administration considered under the novel oral umbrella: buccal, sublingual, and GI delivery. Figure 3-1 shows an illustrative depiction of the three different types of oral drug delivery. Figure 3-1 Oral drug delivery via (a) the GI tract , (b) the buccal route , (c) the sublingual route .This section goes into the differences between these three routes.

3.1.1 Buccal & Sublingual Routes of Administration

The buccal and sublingual routes of administration are rather similar to each other. The buccal route involves drug delivery through the cheek, while the sublingual route involves drug delivery through the tissue under the tongue (Figure 3-1 (b) and (c) respectively).

In these two routes, drug product is released and travels through the epithelial layers in order to gain access to the highly vascularized tissues underneath (see Figure 3-2). The differences between the buccal and sublingual mucosa are listed in Table 3-1, and discussed in further detail below.

Table 3-1 Comparison of Buccal and Sublingual Delivery Routes

	Buccal	Sublingual
Cell Layers	40-50	8-12
Thickness	500-800 μm	100-200 μm
Surface area	50 cm^2	<50 cm^2
Type	semi-keratinized	non-keratinized
Relative Permeability	Lower	Higher

The buccal mucosa consists of a mucus-lined keratinized stratified squamous epithelium of approximately 40-50 cell layers, which is attached to connective tissue via the basal lamina (Morales, et al., 2017). The connective tissue contains blood vessels that allow for direct systemic circulation of drug product, avoiding hepatic first-pass metabolism (Morales, et al., 2017). This effect occurs when the drug is swallowed by the patient and absorbed into the portal vein system. After digestion of the drug by enzymes in the gut, the portal vein system delivers absorbed drug to the liver prior to wider systemic circulation, where the liver can further metabolize the active drug substance. Although the stratified squamous epithelium does not contain tight junctions, analogous to those described in section 323.1.2, lipid content extruded by the upper third layer of cells limits drug permeation through the numerous cell layers prior to reaching the vascularized tissue (Morales, et al., 2017).

Similar to the buccal mucosa, the sublingual mucosa is divided into two layers consisting of stratified non-keratinized squamous epithelium lined with a thin layer of mucus and connective tissue (Goswami, Jasti, & Li, 2008). The epithelium is comprised of 8-12 cell layers (100-200 μm thick), and is attached to the connective tissue via the basal lamina, otherwise known as the basement membrane (Goswami, Jasti, & Li, 2008). Again, the connective tissue allows for absorption of large molecules directly into systemic circulation, bypassing first pass metabolism.

The major difference between keratinized and non-keratinized epithelia is the type of lipids produced that inhibit the transport of large molecules through the epithelial layer. In keratinized epithelia, the lipids are in the form of lamellar lipid stacks, while they consist of an amorphous material in non-keratinized epithelium (Goswami, Jasti, & Li, 2008). Therefore, non-keratinized epithelia has lower lipid content and disorganized arrays of keratin, resulting in the larger permeability of large molecules in the sublingual mucosa than in the buccal mucosa. This is aided by the fact that the sublingual epithelium is thinner than that of the buccal epithelium. However, although the permeability is higher within the sublingual mucosa,

the surface area is smaller than that of the buccal mucosa, leading to less available space for drug absorption.

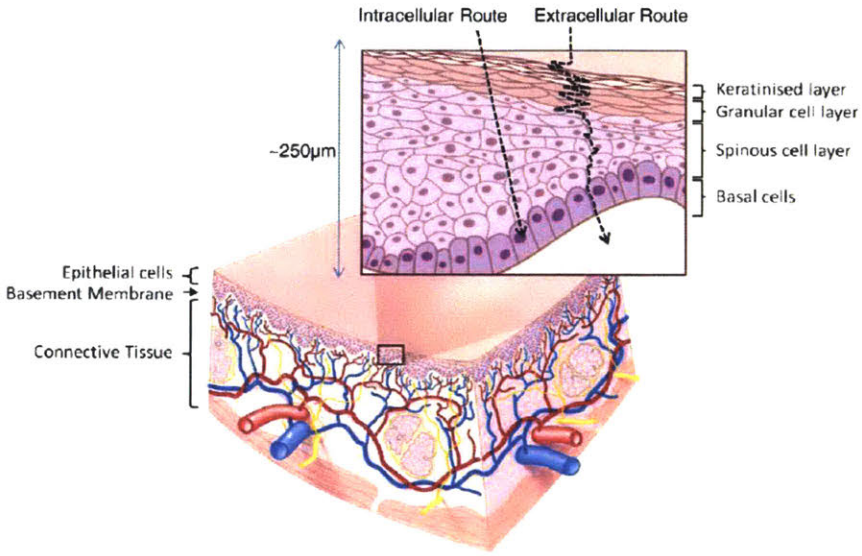

Figure 3-2 Representative illustration of oral mucosa displaying two possible transportation routes for large molecule delivery (Hearnden, et al., 2012)

There are multiple methods by which drug product can travel through the epithelium of the oral mucosa to the underlying vascularized tissue, and two of the passive methods are depicted in Figure 3-2. The intracellular route indicates that molecules pass through cells as they travel via passive diffusion, while the extracellular route indicates that molecules through the lipid rich domains between cells as they filter down. Other routes of transportation include carrier mediated transport and endocytosis/exocytosis (Hearnden, et al., 2012). However, these other routes may metabolize and/or alter the chemical structure of biologics, and are less ideal for drug delivery.

Drug products that consist of lipophilic molecules of small molecular weight are ideal for delivery through the oral epithelium (Morales, et al., 2017). However, given the high molecular weight and hydrophilicity of most of biologics, this puts a strain on the passive diffusion mechanisms within the oral epithelium. In fact, studies have shown that dextran molecules – a polar drug product – can diffuse across the oral epithelium when the molecular weight is less than 20,000 Da (Hearnden, et al., 2012). Any larger, and the dextran molecules are not able to reach the underlying vascularized tissue.

3.1.2 GI Delivery

For oral gastrointestinal (GI) delivery, drug product is generally swallowed in a pill or tablet form factor, and moves through the digestive system, where it is then released for absorption in the small intestine. There are also infusion systems that deliver directly to the small intestine, such as the Duodopa Infusion System, but are not typical used as a delivery mode (Negreanu, et al., 2011).

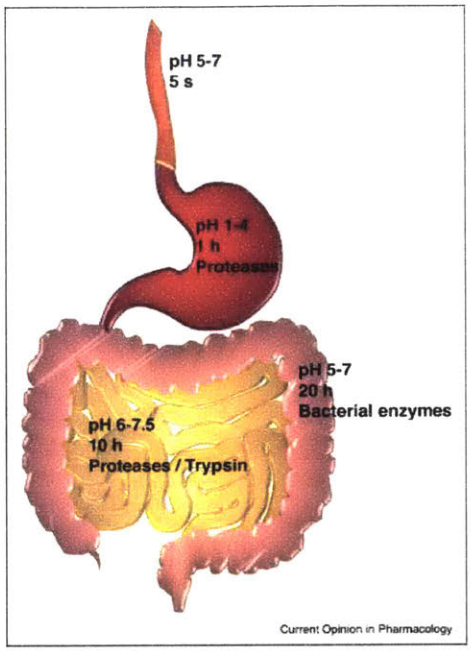

Figure 3-3 Schematic of the GI tract with corresponding pH ranges, average transit times and predominant protein degradative enzymatic activity (Langer & Traverso, 2017)

As seen in Figure 3-3, after a pill is swallowed, it travels through the esophagus with a pH of 5-7, then enters the stomach with a pH of 1-4, moves into the small intestine (yellow) with a pH of 6-7.5, and finally traverses through the large intestine or colon with a pH of 5-7. In general, the drug product is released in the small intestine due to the neutral pH of that system, the long transit time, the smaller inner diameter of the small intestine allowing for localization, the surface area of the small intestine, and the ability to trigger release, all of which aid in drug absorption into systemic circulation.

The small intestine has a large surface area for absorption (400 m^2) that is covered by a thick mucus coating (40-450µm) that sheds frequently (Fox, et al., 2015) (Langer & Traverso, 2017). The mucus layer restricts large molecules from accessing the surface area of epithelial cells, and is comprised of glycoproteins that stabilize the unstirred mucus layer due to their high molecular weight (Hamman, Enslin, & Kotze, 2005).

The small intestine itself is filled with digestive enzymes, which can attack drug product prior to its absorption across the small intestinal wall. Proteolytic enzymes are ubiquitous throughout the GI tract, and digestion can take place along multiple places within the GI tract and generally attack the peptide backbone of the drug substance itself (Hamman, Enslin, & Kotze, 2005). Large molecule drugs are broken down into units that are sufficient for absorption, such as single amino acids, and di- and tri- peptide units (Hamman, Enslin, & Kotze, 2005). While these units can be easily absorbed as a nutrient, the drug substance is no longer in its bioactive form, and has no therapeutic activity by the time it reaches its target area, decreasing bioavailability. Enzymes that can break down drug substance include, but are not limited to, pepsin within the stomach, trypsin, peptidases, and other derivatives in the small intestine lumen, and

enzymes residing in the brush border membrane of the small intestine epithelium (Hamman, Enslin, & Kotze, 2005).

The small intestinal wall consists of a mucus layer followed by a single-celled epithelial layer, which is connected to the lamina propria, rich with blood vessels and lymph nodes that carry drug product into systemic circulation via the portal vein. A simplified illustration of the wall of the small intestine and the various delivery pathways across it can be seen in Figure 3-4.

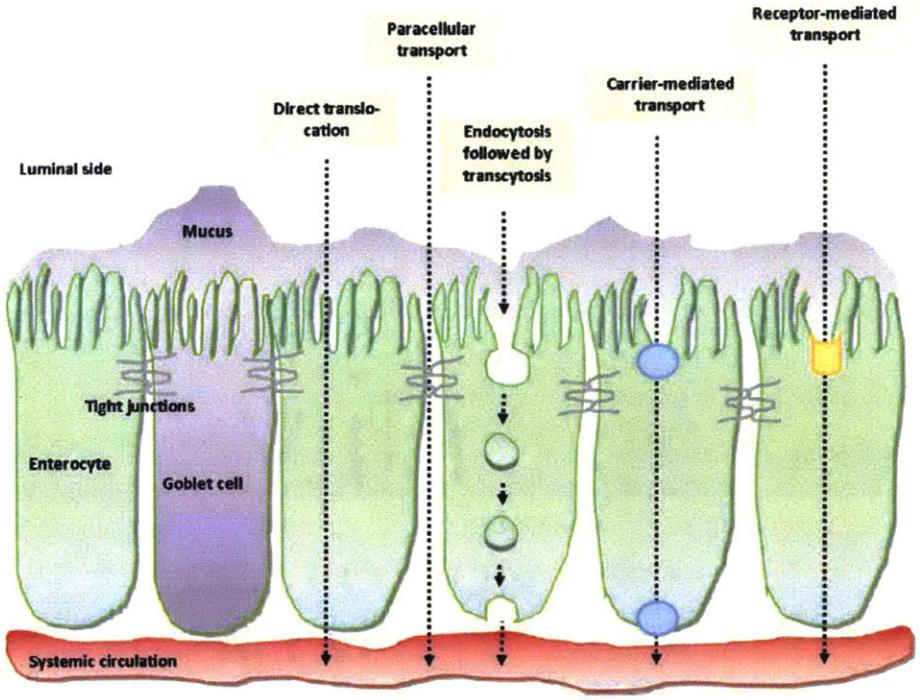

Figure 3-4 Schematic of Wall of Small Intestine and Transport Pathways across Epithelial Barrier (Kristensen & Nielsen, 2015)

Both direct translocation and paracellular transport occur through passive diffusion mechanisms within the small intestine driven by a concentration gradient imbalance. Direct translocation, or transcellular transport, requires passage through the cell, with preference for lipophilic molecules that can disrupt the cell membrane (Kristensen & Nielsen, 2015). Paracellular transport requires passage through the tight junctions that only leave 1-5nm of space between cells for molecules to move across (Tibbitt, Dahlman, & Langer, 2016). Therefore, only hydrophilic molecules less than 200 Da can traverse the epithelium through the paracellular route (Montenegro-Nicolini & Morales, 2017).

Carrier mediated transport, receptor-mediated transport, and endocytosis & transcytosis are considered active transport mechanisms across the epithelium, and require the interaction between cell-contents and the drug molecule in question. These transport mechanisms are not considered ideal for biologics, since only a small fraction are transported across the epithelium in their bioactive form (Tibbitt, Dahlman, & Langer, 2016). Furthermore, carrier- and receptor- mediated transport pathways require conjugation and targeting of the drug substance to specific ligands on the cell-surface.

Not shown in Figure 3-4 are regions of the small intestine called Peyer's Patches, which contain M cells. Although Peyer's patches only account for approximately 1% of the surface area of the small intestine, there is evidence that M cells have adapted to absorb many different types of materials, making them a possible location for drug delivery (Rieux, Fievez, Garinot, Schneider, & Preat, 2006). Furthermore, absorption via Peyer's patches allows drug product to travel across a thinner mucus lining, allowing for potentially faster drug uptake (Langer & Traverso, 2017). However, absorption via M-cells requires significant targeting and size dependencies that are species dependent, making the method of M-cell targeting not ideal as a platform solution (Rieux, Fievez, Garinot, Schneider, & Preat, 2006).

The molecular weight limit to gastrointestinal permeability is 20 kDa, equivalent to the permeability limit exhibited by the oral mucosa (Chirra & Desai, 2012).

3.1.3 Comparison of Buccal, Sublingual, and GI Delivery

Although both the oral mucosa routes (buccal and sublingual) exhibit the same approximate molecular weight limit to biologics as the GI route (20 kDa), there are other aspects that can be compared across the two locations for delivery. For the purposes of this comparison, buccal and sublingual will be referred to as "oral mucosa routes".

Although the oral mucosa routes are less commonly used, their environment may be more amenable to delivery. Due to their lack of tight junctions, higher volumes of drug product are able to travel through the epithelium to the vascularized underlying tissue (Montenegro-Nicolini & Morales, 2017). The oral mucosa lacks the harsh acidic environment and pH variability, as well as the intense enzymatic environment found in the gut. Absorption through the oral mucosa allows for avoidance of first-pass metabolism, and has a faster time to max concentration due to its convenient delivery location. Finally, the device used to deliver the drug can be immobilized during the event and localized to the oral mucosa, which cannot be guaranteed in GI delivery due to the constant motion of fluid within the GI tract. Furthermore, the drug delivery vehicle does not need to be swallowed when delivered via the oral mucosa, which is a major hindrance for both children and the elderly.

However, there are some drawbacks to delivery via the oral mucosa. Although not to the same extent as in the GI tract, there are still enzymes present in this environment that can lead to degradation (Morales, et al., 2017). Furthermore, drug product can be lost through the production and flow of saliva throughout the cavity. Delivery through the oral mucosa also requires the taste of the drug product to be considered and is a foreign route of administration to most patients. Finally, if the drug requires GI localization to reduce off-target side-effects or increase efficacy, it will not be able to achieve that through delivery via the oral mucosa.

Delivery via the GI tract is more traditionally accepted by and familiar to patients and physicians (Langer & Traverso, 2017). As noted above, it can allow for local delivery of drug products that act within the GI tract, and has a longer transit time and larger surface area that can help with drug absorption.

However, there are notable drawbacks to delivery via the GI tract around variability and predictability. The thick mucus coating that sheds frequently makes it hard to localize delivery and build a concentration gradient in a single location. Furthermore, variability is present in pH between different humans at the

same site, and within a single human depending on the time of day (Montenegro-Nicolini & Morales, 2017). Drug delivery can also vary depending on the age, diet, and disease state of the patient in question (Morishita & Peppas, 2006). Finally, the tight junctions, first pass metabolism, harsh enzymatic environment, and dosage that is limited by the size of the pill present further barriers to delivery via the gastrointestinal tract.

3.2 History of attempts

Oral delivery of large molecules has been attempted since 1923, two years after the discovery of insulin (Langer & Traverso, 2017). Over that time, attempts to increase the oral bioavailability of biologics has been attempted with little success.

3.2.1 Formulation Strategies

Formulation strategies aim to increase the bioavailability of drug product through a couple of different routes. Permeation enhancers are chemical agents added to the drug product formulation to increase the permeability of the epithelium via chemical interaction with the cellular structure of the epithelial barrier. They aim to increase transport either across the transcellular or paracellular route, depending on the cellular structures that are chemically altered (Gupta, Hwang, Doshi, & Mitragotri, 2013). They work through numerous mechanisms, such as changing the cell membrane fluidity via partial solubilization, decreasing the mucus layer viscosity, and opening of the tight junctions of the GI tract (Hamman, Enslin, & Kotze, 2005). Numerous entities have been tested for efficacy, including surfactants, bile salts, fatty acids, chitosan derivatives, and poly (acrylic acid) (Gupta, Hwang, Doshi, & Mitragotri, 2013). However, some of the mechanisms of action, such as solubilization of the cell membrane, can lead to damage and local inflammation if used over long periods (Muheem, et al., 2016). This leads to concerns over potency and toxicity when formulated with drug substance, making permeation enhancers a non-ideal solution for oral delivery of biologics.

Protease and enzyme inhibitors are chemicals that deactivate or block the digestive enzymes of the stomach and small intestine from attacking and degrading the drug product while in its bioactive form. However, there is concern over long term use of these types of formulation agents due to their potential to disturb the digestion patterns of nutrients and to actually increase future enzyme secretion due to the disturbance of the biological feedback control system (Hamman, Enslin, & Kotze, 2005).

Mucoadhesion, or bioadhesion, indicates adhesion between the drug delivery system carrying the drug product and the GI (or oral) mucosa. By promoting mucoadhesion, the drug delivery system is immobilized to the wall, and a concentration gradient of drug product is allowed to form over time without being disturbed, theoretically increasing the absorption of drug product across the epithelial layer. Multiple chemicals have been studied for their mucoadhesive abilities, including chitosan, PLGA, thiolated polymers, and alginates (Muheem, et al., 2016). For example, entities containing thiomers aid in the formation of covalent bonds with cysteine rich sub-domains of mucus glycoproteins, allowing for drug substance to remain in the mucus for longer (Hamman, Enslin, & Kotze, 2005). However, given that these types of agents only build up the concentration gradient, but do not actively aid in absorption, mucoadhesive agents alone have had limited success in increasing oral bioavailability of drugs of weight larger than the permeability limit of 20 kDa.

Enteric capsules are currently widely used as delivery vehicles for small molecules. They dissolve when triggered by a certain pH range, and dissolve once this trigger has been reached. As such, enteric capsules release drug in the desired region of the GI tract based on the absorption profile of the drug in question. However, once large molecule drug product is released, it is susceptible to attack by the enzymes in the luminal space and is not aided in absorption. Furthermore, the pH variability between humans leads to unpredictable dissolution of enteric capsules. This leaves enteric capsules unable to increase the oral bioavailability of large molecules alone.

Finally, other formulation techniques aimed at encapsulation of the drug product to increase absorption, such as nanoparticles, microspheres, liposomes, and emulsions, aim to protect drug product against degradation, control its release rate, and target drug delivery to specific cells. For example, many of these systems target the Peyer's patches of the small intestine, that show increased ability to absorb many types of materials (Mitragotri, Burke, & Langer, Overcoming the challenges in administering biopharmaceuticals: formulation and delivery strategies, 2014). However, formulation strategies have only increased the oral bioavailability of biologics by 1-2% (Langer & Traverso, 2017).

3.2.2 Drug modifications

Prodrugs are pharmacologically inactive chemical derivatives of a parent drug that requires transformation within the body to become therapeutically active (Hamman, Enslin, & Kotze, 2005). However, these types of drugs are difficult to design and manufacture due to the increasing complexity of the drug as its molecular weight increases and its structure becomes more difficult to fully comprehend.

Other structural modifications such as the addition of PEG groups (PEGylation) and lipidization via the conjugation of fatty acid polypeptide groups have also been attempted (Hamman, Enslin, & Kotze, 2005). However, chemical modifications such at mutagenesis, glycosylation, PEGylation and prodrugs have only increased the bioavailability of oral biologics by 1-2% in comparison to ingestion of the unmodified drug substance (Langer & Traverso, 2017).

Direct chemical modification is unable to become a platform technology unless incorporated at the protein engineering stage of research and development. Given the nature of this investigation from the device group, chemical drug modifications are not widely considered in the following sections, although there is some promising research in this area.

3.2.3 Robotic pills

Robotic pill technologies have been researched and manufactured to act as a non-dissolvable enteric coating. In general, the robotic pill holds a payload of large molecule drug product in liquid form, and releases the drug product within the GI tract once it receives a signal. This signal could either be internally sourced from the biology and anatomy of the GI tract (e.g. a pH change) or it could be externally sourced from a wireless transmitter.

Examples of these types of robotic pills include: Intellicap, Pulsincap, Intelisite®, and capsules in research stages from the University of Kentucky, the Battele Institute in Germany, Vanderbilt University, Imperial College London, and Harvard (Mapara & Patravale, 2017). External activation can occur through wireless signal transmission after tracking via gamma scintigraphy, radio frequency trigger, and magnetic forces,

while internal activation can occur through sensing of pH, temperature, or other biological changes (Mapara & Patravale, 2017).

Even though these capsules protect drug product during transportation through the stomach and release drug product in the best location optimal for delivery, they do not, by themselves, aid in the absorption of drug product across the epithelial barrier. By passively releasing the drug product into the lumen of the small intestine, drug product is still susceptible to proteolytic activity and poor absorption, ultimately leading to low bioavailability. This makes passive robotic pills unsuitable for delivery of large molecules biologics.

3.3 Three Main Challenges:

In summary, there are three main challenges associated with oral delivery of large molecules: overall lack of systemic bioavailability, clinical relevance of delivered dose, and long term safety.

3.3.1 Lack of Bioavailability

Recall, bioavailability is defined as the proportion of active drug substance that enters into systemic circulation when introduced into the body and so is able to have an effect on the intended condition. There are many issues when drug is delivered via an oral route that could potentially disrupt the bioavailability of the active drug substance, including but not limited to:

- pH denaturation (GI only)
- enzymatic degradation
- inability to access epithelium due to mucus lining
- inability to cross the epithelium due to poor absorption

All of these phenomena combine to yield poor bioavailability for large molecule when delivered via the sublingual, buccal, or GI routes. While techniques have been developed to effectively protect the drug product against pH denaturation and enzymatic degradation, solutions to address the poor absorption across the mucus and epithelial linings have not yet been full realized.

3.3.2 Clinical Relevance for GI delivery

Many large molecule drugs require a large dosage to achieve their desired effect – specifically antagonist type drugs, which blocks or dampens a biological response by binding to and blocking a receptor. Agonist type drugs work in reverse – they turn on or activate a response, and thus require a smaller amount of drug product to activate the intended mechanism. Two of the top-20 selling drugs in the world in 2016 were Amgen's Enbrel and Neulasta (Philippidis, 2017). Enbrel® is an antagonist, with a recommended dosage of 50 mg once a week (Amgen, Inc.), while Neulasta® is an agonist, with a dose of 6mg taken 27 hours after completion of chemotherapy (Drugbank, n.d.). In comparison of these two drugs, the dosage size difference between agonists and antagonists is clear.

Given that many large molecules drugs tend to be antagonists, in order for oral administration of biologics to succeed, a clinically relevant dose must be delivered at a favorable dosing frequency for the patient. Recall in section 2.1.1, limited dosing frequency was the reason some patients preferred injectable to oral

medications. Therefore, enough drug product needs to be delivered in a single dose so as not to increase the dosing frequency to the point where an injectable formulation is preferred.

Video capsule endoscopes (VCEs) have been widely used for non-invasive imaging of the GI tract, and represent an upper boundary to the size of pill that can be swallowed by humans. Measuring 11mm by 26mm, these video endoscopes have a total volume of 2.5mL, and a retention rate of 1.3% (Langer & Traverso, 2017). This retention rate is high for a pill that is taken frequently, especially if the pill is taken over the course of a lifetime for chronic illnesses. Studies have also been done on the OROS system, an extended drug release capsule that leaves an indigestible shell measuring 9mm x 15mm, with a total volume of 0.95 mL (Langer & Traverso, 2017). The retention rate with the OROS system is only 1 in 29 million, which is much less than that with the VCEs, and represents a size that is safe to take frequently, even for daily use (Langer & Traverso, 2017). The comparison is summarized in Table 3-2.

Table 3-2 Details of Two Different Ingestible Pill Systems

	Outer Diameter (mm)	Length (mm)	Approximate Total Volume (mL)	Retention Rate (%)
VCEs	11	26	2.47	1.30%
OROS System	9	15	0.95	0.00%

While retention is a risk, an estimated 16 million people in the U.S. also have difficulty swallowing, called dysphagia (Robbins, Langmore, Hind, & Erlichman, 2002). Studies have found that 54% of people have difficulty swallowing solid medication, and of those patients 20% of patients responded that it was due to pills that were too large (Fields, Go, & Schulze, 2015). This study also cited that extra-large pills were particularly detested, with 4 out of 5 study participants preferring to take 3 or more medium-sized pills instead of a single jumbo pill (Fields, Go, & Schulze, 2015).

Therefore, there is a balance that needs to be achieved for GI delivery between pill size and drug payload. This means that for any large molecule drug product that is considered for delivery via the oral GI route, careful study of the pharmacokinetics will need to be conducted to ensure that the proposed dosage and dosing frequency allow patients to keep plasma drug levels within the effective therapeutic window. Furthermore, more concentrated formulations of drug product will need to be considered in order to further increase the payload within the limited size constraint of the drug product.

3.3.3 Safety

Finally, the safety of patients is of the utmost concern when developing new systems for drug delivery. Given the dubious safety record of permeation enhancers and other methods for delivering drug product via an oral route in the past, the methods considered must be safe when taken frequently. The long-term effects of taking a therapy via an oral route and the immune response from any absorption enhancers must be well understood and characterized prior to use as platform delivery method.

3.4 Summary

This chapter discussed the relative benefits of the three routes for oral drug delivery: buccal, sublingual, and GI. While the GI route is traditionally more accepted by and familiar to patients, it poses challenges due to pH variability, the mucus coating protecting the epithelial barrier, and the tight-junctions and harsh enzymatic environment. The buccal and sublingual routes are decidedly less familiar to patients, but offer a more amenable environment to delivery and allow for avoidance of tight-junctions and first-pass metabolism.

Historical attempts of oral drug delivery were also discussed. Formulation strategies consisted of permeation enhancers, protease and enzyme inhibitors, mucoadhesive additives, and enteric capsules. However, none of these strategies were able to successfully increase the bioavailability of large molecule drugs, either due to concerns over toxicity and other health-effects, or due to ineffectiveness. Drug modifications have been historically used to alter the chemical structure of a drug in order to increase its bioavailability. However, the relative increases in bioavailability were small, and would require direct modification of chemical structures of each drug in the pipeline, disenabling it as a platform approach. Finally, robotic pills offer an interesting alternative to drug delivery by encapsulating drug product and releasing it upon the receipt of a signal. However, this approach leaves drug product susceptible within the lumen of the GI tract, as robotic pills historically do not aid in the absorption across the epithelial barrier.

Finally, the three main challenges of oral drug delivery of biologics were summarized. The first, lack of bioavailability, revolves around the issues encountered when a drug is delivery via an oral route, including pH denaturation, enzymatic degradation, and the barriers of the mucus and epithelial barriers leading to poor absorption. Without a high bioavailability, an oral route will not be feasible as a delivery option for large molecule drugs. The second challenge, clinical relevance for GI delivery, refers to the fact that many large molecule drugs are agonists and require a relatively large dosage to achieve the intended therapeutic effect. This volume is limited by what the human body can swallow, as detailed in Table 3-2. The third challenge, safety, indicates that any oral delivery option needs to be safe for the patient in the long-term. In light of historical attempts, any means to increase absorption needs to be fully understood and characterized prior to use.

Chapter 3 laid the groundwork upon which new technologies could be sourced. By understanding the historical barriers to oral drug delivery, consideration can be placed on new technologies as to how they solve the problems of the past.

Chapter 4 Technology Landscape of Emerging Oral Delivery Methods of Large Molecules

The technology landscape was the last activity remaining in Phase 1 of the project, where the technical approach to Novel Oral Drug Delivery was planned (see Figure 2-2).

In Chapter 4, the methodology and results of the technology landscape are discussed. The chapter further details specific technologies highlighted in the landscape, including novel device-based, hydrogel, and formulation-based technologies.

4.1 Methodology for Technology Landscape

Once the biological barriers and historical attempts of oral drug delivery were researched and understood, a broader technology landscape of current technologies was pursued. The technology landscape was performed in order to understand the current state of research from academic institutions and startup companies in the space of novel oral delivery of biologics.

The literature review into the historical barriers allowed for preliminary criteria for inclusion in the technology landscape, to include technologies that were able to overcome the challenges of low bioavailability, clinical relevance of dose, and safety. Priority was given to technologies able to overcome the issue of low bioavailability. While the issues of clinical relevance and safety are challenges that warrant investigation, these two require further clinical study once a specific technology and drug candidate are chosen. For example, studies of long term damage and the pharmacokinetics require delivery of the drug with the chosen technology in the animal model of choice.

The landscape was performed through a number of different forums. A literature search was completed using combinations of keywords including, but not limited to: oral, gastrointestinal, buccal, sublingual, peptide, protein, monoclonal antibody, biologic, macromolecule, bio-therapeutic, and delivery. Online forums such as FiercePharma were monitored for updates related to oral drug delivery of large molecules. Websites of academic institutions thought to be working on relevant topics were consulted, and contact made with pertinent professors when warranted. Additional sources included attendance at the Partnerships on Drug Delivery (PODD) conference and interviews conducted with Amgen employees and LGO internship advisors.

Due to the device-based nature of the group the LGO student interned with (ADT&I), and the LGO student's past experience with medical devices, priority was placed on sourcing device-based solutions. However, during the landscape review, novel formulation, hydrogel, and other techniques were also captured for further review and shared with the appropriate groups within Amgen's organization.

4.2 Results

This methodology allowed for the sourcing of 86 different technologies. While not all of the technologies were current or fully developed, they allowed for a more complete documentation of the different attempts made to deliver large molecules via an oral route.

Of interest, upon follow up with academic institutions that had published in the space in the past ten years, the author discovered that many projects were discontinued due to lack of interest or funding. Furthermore, there has been an emphasis on the GI delivery route, opposed to the buccal and sublingual routes. Most of the work that is done in the buccal and sublingual space is around the formulation of sprays, patches, films, and gels, rather than on device based solutions. Devices designed for the sublingual

and buccal route, with one exception, are for the delivery of sprays that were purposely reformulated for the oral mucosa route.

The technologies were then split into three different categories: device based, hydrogel based, and formulation based technologies. These three categories were then further segmented by the route of delivery pursued. Figure 4-1 is an illustrative depiction of some representative technologies and how they were categorized based on the method and location of delivery.

In the sections below, pertinent technologies from each category are described in greater detail. Although 86 technologies were sourced, not all technologies will be discussed in the sections below.

Figure 4-1 Segmentation of Technology Landscape by method and location of delivery

4.2.1 Device-Based

As mentioned above, device based technologies were prioritized during the technology landscape due to the LGO's previous experience and the device-based nature of ADT&I. As indicated in Figure 4-1, device-based technologies indicate drug product is packaged into a device and delivered to the site of action via mechanical means. There were multiple technologies sourced in this area, and a few are highlighted below.

4.2.1.1 MIT Microneedles

The *MIT Microneedles* device for GI delivery takes advantage of the lack of pain receptors in the GI tract and features 25G hollow microneedles that protrude from a drug reservoir (Traverso, et al., 2015). Once the device reaches the small intestine, the pH triggered enteric capsule dissolves exposing the microneedles, and upon the peristaltic contractions of the small intestine, injects drug product into the wall of the small intestine. A solid microneedle filled with solid drug product was also conceptualized, and would similarly deploy via peristaltic motion. Both concepts are showcased in Figure 4-2. These technologies were in the prototyping stage at the time that the paper was published, and no clinical studies were performed with the devices themselves.

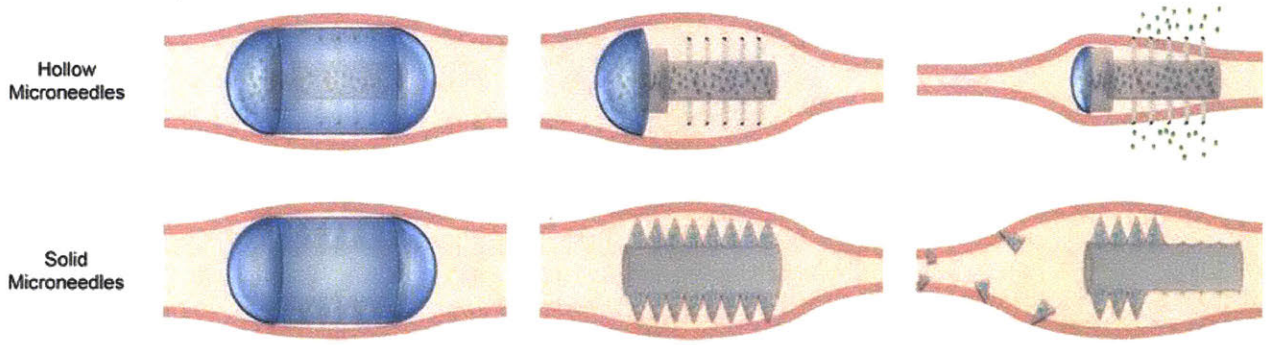

Figure 4-2 MIT Microneedles - Hollow and Solid Microneedle Concepts (Traverso, et al., 2015)

4.2.1.2 UC Berkley Mucojet

UC Berkeley's *Mucojet* device provides options for both buccal and GI delivery. In the one paper published, the buccal version of the device is described (Aran, Chooljian, Parades, Rafi, & Liepmann, 2017). The device features an interior and exterior component that are snapped together to activate the device. The interior component features a power reservoir filled with sodium bicarbonate and citric acid (otherwise known as baking soda) separated by a piston from the drug reservoir containing liquid drug product. The exterior component features a water reservoir. Upon clicking the two components together, the water enters into the power reservoir, reacts with the baking soda to generate CO_2, and pushes the piston forward. The piston then ejects the liquid drug product from the single nozzle of the Mucojet device at a velocity of approximately 50-200 mm/s (Aran, Chooljian, Parades, Rafi, & Liepmann, 2017). The patient has approximately 10 seconds after clicking the two compartments together to place the Mucojet on the inside of the cheek prior to device deployment. Figure 4-3 (a) describes the assembly of the Mucojet device, while (b) and (c) depict the mechanism of action of the device. Delivery of vaccine (ovalbumin-45 kDa) in rabbits yielded favorable antibody production, 7x greater than vaccine delivered orally via solution only (Aran, Chooljian, Parades, Rafi, & Liepmann, 2017). This device does not deliver through the epithelial barrier of the buccal mucosa, but deposits the drug on the epithelial lining itself (Figure 4-3 b). Due to the lack of tight junctions in the buccal epithelium as described in section 3.1.1, ovalbumin (45 kDa) was able to permeate through the epithelial barrier for systemic uptake, evidenced by the production of anti-ovalbumin antibodies.

The Mucojet for GI delivery is still in the conceptualization and prototyping stages from the Liepmann lab at UC Berkeley. It grew out of the buccal version of the delivery device, described in a 2015 paper from the lab (Aran, Chooljian, Parades, Rafi, & Liepmann, 2017). The GI version of the device was proposed in a presentation given by Professor Liepmann at the Medical MEMS and Sensors conference in 2017

(Liepmann, 2017). Instead of placing the device against the side of the cheek, it is swallowed by the patient to deliver drug product directly to the small intestine.

Similar to the buccal version, the version for GI delivery is a capsule that contains a power reservoir, a piston, and a drug reservoir. The power reservoir contains a powdered mixture of sodium bicarbonate and citric acid (baking soda), while the drug reservoir contains the liquid drug product for delivery (Liepmann, 2017).

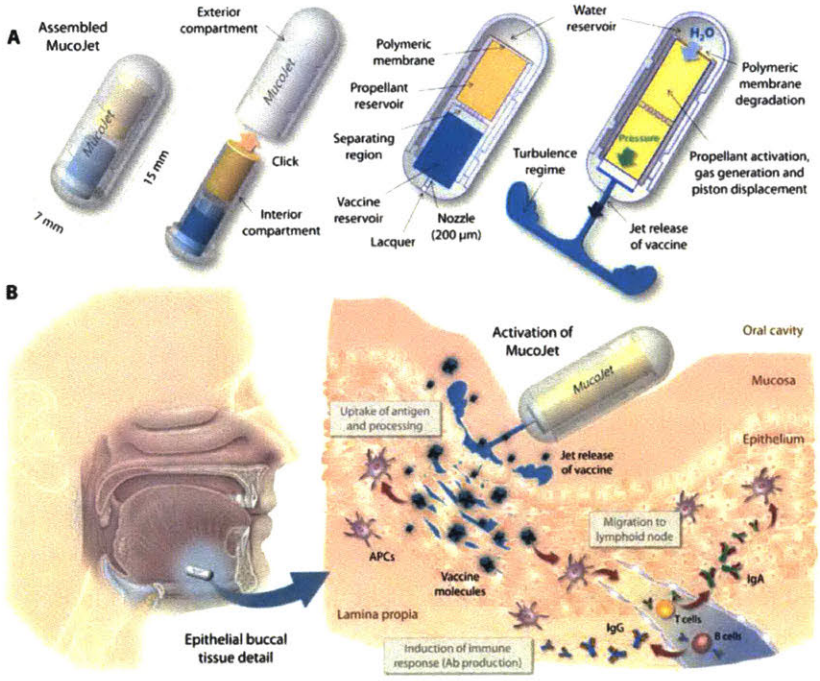

Figure 4-3 Schematic overview of the Mucojet oral, needle-free immunization strategy. Adapted from (Aran, Chooljian, Parades, Rafi, & Liepmann, 2017)

The pH valves located within the region of the power reservoir selectively open in the presence of the pH of the small intestine, which resides between a pH of 6-7.5 (Langer & Traverso, 2017). The valves then allow the luminal fluid containing water to enter into the power reservoir, allowing the propellant to react to produce carbon dioxide (CO_2). The CO_2 drives the pressure in the pill up until the threshold pressure of the nozzle is reached, which is determined by the plug used to cap the nozzle. Once the threshold pressure is met, the nozzles open, the piston moves forward, and the drug product is ejected out of the Mucojet device.

In publicly released testing, the Mucojet underwent early tests to understand how the drug passed through the digestive system of rabbits (Liepmann, 2017). Testing indicated that the Mucojet device was able to pass safely through the rabbit without signs of discomfort, and was excreted 30 hours after ingestion (Liepmann, 2017). However, the drug delivery experiments were unsuccessful due to a couple of factors. Because rabbits are ruminants, their digestive systems vary significantly in function and pH from humans, which is what the system was designed for (Liepmann, 2017). Furthermore, because the transit time through the various organs varied between 1 and 20 hours, the researches had no idea when

the material would actually be delivered, and did not know at which time points to check for the drug concentration levels within the blood plasma (Liepmann, 2017). Of note, the drug product used for these initial tests was not revealed.

However, in *ex vivo* testing with pig intestinal tissue in a Boyden Chamber, drug product showed favorable movement across the intestinal epithelium. Although the drug product was not explicitly stated, it can be assumed to be large molecule drug, due to the nature of the talk given by Professor Liepmann. Drug product was delivered with the Mucojet device across the intestinal tissue and also dropped on the surface of the intestine as a control. The concentration of drug product left on the luminal side of the tissue was then measured and compared for the two methods of delivery. Figure 4-4 shows the results of these experiments, indicating that delivery with the Mucojet Device significantly increases the amount of drug product that transports across the epithelium, thus increasing its chance of reaching systemic circulation.

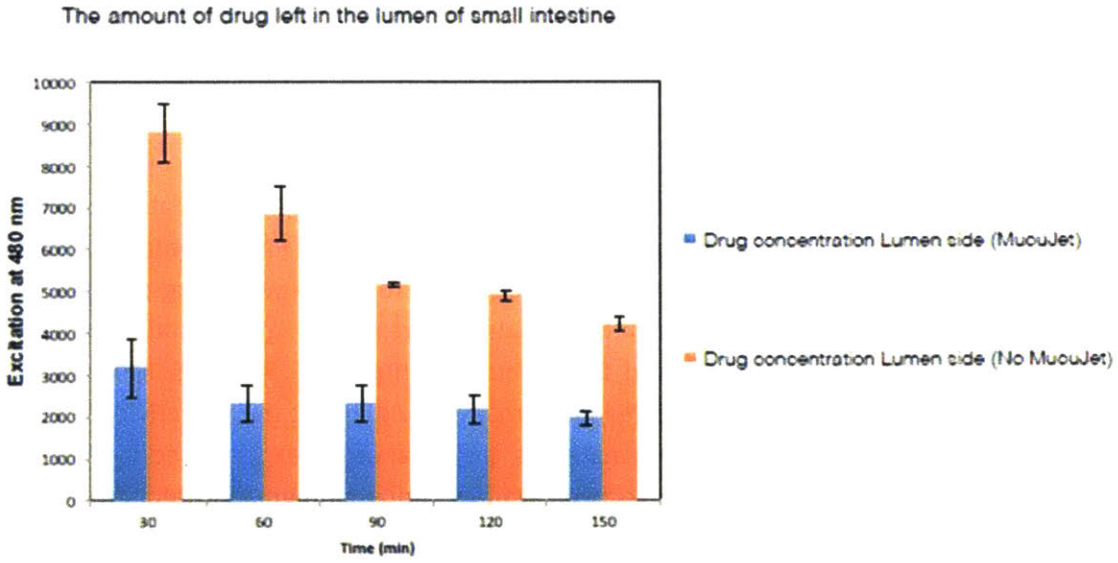

Figure 4-4 Ex Vivo Delivery with Mucojet across Small Intestinal Tissue in Boyden Chamber indicated less drug product was left in lumen when delivered with Mucojet (blue) than without the device (orange). Adapted from (Liepmann, 2017).

4.2.1.3 Rani Therapeutics Pill

Rani Therapeutics, a startup with 31 issued or allowed patents, 110 patent applications filed, $85 million in raised funding initially was founded at inCube Labs, a multi-disciplinary life sciences R&D lab focused on developing breakthrough medical innovations (Rani Therapeutics, 2017). The CEO, Mir Imran, also leads inCube labs, and has founded more than 20 life sciences companies and holds more than 400 issued and pending patents in the US. The investors within Rani Therapeutics include big names such as Novartis, AstraZeneca, Google Ventures, inCube Ventures, Venturehealth.com, KPC, Buttonwood, and Alpha Fund (Rani Therapeutics, 2017). In late 2017, Shire also announced an equity investment in Rani, with the option to negotiate a licensing deal to develop and market the Rani platform for hemophilia drugs (Reuters, 2017).

The *Rani* Pill™ technology involves an enteric coated capsule that contains a cellulose balloon attached to dissolvable microneedles formulated with solid drug product and sugar (Imran M. , 2016) (United States Patent No. US 8.846,040 B2, 2014). Once the capsule reaches the small intestine, the pH change triggers the dissolution of the enteric capsule, and water enters into the device to react with sodium bicarbonate and citric acid. This reaction then produces CO_2 which fills the balloon, and injects the dissolvable microneedles into the wall of the small intestine (Rani Therapeutics, 2017). The rest of the device then detaches from the microneedles and passes through the GI tract. This process is illustrated in Figure 4-5.

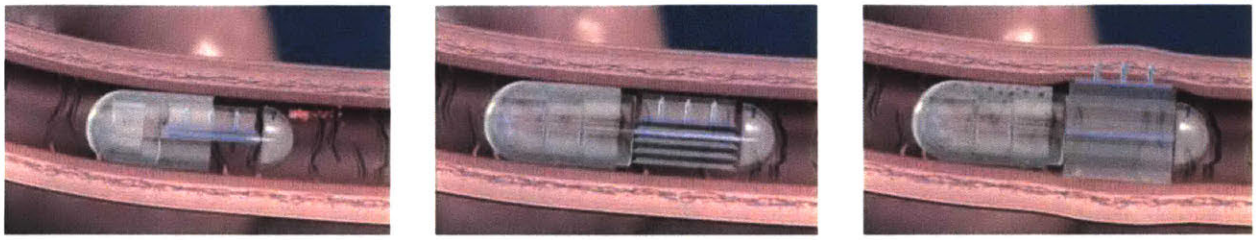

Figure 4-5 As it travels through the GI tract, the capsule remains intact (left), until the pH increases to 6.5/7.0, at which point the capsule dissolves, activating the chemicals within the capsule which react to release CO_2 and begin to inflate the balloon (middle). As the balloon becomes fully inflated, the drug-loaded needles are delivered into the intestinal wall (right). (On Drug Delivery, 2015)

Rani has focused a lot of effort into the formulation of drug product into microneedles able to penetrate the lining of the small intestine. The assumption is that the microneedles are likely created via a process known as hot-melt extrusion, where low-melting point polymers are mixed with drug product in high concentration to create solid forms of drug product. The materials are melted, mixed, and forced through a die or molded in order to achieve the desired form factor (Montenegro-Nicolini & Morales, 2017). Although historically successful for small molecules, this process could inhibit the bioactivity of biologics due to the high temperature needed to melt the materials, the shear stress experienced by the delicate biologic during molding, and the potential for recrystallization during storage (Montenegro-Nicolini & Morales, 2017).

However, if this process is successful, the solid dosage form allows for maximization of the amount of drug product in the small volume of the pill, with up to 3-5 mg of large molecule drug able to be incorporated (Imran M. , 2016), (United States Patent No. US 8.846,040 B2, 2014). Furthermore, Rani claims that the dosage form increases shelf-life and stability of the drug, even in the face of recrystallization effects from hot-melt extrusion.

Finally, the microneedles allow for avoidance of metal needles, which would not be patient-friendly for ingestion. However, despite the lack of metal needles, the pill is currently a triple 000 capsule size, measuring 26mm in length and 11mm in outer diameter (Imran M. , 2016). This size is rather large, and violates the assumptions for daily usage indicated in section 3.3.2 regarding pill size. Considering that not all components of the Rani pill are biodegradable, a portion of the pill is still passed through the body, and poses a risk of retention

In animal testing, the CEO has stated that the Rani Pill™ achieves successful deployment of microneedles 95% of the time, with the failures attributed to manufacturing defects that can be overcome with further

process refinement (Imran M. , 2016). In their introduction deck for the 2017 JPM conference, Rani has claimed the successful delivery of two commercial drugs with 100% equivalence to injections in pre-clinical trials (Rani Therapeutics, 2017). However, the data for these claims have not been presented in a public forum, and therefore rely on the word of the company itself.

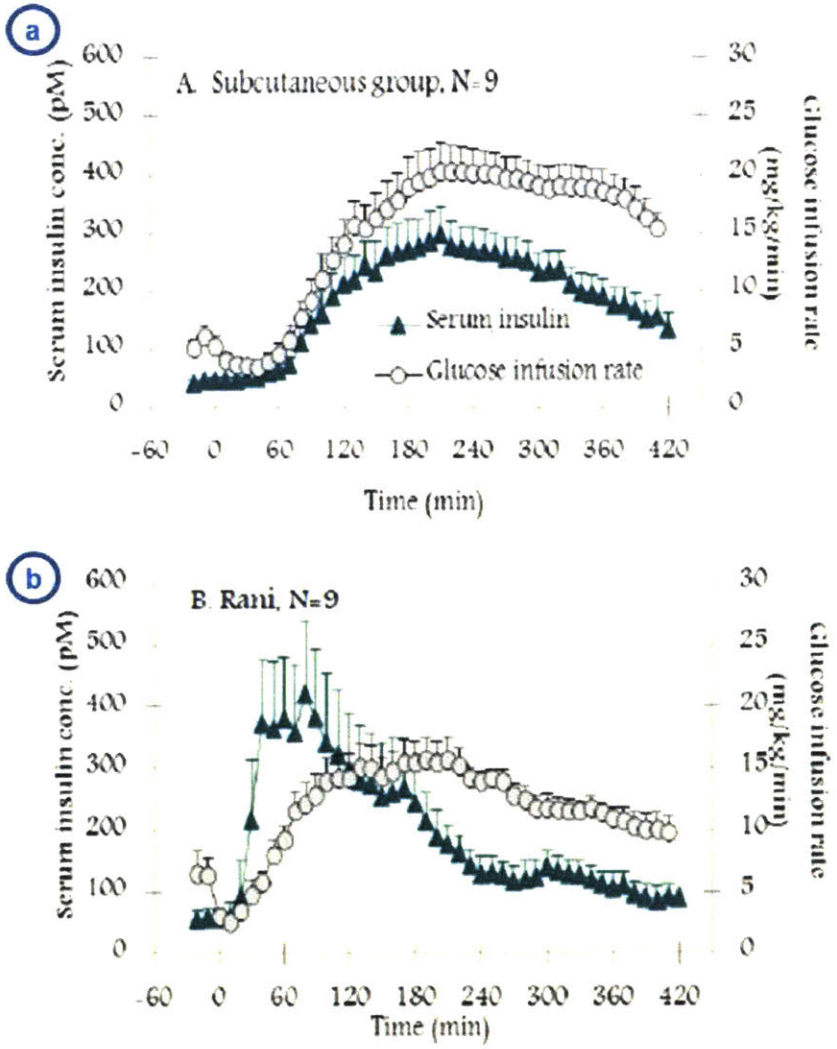

Figure 4-6 Insulin infusion to Yorkshire Pigs using (a) SC Injection and (b) Rani Pill™. Adapted from (Rani Therapeutics, 2017).

Studies comparing the pharmacokinetic profile of insulin delivered with SC injection and the Rani Pill™ to anesthetized, juvenile Yorkshire Pigs under a euglycemic glucose clamp were done to compare the relative effectiveness of the two delivery modes (Rani Therapeutics, 2017). The pharmacokinetic profiles of these two delivery methods are depicted in Figure 4-6. At t=0, 20 units of fast-acting human insulin was delivered either via a SC injection (n=9) or intra-jejunely via autonomously deployed Rani capsules (n=8). Each graph shows the change in serum insulin (green) over time after injection, determined using the ELISA method, and also the gluclose delivered via the euglycemic clamp (grey). In (b), the insulin experiences a more rapid uptake into blood circulation, potentially due to the rapid uptake of the peptide from the highly vascularized wall. Overall, these results indicate that delivery of insulin is just as effective with the Rani platform as with SC injection, considered the gold standard. However, insulin is only a

peptide, and Amgen's products have higher molecular weights than insulin. Furthermore, information regarding how the capsules reached the small intestine and the dosage levels in the SC injection vs. the Rani Pill™ were not explicitly stated.

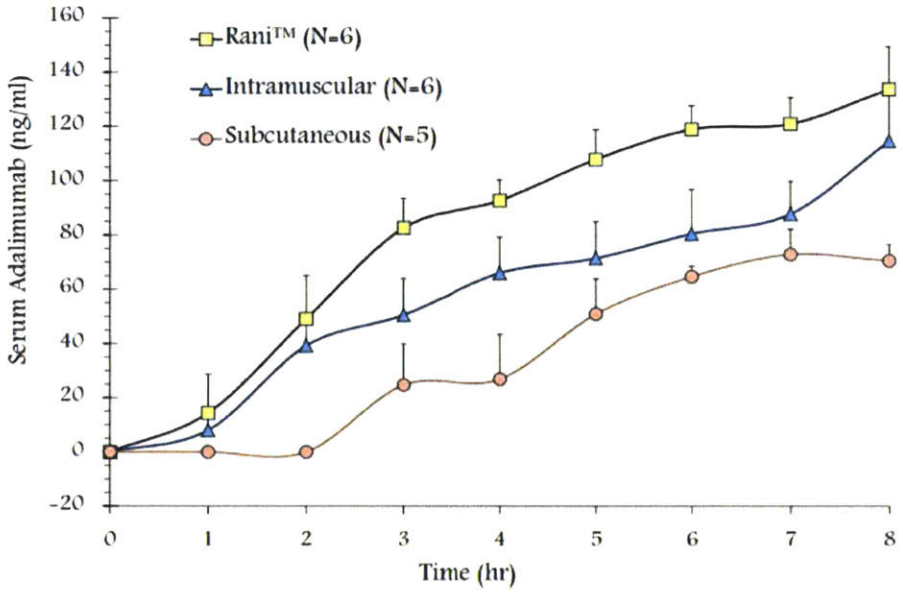

Figure 4-7 Comparison of PK profiles after injection of adalimumab via delivery with Rani(TM), Intramuscular, and Subcutaneous injection (Rani Therapeutics)

Testing of the Rani Pill™ in pig studies have also shown favorable results when compared to intramuscular and subcutaneous administration of adalimumab, a drug with a similar mechanism of action and molecular weight to Enbrel®. As seen from Figure 4-7, depicting the pharmacokinetic (PK) data for adalimumab when delivered via the three different routes of delivery, delivery via the Rani platform achieves a higher blood concentration than with IM or SC routes (Rani Therapeutics). If the same dose was delivered via each of the three systems, this data is very promising, as it would suggest comparable bioavailability between the Rani Platform and traditional routes of administration.

4.2.1.4 UCSF Nanostraws

Tejal Desai's lab at UCSF has also focused on the development of alternative methods to deliver drug product via an oral route. One of those technologies, the *Nanostraw Microdevices*, include circular

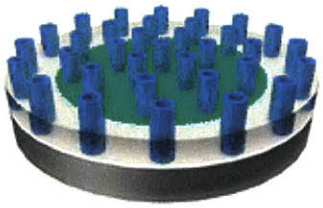

Figure 4-8 Nanostraw Microdevices featuring a circular base with nanostraws containing drug reservoirs on one surface. Adapted from (Fox, et al., 2016)

patches that feature nanostraws on one surface, with drug product loaded in the reservoir of each nanostraw (Fox, et al., 2016). Figure 4-8 includes an illustrative depiction of the device. The devices are intended for delivery to the small intestine via an enteric capsule, where the patches are released and adhere to the lining of the GI tract for release of drug at high local concentrations (Fox, et al., 2016).

4.2.1.5 Other Device Based Technologies

Besides these three platforms, other technologies sourced and considered for GI delivery included artificial micromotor research from UCSD Department of Nanoengineering and ultrasound technology, described in further detail below. For buccal delivery, other technologies sourced included nanotopography microneedle devices from the Desai lab at UCSF.

Although not strictly an oral delivery route, ultrasound technology for large molecule delivery was also considered. This technology, originally out of the MIT Langer lab and spun out into the startup SuonoBio, aims to use low frequency ultrasound to induce cavitation (bubbling) within the colon (Schoellhammer, et al., 2015) (Schoellhammer, et al., 2017). The bubbles become unstable and implode, creating a void that fluid rushes into, generating a microjet which aids in absorption of drug product across the epithelial lining of the colon (Schoellhammer, et al., 2017). Testing in pigs and mice led to increased uptake of insulin, dextran, and siRNA, all molecules greater than 1000 Da (Schoellhammer, et al., 2015) (Schoellhammer, et al., 2017). However, the ultrasound and drug product are currently delivered via a rectal route of administration, although plans in the future could involve miniaturization of the ultrasound into a pill form factor for oral delivery (Schoellhammer & Traverso, Low-frequency ultrasound for drug delivery in the gastrointestinal tract, 2016).

4.2.2 Hydrogels

Although hydrogels were not prioritized, hydrogel technologies were prevalent throughout the course of the literature review. As indicated in Figure 4-1, hydrogel based technologies mix drug product with a cross-linked polymer matrix for delivery. This polymer matrix can have unique properties depending on the type of polymer used to construct it. There were multiple technologies sourced in this area, and a few are highlighted below.

Hydrogels for oral delivery present an interesting body of work. Most hydrogels use swelling properties to fill the space within the small intestine and localize the drug product to the wall in order to create a local concentration gradient to increase absorption. Other hydrogels incorporate mucoadhesive polymers in a similar attempt to localize to a single spot on the small intestinal wall to increase absorption.

Most hydrogels that were considered were in the academic research stage from universities such as Ohio State, MIT, and UT Austin. A couple of the interesting findings from the Technology Landscape are discussed in further detail below.

The Peppas lab from UT Austin focuses on complexation hydrogels made with Poly(methacrylic acid) grafted with PEG (P(MAA-g-EG)) that are loaded with drug product via equilibrium partitioning (Carillo-Conde, Brewer, Lowman, & Peppas, 2015). The hydrogels constrict in low pH environments, such as the stomach, protecting drug product from the acid and enzymes within the stomach fluid. The hydrogel swells in neutral pH environments, such as the small intestine. When swollen, the hydrogel fills the lumen

of the small intestine and drug product can diffuse out of the hydrogel towards the epithelial barrier without contact with proteolytic enzymes. *In vitro* experiments confirmed that bioactivity of Anti-TNF-α

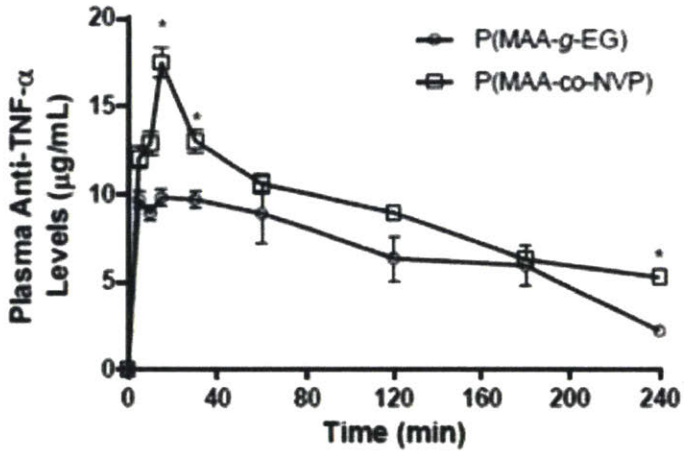

Figure 4-9 Bioavailability of anti-TNF-alpha antibody upon release from hydrogel microparticles. Plasma anti-TNF-α levels versus time profiles following direct injection of anti-TNF-α loaded P(MAA-g-EG) microparticles (n = 6) into an intestinal closed-loop in healthy adult Sprague-Dawley rats. Blood samples were then taken at 5, 10, 15, 30, 60, 120, 180, and 240 min. The dose of anti-TNF-α loaded into microparticles was 70 μg/kg body weight. Anti-TNF-α mAb concentration in diluted serum was measured by ELISA (Carillo-Conde, Brewer, Lowman, & Peppas, 2015)

antibodies were preserved when encapsulated in the hydrogel and subjected to conditions similar to those in the GI tract (Carillo-Conde, Brewer, Lowman, & Peppas, 2015). *Ex vivo* experiments were conducted by injecting hydrogel micro particles loaded with Anti-TNF-α into the intestine of Sprague-Dawley rats and subsequent monitoring of the blood plasma levels of the antibody (Carillo-Conde, Brewer, Lowman, & Peppas, 2015). These results, also seen in Figure 4-9, indicate that there was some permeation of the drug product into systemic circulation following administration of the hydrogel microparticles. Of note, the data from the control group consisting of subcutaneous administration of the same dose of antibodies was not presented in the paper, making a comparison between the relative bioavailability of the hydrogel and SC injection impossible.

While the hydrogels from the Peppas lab are one example of hydrogels for GI delivery, self-folding hydrogels that adhered to the mucus lining of the small intestine from Ohio State (He, Guan, Lee, & Hansford), and trigger-able hydrogels that reside in the stomach were also considered for GI delivery (Liu, et al., 2017). For buccal and sublingual delivery, Aegis Hydrogel™ technology utilizing self-assembling aqueous hydrogels with extended residence time (Aegis Therapeutics, LLC, n.d.) were also included in the technology landscape.

4.2.3 Novel Formulation Approaches

Although hydrogels were not prioritized, formulation technologies were also prevalent throughout the course of the literature review. In Figure 4-1, formulation based approaches are defined as those where drug product is conjugated or encapsulated to or in nanoparticles, microparticles, and liposomes, or are delivered with a cocktail of permeation enhancers and enzyme inhibitors. In addition to this definition, this category acted as a "catch-all", where technologies that didn't necessarily fit into either the device or hydrogel category were placed.

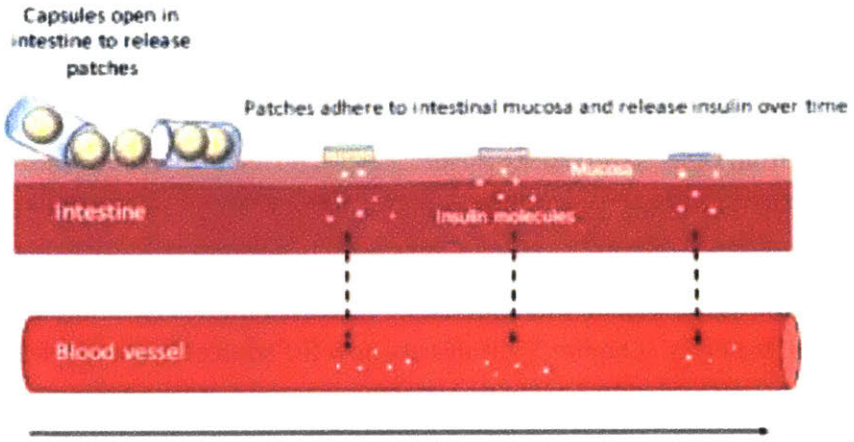

Figure 4-10 Schematic representation of mode of action of oral devices. Mucoadhesive patches are released from enterically coated capsules in the intestine where it adheres to the mucosa and releases insulin over time (Banerjee, Lee, & Mitragotri, 2016)

One such example of that type of technology is that from *Entrega Bio*, a startup in the Cambridge, MA area, which is a combination of a device and formulation play. The startup further developed technology from the Center for Bioengineering at UCSB. The technology consists of mucoadhesive patches that are released from an enterically coated capsule upon movement into the small intestine (Banerjee, Lee, & Mitragotri, 2016). The mucoadhesive patches consist of a mixture of mucoadhesive polymers, insulin, and dimethyl palmitoyl ammonio propanesulfonate (PPS), a studied permeation enhancer (Banerjee, Lee, & Mitragotri, 2016). Once released from the pH sensitive enteric capsule, patches adhere to the mucous layer of the intestine, swell, and release their drug load over time through dissolution of the patch (Banerjee, Lee, & Mitragotri, 2016). All but one side of the patch is coated with a water-impermeable coating, allowing for unidirectional release of the drug (Banerjee, Lee, & Mitragotri, 2016). The mode of action is illustratively depicted in Figure 4-10. The patches allow drug product to surpass the harsh environment of the stomach, and through adhering to the mucus of the small intestine and use of a permeation enhancer, increase the concentration gradient and absorption of insulin into systemic circulation (Banerjee, Lee, & Mitragotri, 2016). While the PK effects were comparable between subcutaneous and oral administration of the drug, the oral drug was given at a dosage level 50-100 times higher than the subcutaneous injection (Banerjee, Lee, & Mitragotri, 2016).

Other formulation technologies considered for GI delivery included those developed by AMT (AMT, n.d.), EnteraBio's platforms (EnteraBio, n.d.), Proxima Concepts (Proxima, n.d.), Ovensa (Ovensa, n.d.), ThioMatrix (ThioMatrix, n.d.), Phloral® by IntractPharma (IntractPharma, n.d.), and Peptelligence by Tarsa Therpeutics (Tarsa Therapeutics, n.d.).

4.3 Summary

Chapter 4 presented the methodology for the technology landscape, which consisted of sourcing technologies through academic journals, online forums, patents, conference attendance and consultations with advisors and colleagues.

The results of the technology landscape were segmented into device-based, hydrogel-based, and formulation-based strategies. Promising device technologies using novel mechanisms for drug absorption included the MIT Microneedle, Rani Therapeutics Auto-Pill, UC Berkeley Mucojet, and UCSF Nanostraws. Hydrogels using swelling properties to protect drug product were also considered, including technologies from Ohio State and UT Austin. Finally, novel formulation approaches such as the technology from Entrega Bio were considered, as a mix between a device and formulation approach to drug delivery.

The technology landscape cast a wide net to understand the vast varieties of technologies to consider for oral drug delivery of biologics. Chapter 5 will discuss how the sourced technologies are pruned down to those most likely to be applicable to Amgen's portfolio.

Chapter 5 Down-Selection of Delivery Methods

Once the technology landscape was completed and Phase 1 of the project was concluded, Phase 2, or "Technology Convergence" commenced (see Figure 2-2 below). In the down-selection activity in this phase, technologies needed to be filtered down to a couple of top-priority technologies for Amgen to further pursue.

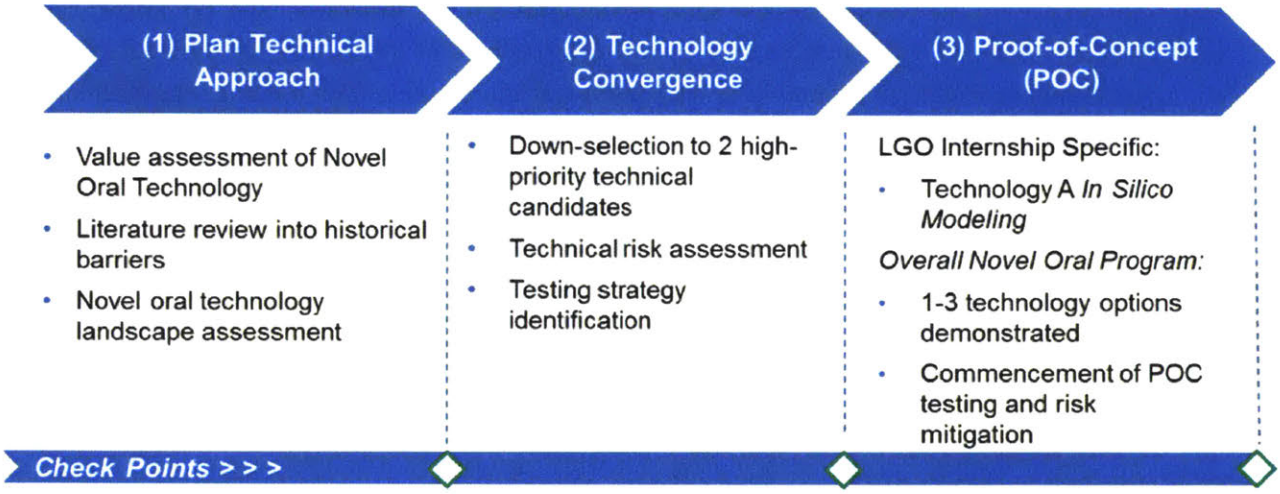

Figure 2-2 (repeated): Project Approach for Novel Oral Program

This chapter details the methodology and results of the down-selection process. The down-selection process consists of two stages: a first- and second- pass filter. The first-pass filter intended to prune the field based on the ability to add value to Amgen, focusing on technologies that would enable a platform approach and could deliver therapies greater than 50 kDa in molecular weight. This resulted in 9 technologies to pass through the second-pass filter. The second pass filter consisted of a more rigorous set of criteria, and utilized a matrix evaluation method to compare and rank the 9 technologies. As an output, two technologies were considered for further pursuit.

Of note, all technologies after the first-pass filter are masked in order to protect Amgen's strategy in the oral drug-delivery space.

5.1 Methodology for Down-Selection

The down-selection was a two-phase filtering process, which started with 86 technologies and resulted in two top-priority technologies to move further into the technology evaluation process.

While sourcing solutions that mitigated the challenge of low bioavailability was the main priority for the technology landscape, this goal was fine-tuned during the down-selection process. Low bioavailability, as discussed in section 3.3.1, is due to both enzymatic and pH degradation of the large molecule drug and low absorption of that drug into systemic circulation. Given that there are conventional methods available today, including enteric capsules, that protect the drug from degradation, focus in the down-selection process shifted to those technologies that included a novel approach for promoting high absorption of the drug product into systemic circulation. This concept is deemed "active absorption", and will be used as a criterion in the down-selection process.

5.1.1 First Pass Filter focused on platform approaches

The first-pass filter was used to prune the technology landscape based on the technology's value to Amgen, with a focus on platform capabilities. This is further explained in the section below.

5.1.1.1 Criteria

In order to identify the technologies that have the highest potential to add value to Amgen, criteria for selection need to be understood. Currently, Amgen has a need for differentiation in competitive therapeutic areas (e.g. cardiovascular and neuroscience) and for lifetime extension of its drug products that are facing a patent-cliff. With that stated, platform-approaches, with emphasis on device-based solutions, to effectively deliver drug product via an oral route were considered as the fastest, least problematic methods to quickly add value back to Amgen's drug portfolio. Device-based, platform solutions align with the vision of ADT&I and the greater device organization, and also allows for the quickest implementation and thus quickest realization of profits from an oral option.

A platform approach is one that allows multiple drugs to work with a single technology option, and was emphasized by senior leadership within the device organization for use as a design criteria in new technology development. Similarly, a platform approach in device form was considered to be the path of least resistance for life cycle management (LCM) strategy, as it will likely not require the drug product to be designated as a new molecular entity, which requires extensive regulatory testing. Furthermore, a platform-approach to the problem aligned with the mission of the ADT&I group, who hosted the LGO internship. Additionally, in order to align with the needs of the company, technologies capable of large molecule delivery greater than 50 kDa were prioritized, as the majority of the pipeline has a molecular weight greater than that of >50kDa.

Effectiveness of delivery was judged through consideration of the historical barriers of delivery, the proposed novel mechanism afforded by the considered technology, and whether or not prior testing of the proposed mechanism has previously occurred. Oftentimes, this required labeling a technology as either an "active" or "passive" mechanism for drug absorption, which is further described in the results section below. This allowed for a quick judgement on effectiveness of the delivery mechanism without an in-depth review and testing of the technology itself.

While there are more criteria that need to be addressed, the first-pass filter was meant to be a quick test that allowed more time, energy, and resources to be committed to researching the output technologies from the filter. Criteria such as intellectual property protection, manufacturability, patient safety, and others are more finely considered in the second-pass down-selection below.

In summary, the first-pass down-selection's criteria revolved around sourcing a preferably device-based platform technology capable of effectively delivering molecules greater than 50 kDa through an oral route.

5.1.1.2 Methodology

An in-depth review of all technologies would not have been resource efficient for determination of the technologies that could pass the first-pass filter. Given the resources dedicated to the initial technology landscape, notes from this exercise and the groupings of the technologies were largely used to make the determination of those technologies that were moved into the second stage for further consideration. The technologies were compared to the criteria above by the LGO intern (who also performed the technology landscape) to determine candidates for further evaluation.

While the LGO intern was the judge of technologies that met the criteria of the first-pass filter, the criteria, candidates, and results of the down-selection were discussed and agreed upon with the team of engineers and managers close to the project. This team included a Director, two Principal Engineers, and a Senior Project Manager within ADT&I, and a Director within Drug Product, all of whom were aware and familiar with the project context and challenges associated with novel oral drug delivery of biologics.

5.1.1.3 Results

Two groupings of technologies were promoted for further study: Active-Device Based and Hydrogel based technologies. These groups were included because they are able to incorporate multiple modalities of drugs, while formulation based technologies may require molecule-targeted reformulation, which was less of a priority for the group given ADT&I's approach. Reformulation, in some cases, may require designation as a new molecular entity, which would further complicate the LCM strategy and extend the timeline required to get these drugs to market, making them potentially more expensive options.

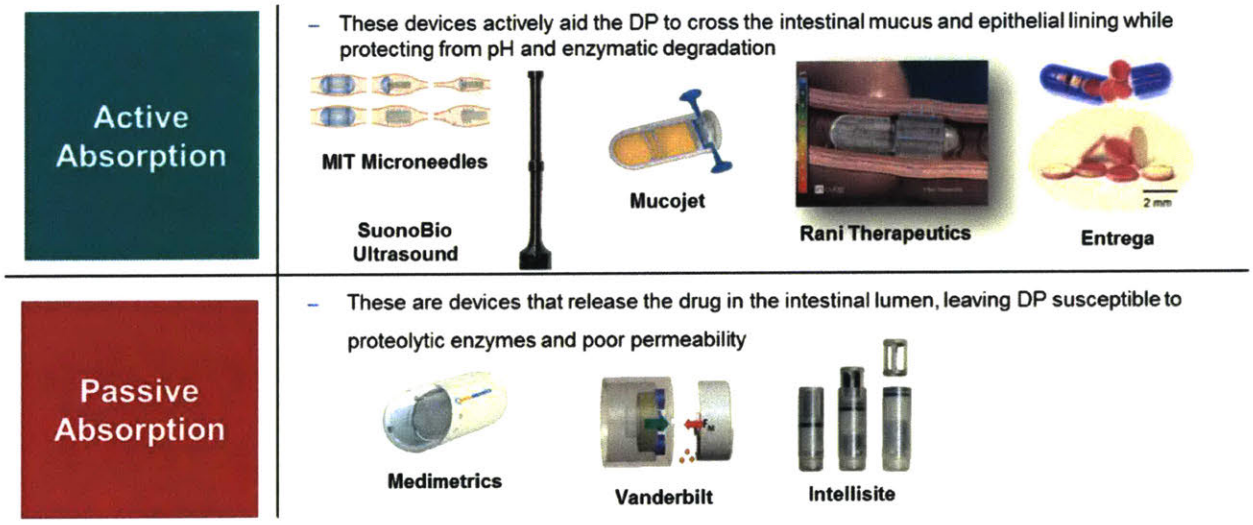

Figure 5-1 Devices that enable active vs. passive delivery of drug product

Active device based technologies are devices that aid in the absorption of drug across the intestinal (or oral) epithelium in a novel way. On the other hand, passive device technologies are devices that just act as a vehicle for the drug product, that release the drug product in the correct anatomical location, but do not aid in any tangible way with absorption. For this reason, passive devices were excluded from further study and did not pass through the first-pass filter. Figure 5-1 further explains the differences between these two types of devices. For example, the Rani technology actively aids by formulating drug product in microneedles that are then deployed into the wall of the small intestine, while the Medimetrics device does not, as it releases drug into the lumen of the small intestine without aiding in the drug's ability to pass through the intestinal wall. Because active mechanisms are likely required for effective drug delivery, no passive devices are included in Table 5-1.

PH-responsive hydrogels were also included for further evaluation, due to their mechanism of action previously described in section 4.2.2. Hydrogels like those from UT Austin promote a novel way for drug product to localize to the wall of the small intestine, while also being protected from the acid and enzymes in other regions of the GI Tract. The self-folding hydrogels from OSU were not considered further due to the lack of continuation of the project, and the trigger-able hydrogels from MIT were not suitable due to delivery within the stomach, leaving drug product susceptible to denaturation.

This led to 9 technologies being considered for the second-pass filter, all previously described in section 4.2. The technologies are listed in Table 5-1 below in no particular order.

Table 5-1 Technologies chosen for further evaluation from first-pass down-selection

Name	Company	Category	Application Area	Brief Description
Entrega	Entrega	Device, Formulation	GI	Entrega embeds drugs in a mucoadhesive patch that unidirectionally attaches to the intestinal lining to drive up the concentration gradient for delivery.
Mucojet	UC Berkeley	Active Device	GI	Mucojet generates CO2 via a chemical reaction to drive up pressure, move a piston, and eject drug through the mucus and into the mucosal layer of the small intestine.
Mucojet	UC Berkeley	Active Device	Buccal	Mucojet generates CO2 via a chemical reaction to drive up pressure, move a piston, and eject drug through the mucus and into the mucosal layer of the cheek; patient activated.
Auto-Pill	Rani	Active Device	GI	Rani uses a gas-powered balloon to dislodge sugar-based microneedles filled with solid drug into the small intestine.
Microneedle Pill	MIT, Langer Lab	Active Device	GI	This pill ejects drug into the small intestine using the peristaltic action of the small intestine; loaded with liquid drug formulation.
pH Responsive Hydrogels	UT Austin, Peppas Lab	Hydrogel	GI	P(MMA-g-EG) hydrogels are able to contract in pH in stomach, protecting drug, and swell in small intestine to release drug; mucoadhesive agents are added to help delivery.
Nanostraw Microdevices	UCSF, Desai Lab	Device	GI	PC base with alumina micro-straws load drug via diffusion; microdevice loaded in enteric capsule for delivery to small intestine via adhesion to and penetration of epithelial lining.
UMGID	MIT, Langer Lab	Active Device	GI (rectal)	Miniaturized ultrasound capsules for delivery of drugs via low frequency US induced diffusion drug delivery. Currently rectal ROA; hope to create pill-sized US. External activation.
Microneedle Patch	USCF, Desai Lab	Active Device	Buccal	Nanotopographic array of microneedles loaded with drug aid in buccal delivery.

5.1.1.4 Knowledge Sharing

The technologies that were filtered out during the down-selection process were collected in an excel database. This database was shared with the Formulation team at Amgen for further consideration.

5.1.2 Second pass filter based on Design for Six Sigma Matrix

The 9 technologies that successfully passed the first filter were then considered in the second down-selection.

5.1.2.1 Criteria Selection

Criteria for selection were based on technical performance, operational considerations, and the value to Amgen. Technical performance included considerations related to the ability of the technology to delivery large molecules via the oral mucosa or GI route, safety of the considered device, protection of the drug product, and the ability to increase absorption. Operational considerations included potential cost of goods manufactured impact, manufacturability, regulatory pathway, and device reliability considerations. Criteria related to the value to Amgen included maturity of the technology, IP generation capability, and patient preference.

The target value of depends on the wording of the criteria, and is specified for each criteria chosen for evaluation. For example, in Table 5-2, the criterion 1.10 "likelihood of long-term health effects" has a target value of "low" because the considered device should not pose any problems for long-term health. Alternatively, the criterion 1.7 "likelihood of high protein integrity from device mechanism of action" has a target value of "high" due to the expectation that any technology would not compromise the drug product that it is intended to deliver. When target values are assigned as "high" or "low", the evaluator uses his or her judgement to assign a score between 0-3 based on how well the device satisfies the criterion. Additionally, there are binary ("yes" or "no") target values as well, where a 3 is awarded if the device, within all likelihood, fulfills the absolute target value. For any device that answers the question with a "maybe", a score of 1 or 2 is given by the evaluator based on his or her judgement.

The full list of criteria, their rationale for inclusion, and their target value is listed in Table 5-2. In Table 5-2, criteria 1.9, 1.15, and 1.20 are excluded for buccal options, as they do not apply. In total, there are 34 criteria by which the second-pass down-selection judged different technologies. These criteria were agreed upon by all four judges.

Table 5-2 Criteria for Down-Selection

	Criteria	Rationale	Target Value
1	**Technical Performance**		
	Delivery Abilities (Loading Capacity, Location)		
1.1	Compatible with proteins (50 kDa and above)	Enables delivery of monoclonal antibodies	Yes
1.2	Compatible with small proteins (10 kDa to 50 kDa)	Enables delivery of molecules like Neulasta®	Yes
1.3	Compatible with peptides (1 kDa to 10 kDa)	Enables delivery of molecules like Parsabiv®	Yes
1.4	Compatible with small molecules (less than 1kDa)	Enables delivery of molecules like Kyprolis®	Yes
1.5	Volume of delivery / Payload capability	Larger volume of delivery, less likely to increase frequency of dosing	>1 mL
1.6	Reduce side effects & increase efficacy of therapy via GI localization	Could be launch enabling for a molecule & allow for localized delivery	Yes
1.7	Likelihood of high protein integrity from device MOA	If MOA compromises protein integrity, leads to lower bioavailability (i.e. shearing)	High
1.8	Enables systemic delivery	If ROA enables systemic delivery, more applicable assets for inclusion	High
	Safety		
1.9	Retention Time (i.e. risk of retention beyond average digestive cycle, OROS size 9mmx15mm)	Retention time as a proxy for obstruction risk based on OROS pill; exclude buccal	<24 hrs
1.10	Likelihood of long-term health effects	From inclusion of protease inhibitors that affect feedback mechanisms, probability of acting in same place multiple times leading to inflammation	Low
1.11	Biocompatible	Materials have generally regarded as safe (GRAS) status; avoid device toxicity	Yes
1.12	Risk of infection or immune response	If MOA may disrupt epithelial tissue, greater likelihood of health risks	Low
	Bioavailability, Protection, Absorption		
1.13	Efficacy on par with Sub-Q	Probability of relevant bioavailability	High
1.14	Ability to protect from enzymes in GI or oral location	Protein integrity	Yes
1.15	Ability to protect from pH changes in stomach and GI	Protein integrity; exclude buccal options	Yes
1.16	Likelihood of reliable and predictable dose delivery based on mechanism	Does the device deploy reliably and predictably? Location, timing, etc.	High
	Device Characteristics		
1.17	Extent of Reformulation Required	Require difficulties such as: solid formulation, addition of novel excipients, concentration increase?	Low
1.18	Inclusion of Visible Sharps	Sharps have higher likelihood of health concerns, marketing concerns	No
1.19	Ability to deliver highly viscous fluids within size constraint	If drug concentration increased, device needs to be able to deliver without issue	High
1.20	Pill Size (i.e. Ease of Swallowing)	OROS 9mm OD x 15mm Length considered low-risk of retention; larger risk goes up; exclude buccal options	Low
1.21	Large animal in vivo studies performed?	As a measure of technical tractability	Yes
1.22	Requires external activation?	External activation is a foreign concept; requires alternate regulatory pathway & more patient engagement	No
1.23	Confirmation of dosing event?	Relates to predictability of dosing; does patient/HCP know drug delivered after it has been deployed?	Yes
1.24	Potential for significant pain	If patient feels pain even once with device, negative perception will affect adherence	Low

2	**Operational Considerations**		
2.1	Potential cost of goods sold (COGS) Impact	Decrease profitability	Lower
2.2	Manufacturability (Sterility in GMP setting possible?)	Increase cost and timeline	Higher
2.3	Ease of Fit of Regulatory Pathway with current combination products	Increase in cost and timeline due to regulatory uncertainty	Higher
2.4	Protein Stability in Final Form	Protein stability and shelf-life	Higher
2.5	Device Reliability	Robustness of container/packaging leads to predictability of device deployment	Higher
3	**Value to Business**		
3.1	Maturity of Technology	More mature a technology, less risks while investing	Late Stage
3.2	IP - Ability to Extend Molecule Patent	Extend molecule life, extend revenue generation	Yes
3.3	Ownership by a Corporation	Generally easier to work with established companies	Yes
3.4	Patient Preference	Assumption that buccal delivery is not as preferred	Yes

5.1.2.2 Matrix Evaluation

A modified Design for Six Sigma (DFSS) matrix was used to weight and score the different technologies based on a set of criteria (described above). Each technology is scored within each specified criterion on a 0-3 scale with a 3 awarded to the target value. These scores are then multiplied by the weighting factor, summed, and divided by the possible number of points available to score each technology. Criteria were agreed on among stakeholders, designed to rank technologies on their ability to enable oral delivery of biologics. Each criteria was assigned a weight between 1-10 based on its importance for oral drug delivery of biologics.

Figure 5-2 Example Evaluation of Devices based on Criteria and Weighting Factors an example evaluation of the technologies by one of the judges. On the top, we see each device that is considered (A-I), total value of points allotted to that technology by the evaluator, the total number of points possible for that technology to achieve based on whether or not the criteria are applicable to it, and the percentage of points received as a function of the total possible. This allowed the technologies to be ranked by each evaluator.

Mathematically speaking, the total number of points scored by each device (j) within each criteria (i) follows the formula below:

$$V_{i,j} = W_i \, S_{i,j} \qquad (1)$$

$$TV_j = \sum_{i=1}^{35} V_{i,j} \qquad (2)$$

In these formulas, $V_{i,j}$ refers to the weighted score of a device (j) within a specific criterion (i). W_i is the weighting factor (between 1 and 10) for each criterion (i) based on its importance to the overall down-selection. $S_{i,j}$ is the score from 0 to 3 assigned by the evaluator to each device (j) within each criterion

(i). Multiplied together yields the weighted score, $V_{i,j}$. For example, in Figure 5-2, $V_{1,H}$ refers to the score given to device H for criterion 1, which is equal to 10 when calculated from the figure.

Similarly, TV_j is the total value assigned to device (*j*), which is just the summation of the weighted scores from each of the 35 criteria. In Figure 5-2, TV_H is 407 (second row of the figure).

This method has been previously used in the ADT&I group for ranking of technologies on previous projects, and was considered an acceptable ranking method for determination of the best candidates to move forward with. The main difference between this methodology and others previously used was the team-based approach to establishing the criteria, weighting, and scoring of the individual technologies. The two principal engineers in ADT&I and Director from drug formulation, along with the LGO intern, all agreed upon the set of criteria for ranking. Each of the four "judges" then independently weighted the criteria and scored each technology within each criteria. The scores and weights of all the different stakeholders were compared for determination of the top two candidates for further evaluation. Prior to scoring and weighting by the other judges, documents were sent out to all for consideration, explaining the historical barriers of oral delivery and an in-depth review of the top 9 technologies. Incorporation of

the scores and weights of all judges allowed for all stakeholders to come to a consensus regarding the technologies pursued for further evaluation.

Device	H	A	B	c	D	F	I	E	G
Total Value (TV_j)	407	499	406	492	432	410	335	422	347
Total Possible	702	702	630	687	702	702	702	702	630
Percentage	58%	71%	64%	72%	62%	58%	48%	60%	55%
Rank	7	2	3	1	4	6	9	5	8

Criteria	Weighting Factor (W_i)	Scores for Individual Technologies ($S_{i,j}$)								
1.1	10	1	3	3	3	3	1	2	3	3
1.2	7	1	3	3	3	3	2	3	3	3
1.3	5	3	3	3	3	3	3	3	3	3
1.4	1	3	3	3	3	3	3	3	3	3
1.5	7	1	3	3	2	3	2	0	1	3
1.6	5	3	3	0	3	3	2	3	3	0
1.7	7	1	1	1	2	1	1	1	2	2
1.8	10	1	3	3	3	3	1	2	1	2
1.9	7	3	3	N/A	2	1	3	1	3	N/A
1.10	7	3	2	1	2	1	2	3	3	2
1.11	10	3	3	3	3	1	3	2	3	2
1.12	10	3	2	2	1	1	2	2	1	1
1.13	7	0	1	2	3	3	1	1	1	1
1.14	10	1	2	2	3	3	2	1	2	1
1.15	10	3	3	N/A	3	3	3	2	3	N/A
1.16	10	0	1	3	1	2	1	1	0	2
1.18	8	0	2	2	1	2	1	2	1	2
1.19	5	3	3	3	2	0	2	3	3	1
1.20	5	0	1	3	N/A	1	1	1	1	1
1.21	7	3	3	N/A	1	1	3	1	3	N/A
1.22	7	0	0	0	3	1	0	2	0	1
1.23	7	3	3	1	3	3	3	0	3	1
1.24	4	0	0	3	0	0	0	0	0	2
1.25	7	3	3	1	2	1	1	0	2	1
2.1	4	1	3	3	1	1	1	0	1	1
2.2	6	3	2	2	1	1	1	1	1	1
2.3	4	1	2	2	1	2	1	1	0	2
2.4	7	1	2	2	3	2	2	1	2	2
2.5	10	3	1	1	1	2	2	1	1	2
3.1	5	1	1	1	2	1	0	0	1	0
3.2	10	0	1	1	1	1	2	2	2	2
3.3	5	3	1	1	3	1	1	1	1	1
3.4	10	3	3	1	3	2	3	1	2	1

Figure 5-2 Example Evaluation of Devices based on Criteria and Weighting Factors

5.1.2.3 Scoring & Weighting

Each judge independently applied a weight to and scored each technology within each criteria. As a reminder, the weighting factor (from 0-10) is used to multiply the score in the range of 0-3, depending on the judge's interpretation of the importance of the criteria to success. Appendix 1 includes the differences in weighting and scoring between each of the four judges. Given the ranges of maturity of the considered technologies, and the uneven base of knowledge for the different technologies, judgement calls were often made for scoring of the different technologies. By allowing all stakeholders to have the opportunity to review and judge the different technologies, different perspectives were incorporated into the ranking

process, and spurred fruitful conversation about the best method to continue forward with. The outputs of the scoring were then compared and discussed with the team, and two clear front runners were selected for further evaluation.

Of note, all the three judges within the ADT&I group (two principal engineers and LGO intern) were of a similar mindset, that a device was the best approach to effectively package, protect, and enable active absorption of the drug product. This group also took on the mindset to test the worst-case scenario first, meaning that technologies that could deliver the largest molecules would also be able to deliver the smaller molecules. On the other hand, the Director of formulation was more familiar with non-device approaches to oral drug delivery and also preferred to test easier cases (smaller molecules) first. These biases are evident in Appendix 1, which clearly shows the different scoring patterns between the evaluators from ADT&I vs. formulation.

5.2 Output of Down-Selection

The output of the second stage down-selection was a ranking of the different technologies, determined by the score each technology received within each applicable criteria, multiplied by the assigned weighting factor, and divided by the total number of points achievable by the technology. The relative rankings of the four evaluators are graphically depicted in Figure 5-3 and the top three options for each evaluator are compared in Table 5-3.

For the rest of this thesis, the technologies are masked due to the wishes of Amgen not to disclose its strategy within the Novel Oral space.

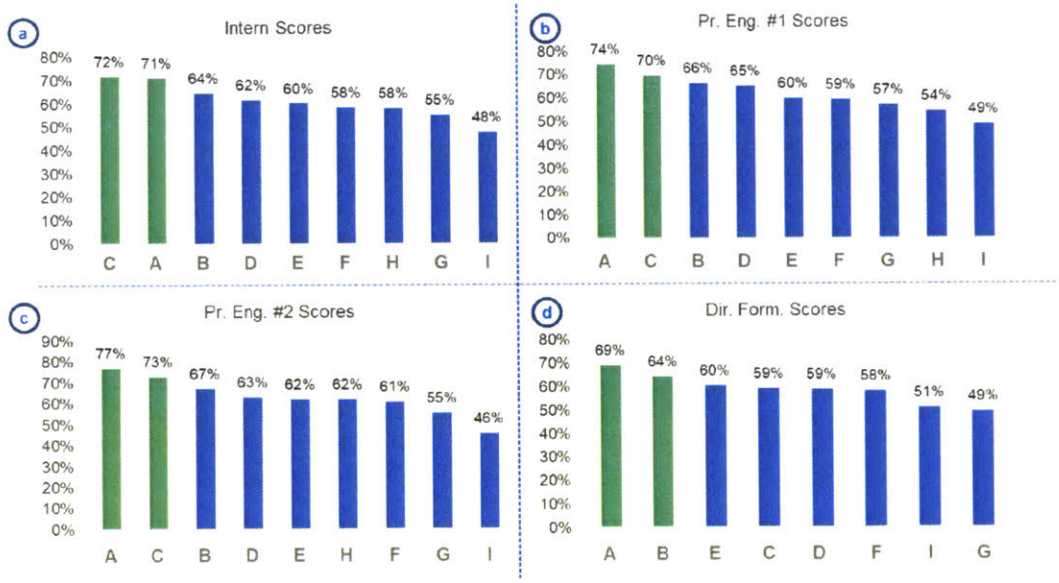

Figure 5-3 Relative Rankings of Technologies for 4 Evaluators. (a) Intern (b) Principal Engineer #1 (c) Principal Engineer #2 (d) Director of Formulation

Table 5-3 Top Three Ranked Technologies for each of the Four Evaluators

Evaluator	1st Rank	2nd Rank	3rd Rank
Intern	C	A	B
Pr. Eng. #1	A	C	B
Pr. Eng. #2	A	C	B
Dir. Form.	A	B	E

Technology A, B, and C were chosen most frequently by all evaluators. Of note, Technology E scored high for the Director of Formulation, but not for any of the employees within the device organization. This may have to do with the solid formulation that would be necessary for the Technology C, which Amgen does not have extensive experience with, while Technologies A, B, and E allow for the standard liquid formulation to be used.

Of note, the LGO intern was the only evaluator to rank the technology "C" first; this is due to her weighting of the maturity of that technology and belief that it had a superior mechanism of action to disrupt the epithelial barrier as opposed to the alternative technology options.

After discussion of these top-ranked choices, Technologies A and C were chosen to continue into technology evaluation, as these two choices were most often ranked in the top two spots.

Technology B was not chosen for pursuit at this time due to a number of reasons. Technology B employs buccal administration, which may make more sense for vaccine delivery due to the large number of immune cells in the mouth. Furthermore, there are many nerve cells in the mouth, which means that buccal administration may not be entirely pain-free, and thus negates some of the proposed value. Finally, it is unclear whether the patient would prefer Technology B to other delivery technologies, due to the fact that it requires a lot of user preparation and may be cumbersome to deploy.

Technology E was not chosen for pursuit at this time due a number of reasons. The inefficient drug loading (40-60% loading efficiency of drug product) into the body of Technology E makes it economically less appealing for pursuit. Furthermore, Technology E functions to locally increase the concentration gradient of the drug, but does not necessarily include a novel mechanism by which drug is absorbed across the epithelium. The Director of Formulation likely ranked this technology higher due to his familiarity with the technology and experience with similar delivery options in the past. However, even in light of the Director's ranking, Technology E may be more applicable to local delivery of drugs in the GI system, where drug product either acts in the lumen, or is absorbed through the compromised epithelium often associated with diseases of the gut.

5.2.1.1 LGO Thesis focused on Technology A

This analysis, in comparison with the needs of the LGO internship, called for the focus on the Technology A for a number of reasons. Given the academic, early stage nature and breadth of literature published on Technology A, it lends itself better to an engineering-focused analysis that is described in Chapter 7.

For the overall novel oral program at Amgen, both Technology A and C warrant further review. While Technology A will be further assessed by the LGO intern, recommendations for outreach to both technology owners were made and pursued by the wider ADT&I group at Amgen.

5.3 Summary

Chapter 5 focused on the down-selection of technology candidates sourced through the technology landscape. The first-pass filter, focused on identifying technologies able to be a platform play for Amgen capable of delivering molecules greater than 50 kDa, resulted in 9 technologies for consideration, detailed in Table 5-1. These technologies had novel approaches to enabling active absorption of drug product via the buccal and GI routes.

In the second-pass filter, these 9 technologies were further pruned through a rigorous matrix analysis with a well-defined set of criteria. The criteria were based on technical and operational, as well as the potential to bring value to Amgen. Four evaluators judged the 9 technologies and agreed upon the pursuit of the resulting two candidates that stood out in the evaluation: Technology A and Technology C. Technology A will be further pursued by the LGO student, while Technology C will be pursued by the wider ADT&I group.

Chapter 6 Risk Assessment of Prioritized Technologies

Given the nature of the LGO project, Technology A remains the focus for the risk assessment and technological evaluation segment of this project. To complete Phase 2 of the project plan (Figure 2-2), a technical risk assessment to inform the testing strategy was completed for Technology A. Here, the testing strategy refers to the steps taken to perform due diligence on the feasibility of the technology against the risk profile outlined in the sections below.

Chapter 6 outlines two methods used to assess the risk associated with Technology A. The first is a Failure Modes and Effects Analysis (FMEA), a widely used risk assessment tool in the industry, and the second is a Fishbone Diagram, intended to catch the design features that could lead to variability in the intended performance of Technology A.

6.1 Technical Risks

The technical risks were assessed in two ways. The first was through a Failure Mode and Effects analysis (FMEA), which took a broader view of the technical risks of the Technology A device. The FMEA analysis is often used in the medical device and pharmaceutical industries, and so was appropriate to apply to Technology A.

The second risk assessment was completed through the identification of the design risks in relation to the ability of the device to successfully deploy, through a fishbone diagram. This method was employed to

detail the different ways in which a device could not perform its function, and goes into more detail related to the specific design of the device than the FMEA analysis.

6.1.1 Failure mode and effects analysis (FMEA) and Mitigation Strategies

FMEA is a highly structured tool for the analysis of failure modes that may arise from the malfunctions of systems. Given that this study is usually applied to systems that already exist and are in place, the FMEA for Technology A was adapted to take a macroscopic, qualitative approach to the analysis.

Key risks were identified through a literature review of Technology A, and discussions with toxicology, regulatory, formulation, pathology, device, pharmacokinetic, attribute sciences, and other groups within Amgen. All risks are "ex ante", based on predictions of the device function rather than on actual device performance. The identified risks were then grouped into the top five highest priority risks, which were prioritized through discussion with the groups mentioned above. The prioritized risks were then categorized by the severity of the outcome if the risk were realized, as well as the probability of risk occurrence on a qualitative scale. Risk severity scores ranged from Low (1) to Severe (9), with low indicating a negligible effect on the patient and severe indicating serious harm or death. Risk likelihood scores ranges from remote (1) to very likely (9), with very likely indicating near inevitable occurrence. Mitigation options were then designated to each risk, sourced from research and discussions with LGO advisors and Amgen colleagues within the groups identified above. The outputs of this analysis can be seen in Figure 6-1, where the highest priority risks, their impact, and the suggested mitigation options are detailed.

The first risk is that of low bioavailability, which is reflective of the major challenges associated with oral drug delivery of biologics initially described in section 3.3.1. If the drug is not able to reach a relevant level of bioavailability, the necessary concentration of drug within the blood for effective therapy will not be attained. If this happens, the patient will not get the benefits associated with therapy. Depending on the drug and disease state of the patient, this represents a moderate to major ranking on the severity index. Given the challenges with delivery of oral bio therapeutics, this risk was allotted a high likelihood of occurrence. The design attributes of the device and the risks are further described in the section below. To initially mitigate this risk, simulation of the device deployment as it relates to drug transport within the small intestine is suggested for completion by the LGO intern.

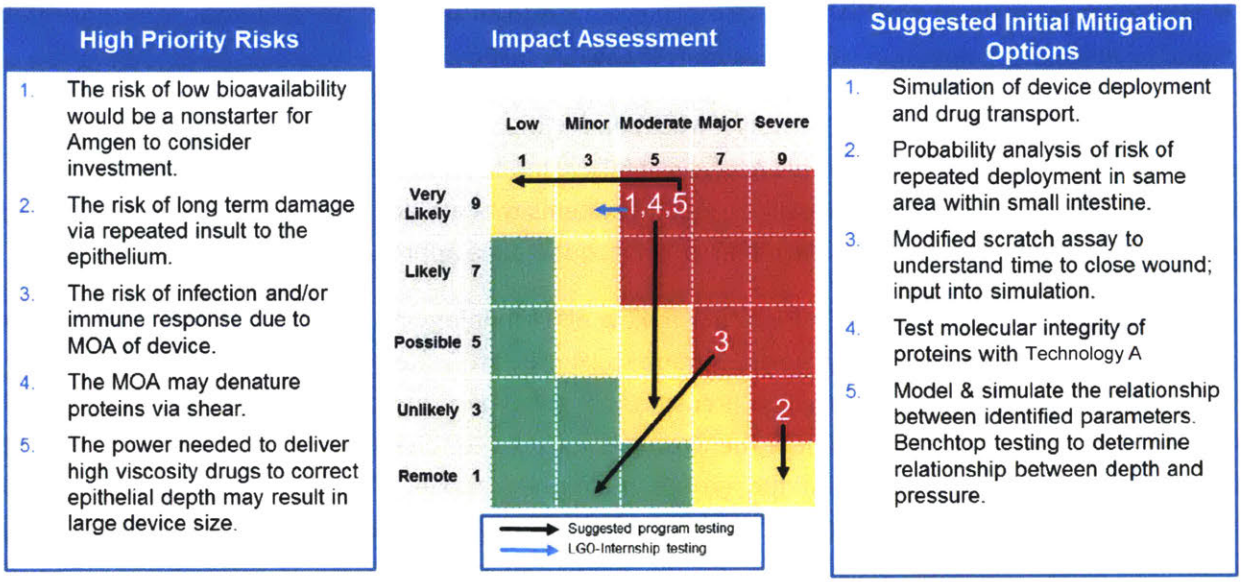

Figure 6-1 Risk Identification, Impact Assessment (FMEA), and Suggested Mitigation Options for Technology A

Risk 2 and Risk 3, detailing the risks of long term damage and infection due to the mechanism of action (MOA) of Technology A are related. Since the device aims to disrupt the mucus, and potentially the epithelial lining, of the small intestine to deliver drug product, there is risk of both long term damage and a localized infection or immune response. Risk 2 for long term damage was indicated as severe due to the potential for serious harm from long term damage, but was considered unlikely due to the large volume of the small intestine. To initially mitigate this risk, a probability analysis of the risk of repeated deployment in the same area along the surface area of the small intestine should be conducted. Risk 3, relating to immune response and infection, was indicated as a major risk on the severity scale due to the potential for serious side-effects that could require medical intervention, and was deemed more likely to occur than risk 2, due to the potential for an immune response or infection to occur after every deployment that takes place. In order to initially mitigate Risk 3, a modified scratch assay with CaCo2 cells (representative of the small intestine epithelium) could be performed to understand the time needed to close the wound inflicted by Technology A during delivery.

For similar reasons as Risk 1, Risk 4 was assigned the same severity and likelihood ratings. If the drug product packaged with Technology A is denatured via shear stress produced by the high-velocity jet, then the drug will never reach the concentration it needs to be therapeutic to the patient, posing a moderate risk. To initially mitigate this risk, protein molecular testing integrity is suggested to determine whether aggregates or fragments occur from deployment with Technology A.

Risk 5 details the potential for the device size to be driven up due to the balance between needing enough power to deliver drug product successfully, and also including an adequate payload of drug in the device for a favorable dosing frequency to the patient. If this drives the device size up past the 9mm x 15mm size indicated in section 3.3.2, there is an increased risk of retention. Retention may require medical intervention for removal of the device components, and is thus given a moderate severity rating. This

was also deemed likely to happen, because drug product will likely need to be produced in a more concentrated form to achieve the necessary payloads, which will drive viscosity up, and potentially also increase the power needed for delivery, thereby increasing the overall device size. Similar to Risk 1, simulation of the device parameters and benchtop testing is suggested for initial mitigation to understand the power requirements to inject the desired drug product to the desired location within the small intestine wall.

In further technical assessment of Technology A by the LGO student, risk 1 of low bioavailability will be simulated through *in silico* testing. Low bioavailability of the drug product when delivered via an oral route is not only likely from a historical perspective, but would also prevent the patient from getting the desired effect of their medicine. Thus, this risk is not only meaningful to Amgen, it is meaningful to the patient, and lends itself to modeling and simulation to be performed by the LGO student.

6.1.2 Sources of Variability related to Expected Performance of Technology A

There are multiple malfunctions that can occur that could lead to low bioavailability. In Figure 6-2, these sources of variability are categorized and detailed in a Fish-Bone diagram. Expected device performance in this context refers to the successful delivery of drug product via Technology A into systemic circulation with bioavailability comparable to subcutaneous injection.

This diagram highlights some of the difficulty in producing the desired performance of Technology A. For Risk 1 detailed in the previous section, low bioavailability could be the result of any of the sources of variability outlined above. For example, under the Materials section, a source of variability was listed as the mechanical properties of the small intestine. If one person's small intestine requires more force for delivery of drug product than another person's, Technology A may not deliver drug product successfully in both patients.

Alternatively, under the "Personnel" section, if the end-used of the technology does not comply with the instructions for use (IFU), then it will compromise the ability of the device to perform. For example, if a patient compromised the integrity of the device by splitting it in half, keeping it out of the refrigerator, or consuming the medicine in the inappropriate state of fasting, the device will not be able to deliver the medicine appropriately.

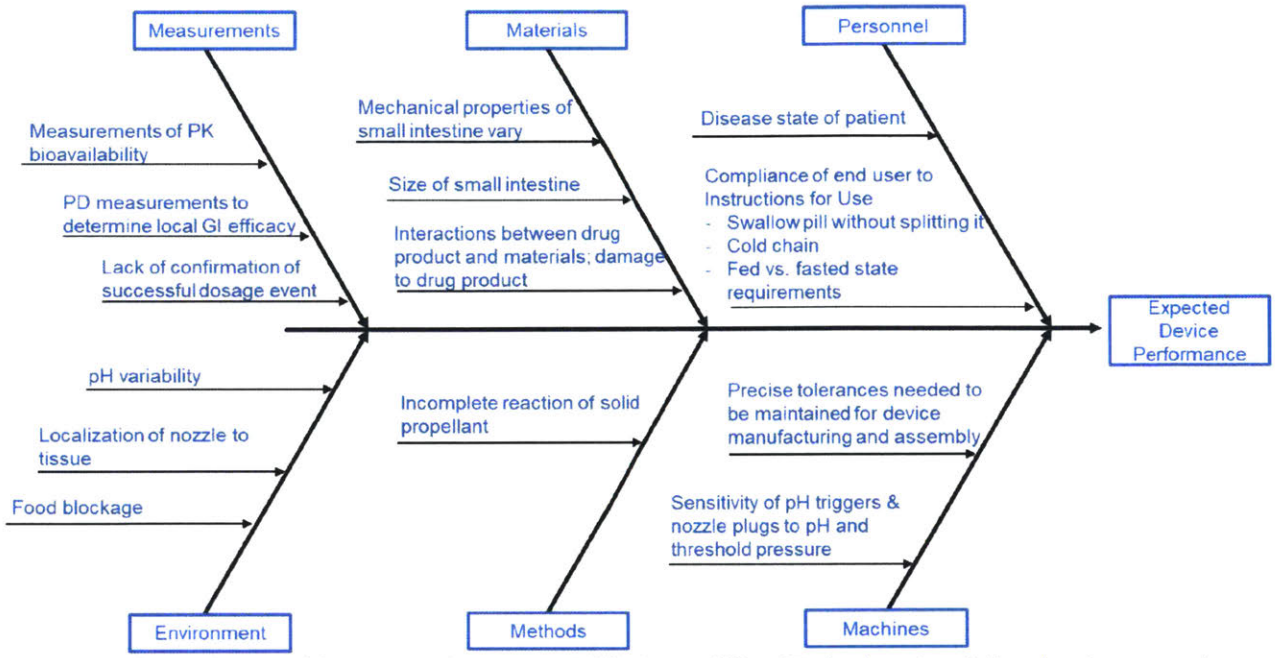

Figure 6-2 Fishbone diagram of factors contributing to variability in capability of Technology A to deliver drug into systemic circulation

As another example, under the "Machines" section, if manufacturing of the device is not in spec, this can affect both the sensitivity of the pH triggers and nozzle plugs, as well as affect the tolerances and thereby affecting the flow of the drug product through the multiple nozzles of Technology A. Any variability in the sensitivity of crucial components and tolerances can affect the deployment of Technology A.

From the different sources of variability considered under the six categories, the device needs rigorous verification and validation testing to ensure it can deliver medicine to patients reliably and accurately.

6.2 Summary

The technical risks of Technology A were assessed through an FMEA analysis and a Fishbone Diagram documenting the sources of variability. The FMEA analysis revealed that the risk of low bioavailability of any drug product combined with Technology A is of high important both on the severity and likelihood scales, and was chosen as the risk to mitigate during technical feasibility testing.

The fishbone diagram documenting the numerous sources of variability within the design and handling of Technology A revealed that variability stems from, among others, the environment in which the technology deploys, the manufacturing of the technology, and the state in which the technology is handled by the patient once produced.

Although there are multiple sources of variability and risks to pursue further, the risk of low bioavailability was prioritized for further mitigation by the LGO student. This was done due to ease of access to software enabling modeling and simulation, the important of the risk of low bioavailability, and timeline of the overall project.

Chapter 7 Technical Assessment of Technology A

Chapter 7 walks through the technical assessment of Technology A performed by the LGO student. As Technology A utilizes a jet of drug product for delivery, the chapter first evaluates other jet injection devices historically considered for delivery of large molecules.

Next, the chapter considers the technical assessment of Technology A through *in silico* modeling and simulation in COMSOL Multiphysics®. Two models were built to understand whether Technology A will be able to deliver drug product in a meaningful concentration to achieve high bioavailability. The first model assesses the internal mechanisms of Technology A with respect to different combinations of input parameters to judge their effects on the output velocity profiles of drug product from the device. The second model takes the output velocity profiles from Model 1, and simulates their flow into the modeled layers of the small intestinal wall. Through this, the volume of drug product in the desired anatomical location can be measured, and related back to the bioavailability enabled by the device.

The setup, methodology, and results of the two models are discussed in the sections below.

7.1 Jet Injection in Drug Delivery

While jet injection for intestinal delivery is a novel concept to enhance absorption, this concept is not necessarily new in transdermal delivery of biologics. To consider the invention of Technology A in comparison to other jet injection devices in literature, a mini-literature review into these transdermal options was performed. Most studies for drug delivery via jet injection are conducted for study of transdermal drug delivery, rather than drug delivery across the mucus and epithelial layers of the small intestine. Needle Free Injection Technology (NFIT) aims to deliver liquid drug product via a transdermal route to replace intradermal, subcutaneous, and intramuscular injection. These technologies generally exhibit turbulent flow and induce exit velocities >100 m/s in order to generate the force necessary to penetrate through the skin, with nozzle diameters typically between 150-300 µm (Kale & Momin, 2014).

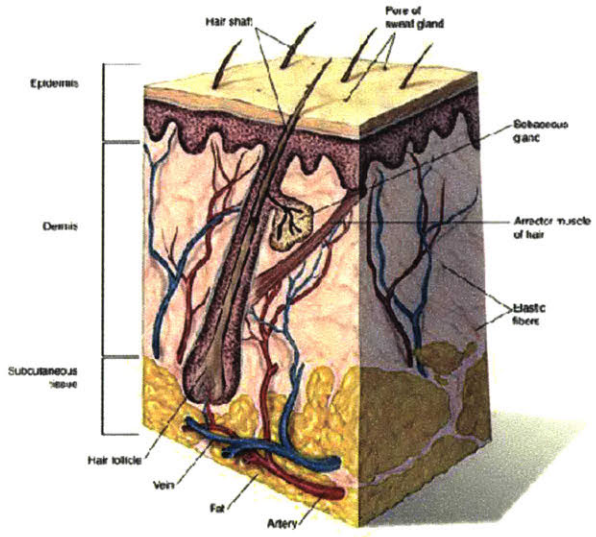

Figure 7-1 Schematic of the transdermal layer of skin. Adapted from http://www.esthetique.com.cy/?pageid=35

These velocities are nearly three orders of magnitude larger than the proposed exit velocity from Technology A, expected to be around 200 mm/s. These larger velocities may be required to penetrate through the thicker layers of the epidermis (Figure 7-1), which require an estimated 15 MPa of pressure or at least a threshold velocity of 80 m/s to ensure penetration of the stratum corneum (Shergold, Fleck, & King, 2006) (Tagawa, Oudalov, Ghalbzouri, Sun, & Lohse, 2013). For subcutaneous delivery through the skin, the drug needs to travel past the stratum corneum, a thin but hard layer, through the dermis, and into the subcutaneous tissue to a final depth on the order of millimeters to centimeters.

Other microjet technologies aim to deliver molecules across the cell membrane and into the cell cytoplasm (Adamo, 2013). They aim for exit velocities between 5-6 m/s in order to puncture the cell membrane without harming the vitality of cells. However, the limitations of this type of technology is that it requires clear access to the cell, requires microfabrication of nozzle diameters on the order of 2μm, and can only deliver picoliters of liquid product at a time (Adamo, 2013). However, this technology uses laminar flow, in contrast to other NFIT technologies, to deliver drug product via jet injection, which is more amenable to the expected jet production by Technology A.

There is a gap in the knowledge between the microjet technologies and the high-power needle free injection technologies. The microjet technologies work to deliver intracellularly, through epithelial barriers that are 10s of microns thick, while the NFIT devices deliver drugs subcutaneously, through dense tissue that is 1-10mm thick. Technology A plays in between these two technologies, delivering into the wall of the small intestine, aiming for a delivery depth of at least 50-500 μm to access the lamina propria, but not exceeding 3mm, which is the upper limit of the wall thickness of the small intestine.

7.2 Technology A - *In Silico* modeling with COMSOL Multiphysics®

Technology A was chosen for further evaluation through *in silico* modeling in COMSOL Multiphysics® to test the prioritized risk of low bioavailability identified in Section 6.1.

7.2.1 Hypothesis related to low bioavailability

In order to test the risk of low bioavailability as related to Technology A, a hypothesis related to the optimal location for uptake of large molecules into systemic circulation needs to be made.

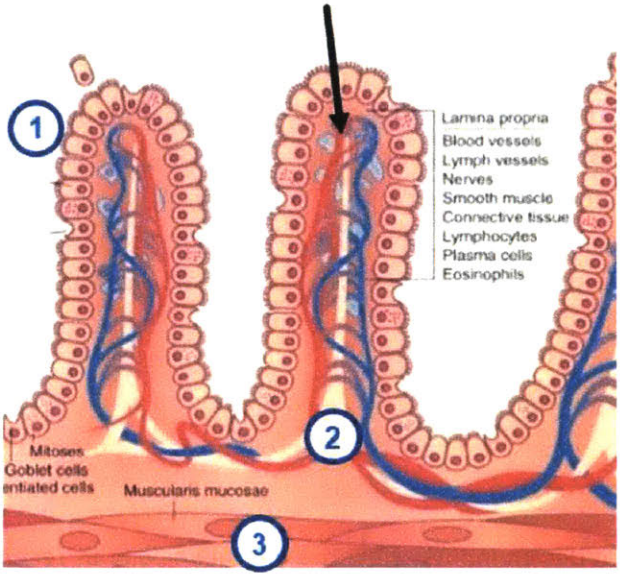

Figure 7-2 Layers of small intestinal wall. (1) Epithelial barrier of small intestine that has very low permeability to large molecules. (2) Lamina propria (LP) which is rich with blood and lymph vessels, (3) Muscularis Mucosa (MM) also rich with blood and lymph vessels. Missing: mucus layer that sits on top of epithelial layer. (Adapted from Sobotta J, Figge FHJ, Hild WJ: Atlas of human anatomy, New York, 1974, Hafner.)

However, for systemic delivery through the gastrointestinal tract, deposition of drug on the epithelial lining of the small intestine will not be sufficient for systemic bioavailability. Due to the epithelial barrier's low permeability to large molecules and the frequent shedding of the mucus layer described in section in Chapter 3, drug product needs to enter into the lamina propria in order to have relevant levels of bioavailability. Relevant levels of bioavailability are considered those approximate to subcutaneous injection, which will be different for each drug used.

In subcutaneous injection, studies have shown that molecules larger than 16 kDa travel into systemic circulation via the lymphatic system, while those less than 16 kDa are taken up by blood capillaries (Richter, Bhansali, & Morris, 2012). Bioavailability levels for different drugs can vary widely, depending on the specific properties and characteristics of the drug product in question. However, the lamina propria and muscularis mucosa layers, which are rich with blood and lymph vessels, represent a very good delivery location to enable systemic circulation for large molecule drugs.

Thus, Chapter 7 of this thesis uses the hypothesis that large molecule drug product needs to enter into the sub-epithelial space consisting of the lamina propria and muscularis mucosa (Figure 7-2) in order to achieve relevant levels of bioavailability.

7.2.2 Modeling vs. Benchtop Testing

Due to the lack of Technology A prototypes accessible to the student and time constraints associated with the LGO Internship, benchtop testing was not pursued to test the ability of the device to penetrate

through the mucus and epithelial layers of the small intestine. *In Silico* modeling with COMSOL Multiphysics® was pursued as an alternative option to benchtop testing, to model the abilities of Technology A and initiate mitigation of the risk of low bioavailability.

Two models were developed to mitigate this risk. Model 1 focuses on Technology A's internal mechanism of action, to understand which input design parameters affect the output velocity of the liquid drug product exiting the device. Model 2 simulates the inflow of the drug product into the various layers of the small intestine, from the input velocity profiles produced by Model 1. The outputs from both of these models allows for understanding of whether or not Technology A would enable drug product to be delivered with a high probability of relevant bioavailability, but to also understand which input design parameters are the most significant for the optimal dispersion of drug product in the small intestine.

7.3 Model 1 – Assessment of Internal Mechanics of Technology A

7.3.1 Technology A Mechanism of Action

The first model was designed to understand how the different design inputs into Technology A affect the exit velocity of the drug product from the device nozzle.

To understand how the different design inputs affect the output velocity of Technology A, it is necessary to understand the proposed mechanism of action of the device itself. The device is a capsule that contains a power reservoir, a piston, and a drug reservoir (Figure 7-3). The power reservoir contains a powdered mixture of sodium bicarbonate and citric acid (baking soda), while the drug reservoir contains the liquid drug product for delivery *(Reference Redacted)*.

The pH valves located within the region of the power reservoir selectively open in the presence of the pH of the small intestine, which resides between a pH of 6-7.5 (Langer & Traverso, 2017). The valves then allow the luminal fluid containing water to enter into the power reservoir, allowing the propellant to react to produce carbon dioxide (CO_2). The CO_2 drives the pressure in the pill up until the threshold pressure of the nozzle is reached, which is determined by the plug used to cap the nozzle. Once the threshold pressure is met, the nozzles open, the piston moves forward, and the drug product is ejected at a high velocity out of Technology A.

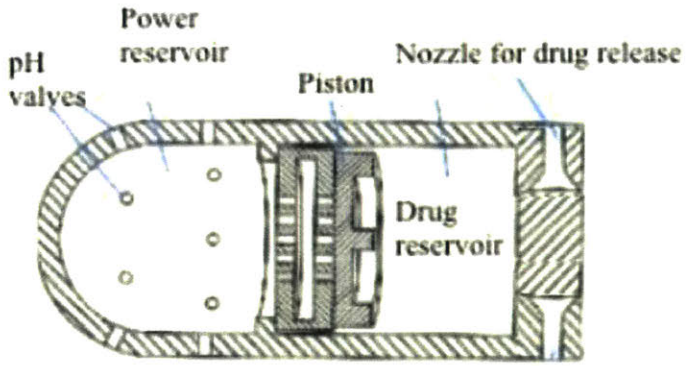

Figure 7-3 Schematic of Technology A. Adapted from *Reference Redacted.*

There are multiple design parameters that can be studied, including but not limited to, the threshold pressure and nozzle diameter. Furthermore, the liquid drug product intended for delivery with the device also presents a number of additional input parameters, including but not limited to the drug viscosity. These three inputs: nozzle diameter, threshold pressure, and drug viscosity, will be studied for their effect on the output velocity in Model 1.

7.3.2 Methodology & Assumptions for Computational Modeling (Model 1)

7.3.2.1 Hypothesis on Impact of Nozzle Diameter, Threshold Pressure, and Drug Viscosity on Exit Velocity

Assuming incompressible flow with constant flow rate, the nozzle diameter of Technology A will likely have an effect on the output velocity. The equations below demonstrate the relationship between the nozzle diameter and the exit velocity,

$$v_{piston}A_{piston} = v_{exit}A_{nozzle} \quad (3)$$

$$\frac{v_{piston}A_{piston}}{d_{nozzle}^2} \sim v_{exit} \quad (4)$$

Where v_{piston} is the piston velocity, A_{piston} is the cross-sectional area of the piston, v_{exit} is the exit velocity of the drug product, A_{nozzle} is the cross-sectional area of the nozzle, and d_{nozzle} is the nozzle diameter. It is evident that as the nozzle diameter increases, the exit velocity should decrease by a factor of four. However, the assumption of a constant flow rate may not be entirely realistic, since the fluid will be accelerating as the piston moves forward.

Similarly, the threshold pressure should also have an effect on the exit velocity of the drug product - the higher the threshold pressure, the higher the exit velocity of the drug product. Assuming that the Reynold's number is greater than one, indicating that inertial effects dominate over viscous ones, and that the flow is quasi-steady, Bernoulli's equation can be used to analyze this relationship. The equation below describes this relationship, where the external pressure is assumed to be zero and the initial velocity of the drug product is assumed to be zero,

$$P_{threshold} - P_{lumen} = {}^1/_2\,\rho\left(v_{exit}^2 - v_{initial}^2\right) \quad (5)$$

$$P_{threshold} \sim v_{exit}^2 \quad (6)$$

Where $P_{threshold}$ is the threshold pressure, P_{lumen} is the luminal pressure (assumed to be zero), $v_{initial}$ is the initial velocity of the drug product (assumed to be zero), and ρ is the density of the drug product. It is evident that as the threshold pressure increases, the exit velocity should increase by a factor of $\sqrt{2}$. This relationship relies on the assumption that inertial effects dominate during ejection, and the Reynold's number will be calculated after simulation to confirm this assumption. Additionally, this also assumes that fluid flow is quasi-steady, which may not be entirely reasonable due to the time dependent nature of the flow.

Finally, to the extent that viscous shear stress influences ejection velocities, the viscosity of the drug product should also have an effect. Viscosity induces a shear force on the different layers of liquid moving

past each other in laminar flows, proportional to the dynamic viscosity measurement. Poiseuille's Law below describes the flow rate of Newtonian fluids in laminar flow,

$$Q_{fluid} = \left(\Delta p\, \pi\, r_{reservoir}^4\right)/(8\mu l_{reservoir}), \quad (7)$$

$$Q_{fluid} \sim v_{fluid} A_{fluid}, \quad (8)$$

$$v_{fluid} \propto {}^{1}/_{\mu}, \quad (9)$$

where Q_{fluid} is the flow rate of the fluid (volume/s), Δp is the pressure difference caused by the force of the piston on the fluid, $r_{reservoir}$ is the radius of the drug reservoir of Technology A, $l_{reservoir}$ is the length of the drug reservoir of Technology A, v_{fluid} is the velocity of the fluid in the drug reservoir, A_{fluid} is the cross sectional area of the drug reservoir, and μ is the dynamic viscosity of the drug product contained in the drug reservoir. Approximating the flow rate as the area multiplied by the velocity, it is evident that the velocity of the fluid is indirectly proportional to the dynamic viscosity, and therefore would likely have an effect on the final exit velocity of the fluid from the nozzle.

7.3.2.2 Geometry

The geometry of Technology A was estimated by applying a scaling factor to the schematic in Figure 7-3 of 10mm across the length of the pill. This factor was chosen by looking at the comparison of the device to a 500mg Tylenol capsule in Figure 7-4.

Figure 7-4 Comparison of Technology A (right) to Tylenol Capsule.

The scaling factor was applied to the schematic in ImageJ (Rasband, 1997-2017), and used to estimate the 2-D dimensions of Technology A, which were then translated into a 3-D model in COMSOL Multiphysics® (COMSOL AB).

A schematic of Technology A labeled with dimensions and a table with the matching measurements can be seen in Figure 7-6 and Table 7-1.

Table 7-1 Measurements of Important Parameters of Technology A

Parameter	Measurement (mm)	Parameter	Measurement (mm)
d_o	4.5	l_nozzle	0.9
l_o	10.0	d_nozzle	0.2
l_i	8.3	h_transition	1.1
l_power	1.9	d_transition	2.0
th	0.5	Piston_Travel_Distance	2.6
l_piston	6.3	l_s_i	6.6
l_piston_z	4.1	stop_distance	0.6
d_i	3.5	t_back_nozzle	0.4
d_cone_bottom	0.6	t_wall_end	0.1
h_cone	0.4	t_back	1.2

Of note, due to the 10mm length and scaling size, the included volume in the drug reservoir is only 0.027 mL, calculated from the equation below. While there is room to grow the overall device size of Technology A, this volume is rather low in face of the range of volumes delivered for Amgen's commercial prodcuts (>1mL). This calculated volume will be used to validate the models in later sections of this thesis.

$$Volume_{Drug} = V_{reservoir} + V_{transition\ zone} + 2 * V_{nozzle} + 2 * V_{cone} \quad (10)$$

$$Volume_{Drug} = \pi l_{drug}\left(\frac{d_o - 2t}{2}\right)^2 + \pi h_{transition}\left(\frac{d_{transition}}{2}\right)^2 + 2\pi l_{nozzle}\left(\frac{d_{nozzle}}{2}\right)^2 + \frac{2\pi h_{cone}}{3}\left(\left(\frac{d_{nozzle}}{2}\right)^2 + \left(\frac{d_{cone}}{2}\right)^2 + \left(\frac{d_{nozzle}d_{cone}}{4}\right)\right) \quad (11)$$

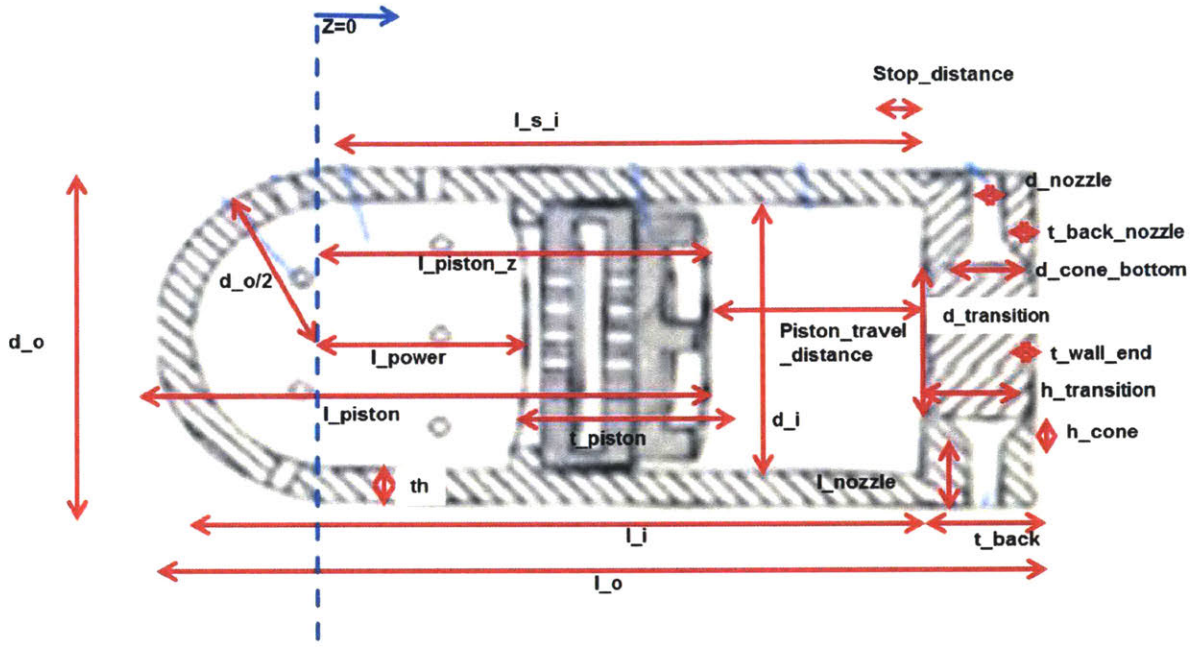

Figure 7-5 Schematic of Technology A with parameters measured from ImageJ and used in Model 1

A 3D model was then created in COMSOL Multiphysics® that allowed for the geometry to be manipulated as part of the studies (Figure 7-6 (a)). The geometry was then divided into four symmetrical partitions for ease of computation and efficiency when running the parametric studies (Figure 7-6 (b)).

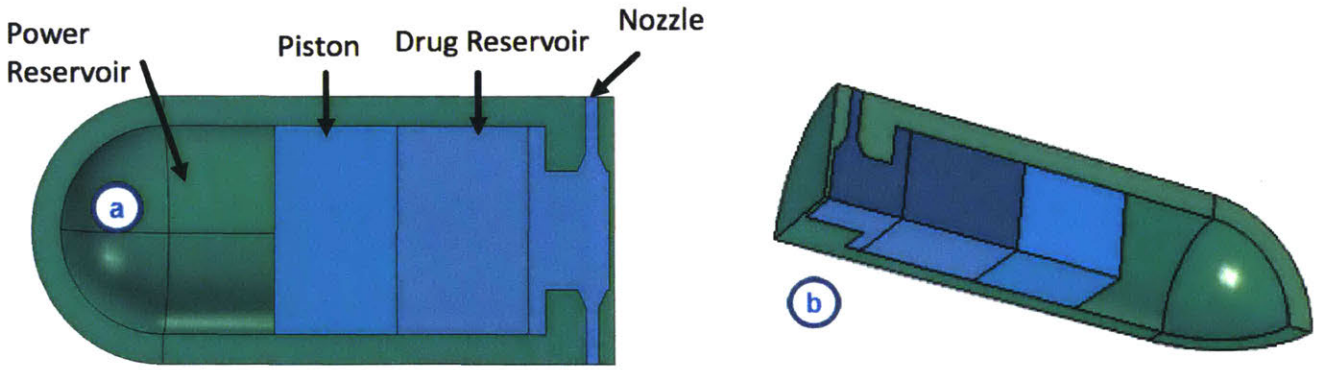

Figure 7-6 a) 3D representation of Technology A in COMSOL Multiphysics b) View of symmetric partition used for computational ease. The dark blue region containing the fluid drug product will be the only part of Technology A studied in the subsequent sections.

7.3.2.3 Laminar Flow

The Laminar Flow Multiphysics® module was used to simulate the flow of the drug product within Technology A.

7.3.2.3.1 Reynold's number calculations

This module was able to be used due to the relatively low Reynold's numbers expected for the exit velocity of the device. The Reynold's number was calculated as,

$$Re = \frac{\rho v_{exit} d_{nozzle}}{\mu} \quad (12)$$

Table 7-2 Reynold's Number Calculations

Nozzle Diameter (µm)	Dynamic Viscosity (mPa-s)	Velocity (mm/s)	Reynold's #
200	1	200	40
200	1	10000	2000
200	50	200	0.8
200	50	10000	40
200	25	200	1.6
200	25	10000	80
100	1	200	20
100	1	10000	1000
100	50	200	0.4
100	50	10000	20
100	25	200	0.8
100	25	10000	40

Where ρ is the density of the drug, assumed to be that of water at 1000 kg/m^3, v_{exit} is the exit velocity of the fluid, and d_{nozzle} is the diameter of the nozzle as the characteristic length of the pipe, and μ asthe dynamic viscosity in Pa-s. To make this assumption, representative values of the dynamic viscosity (1, 25, and 50 mPa-s) and nozzle diameter (100 and 200 µm) were used for calculations, along with a wide range of exit velocities. The minimum velocity used for calculation was 200 mm/s and the maximum value was 10,000 mm/s, to calculate a wide range of Reynold's numbers (Table 7-2). Although only applicable in a long, straight tube, a Reynold's number of ~2300 indicates that the flow has transitioned from the laminar to the turbulent regime. The flow parameters for Technology A do not come near this Reynold's number, even with highly exaggerated exit velocities.

7.3.2.3.2 Laminar Module and Boundary Conditions in COMSOL Multiphysics®

Given these calculations, the laminar flow module was used in COMSOL Multiphysics for the fluid within the drug reservoir, which solve the Navier-Stokes equations for conservation of momentum and the continuity equation for conservation of mass (COMSOL AB). Due to the incorporation of a moving mesh interface described in section 7.3.2.4.1, a weakly compressible flow was chosen. The reference temperature outside of the fluid of the system was set to 1[atm] and the reference temperature of the system was set to body temperature at 310 [K].

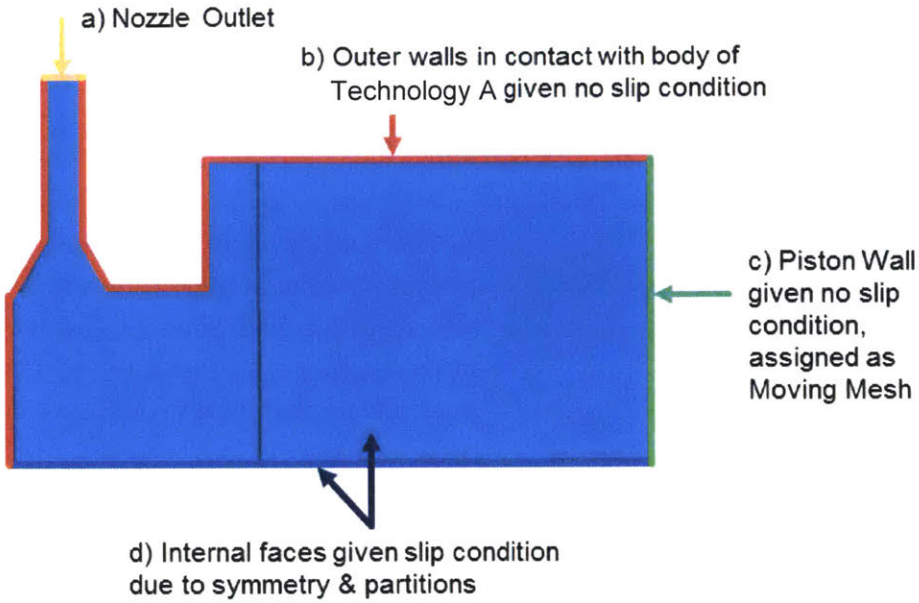

Figure 7-7 Boundary Conditions for Model 1

Initial values for the velocity field and pressure within the fluid was set to zero, and the boundary conditions for the fluid are described in Figure 7-7 for the symmetrical ¼ partition of the fluid in the device (recall from Figure 7-6 (b)).

In Figure 7-7 part a, the yellow line indicates the only outlet for the fluid from Technology A specified in the model. This nozzle outlet is where the exit velocity will be measured from as the output of the model.

In Figure 7-7 part b, the red lines indicate the walls that are prescribed a no-slip condition, consistent with what we would expect for a fluid in a laminar flow regime when in contact with a solid surface. The red lines all indicate where fluid is in contact with the actual body of the capsule, rather than in contact with another layer of fluid. The no-slip condition indicates that the velocity of the fluid at those walls is equal to zero.

In Figure 7-7 part c, the green line indicates the boundary between the piston and the drug reservoir. It is assigned a no-slip condition in the laminar flow module due to the contact between fluid and solid material, but is assigned a moving mesh condition described in Section 7.3.2.4.1.

In Figure 7-7 part d. the rest of the lines and faces that are shaded with dark and light blue indicate fluid surfaces that are in contact with other fluid layers, and are assigned a slip condition due to the ability of the layers to slide past each other in the laminar regime.

7.3.2.4 Ideal Gas Law

The ideal gas law was used to govern the movement of the piston against the fluid. In order to use this law effectively, a moving mesh and a series of global equations were required to get the desired results.

7.3.2.4.1 Moving Piston Boundary & Global Equations

A partition was included in the geometry of Technology A to indicate where the moving mesh should discontinue forward motion in the z-direction. This boundary was not placed at the realistic site of where the mesh would stop (see red arrow in Figure 7-8), but rather a small distance before it to allow for computational convergence (see black arrow in Figure 7-8). In section 7.3.2.2, the volume of drug product deliverable by Technology A was calculated to be 0.027 mL. However, due to the inclusion of the partition where the piston wall stops, the ejected volume is now limited to 0.018mL, since the drug product to the left of the vertical, black dotted line will not be ejected due the setup of the model. The volume ejected is equal to the cross-sectional area of the piston multiplied by the length that it moves, which is only 1.9mm. Further iterations of the model will look to account for this discrepancy.

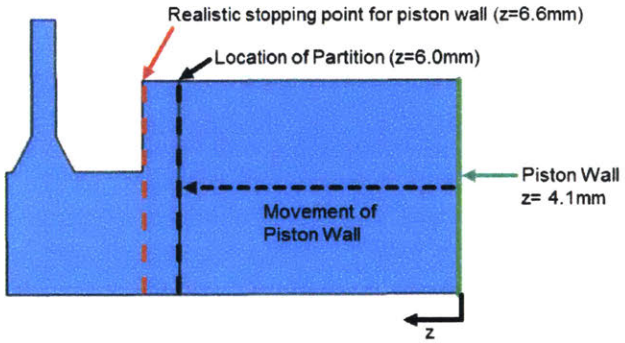

Figure 7-8 Movement of Moving Piston Boundary

The Moving Mesh module was applied to the fluid domains of the model. The region to the left of the partition line (z>6.25mm) was assigned as a fixed mesh, the partition boundary at z=6.25mm was prescribed a mesh displacement of zero, and the region to the right of the partition line (z<6.25mm) was assigned as a "Free Deformation" domain, with an initial deformation of zero in all directions. The piston wall boundary was prescribed a mesh velocity in the z-direction with the variable $piston_{velocity}$, which will be described in more detail below. The rest of the walls in the drug reservoir were prescribed a mesh displacement of zero in the x- and y-directions.

Prescription of the moving mesh allowed for simulation of the piston moving against the fluid. The velocity of the piston wall was determined through a series of global equations and variables described in the next section.

7.3.2.4.2 Reaction Efficiency and Ideal Gas Law

In the variable sections, three variables are defined to govern motion:

$$p_{piston} = p_{threshold} * \frac{volume_{initial}}{volume_{final}} \quad (13)$$

$$volume_{final} = volume_{initial} + A_{piston} * z_{piston} \quad (14)$$

$$F_{piston} = p_{stop\ piston} * A_{piston} \quad (15)$$

In the parameter section, the initial volume of carbon dioxide is defined:

$$volume_{initial} = efficiency_{reaction} * \left[A_{piston} l_{power} + \left(\frac{4}{3}\pi * \frac{d_i^3}{8}\right)\right] \quad (16)$$

In the global variable sections, the following global equations are defined:

$$0 = \frac{d(z_{iston})}{dt} - piston_{velocity} \quad (17)$$

$$0 = F_{piston} - (k_{damping} * piston_{velocity}) - F_{piston\ measured} \quad (18)$$

Table 7-3 describes the meaning of each of the terms in the equations above.

Table 7-3 Description of Parameters Governing Motion and Ideal Gas Law

Parameter	Description	Value (if constant)
p_{piston}	The pressure applied by the piston governed by the ideal gas law, assuming temperature is constant at 310 [K].	N/A
$p_{threshold}$	Threshold pressure assigned to nozzle outlet.	10, 30, or 50 [kPa]
$volume_{initial}$	Initial volume of the carbon dioxide in the power reservoir from the sodium bicarbonate and cirtic acid reaction.	2.95×10^{-9} m^3
$volume_{final}$	Final volume of the carbon dioxide in the power reservoir given the z displacement of the piston, assuming no additional carbon dioxide is produce by the reaction.	N/A
A_{piston}	Area of the piston	9.62×10^{-6} m^2
z_{piston}	The position of the piston relative to the starting position.	N/A
F_{piston}	The force the piston is applying to the water at any given time.	N/A
$piston_{velocity}$	The velocity of the piston at a given time.	N/A
$k_{damping}$	The damping coefficient used to govern the friction between the piston and the Technology A capsule, assumed to be a function of velocity. See assumptions section for more information	800 N*s/m
$F_{piston\ measured}$	Measure piston force through boundary probe set up on piston wall as an integral of the measured pressure at a given point in time.	N/A
$efficiency_{reactio}$	Assumed percentage of the total volume of the power reservoir that holds consist of carbon dioxide (for more information see assumptions section).	10 %
l_{power}	Length of cylindrical portion of power reservoir	1.9 mm
d_i	Inner diameter of power reservoir, used for calculation of the total volume of the hemi-spherical and cylindrical portions of the power reservoir.	3.5 mm

Through the equations above, the laws of motion in the model become apparent. Equation 13 describes how the pressure the piston applies to the fluid changes over time in accordance with the ideal gas law. The ideal gas law, described in Equation 19 below, describes how the pressure, volume, and temperature relate to each other for an ideal gas,

$$PV = nRT, \quad (19)$$

Where P is the pressure of the system, V is the volume of the gas, n is the amount of substance of the gas in [mols], R is the ideal gas constant (8.314 [J/K-mol]), and T is the temperature in [K]. Assuming that the temperature of the carbon dioxide does not change, and carbon dioxide neither enters nor escapes the system, the equality in Equation 20 can be made:

$$P_1 V_1 = P_2 V_2, \tag{20}$$

where the subscripts 1 and 2 indicate two points in time. Equation 20 is the same equality that is written in equation 13, with P_2 substituted for $p_{stop\ piston}$, P_1 substituted for $p_{threshold}$, V_1 for $volume_{initial}$, and finally V_2 for $volume_{final}$. $p_{threshold}$ is an input into the Model 1, chosen for parametric study.

The initial volume ($volume_{initial}$) described in equation 16 indicates the starting volume of carbon dioxide in the system at the time of deployment, assumed to be a fraction of the total volume of the power reservoir. The parameter $efficiency_{reaction}$ was arbitrarily chosen at 10%, but requires further study and information from the creators of Technology A to understand the power drive of the system.

The final volume of carbon dioxide in the system ($volume_{final}$) is described in equation 14, as the intial volume plus the additional space the carbon dioxide is allowed to fill into as the piston moves in the forward z direction (z_{piston}).

The force that is applied to the fluid ($F_{stop\ piston}$) is described in equation 15 simply as the pressure multiplied by the cross-sectional area.

In the global equations, further calculation is done to yield the desired input.

In Equation 18, the force the piston applies to the fluid (F_{piston}) less the frictional force it experiences with the body of the capsule of Technology A ($k_{damping} * piston_{velocity}$) should equal the measured piston force from the boundary probe that calculates data as the simulation runs ($F_{piston\ measured}$). $piston_{velocity}$ is calculated through integration of the force balance equation indicated in Equation 18.

Finally, the displacement of the piston (z_{piston}) is calculated through integration of Equation 17, which equates the derivative of the piston displacement to the piston velocity calculated in Equation 18. The value for the displacement (z_{piston}) is then fed back into Equation 14 for calculation of the volume.

Through these sets of equations, the model is able to calculate the displacement of and the force applied by the piston as it ejects fluid out of Technology A.

7.3.2.1 Mesh

Two different regions of mesh were used for computation. In Figure 7-9, the red dotted line indicates the transition between the two meshes. On the right, a swept mesh using a quadrilateral face meshing method that generates hexahedrons was chosen, using an extra course mesh on the inside, with a coarse mesh size chosen for all of the sides in contact with a boundary (cyan lines). To the left of the red dotted line, a free tetrahedral mesh is chosen, with extra coarse elements chosen for the inside, and a coarse size chosen for walls in contact with a boundary layer (cyan lines). The "no-slip" boundary walls are all indicated as boundary layers within the mesh (cyan lines), with the properties in Table 7-4.

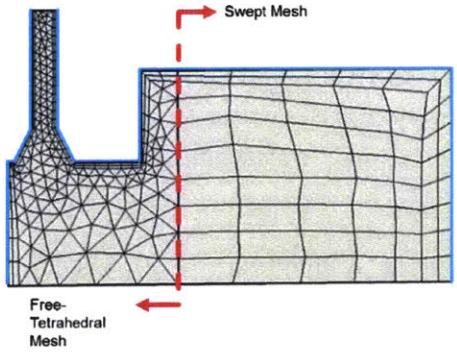

Figure 7-9 Mesh for Model 1

A coarse, swept mesh was chosen based on the need for efficient and smooth computation as the software solved for the moving mesh wall to the right of the red-dotted line. A free-tetrahedral mesh was used after the partition that indicates the "stop" for the piston movement to allow for more mesh elements to fill the space of the more complicated geometry to the left of the red-dotted line. The smallest elements of the mesh are located in the nozzle, which makes sense given that the velocity of fluid out of the nozzle was the desired output from Model 1.

Table 7-4 Mesh Properties for Model 1

Parameter	Extra Coarse	Coarse
Maximum Element Size	4.7e-4 m	2.35E-04
Minimum Element Size	1.17E-04	7.05E-05
Maximum Element Growth Rate	1.3	1.2
Curvature Factor	0.9	0.7
Resolution of Narrow Regions	0.4	0.6

Parameter	Boundary Layers
# of Boundary Layers	2
Boundary Layer Stretching Factor	1.2
Thickness Adjustment Factor	5

7.3.2.2 Deployment

Although specific studies that are executed are described in Section 7.3.2.4, this section outlines how the model deploys once a study is executed. The model starts as is seen in Figure 7-10 (a), and the piston wall continues to move towards the nozzle as the images progress from (a) to (d). This emulates how the piston would move in the actual device. During this deployment, measurements of the piston velocity,

displacement, force, and the fluid pressure and velocity are continuously monitored and recorded for post-processing and analysis.

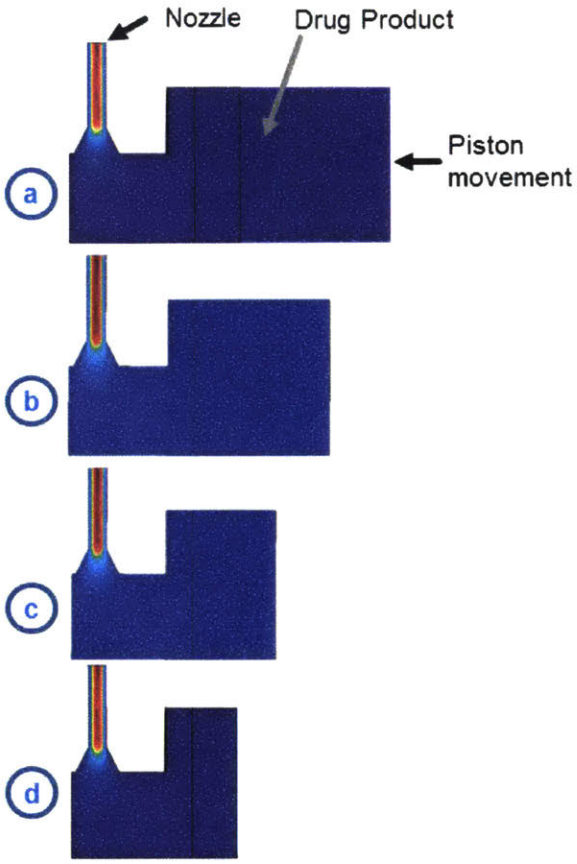

Figure 7-10 Model 1 deployment. Progressing from image (a)-(d), the piston boundary moves further towards the nozzle, simulating the movement of the piston in an actual device.

7.3.2.3 Assumptions & Simplifications

7.3.2.3.1 Friction

As indicated in Section 7.3.2.4.2, the friction force is a major input into the model that determines the physics of motion of the piston. The frictional force can affect the output results of Model 1. For instance, when the model was run without taking into account any frictional forces (i.e. $k_{damping} = 0$), the maximum velocities ranged from 449-16,892 mm/s much higher than the range of 36-925 mm/s tabulated in Table 7-12.

The value for the damping term ($k_{damping}$) was determined from separate testing conducted within Amgen to determine the damping coefficient for a standard syringe and plunger assembly. This assembly did not have the same size, dimensions, or materials as Technology A. Due to this, the actual damping coefficient should be determined via empirical testing of Technology A prototypes for continual

refinement of the model. Empirical testing of the damping coefficient of the actual device was out of scope for the LGO internship due to time constraints.

7.3.2.3.2 Reaction Efficiency

As indicated in Section 7.3.2.4.2, the reaction efficiency coefficient ($efficiency_{reaction}$) was assumed to be 10%. This coefficient is used to determine the fraction of the total volume of the power reservoir that was assumed to contain carbon dioxide at the time that the threshold pressure is reached. In reality, this fraction is likely influenced by multiple parameters, including but not limited to: threshold pressure, carbon dioxide loss through pH valves, reaction rate dynamics of carbon dioxide and citric acid, and the initial volume of the power reservoir that is filled with powdered propellant. Due to the fact that a lot of the design considerations for the propellant reservoir were unknown at the time the simulation was constructed, 10% was assumed as a conservative estimate of the volume.

7.3.2.3.3 Shear-thinning

Studies have shown that solutions of IgG1 and IgG2, well known large molecule constructs with approximate molecular weights of 150kDa (ThermoFisher Scientific, n.d.), do not experience significant shear thinning when concentrated at, and presumably above, 70 mg/ml (Gleason, Yee, Masatani, Middaugh, & Vance, 2016). Figure 7-11 shows the results of these studies, where solutions concentrated at 70 mg/ml do not vary viscosity over a large range of shear rates. Given that some of Amgen's self-administered commercial drugs are concentrated in proximity to or above 70 mg/ml (Table 7-5), shear-thinning behavior was not assumed to take place.

Table 7-5 Concentration of Self-Administered, Commercial Amgen Products

Drug	Concentration (mg/ml)	Source
Enbrel®	50	(Amgen, Inc.)
Repatha®	140	(Amgen, Inc.)

The shear rate was calculated using the maximum velocity and nozzle diameter from Table 7-12, yielding a range of 181-9246 s^{-1}. These shear rates represent a worst case scenario, as they assume steady flow at the maximum velocity. However, when calculated using the sustained flow from Table 7-12, the shear rates drop to 29-1259 s^{-1}. Given the high range of shear rates experienced in Technology A, some shear-thinning is likely to occur, and this phenomena should be measured for Amgen drug product of interest and incorporated into future iterations of Model 1.

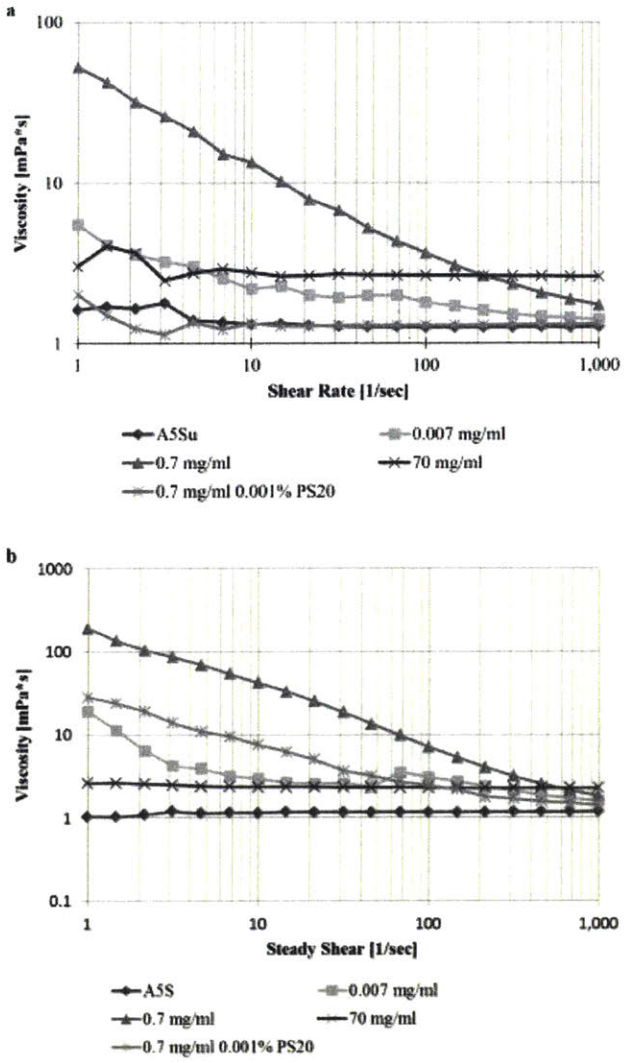

Figure 7-11 (a) Viscosity behavior of IgG1 at 3 different protein concentrations at 20 °C (0.007–70 mg/mL). (b) Viscosity behavior at varying concentrations of IgG2 at 20°C (0.007–70 mg/mL). Adapted from (Gleason, Yee, Masatani, Middaugh, & Vance, 2016).

7.3.2.3.4 Model drug product as water with varying viscosities

As a simplification, the liquid drug product was modeled as water that is varied in viscosity. This assumption applies to both Model 1 and Model 2. This same assumption is also employed by the creators of Technology A for the Ansys simulations done on earlier versions of the device (*Reference Redacted)*. In future iterations of the model, the Particle Tracking module in COMSOL Multiphysics® can be used for a microscopic view of the model, as opposed to the macroscopic view presented in this thesis.

7.3.2.3.5 Convective Flow

The flow out of Technology A (Model 1) and into the layers of the small intestine (Model 2) was assumed to be flow dominated entirely by convection, rather than diffusion. This assumption is justified by the

calculation of the Peclet number, which is the ratio between convective and diffusive flow. The Peclet Number (Pe) is described in the equations below for mass transfer,

$$Pe = \frac{convective\ transport\ rate}{diffusive\ transport\ rate}, \quad (21)$$

$$Pe = \frac{Lv}{D}, \quad (22)$$

$$D = \frac{RT}{6\pi N_o \mu r}, \quad (23)$$

Where L is the characteristic length (the diameter of the nozzle [m]), v is the local flow velocity (the velocity of the drug product as it exits the nozzle [m/s]), D is the mass diffusion coefficient, R is the ideal gas constant [J/mol-k], T is the temperature [K], N_o is the Avogadro's constant (6.02e23 [1/mol]), μ is the dynamic viscosity of the drug product [Pa-s], and r is the radius of the particle in question [m]. For proteins, studies have shown that the hydrodynamic radius of various monoclonal antibodies and fusion proteins lie between 5-10 [nm], and so the hydrodynamic radius is assumed to be 10 [nm] (Hawe, Hulse, Jiskoot, & Forbes, 2011).

Table 7-6 Peclet Number Calculations

Nozzle Diameter (m)	Dynamic Viscosity (Pa-s)	Velocity (m/s)	Mass Diffusion Constant (m^2/s)	Peclet #
0.0002	0.001	0.2	2.27054E-11	1.76E+06
0.0002	0.001	10	2.27054E-11	8.81E+07
0.0002	0.05	0.2	4.54109E-13	8.81E+07
0.0002	0.05	10	4.54109E-13	4.40E+09
0.0002	0.025	0.2	9.08217E-13	4.40E+07
0.0002	0.025	10	9.08217E-13	2.20E+09
0.0001	0.001	0.2	2.27054E-11	8.81E+05
0.0001	0.001	10	2.27054E-11	4.40E+07
0.0001	0.05	0.2	4.54109E-13	4.40E+07
0.0001	0.05	10	4.54109E-13	2.20E+09
0.0001	0.025	0.2	9.08217E-13	2.20E+07
0.0001	0.025	10	9.08217E-13	1.10E+09

In Table 7-6, for the same values used to assume laminar flow as in Table 7-2, the diffusion mass constant and Peclet number are calculated. Given that all of the Peclet numbers are well above 1, the assumption can be made that convective transport dominates over diffusive mass transport for both models. Therefore, the fluid moves via bulk mass transport properties, and the molecular weight of the particles and their concentrations are not taken into direct account in the simulation.

7.3.2.3.6 Temperature

The temperature of the entire Technology A system was assumed to be constant at body temperature (310 [K]). Assuming that the heating of Technology A has a first-order response, the time constant of the system is described by:

$$\tau = \frac{mc}{hA}, \quad (24)$$

Where τ is the time constant [s], m is the mass of the system [kg], h is the coefficient of heat transfer [W/m^2-k], c is the heat capacity [J/kg-K], and A is the surface area of Technology A [m^2]. For calculation purposes, the thermal conductivity is approximated by

$$h = \frac{k}{t}, \qquad (25)$$

where k is the thermal conductivity of material [W/m-K] and t is the thickness of the material, approximated as the radius of the capsule (2.5mm).

If the assumption is made that the Technology A capsule is solid and made of either plastic or water, time constants of 40 and 44 seconds are calculated (Table 7-7). At a value of 5* τ, the system is considered to be at 99% of the final equilibrium temperature value (University of Colorado, 2018), indicating that Technology A reaches equilibrium with body temperature between 200 and 220 seconds after the pill is swallowed. Considering that the minimum studied amount of time it takes for 10% of stomach contents to empty from the stomach is 56 minutes post-ingestion (Degen & Phillips, 1996), much longer than five times the time constant, the assumption of temperature equilibrium is made.

Table 7-7 Time Constant Calculations for Thermal Equilibrium of Technology A

Material	Density (kg/m^3)	Volume (m^3)	Mass (kg)	Surface Area (m^2)	Heat Capacity (J/(kg-K))	Thermal Conductivity of Material (W/(m-K))	Thickness (m)	Tau (s)
Plastic (General)	1140	1.96E-07	0.0002	0.00016	1670	0.3	0.005	**39.7**
Water	1000	1.96E-07	0.0002	0.00016	4187	0.6	0.005	**43.6**
Source	(Stelray, Inc., n.d.)				(The Engineering Toolbox, n.d.)	(The Engineering Toolbox, n.d.)		

Of note, the reaction of sodium bicarbonate and citric acid is endothermic, and could potentially cool down the surrounding Technology A device and drug product during reaction, depending on the relative time scales of the reaction and of device deployment. Given that there is a long time to reach thermal equilibrium, the assumption of an isothermal ejection of the liquid from Technology A needs to be further considered. This can be done in further iterations of modeling when the chemical reaction is taken into account in the COMSOL Multiphysics Model as well as during empirical testing of the device.

7.3.2.4 Study Design and Parametric Inputs to Model

In order to study their effect on exit velocity, a parametric sweep of the following parameters was employed: threshold pressure, nozzle diameter, and drug viscosity. Section 7.3.2.1 outlines the expected effect those parameters should have on the exit velocity of drug product out of the device nozzle. To recap, these parameters are described again below:

- **Threshold Pressure:** the internal pressure that Technology A needs to reach via the generation of CO_2 before the nozzles open, allowing for the release of drug product.
- **Nozzle Diameter:** the diameter of the exit nozzle where drug product exits Technology A.

- **Drug Viscosity:** the dynamic viscosity of the drug product contained in Technology A.

Table 7-8 Input Range for Parametric sweep

Drug Viscosity	mPa-s	1 - 50
Threshold Pressure	kPa	10-50
Nozzle Diameter	µm	100-200

The ranges for the different input parameters are described in Table 7-8. The viscosity of water is approximately 1-5 mPa-s, while the viscosity of corn syrup is between 50-100 mPa-s (The Composites Store, n.d.). Given this information and the knowledge of Amgen's commercial and pipeline assets, the range of 1-50 mPa-s was chosen for testing.

For threshold pressure, the earlier version of the technology, which was empirically tested, was designed with a 30 kPa threshold pressure, but was hypothesized to have the same effect with a 10 kPa pressure (*Reference Redacted*). Given this information, and the fact that in order to disrupt the epithelial barrier, the drug product may have to be delivered with more power, values of 10, 30, and 50 kPa were chosen as representative parameters for the threshold pressure input.

A typical lower limit size range is approximately 200 µm as a nozzle diameter. Given that the nozzle diameter is indirectly related to exit velocity (see Section 7.3.2.1), a smaller diameter was chosen for testing as well (100 µm).

Once the parameters were chosen, a time-dependent study was set up in COMSOL and took approximately 30 minutes to run on an HP EliteBook with an Intel® Core™ i7-6600U CPU Processor as it swept through the 24 different combinations of inputs. In order to get the appropriate granularity of data while balancing the need for efficient computation, data from the solution was stored at a higher frequency for the first .02 seconds, and at a lower frequency for the remaining time up until the limit of 50 seconds.

In order to allow the model to converge, stop-conditions were added to ensure that the model did not continue to solve for the full 50 seconds if the piston had reached its end condition. The equations below outline these stop conditions:

$$(1)\ z_{displacement} \geq piston_{travel\ distance} - stop_{distance} \quad (26)$$

$$(2)\ piston_{velocity} < 0 \quad (27)$$

The first equation looks at the displacement of the piston wall from its initial position (z=4.1mm) in relation to the partition that is set up, described in Table 7-5. The total piston travel distance that is allowed by the geometry is approximately 2.5mm, while the stop distance that is built into the partition is 0.5mm, allowing for a total travel distance of 1.9mm. Once the piston has moved further than this, the model stops computing.

The second equation ensures that if there are negative piston velocities due to erroneous input forces to the model, the piston does not move backwards in the negative z-direction.

Once the model is run, the pressure and velocity field is computed across the entire fluid domain for all times in question and can be post-processed rather easily to understand the effects of the input parameters to the model.

7.3.3 Outputs and Analysis

The model was run successfully for the 24 different combinations of input parameters.

7.3.3.1 Model Validation

Although no prototypes existed at the time for comparison of the simulated testing to empirical results, other methods of model validation were utilized to make sure the model was working as expected.

7.3.3.1.1 Exit velocity in range of Empirical Tests

Earlier versions of Technology A, although of a different design than the current version, measured the exit velocity of drug product from the device empirically for a threshold pressure of 30 kPa and a nozzle diameter of 200 µm (*Reference Redacted)*. This allowed for a direct comparison of the exit velocities from the *in silico* model to the empirically tested model, even though the two devices are of slightly different designs. Table 7-9 details the range of measured velocities for the earlier version compared to the model's prediction.

Table 7-9 Comparison of Velocity for Empirically Tested Earlier Prototype to the *In Silico* simulation for a threshold pressure of 30 kPa and a nozzle diameter of 200 microns

Empirical Testing Earlier Prototype	Model Prediction
50-200 mm/s	109-113 mm/s

While empirical testing resulted in a range of velocities between 50-200 mm/s, the model predicted between 109-113 mm/s, with the differences in exit velocity for the *in silico* predictions depending on the specific viscosity that was simulated. Even though the viscosity of the fluid used for the empirical measurements is not specified, the fact that the model predictions were within the range of the empirical testing serves as validation of the model.

7.3.3.1.2 Volume as expected based on setup

Table 7-10 Comparison between Contained Volume, Allowable Delivered Volume, and Predicted Volume output from Technology A

Current Design	Allowable Volume	Measured Volume	Without 10 kPa Runs
0.027 mL	0.018 mL	0.0169 ± 0.0015 mL	0.0177 ± 0.0058 mL

In section 7.3.2.2, the overall volume that the device contains is 0.027 mL, while the deliverable volume set up by the limitations of the model is calculated in section 7.3.2.4.1 to be 0.018 mL. In the model itself, a probe was set up to measure the output volume of the outlet based on the integration of the normal velocity to the outlet boundary. Because of the symmetry of the model, this value was then multiplied by 2 to obtain the total volume output from one nozzle, and then multiplied by 2 again in order to get the

total volume output by the two nozzles included in Technology A. When averaged across the 24 runs of the simulation, the average volume output was 0.0169 ± 0.0015 mL. These results are tabulated in Table 7-10.

This calculation represents some error, as ~94% of the allowable volume is ejected during the simulations. Of note, for the 6 runs conducted with an input threshold pressure of 10 kPa, the model does not completely deploy (i.e. the piston never reaches the stop condition), meaning that not all of the allowable volume will be measured as output. Taking these six runs out of consideration, the average increases to 0.018 ± 0.006 mL, the same value as the allowable volume.

Therefore, the conclusion is made that the model is working as expected in regard to mass conservation.

7.3.3.1.3 Delivery Time

Table 7-11 Comparison between delivery times for empirically tested earlier prototype and simulation of Technology A

Ejection Time Calculated for Earlier Prototype	Model Prediction – All Runs	Model Prediction – Runs with 30 kPa and 200 µm
16 s	28.1 ± 16.2 s	18.8 ± 1.2 s

The earlier version of Technology A indicates that its jet can penetrate the mucosa on the order of milliseconds and its delivery time is on the order of hundreds of milliseconds (*Reference Redacted)*. However, given that the maximum average velocity measured of the earlier prototype was 200 mm/s, with a nozzle diameter of 200 µm and a payload of 100 µL (0.1 mL) (*reference redacted)*, the expected delivery time is ~16 seconds if the maximum velocity was maintained over the entire ejection regime.

Given this calculation, and disregarding the claim that the entire ejection takes place within the range of a second, we can compare the ejection times from the *in silico* model to the empirical model. Indicated

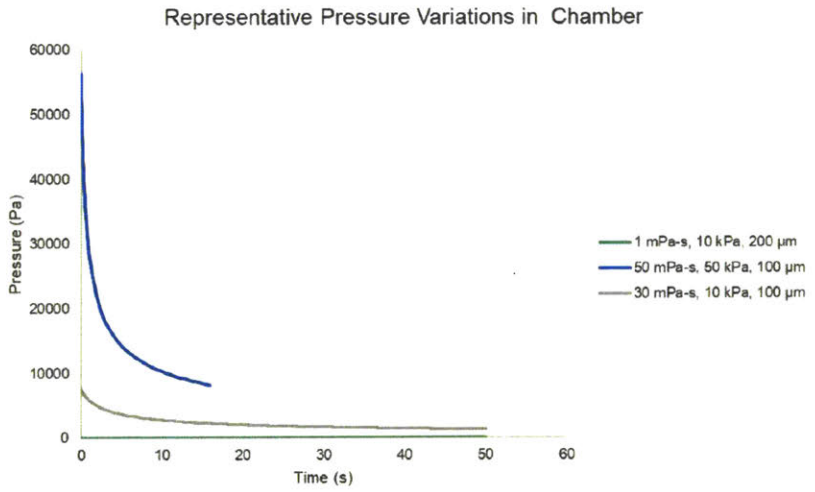

Figure 7-12 Representative Pressure Profiles measured from point evaluation in Model 1

in Table 7-11, when the deployment times for all of the runs are averaged, we see a simulated ejection time of 28 seconds, which is much greater than the calculation for the ejection time from the earlier version of Technology A of 16 seconds. However, segmentation by the same parameters used in the a study of the earlier prototype (threshold pressure of 30 kPa and nozzle diameter of 200 μm) reveals an average ejection time of 18.8 ± 1.2 s by the simulation, which is within the range of the ejection time described in the earlier study. Therefore, the conclusion is made that the model is working as expected in regard to expected delivery time.

7.3.3.1.4 Pressure

Three representative pressure profiles are exhibited in Figure 7-12, with the indicated point of measurement within the drug reservoir chamber indicated in Figure 7-13. The three pressure profiles in Figure 7-12 correlate to cases b (green line), n (blue line), and i (gray line) in Figure 7-12. These pressure profiles make sense, as the case with the highest threshold pressure and smaller nozzle diameter has a relatively higher pressure profile than those with smaller input pressures and nozzle diameters.

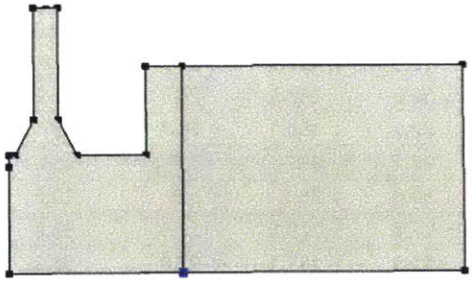

Figure 7-13 Point for Evaluation in Figure 7-12 highlighted in Blue

7.3.3.2 Exit Velocity

The main outputs of interest were the exit velocity profiles from Technology A. These profiles were analyzed, and then select profiles were chosen for input into Model 2, for simulation of the ejection into the small intestinal wall. In Table 7-12, the characteristics of the velocity profile are detailed for the 24 combinations of input parameters. In the case column, the runs labeled with a number were chosen for input into Model 2, while those indicated with a letter were not. The reasoning behind selection will be detailed in later sections.

Table 7-12 Output Velocity Profile Characteristics for 24 combinations of input parameters

Case	Viscosity (mPa-s)	Threshold Pressure (kPa)	Nozzle (μm)	Ejection Time (s)	Max Velocity (mm/s)	Sustained Velocity (mm/s)	Average Velocity (mm/s)	Ejected Volume (mL)	Reynold's #
1	**1**	**10**	**100**	**50.0**	**184.4**	**27.6**	**90.5**	**0.016**	18.4
a	1	30	100	21.5	564.3	74.6	344.5	0.016	56.4
2	**1**	**50**	**100**	**13.0**	**924.7**	**125.9**	**637.3**	**0.017**	92.5
b	1	10	200	50.0	37.4	5.8	18.2	0.016	7.5
c	1	30	200	19.0	113.2	16.4	70.8	0.018	22.6
d	1	50	200	12.5	188.9	26.2	128.0	0.018	37.8
e	10	10	100	50.0	162.8	26.3	82.0	0.015	1.6
3	**10**	**30**	**100**	**22.1**	**496.1**	**68.7**	**137.7**	**0.018**	5.0
f	10	50	100	12.7	837.7	117.1	253.1	0.018	8.4
g	10	10	200	50.0	36.9	5.8	10.6	0.016	0.7
h	10	30	200	17.6	110.9	16.9	33.8	0.018	2.2
6	**10**	**50**	**200**	**11.5**	**185.1**	**27.0**	**58.3**	**0.018**	3.7
i	30	10	100	50.0	141.1	24.5	43.7	0.014	0.5
j	30	30	100	23.5	425.4	62.1	121.7	0.018	1.4
4*	**30**	**50**	**100**	**16.4**	**712.4**	**96.0**	**201.1**	**0.018**	2.4
k	30	10	200	50.0	36.5	5.8	10.5	0.016	0.2
7	**30**	**30**	**200**	**20.5**	**109.7**	**15.6**	**31.3**	**0.018**	0.7
l	30	50	200	12.2	182.8	26.2	56.3	0.017	1.2
m	50	10	100	50.0	125.1	23.0	40.6	0.013	0.3
5	**50**	**30**	**100**	**27.6**	**376.4**	**54.0**	**104.5**	**0.018**	0.8
n	50	50	100	15.9	628.8	91.6	188.3	0.017	1.3
8	**50**	**10**	**200**	**50.0**	**36.2**	**5.7**	**10.5**	**0.016**	0.1
o	50	30	200	18.2	108.7	16.5	32.9	0.017	0.4
p	50	50	200	10.9	181.1	27.5	59.1	0.017	0.7

*This was chosen as a velocity profile to run in the Model 2, but the simulation never successfully converged to a singular solution.

Figure 7-14 graphs all of these velocity profiles into one image, and at a glance does not allow for much information to be gleaned for sense making. However, further segmentation in the following sections allows conclusions to be drawn about the most significant parameters affecting exit velocity. Some of the velocity curves end early due to their short deployment times (see Table 7-12).

The maximum velocity ranged from 36 to 920 mm/s depending on the input parameters, and the average velocity was 287 ± 267 mm/s, indicating that the input parameters do have a significant effect on the exit

velocity. Of note, none of the simulations with a threshold pressure of 10 kPa fully deployed, indicating that this pressure does not allow the piston to overcome the frictional forces incorporated into the model.

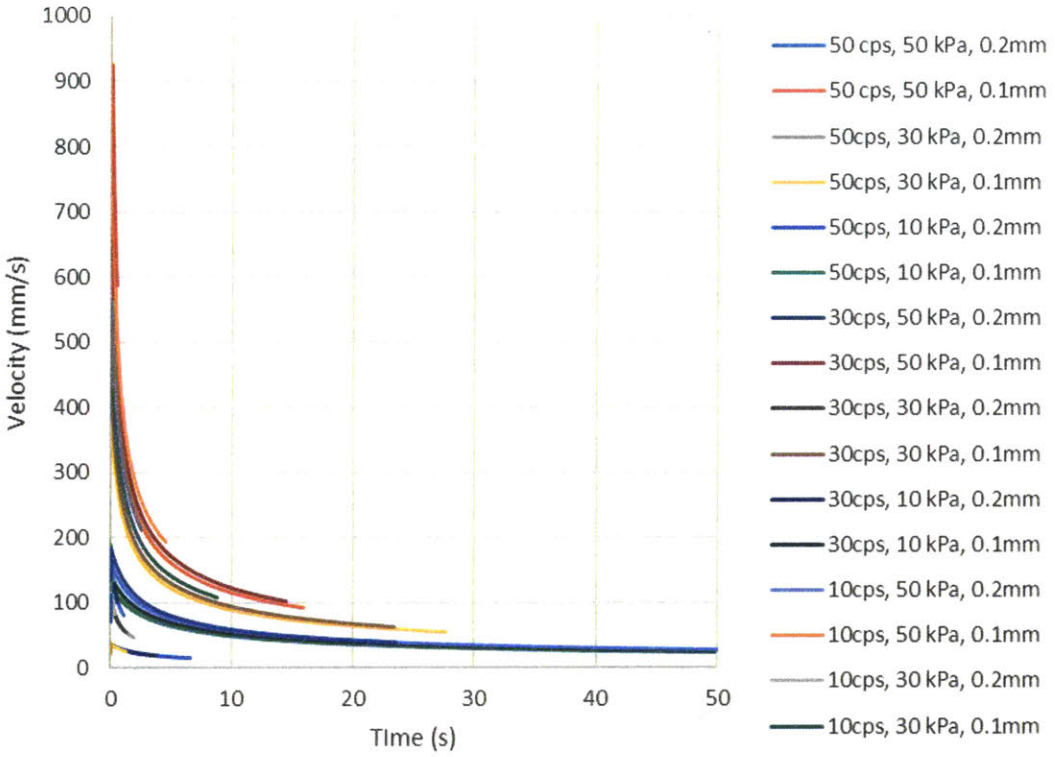

Figure 7-14 Output velocity profiles for all 24 combinations of input parameters

In Figure 7-15, all velocity profiles can be seen on a short time scale, where it is evident that the maximum velocity occurs prior to 0.0002 seconds. This is consistent with the calculated expected times to reach maximum velocity based on Euler's Equation, which considers that inertia is a major factor in periods of large acceleration. Using the simplified formula below for Euler's equation,

$$\Delta p = \rho \frac{v\_max}{t\_max} l\_nozzle \qquad (28)$$

With Δp approximated as the threshold pressure, v_max as the maximum velocity, ρ as the density of the liquid, and l_nozzle as the length of the nozzle, the time to reach maximum velocity can be approximated. These values ranged from 0.1-2.2 μs for all of the runs, consistent with Figure 7-15 below. Thus, the model is working as expected.

When the graph in Figure 7-14 is normalized by dividing the velocity profile by the threshold pressure used in each run, and multiplying the time by the threshold pressure, the resulting graph can be seen in Figure 7-16 All runs with Velocity divided by threshold pressure and time multiplied by threshold pressure Normalizing the data in this way indicates that nozzle diameter and threshold pressure are the main two

determinants of exit velocity from Technology A, since normalization with threshold pressure leads to clear segmentation in the resulting groupings of runs by the nozzle diameter. Of note, however, is that for the 0.1mm nozzle, there is more fine segmentation by viscosity between the runs; the lower viscosities achieve higher velocities, while the larger viscosities exit the nozzle at slightly lower velocities. This indicates that viscous effects only have an apparent effect on velocity when a smaller nozzle diameter is used.

This is consistent with what we see regarding the changes in friction discussed in section 837.3.2.3.1. As the friction between the plunger and the body of Technology A is decreased to zero, the maximum velocities increase by ~10-fold. This indicates that the most important factor to output velocity may be the friction in the plunger. The friction affects the pressure drop that occurs across the path from the piston to the exit nozzle, thereby affecting the resultant exit velocity. As the velocity of the piston is different for the same input pressure with different friction coefficients, the outlet diameter and that initial input of threshold pressure should be the only two factors that make a huge impact on the exit velocity.

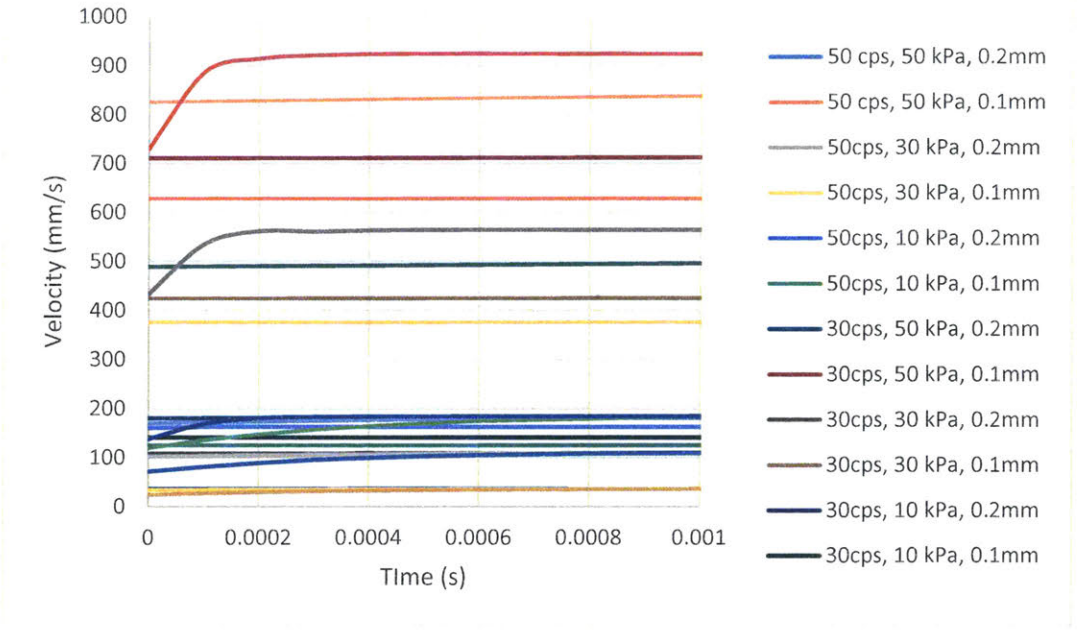

Figure 7-15 All velocity profiles at short timescale

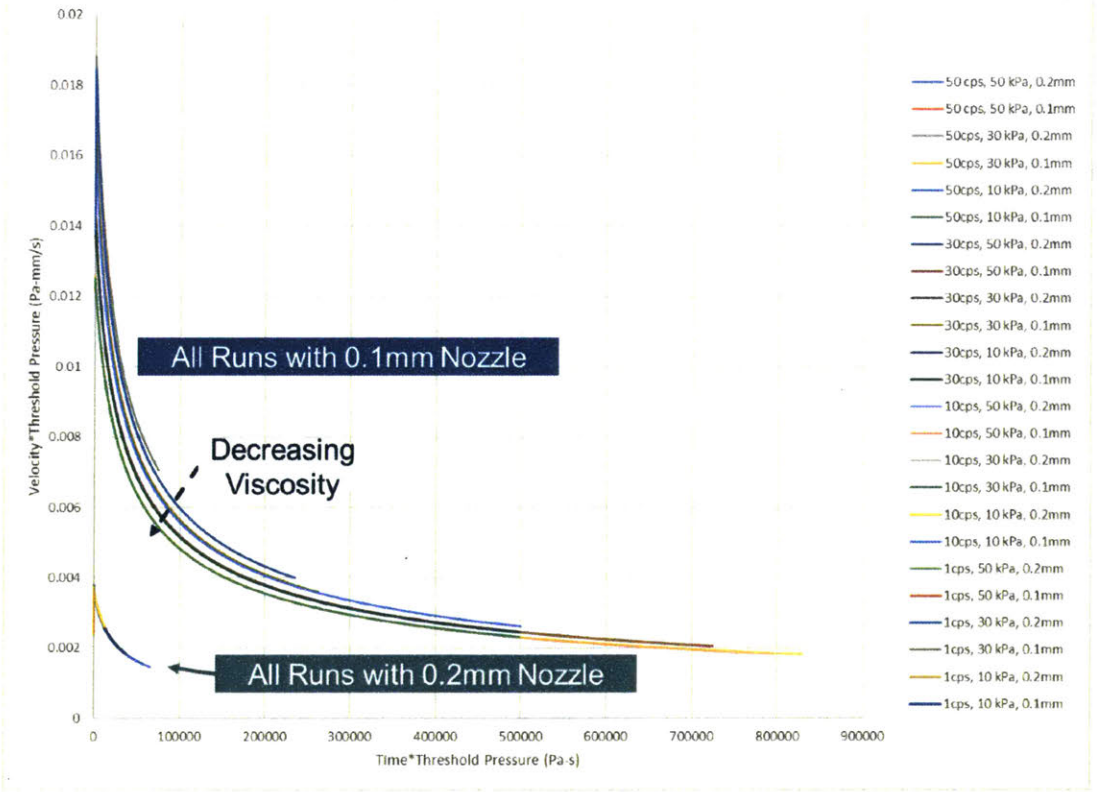

Figure 7-16 All runs with Velocity divided by threshold pressure and time multiplied by threshold pressure

7.3.3.2.1 Relationship to Viscosity

As indicated in section 7.3.2.1, the exit velocity of the fluid is expected to be inversely related to the dynamic viscosity if viscous effects dominate, although the initial findings in Figure 7-16 already seem to negate that. In Figure 7-17, the velocity profiles are segmented by the viscosity input, with four graphs detailing the output from all runs with the 1, 10, 30, and 50 mPa-s viscosity respectively.

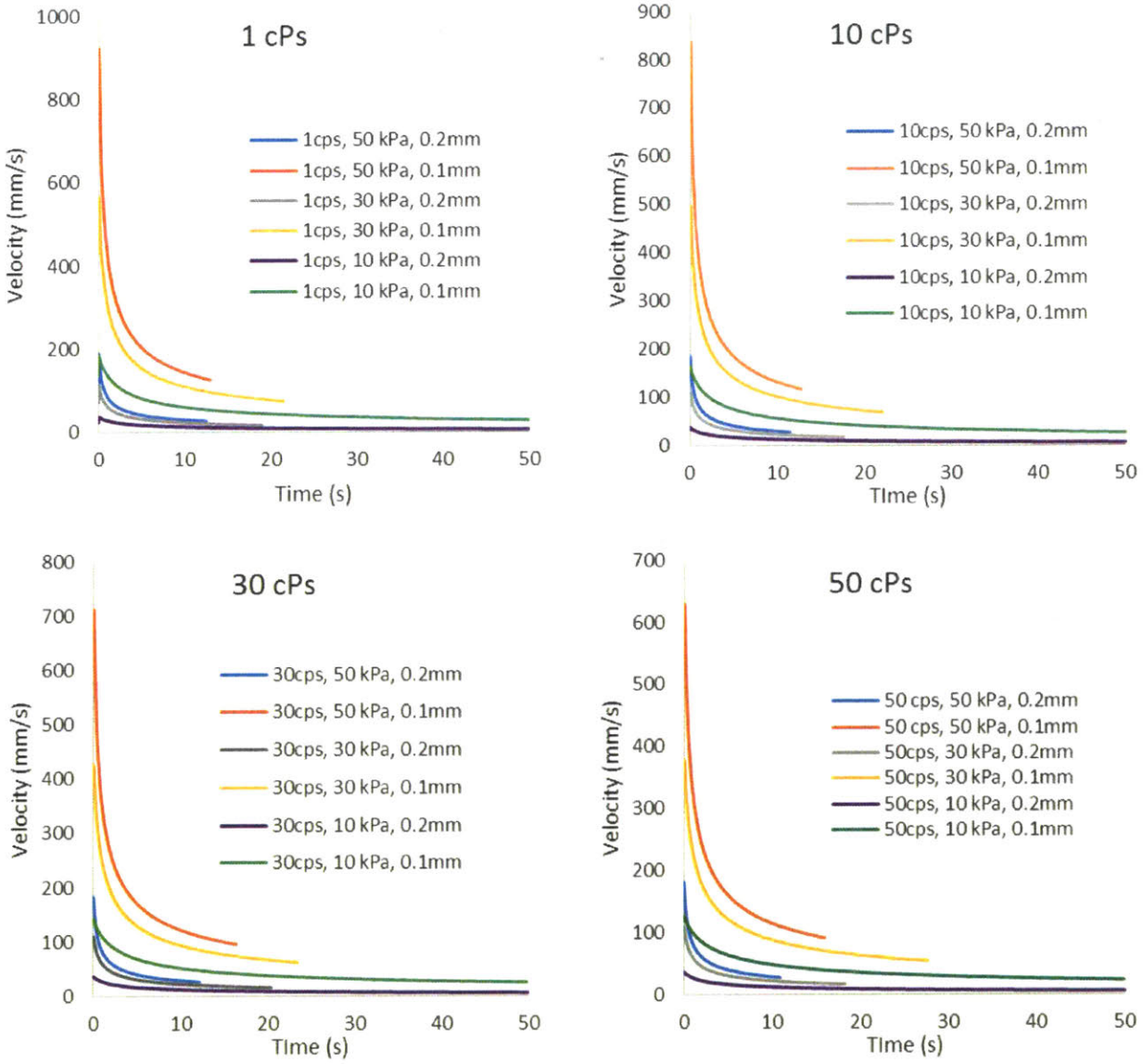

Figure 7-17 Comparison of ejection profiles segmented by viscosity

When segmented this way, it is not entirely clear that viscosity plays a large role due to the similarity between the four graphs. In each of the four graphs, there is a clear hierarchy for both the maximum and sustained velocity rankings within each viscosity segmentation. In all of the above graphs the maximum velocity is ranked in descending order by the following parameters:

1. 50 kPa, 0.1mm (orange line)

2. 30 kPa, 0.1mm (yellow line)
3. 50 kPa, 0.2mm (blue line)
4. 10 kPa, 0.1mm (green line)
5. 30 kPa, 0.2mm (gray line)
6. 10 kPa, 0.2mm (purple line)

While sustained velocity takes on a slightly different order:

1. 50 kPa, 0.1mm (orange line)
2. 30 kPa, 0.1mm (yellow line)
3. **10 kPa, 0.1mm (green line)**
4. **50 kPa, 0.2mm (blue line)**
5. 30 kPa, 0.2mm (gray line)
6. 10 kPa, 0.2mm (purple line)

These rankings persist regardless of the viscosity, as simulations run with the highest threshold pressure and smaller nozzle diameter should have the highest exit velocities, as hypothesized in section 7.3.2.1. Of note, there is a switch between the ranking for maximum and sustained velocity; for maximum velocity, the run with a threshold pressure of 50 kPa and nozzle diameter of 0.2mm has a higher maximum velocity compared to the run with 10 kPa and 0.1mm, while their relative rankings are switched when looking at the sustained, or ending velocity, for the different runs.

In comparison of velocities in Table 7-13Figure 7-17, there is not a large difference in the maximum and sustained velocities achieved by the different viscosities. Although there are differences present, more notably in the comparison between maximum velocities, the larger driver in exit velocity seems to be the threshold pressure and nozzle diameter, within a given viscosity input. This is consistent with the conclusions drawn from Figure 7-16, indicating that nozzle diameter and threshold pressure have the most significant effect on output velocity.

Table 7-13 Comparison of Maximum and Sustained Velocities across various viscosities

		Maximum Velocity (mm/s)				Sustained Velocity (mm/s)			
Threshold Pressure (kPa)	Nozzle Diameter (mm)	1 mPa-s	10 mPa-s	30 mPa-s	50 mPa-s	1 mPa-s	10 mPa-s	30 mPa-s	50 mPa-s
10.0	0.1	184.4	162.8	141.1	125.1	27.6	26.3	24.5	23.0
30.0	0.1	564.3	496.1	425.4	376.4	74.6	68.7	62.1	54.0
50.0	0.1	924.7	837.7	712.4	628.8	125.9	117.1	96.0	91.6
10.0	0.2	37.4	36.9	36.5	36.2	5.8	5.8	5.8	5.7
30.0	0.2	113.2	110.9	109.7	108.7	16.4	16.9	15.6	16.5
50.0	0.2	188.9	185.1	182.8	181.1	26.2	27.0	26.2	27.5

7.3.3.2.2 Relationship to Nozzle Diameter

As indicated in section 7.3.2.1, the exit velocity of the fluid is expected to be inversely related to the nozzle diameter. The exit velocity profiles are segmented by nozzle diameter in Figure 7-18, revealing that there is a strong relationship between the threshold pressure and the output velocity.

When segmented by the 200 µm nozzle diameter (graph a), there are three clear groupings of runs, characterized by the threshold pressure simulated. The green grouping consists of runs conducted with 50kPa threshold pressure, while red indicates 30 kPa, and blue for 10 kPa. In graph a, there are 24 velocity profiles plotted, but the groupings are so tight that only 3 velocity profiles appear to be plotted.

Similarly, when segmented by the 100 µm nozzle diameter (graph b), there is still segmentation by threshold pressure, but this segmentation is more stratified across the different viscosities. The graph indicates that as the viscosity increases across a given group, there is a slower velocity profile.

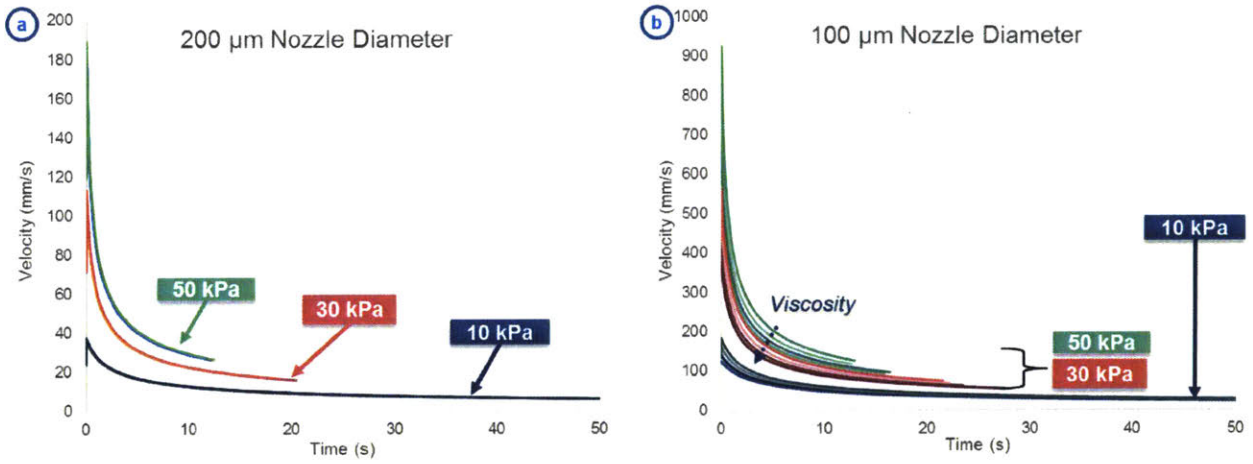

Figure 7-18 Segmentation by nozzle diameter reveals threshold pressure as a significant parameter

Table 7-14 Analysis by nozzle diameter reveals relationship to exit velocity

		Maximum Velocity (mm/s)		Sustained Velocity (mm/s)	
Viscosity (mPa-s)	Threshold Pressure (kPa)	0.1mm	0.2mm	0.1 mm	0.2 mm
1	10	184.4	37.4	27.6	5.8
1	30	564.3	113.2	74.6	16.4
1	50	924.7	188.9	125.9	26.2
10	10	162.8	36.9	26.3	5.8
10	30	496.1	110.9	68.7	16.9
10	50	837.7	185.1	117.1	27.0
30	10	141.1	36.5	24.5	5.8
30	30	425.4	109.7	62.1	15.6
30	50	712.4	182.8	96.0	26.2
50	10	125.1	36.2	23.0	5.7
50	30	376.4	108.7	54.0	16.5
50	50	628.8	181.1	91.6	27.5

These findings indicate that both nozzle diameter and threshold pressure have a strong effect on the output velocity. When the maximum and sustained velocities are compared across the same viscosity and threshold pressure for the two possible nozzle diameters in Table 7-14, it is revealed that the nozzle diameter plays a big role in both the maximum and sustained velocities. For example, looking at the runs with a viscosity of 1 mPa-s and a threshold pressure of 10 kPa, the maximum velocity achieved for the 100

µm nozzle is 184 mm/s, compared to 37 mm/s for the 200 µm nozzle, which is a difference of a factor of 5.

These findings are also consistent with the conclusions drawn from Figure 7-16, indicating that nozzle diameter and threshold pressure have the biggest effects on output velocity.

7.3.3.2.3 Relationship to Threshold Pressure

As indicated in section 7.3.2.1, the exit velocity of the fluid is expected to be directly correlated to the threshold pressure. This was evident in Figure 7-18, where when segmented by nozzle diameter, the exit velocity increased as the threshold pressure increased.

Segmentation by threshold pressure revealed that there was a strong dependence on nozzle diameter, evident in Figure 7-19. In each of the three graphs (a)-(c), the runs conducted with a 100 µm nozzle had faster maximum and sustained velocities than those conducted with a 200 µm nozzle.

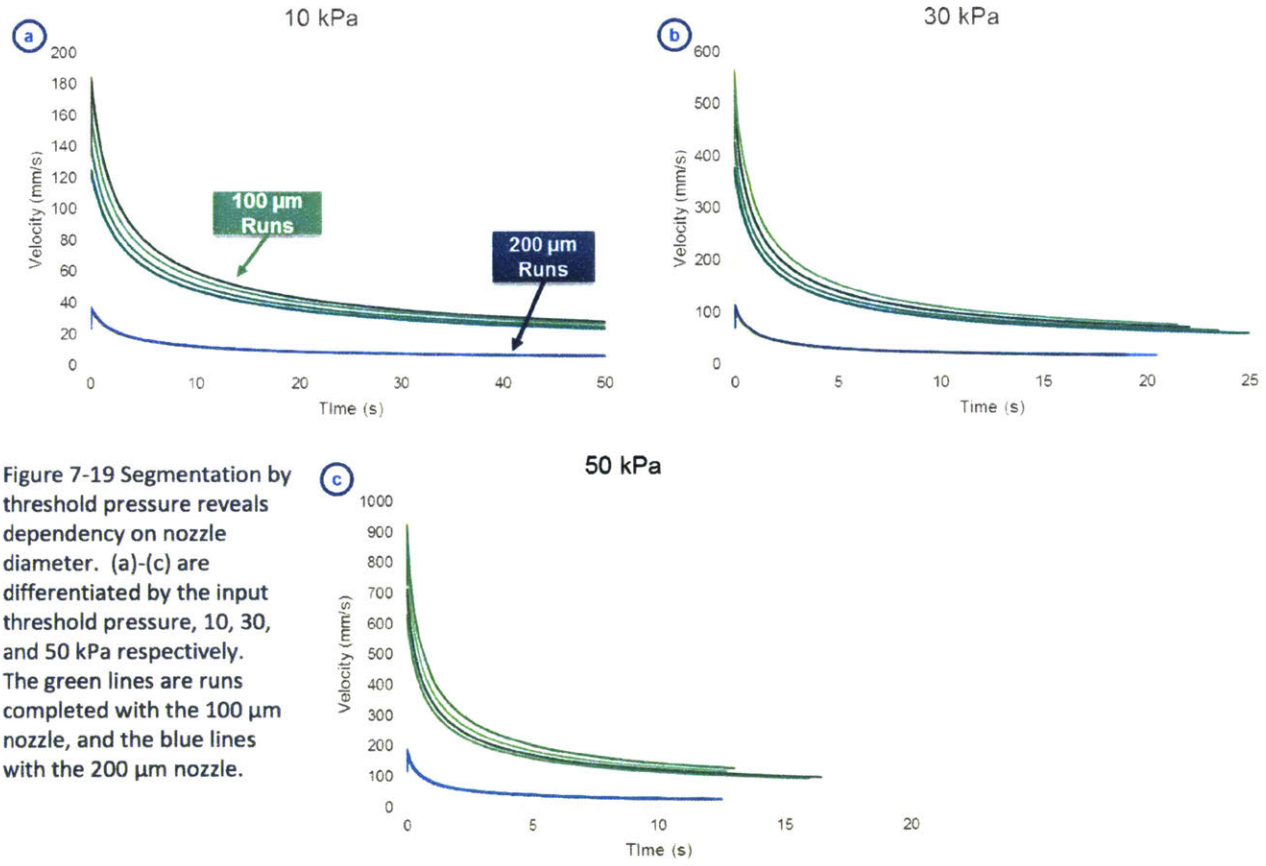

Figure 7-19 Segmentation by threshold pressure reveals dependency on nozzle diameter. (a)-(c) are differentiated by the input threshold pressure, 10, 30, and 50 kPa respectively. The green lines are runs completed with the 100 µm nozzle, and the blue lines with the 200 µm nozzle.

Table 7-15 details the maximum and sustained velocities for the same viscosity and nozzle diameter inputs across the different threshold pressures. It is evident from this table that as the threshold pressure is increased for a given set of inputs, the maximum and sustained velocities increase. For example, with a viscosity of 1mPa-s and a nozzle diameter of 100 µm, the maximum velocity increases from 184 mm/s to 925 mm/s and the sustained velocity increases from 28 mm/s to 126 mm/s when the threshold pressure is increased from 10 kPa to 50 kPa. This relationship occurs for all combinations of input viscosity and

nozzle diameter. These findings are also consistent with the conclusions drawn from Figure 7-16, indicating that nozzle diameter and threshold pressure have the biggest effects on output velocity.

Table 7-15 Segmentation by threshold pressure reveals dependency on nozzle diameter

		Maximum Velocity (mm/s)			Sustained Velocity (mm/s)		
Viscosity (mPa-s)	Nozzle Diameter (mm)	10 kPa	30 kPa	50 kPa	10 kPa	30 kPa	50 kPa
1	0.1	184.4	564.3	924.7	27.6	74.6	125.9
1	0.2	37.4	113.2	188.9	5.8	16.4	26.2
10	0.1	162.8	496.1	837.7	26.3	68.7	117.1
10	0.2	36.9	110.9	185.1	5.8	16.9	27.0
30	0.1	141.1	425.4	712.4	24.5	62.1	96.0
30	0.2	36.5	109.7	182.8	5.8	15.6	26.2
50	0.1	125.1	376.4	628.8	23.0	54.0	91.6
50	0.2	36.2	108.7	181.1	5.7	16.5	27.5

7.3.3.2.4 Regression Analyses

The previous three sections indicate that nozzle diameter and threshold pressure seem to have the greatest effect on exit velocity, while the viscosity has a more minor effect once a nozzle diameter and threshold pressure have been chosen. While the general relationships make sense based on the hypotheses made in previous sections, the disparity between the magnitude of the resulting effect on exit velocity from the nozzle diameter and threshold pressure and viscosity is surprising.

Table 7-16 Values for Regression Analysis for Maximum Velocity

Term	Coef	SE Coef	T	P
Constant	503.6	94.7	5.3	0.000
Threshold Pressure (kPa)	10.1	1.6	6.4	0.000
Nozzle (mm)	-3410.2	522.3	-6.5	0.000

General regression analyses were performed with Minitab 16 Statistical Software® (Minitab, Inc., 2010) to confirm which parameters were statistically significant. When the maximum velocity was analyzed with all three input parameters as independent variables, the viscosity had an insignificant p-value (p=0.264). When the viscosity was removed from the equation, the following regression was calculated with significant p-value for all variables (Table 7-16):

$$Max\,Velocity = 503.6 + 10.1 * Threshold\,Pressure - 3410.2 * Nozzle \qquad (29)$$

This model has an R-squared value of 82.4%, indicating that the regression fits the data pretty well. As expected, the threshold pressure has a positive coefficient due to its direct relationship to exit velocity, and the nozzle diameter has a negative coefficient due to its inverse relationship to maximum velocity.

However, the regression indicates that a maximum velocity of 503.6 mm/s is possible if all parameters values are equal to zero, which would be impossible in reality.

When a regression was run to model the sustained velocity, the viscosity was yet again found to be insignificant (p-value = 0.35). When re-run using only nozzle diameter and threshold pressure as input variables, the following regression was calculated with an r-squared value of 84.4% (important regression parameters are tabulated in Table 7-17):

$$Sustained\ Velocity = 73.71 + 1.35 * Threshold\ Pressure - 481.04 * Nozzle\ Diameter \quad (30)$$

Table 7-17 Values for Regression Analysis for Maximum Velocity

Term	Coef	SE Coef	T	P
Constant	73.71	12.08	6.10	0.000
Threshold Pressure (kPa)	1.35	0.20	6.68	0.000
Nozzle (mm)	-481.04	66.63	-7.22	0.000

Similarly, the model has an acceptable R-squared value and coefficients make sense based on the relationship of the parameters. Once again, the regression indicates that a sustained velocity of 74 mm/s will be achieved if all inputs are set to zero, which is likely not possible.

Regardless of the regressions true interpretation in reality, they indicate that the viscosity will likely not impact the output velocity as much as other design inputs. This indicates that Technology A can be used as a platform technology, able to deliver a wide range of drugs without changes to the design of the device itself. While this finding needs to be validated with empirical testing, it serves as evidence to continue moving forward with investigation.

These findings are also consistent with the conclusions drawn from Figure 7-16, indicating that nozzle diameter and threshold pressure have the biggest effects on output velocity.

7.3.3.3 Friction Dominates Over Viscous Effects

The Reynold's numbers were calculated for the output velocity for all 24 combinations of Technology A using the same equation in section 7.3.2.3.1 using the necessary parameters in Table 7-12. The initial calculations in section 7.3.2.3.1 were calculated with representative values for the output flow, to justify the use of the Laminar flow module, and do not include the actual output velocities simulated via Model 1. When re-calculated with numbers from the results of the simulation, the Reynold's numbers range from 0.1 to 92.5, as seen in Table 7-12. However, 9 out of the 24 combinations of input parameters result in a Reynold's number less than one. This does not invalidate the model, since the model assume laminar flow, or Re<2300. Because the Reynold's number represents the ratio of the inertial forces to the viscous forces that determine fluid flow, the conclusion cannot be made that inertial or viscous effects dominate the fluid flow under this simulation.

To further corroborate that inertial forces do not play a significant role, Model 1 was run with a higher density of 10,000 kg/m^3. The resulting maximum velocities from Technology A were on the same order of magnitude as when run with a density of 1000 kg/m^3. Because the output velocity does not scale linearly with the density, this negates the possibility that inertial flow dominates over viscous flow. In some cases, the velocity increases marginally, while in others it decreases. This indicates that density does seem to make a difference when it is increased by a factor of ten, but the effects are small. This is consistent with the fact that the entire system is dominated by the friction of the piston.

Looking at viscous forces, peak velocities tend to scale linearly with the threshold pressure input, rather than the viscosity, suggesting that viscous forces are also not the dominant feature of the Navier Stokes equations.

Given these findings, fluid flow is likely to be influenced by both inertial and viscous forces under the current model setup. However, the Reynold's number is likely to change with the change in the input friction to the model. As mentioned in section 7.3.2.3.1 detailing the assumptions of Model 1, the resulting velocity of the output flow from the nozzle increases approximately by a factor of ten for all input parameters when run with no friction. This indicates that as the friction coefficient increases, the piston is harder to move, and the threshold pressure built up in the gas chamber cannot transfer as much energy to the drug product, resulting in a slower output flow. Therefore, as friction increases, the inertial forces of the fluid decrease, and the resulting Reynold's number also decreases. This seems to indicate that with a frictional coefficient lower than the one used, inertial forces may dominate; but if friction increases, this may drive viscous forces to dominate.

Therefore, in further iterations of the model as well as in empirical testing, special attention should be paid to friction between the piston and the body of the device, as this can significantly affect the output velocity from the nozzle of the device.

7.3.3.4 Jet Impact Pressure

The impact pressure from the jet can be estimated by using Bernoulli's law and assuming that Technology A is localized to the wall of the small intestine,

$$P_{impact} = \frac{1}{2} * \rho * v_{exit}^2 \qquad (31)$$

where P_{impact} is the impact pressure in Pa, ρ is the fluid density, and v_{exit} is the maximum velocity of the fluid. When calculated for the maximum velocities indicated in Table 7-12, the impact pressure ranges from of 0.7 Pa to 427 Pa. However, when the maximum pressure of the outlet velocity is derived from analysis in COMSOL, the maximum pressures range from 1.5 to 1467 Pa, which is slightly higher than that calculated with the Bernoulli equation.

Studies have shown that the cell adhesion force for epithelial cells is between 17-50 Pa (Gallant, Michael, & Garcia, 2005) (Hagerman, Chao, Dunn, & Wu, 2005) (Garcia & Boettiger, 1999). Figure 7-20 groups the values for impact pressure based on the cell adhesion strength range. The 15 (or 7 depending on the measurement system used) input combinations that yield pressures below 17.5 Pa will likely not be able to disrupt the epithelial barrier, due to the low impact pressure imparted by the jet on the wall of the

small intestine. However, those within the range of 17.5-50 Pa may be able to disrupt the barrier, depending on a number of factors including but not limited to the localization of Technology A to the small intestine wall and the force required to disrupt the mucus layer that sits on top of the epithelial barrier. Given that the cell-adhesion force is not the only force that governs the disruption of the epithelial barrier, empirical testing needs to be done to validate the forces needed to deliver drug product into the sub-epithelial space.

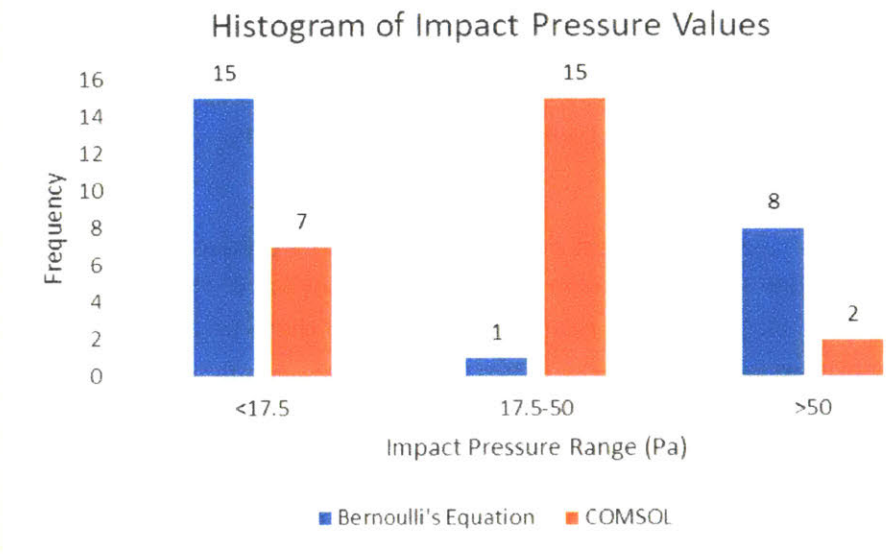

Figure 7-20 Histogram of Impact Pressure Values, grouped into bins depending on range of values

7.3.4 Conclusions

Model 1 was designed to simulate the effect of threshold pressure, drug viscosity, and nozzle diameter on the exit velocity of liquid drug product from Technology A. Simulation via COMSOL Multiphysics® revealed that the nozzle diameter and the threshold pressure are far more significant to the magnitude of the maximum and sustained exit velocity profiles than the viscosity of the drug product. Further testing needs to be performed to validate these claims, but this could possibly indicate Technology A as a platform technology, able to deliver multiple drugs of different viscosities using the same design.

However, it is noted that the friction between the piston and body of the device needs to be thoroughly understood in further iterations of the model and in any empirical testing, as this can have a large effect on the resulting output velocity. Therefore, in further iterations of the model, the friction should be considered as a design variable to calculate the optimal output velocity.

Furthermore, analysis of the impact pressure and cell adhesion force indicate that all but 9 combinations of the 24 possible are able to disrupt the epithelial barrier, when considering the cell adhesion force to the lamina propria. While other forces need to be accounted for, such as the force required to disrupt the mucus layer, this is a promising start to the investigation indicating the need for further empirical evaluation.

7.4 Model 2 – Drug Transport in Small Intestine

The second model was built to understand how the different exit velocity profiles from Model 1 travel through the various layers of the small intestine. This analysis allows for determination of the input parameters optimal for delivery efficiency, or stated differently, the volumetric percentage of drug product that remains in the sub-epithelial layers optimal for bioavailability, as described in the hypothesis in section 7.2.1.

The inputs to this model include 7 different velocity vs. time profiles imported from Model 1, and the outputs include, but are not limited to, the volumetric percentage of drug product in the lamina propria and muscularis mucosa after Technology A deployment and the pressure underneath the epithelial barrier to determine whether or not Technology A could compromise its integrity.

7.4.1 Hypothesis on Drug Transport

The exit velocity will likely have a large effect on the amount of drug product in the sub-epithelial layers of interest. Because the exit velocities are correlated to the input parameters of Model 1 – threshold pressure, viscosity, and nozzle diameter – relationships between these parameters and the volumetric percentage will likely exist as well.

In studies of jet injection for transdermal delivery, it is clear that the velocity of the fluid plays a clear role in the penetration depth of the drug product.

In a study by Tagawa et. al., a viscous shear model was developed to govern the dynamics of jet penetration (Tagawa, Oudalov, Ghalbzouri, Sun, & Lohse, 2013):

$$D_p = \frac{1}{c_v}\left(v_{fluid} - v_c\right) \qquad (32)$$

Where D_p is the final penetration depth, v_{fluid} is the velocity of the fluid at impact, v_c is the critical velocity needed to penetrate the interface of the material, and c_v is a fitting parameter with units of inverse time (Tagawa, Oudalov, Ghalbzouri, Sun, & Lohse, 2013). Given that there is a needed critical velocity to disturb the mucus and epithelial layers of the small intestine, the larger the velocity, the higher the probability of getting a suitable depth of penetration. However, there is a danger of overshooting in terms of penetration depth; if liquid breaks through all layers of the small intestinal wall and perforates, this could leave the patient at risk of infection and sepsis.

Similarly, another study developed a critical stress to failure model (Mitragotri, 2005). Baxter et. Al used the critical stress for the failure of a surface to derive a relationship to the depth of penetration from jet impingement using Bernoulli's law:

$$\sigma_c = \frac{1}{2}\rho v_{mc} \qquad (33)$$

Where σ_c is the critical stress required for failure, ρ is the density of fluid, and v_{mc} is the critical centerline velocity required to induce failure. This critical stress is currently undetermined for the mucus and epithelial layers of the small intestine, but could be experimentally determined via empirical testing.

Assuming jets with no backflow of fluid out of the created hole, the centerline velocity can be characterized as:

$$v_m = \frac{1}{2C_2}\frac{v_0 D_0}{x} \quad (34)$$

Where v_0 is the exit velocity from the device, D_0 is the nozzle diameter, C_2 is an experimentally determined constant characterizing the spread of the jet reported to be 0.081 for submerged turbulent jets, and x is the distance the jet has traveled from the nozzle exit. When v_m=v_0, x_0 can be solved for. When the equation, $x = D_p + x_s$, where x_s is the standoff distance (i.e. gap between substrate and nozzle exit) and $D_p$is the penetration depth is substituted in the above equation, the penetration depth in gel can be characterized as:

$$D_p = \frac{v_0 D_0}{2C_2}\sqrt{\frac{\rho}{2\sigma_c}} - x_s \quad (35)$$

In this equation, it is evident that the velocity of the jet is directly proportional to the penetration depth.

Although these equations were developed for turbulent jets, it is clear that the exit velocity should play a role in the ability of the liquid drug product to penetrate into a material and to disperse in the sub-epithelial layers of the small intestine.

7.4.2 Methodology

7.4.2.1 Selected Velocity Profiles for Analysis in Model 2

Simulation via Model 1 produced 24 velocity outputs based on the various combinations of input variables. Seven of these velocity profiles were chosen for analysis in Model 2 (

Table 7-18 Selected Velocity profiles for Analysis in Model 2).

Case	Viscosity (mPa-s)	Threshold Pressure (kPa)	Nozzle (μm)	Ejection Time (s)	Max Velocity (mm/s)	Sustained Velocity (mm/s)	Average Velocity (mm/s)	Ejected Volume (mL)
1	1	10	100	50.0	184.4	27.6	90.5	0.016
2	1	50	100	13.0	924.7	125.9	637.3	0.017
3	10	30	100	22.1	496.1	68.7	137.7	0.018
6	10	50	200	11.5	185.1	27.0	58.3	0.018
7	30	30	200	20.5	109.7	15.6	31.3	0.018
5	50	30	100	27.6	376.4	54.0	104.5	0.018
8	50	10	200	50.0	36.2	5.7	10.5	0.016

Table 7-18 Selected Velocity profiles for Analysis in Model 2

The selected velocity profiles represent a variety of maximum and sustained velocities, as well as varied inputs of viscosity, threshold pressure, and nozzle diameter. Case 4 never completed its computation within Model 2 due to a lack of convergence, and so was eliminated as a possible case for analysis.

Four different models were built for analysis, models a through d as described in Figure 7-21.

		Epithelium	
		With	Without
Nozzle Diameter (µm)	100	**a**	**c**
	200	**b**	**d**

Figure 7-21 Sub-models for Analysis in Model 2

Sub-models were created both with and without an epithelial barrier in order to simulate the inflow of drug product in both a compromised and intact state of the epithelial barrier. If the pressure generated underneath the epithelial barrier is greater than the cell adhesion force first described in section 7.3.3.4, it is postulated that the epithelial barrier may not be intact after Technology A deployment due to the pressure exerted by the drug product. Therefore, the flow of liquid drug product from Technology A is simulated in both conditions – with and without an epithelial barrier – to help determine whether or not Technology A is a viable method for delivery of large molecule drugs via the GI tract.

The two different geometries for the nozzle inlet were built in order to accurately reflect the conditions from which inlet velocity profiles were sourced. In the 100 µm nozzle models, cases 1,2,3 and 5 were analyzed, while in the 200 µm nozzle models, cases 6-8 were analyzed. Each velocity profile was uploaded as an interpolation function within the model itself and given a function name detailing the input variables used to generate the profile in model 1. For example, case 6 was named v_fric_10mPa-s_50kPa_02mm to reflect the input parameters used to generate it.

In order to run the analysis on the various equations sequentially, a set of equations were set up within the variables section to sweep through the various velocity profiles.

For the 100 µm nozzle models:

$$inlet_{velocity} = (case == 1) * \left(v_{fric_{1cps_{10kPa_{01mm(t)}}}}\right) + (case == 2) * \left(v_{fric_{1cps_{50kPa_{01mm(t)}}}}\right) + (case == 3) * \left(v_{fric_{10cps_{30kPa_{01mm(t)}}}}\right) + (case == 4) * \left(v_{fric_{30cps_{50kPa_{01mm(t)}}}}\right) + (case == 5) * (v\_fric\_50cps\_30kPa\_01mm(t)) \quad (36)$$

For the 200 µm nozzle models:

$$inlet_{velocity} = (case == 6) * \left(v_{fric_{10cps_{50kPa_{02mm(t)}}}}\right) + (case == 7) * \left(v_{fric_{30cps_{30kPa_{02mm(t)}}}}\right) + (case == 8) * (v\_fric\_50cps\_10kPa\_02mm(t)) \quad (37)$$

As the parametric study sweeps through the different cases, it will choose the inlet velocity interpolation function associated with that case due to the Boolean operators incorporated into the above equations. This inlet velocity function is then incorporated into the laminar flow module, which is further explained in section 7.4.2.3.

7.4.2.2 Geometry and Properties of Layers of Small Intestinal Wall

The geometry and properties of the small intestine wall were translated from studies and schematics sourced in the literature. Figure 7-22 depicts the layers of the small intestine, where the area denoted "mucous membrane" is of most interest to Technology A delivery.

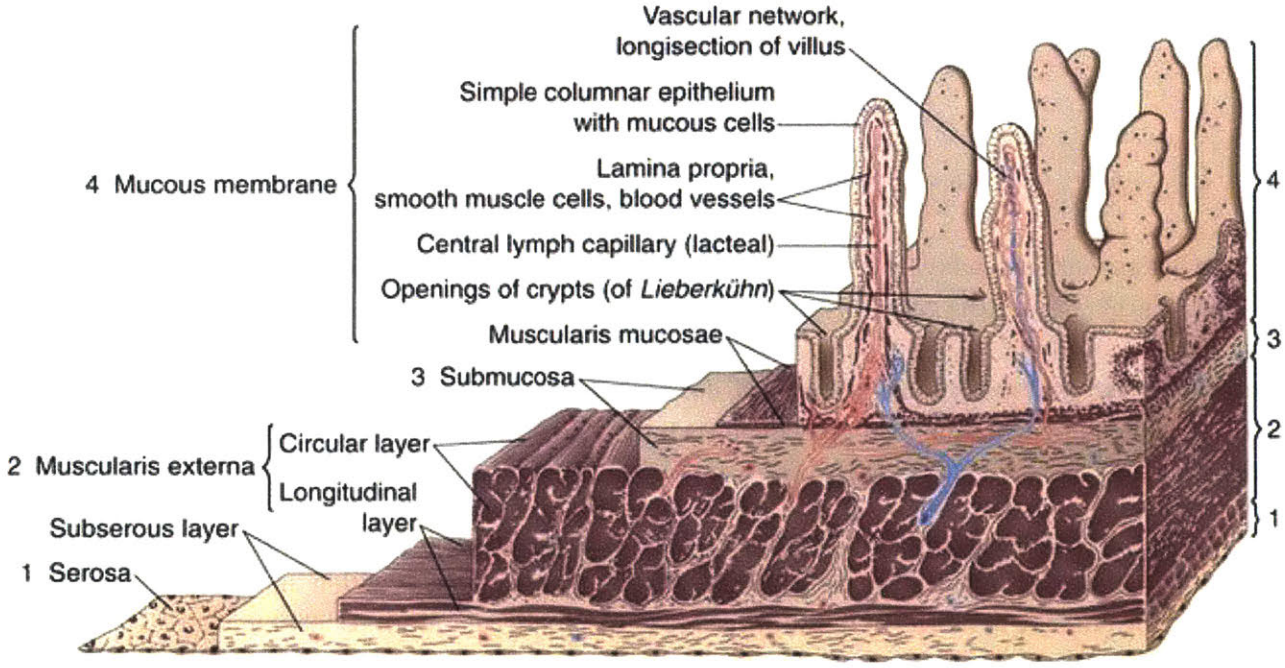

Figure 7-22 The layers of the small intestine wall, adapted from Sobotta J, Figge FHJ, Hild WJ: Atlas of human anatomy, New York, 1974, Hafner.

The lamina propria, muscularis mucosa, and submucosa layers all contain blood and lymph vessels (McKenzie & Evers, 2016), where large molecules can access systemic circulation. For simplicity, the two layers closest to the epithelial surface were considered in the model, the lamina propria and muscularis mucosa.

The muscularis mucosa is a thin layer of muscle that separates the mucosa from the submucosa. The lamina propria is a layer of connective tissue that contains a variety of cells, including immune and muscle cells, as well as non-cellular material (McKenzie & Evers, 2016). The epithelial layer is a single sheet of columnar cells, continuously covering both the villi and crypts present in the small intestinal wall. Not depicted in Figure 7-22 is the mucus layer that covers the epithelial surface, to further protect the small intestine from damage.

The size of an individual villus is approximately 0.1mm in diameter and 0.25mm in height (UCI, n.d.), and the mucus lining that is deposited on top of the epithelial surface is between 120-480 µm thick, with 15 µm of that being firmly adherent to the epithelial surface (Atuma, Strugala, Allen, & Holm, 2001). The

image in Figure 7-23 of the epithelial cells contained in the small intestine was processed in ImageJ Software (Rasband, 1997-2017), indicating that the epithelial cell measures approximately 45-50μm in height.

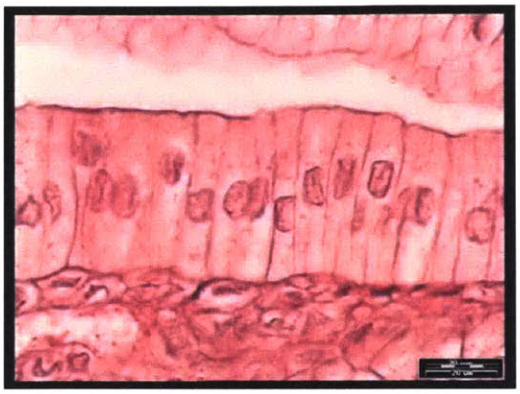

Figure 7-23 Image of Epithelial Surface of Intestinal Wall; Cell height measured to be 45-50 micrometers in ImageJ software. (Into to Anatomy 6: Tissues, Membranes, Organs, 2007)

These measurements were then adapted into the small intestinal model constructed in COMSOL Multiphysics®. depicts the geometry of the small intestinal wall and Table 7-19 summarizes the important parameters for Model 2. The luminal fluid (dark grey rectangle) represents the inner lumen of the small intestine, filled with food products, bacteria, digestive fluids, etc. The lumen is modeled as water and the height of the lumen was made large enough such that the flow lines were not affected by the geometry of Technology A.

The epithelial boundary depicted by the red rectangle is 50 μm in height, and modeled as a porous media domain filled with water. Studies have indicated that the pore diameter within the epithelial boundary is 10Å and the porosity to be 10^{-7} of the surface area of the epithelial surface (Linnankoski, et al., 2010). The permeability has been proven to be a function of the square of the pore size (Loh & Choong, 2013) (Muntz, 2008) (O'Brien, et al., 2007), and so the permeability is considered to be the square of the pore diameter, resulting in a permeability of 10^{-18} m^2. Given that the epithelium has a low porosity, this estimation for permeability may be inaccurate. Further iterations of the model should include a better defined permeability for the epithelial barrier. When an epithelial barrier is included in the model (sub-models a and b), no fluid escapes through the epithelial barrier during simulation, which is expected. Therefore, we can still conclude that the model works as expected, even given the likely inaccuracy of this permeability value.

Indicated in Figure 7-21, sub-models were created to run simulations both with (sub-models a and b) and without the epithelial barrier (sub-models c and d). For cases run without the epithelial barrier (sub-models c and d), the red rectangle referenced in Figure 7-24 and the properties of the epithelial barriers that it represents are not included in the simulation.

The lamina propria depicted by the yellow rectangle is 125 μm, modeled as half the height of the villi structure. This assumption was made for simplification, and is representative of the height of the lamina propria if it took on a smooth surface configuration rather than that of the villi structures. The lamina propria is also modeled as a porous media domain filled with water, with a porosity of 8% and a pore size

of 1.25 μm (Takahashi-Iwanaga, Iwanaga, & Isayama, 1999). Assuming the permeability can be approximated by the square of the pore diameter, the permeability of the lamina propria is $1.6x10^{-12}$ m^2.

The muscularis mucosa, depicted by the green rectangle, is also modeled as a porous media domain filled with water. Although much thinner than the lamina propria in reality, the muscularis mucosa was modeled with a height of ten times the height of the lamina propria, at 1.25mm. This simplification was made for two reasons. The first is that to add another layer of the sub-epithelial space – the submucosa – modeled as a porous media domain filled with water, would require extensive computation by the software, leading to long time frames for solution generation. The second is that the height was exaggerated in nature in order to not disturb the natural trajectory of the flow lines of the fluid in the simulation. As a muscle layer, the muscularis mucosa was assumed to have the same porosity as the lamina propria, but an order of magnitude lower permeability than the lamina propria, leaving it was a permeability of $1.6x10^{-13}$ m^2.

Table 7-19 Parameter Values for 2D Small Intestine Schematic

Parameter	Value	Description
h_{lumen}	2 mm	Height of luminal fluid
r_{nozzle}	50 or 100 μm	radius of the nozzle diameter; radius depends on input of 100 μm or 200 μm for nozzle diameter
h_{nozzle}	100 μm	height of nozzle, arbitrarily chosen
d_{techa}	0.3 mm	length of device from nozzle edge to distal part of devic
w	4 mm	width of small intestinal wall
h_{EB}	50 μm	height of epithelial boundary
$\emptyset_{EB}$	10^{-7}	porosity of epithelial boundary as fraction of surface area
d_{EB}	10 Å	diameter of pore size in epithelial boundary
k_{EB}	10^{-18} m^2	permeability of epithelial boundary
h_{LP}	125 μm	height of lamina propria
$\emptyset_{LP}$	8%	porosity of lamina propria as function of surface area
d_{LP}	1.25 μm	diameter of pore size in lamina propria
k_{LP}	1.6×10^{-12} m^2	permeability of lamina propria
h_{MM}	1.25 mm	height of muscularis mucosa
$\emptyset_{MM}$	8%	porosity of muscularis mucosa
k_{MM}	$1.6x10^{-13}$ m^2	permeability of muscularis mucosa

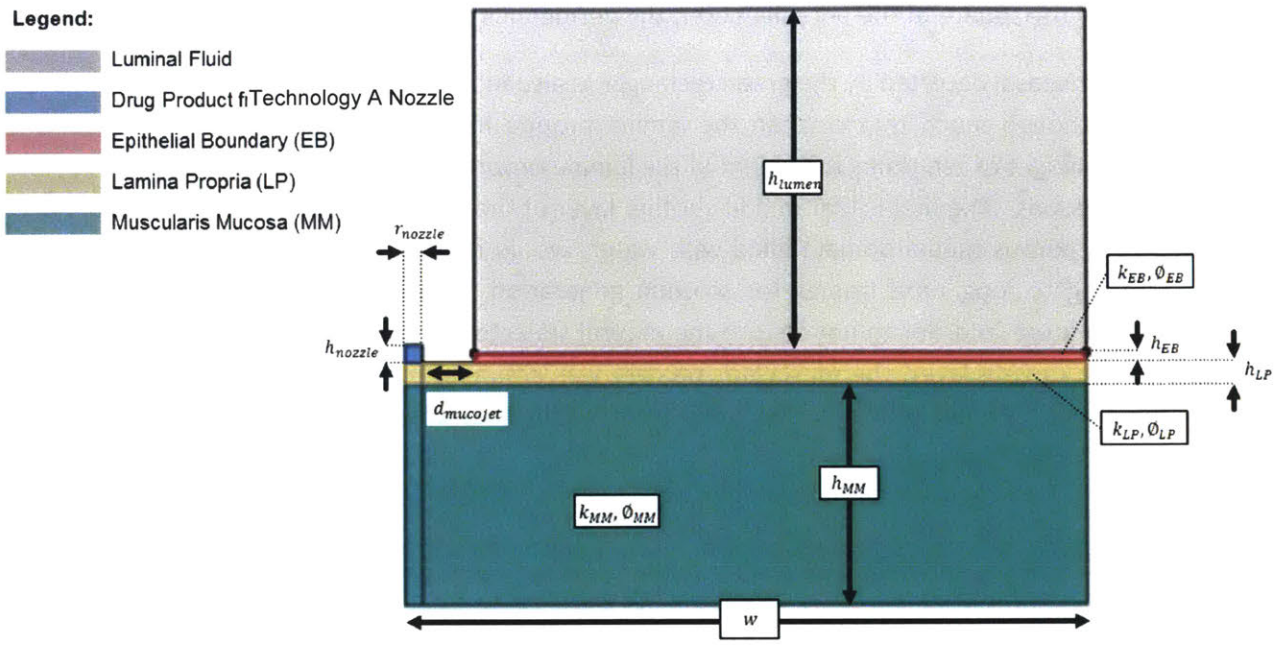

Figure 7-24 Schematic of Small Intestinal Wall in Model 2

The height of the three layers compromising the small intestine wall (epithelial barrier, lamina propria, and muscularis mucosa) add up to a height of 1.425 mm. Given that the thickness of the small intestinal wall is reported to be approximately 1.2mm (Langer & Traverso, 2017), the entirety of the small intestine geometry is represented in Model 2.

The width of the entire structure was assumed to be 4mm, which is twenty times the 200 μm nozzle diameter, such that the fluid would have enough room to spread during the time of simulation without flowing out of the simulated geometry.

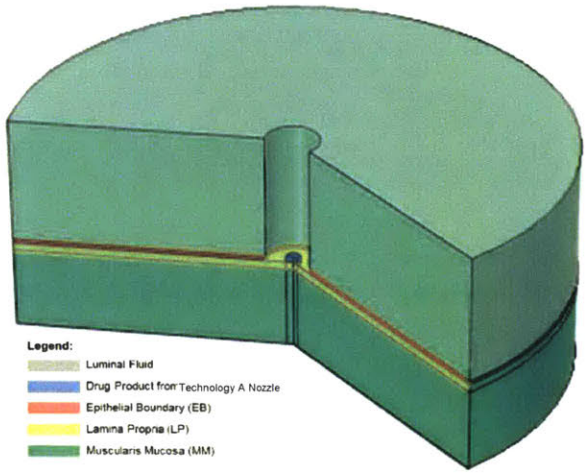

Figure 7-25 Axisymmetric schematic of small intestinal wall in Model 2

The rectangular geometry present in Figure 7-24 is the surface that is swept about an axis to create the axisymmetric geometry present in Figure 7-25. The circular space in the middle of Figure 7-25 is where

Technology A will sit. In order to use the axisymmetric model, rather than building a 3D model which is computationally less efficient, simplifications were made about Technology A. The nozzle was assumed to be placed symmetrically on the body of Technology A, while in actuality, the nozzle is not placed symmetrically. This assumption was made for simplicity, and can be remedied from future work of an intestinal transport model built in 3D, without usage of the axisymmetric function.

7.4.2.3 Laminar Flow and the Porous Media Domains

All five domains in Figure 7-24 are initially defined as water and assigned to the laminar flow interface in COMSOL Multiphysics®. The laminar flow interface was chosen for the same reasons as in Model 1, described in section 7.3.2.3.1. Due to the laminar nature of the exit velocity from Technology A, the flow from Technology A and into the small intestinal layers was also considered to be laminar.

Within the laminar flow interface, the flow was considered to be incompressible and the porous media domain option was enabled. The reference pressure is 1 atm and reference temperature 310 K. This interface calculated the velocity field within the five domains and also the pressure throughout the system. The viscosity of the fluid in all five domains was assigned to a variable termed "viscosity", which is defined in section 7.4.2.4.2. The initial pressure and velocity field within all five domains was assigned a value of zero.

The boundary conditions were assigned to the layers of the small intestine as specified in Figure 7-26. The green line on the nozzle domain specifies the inlet, where the velocity profiles Model 1 initialize. The red lines indicate walls, or zero-flow boundaries. The yellow line indicates the outlet, where flow is allowed out of the modeled system. Finally, the dotted black line indicates the axisymmetric boundary, where the 2D image is revolved to create the 3D representation depicted in Figure 7-25.

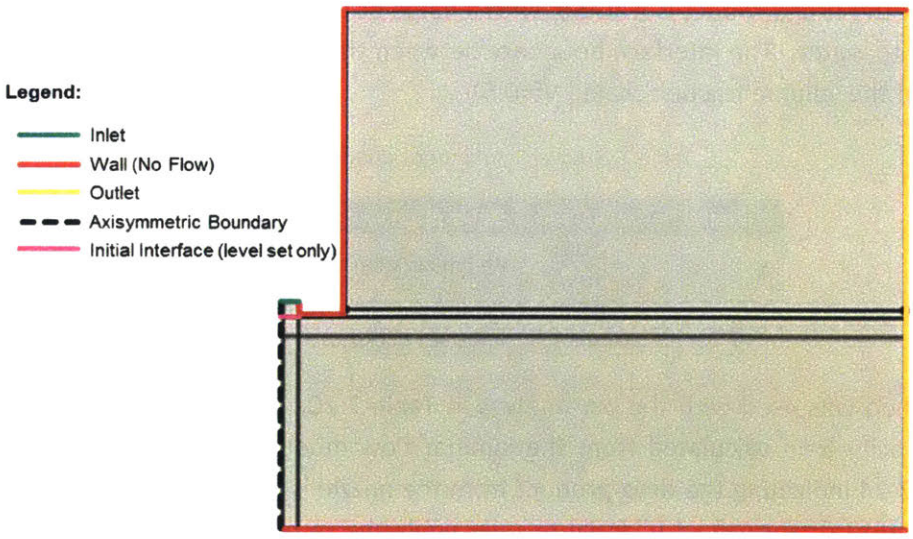

Figure 7-26 Laminar Flow (and level set) boundary conditions for 2D Schematic of Small Intestine

As mentioned in the section above, there are three domains (epithelial boundary, lamina propria, muscularis mucosa) that are modeled as porous media domains filled with water. Enabling the porous domains allowed for simulation of the different resistances between the various layers of the small

intestinal wall and for simulation of the viscous shear stress the fluid experiences at it move through the various layers. Because the option is built in to the laminar flow module, modeling these layers in this fashion allowed for simpler computation by the software.

With the porous media domain option enabled, the software takes a macroscale approach to solving the flow equations, defined by the material's porosity and the permeability. The porosity is defined as the fractional volume of the pore space within the total volume of the material, while the permeability characterizes the resistance to flow through the pores, and as indicated in the previous section, can be estimated as the squared value of the pore diameter.

For areas of free flow – the drug product from nozzle (blue) and luminal fluid (grey) domains in Figure 7-24– the Navier-Stokes equations are solved for the free flow of fluid through the laminar flow interphase. However, in the domains where the porous media has been enabled, the Brinkman equations are solved to determine the pressure and velocity field throughout the simulated material.

7.4.2.4 Level Set Method for Volume Tracking

The Level Set method was chosen to track the dispersed volume within the model. This method was chosen as it allows for a clear, defined boundary between the two liquids that are tracked, with a boundary thickness that is pre-defined as a parameter. Because the flow is considered to be dominated by convection (see section 7.4.2.4.1 below), the level set method is ideal because it limits the diffusive nature of the fluid. However, the clear boundary between the two layers comes at a high computational cost, as the simulation took hours to run.

The level set method solves three different sets of equations while tracking the interface of the fluid: the Navier-Stokes equations, one continuity equation, and one transport equation (Schlegel, 2015). The volume fraction of the drug product is tracked, with a value of one equal to the pure drug product and that of zero equal to water. The interface boundary between the two liquids is diffuse and centered on the center-value of the volume fraction scale (Vf=0.5).

Table 7-20 Level Set method parameters

Parameter	Value	Description
γ	0.001 m/s	Re-initialization parameter
ε_ls	0.015 mm	Parameter controlling interface thickness

The level set method was used with the parameters in Table 7-20. The velocity field for convection is chosen as the velocity field calculated from the laminar flow module (Velocity Field (spf)). The blue domain in Figure 7-24 indicating the drug product from the nozzle is indicated as the initial value where the volume fraction of drug product is equal to one, while the remaining domains are given an initial volume fraction equal to zero. The same axisymmetric, no flow, and outlet boundaries are chosen as for the laminar flow interface, as depicted in Figure 7-26. The initial interface boundary between the drug product and the water is assigned as the pink line in Figure 7-26.

The level set method requires two study steps – Step 1: Phase Initialization and Step 2: Time Dependent. The first step is specifically to ready the level set method for use with the laminar flow interface in the time dependent study, by initialization of the boundary between the two fluids that are tracked. Because the transition between the two phases is smooth, rather than discontinuous and the border between the two fluids is represented as an edge at t=0, a phase initialization step is needed. During this step, the study reads the geometry of the model, and creates the smooth scalar interface between the two fluids by replacing the edge between the two regions with a smooth function. Then the time dependent study begins from the smooth field at t=0, using it as an initial value.

7.4.2.4.1 Convective Flow and Peclet Numbers in Model 2

In the section above, the claim is made that the flow is dominated by convection. In section 7.3.2.3.5, the Peclet numbers were calculated for various combinations of parameters for the fluid flow in the nozzle of Technology A, all with values well over 1 indicating flow dominated by convection.

Table 7-21 Peclet Number Calculations for Model 2

Sustained Velocity (mm/s)	Mass Diffusion Constant (m^2/s)	Peclet # (nozzle)	Peclet # (small intestine)
27.6	2.27054E-11	1.22E+05	4.86E+06
74.6	2.27054E-11	3.28E+05	1.31E+07
125.9	2.27054E-11	5.54E+05	2.22E+07
5.8	2.27054E-11	5.13E+04	1.03E+06
16.4	2.27054E-11	1.45E+05	2.89E+06
26.2	2.27054E-11	2.31E+05	4.62E+06
26.3	2.27054E-12	1.16E+06	4.63E+07
68.7	2.27054E-12	3.02E+06	1.21E+08
117.1	2.27054E-12	5.16E+06	2.06E+08
5.8	2.27054E-12	5.11E+05	1.02E+07
16.9	2.27054E-12	1.49E+06	2.98E+07
27.0	2.27054E-12	2.38E+06	4.76E+07
24.5	7.56848E-13	3.23E+06	1.29E+08
62.1	7.56848E-13	8.20E+06	3.28E+08
96.0	7.56848E-13	1.27E+07	5.08E+08
5.8	7.56848E-13	1.52E+06	3.05E+07
15.6	7.56848E-13	4.13E+06	8.26E+07
26.2	7.56848E-13	6.92E+06	1.38E+08
23.0	4.54109E-13	5.07E+06	2.03E+08
54.0	4.54109E-13	1.19E+07	4.76E+08
91.6	4.54109E-13	2.02E+07	8.07E+08
5.7	4.54109E-13	2.53E+06	5.06E+07
16	4.54109E-13	7.25E+06	1.45E+08
27	4.54109E-13	1.21E+07	2.42E+08

Now, with the actual velocity outputs from Model 1, the Peclet numbers can be recalculated using the sustained velocity, which is the minimum velocity of fluid ejected by Technology A. Recall in section 7.3.2.3.5, the Peclet number is defined as:

$$Pe = \frac{advective\ transport\ rate}{diffusive\ transport\ rate}, \quad (38)$$

$$Pe = \frac{Lv}{D}, \quad (39)$$

Therefore, if the calculation of the Peclet number is performed when the velocity of fluid is at a minimum, a worst-case scenario is presented for analysis. Additionally, the characteristic for the diffusive length in the nozzle is considered to be the diameter of the nozzle, but in the small intestinal model, the diffusive length is considered to be the width of the small intestine, equal to 4mm.

Table 7-21 Peclet Number Calculations for Model 2details the value for the Peclet number, calculated with the sustained velocity within the nozzle (characteristic length of the nozzle diameter) and within the small intestine (characteristic length of 4mm). The peclet numbers are larger within the small intestine than in the nozzle, due to the larger length scale over which diffusion may happen. The Peclet numbers range from $5x10^4$ to $2x10^7$ for the nozzle and between $1x10^6$ and $8x10^8$ for the small intestine, indicating that the flow is dominated by convection and the level set method is justified for use.

However, the Peclet numbers in Table 7-21 are calculated with the sustained velocity from the output of Model 1. Necessarily, as the Model 2 simulation runs and the liquid drug product flows through the porous media domains in the small intestinal layers, the velocity will slow down and potentially drive the Peclet number down. To check if the convective flow assumption remains valid, the minimum velocity of the liquid drug product is calculated to determine the point at which the Peclet number is equal to one, assuming that the characteristic length and the mass diffusion constant remain constant. The mass diffusion rate will likely stay constant since it is determined by the viscosity of the drug product, but the characteristic length of 4mm is assumed to stay constant as a simplification, although it will likely change based on the position of the drug product within model. Using these simplifications, the following equation is used to calculate the velocity needed to achieve a Peclet number equal to 1:

$$Pe = 1 = v_{fluid} = \frac{D}{L} \quad (40)$$

Where D is the mass diffusion constant and L is the characteristic length. This equation indicates that a velocity ranging between $1.1x10^{-10}$ to $5.7x10^{-9}$ m/s will result in a Peclet number equal to one.

Figure 7-27 depicts the volume fraction of drug product and the velocity magnitude contours around the regions of minimum velocity for Case 6, the velocity profile from model 1 with input parameters of 1 mPa-s for viscosity, 50 kPa for threshold pressure, and 200 µm for the nozzle diameter. The end of the velocity profile was chosen as this is the time at which the velocity profile from Model 1 is at a minimum (i.e. the value for sustained velocity). The grayscale legend indicates the volume fraction (Vf) of drug product within the various levels of the small intestine, with a value of one (white) indicating pure drug product

and a vale of zero (black) indicating water. The cyan lines indicate the velocity streamlines. The green to red scale indicates drug product velocities between 1x10-7 m/s (red) and 1x10-10 m/s (green).

In Figure 7-27 (a) and (b), it is evident that at the boundary between the liquid drug product, the velocity remains above the minimum needed for convective flow to remain dominant, since the red lines indicate velocities at or near $1x10^{-7}$ m/s, above the velocity at which the Peclet number nears 1. This confirms the hypothesis of convective flow within the small intestinal layers and justifies the use of the level set method.

Of note, in Figure 7-27 (a), there are green lines indicating a velocity magnitude at or near $1x10^{-10}$ m/s within the epithelial barrier itself, indicating that the epithelial barrier is working as expected by disrupting flow across the membrane.

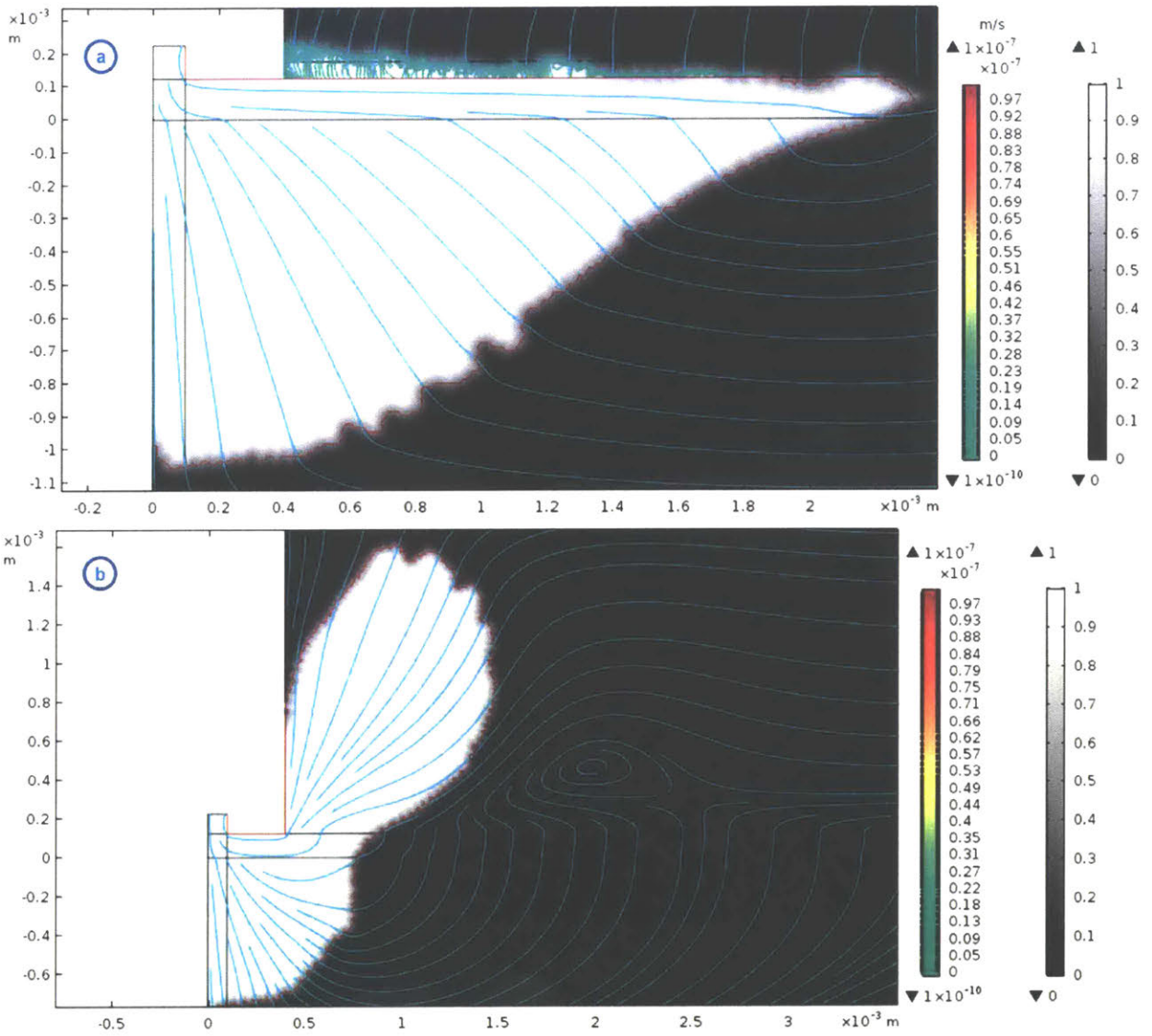

Figure 7-27 Surface plot of Case 6 (10mPa-s, 50 kPa, 200µm) at end of Technology A Deployment (t=11.53s). Green to red scale indicates drug product velocities between $1x10^{-7}$ m/s (red) and $1x10^{-10}$ m/s (green). Cyan lines indicate velocity streamlines. Grayscale legend indicates volume fraction (Vf) of drug product, with a value of one (white) indicating pure drug product and a value of zero (black) indicating water. In both figures, (a) With Epithelium and (b) without epithelium, a red line lines the barrier between the drug product (white) and the water (black), indicating that the drug product stays above a peclet number of one, confirming hypothesis of convective flow. In (a) there are green lines within the epithelial barrier itself, indicating that the epithelial barrier is working as expected by disrupting flow across the membrane.

7.4.2.4.2 Viscosity Tracking

The viscosity of the fluid is tracked through a series of equations sourcing parameters from the level set method, the laminar flow interface, and from the input variables of the selected velocity profiles from Model 1.

The viscosity of the drug product changes with each different case that is run within the model. The viscosity of the drug product is described in the equation below, with the parameters for various constant inputs detailed in Table 7-22 Input Constant Parameters for Viscosity Determination in Model 2Table 7-22.

Table 7-22 Input Constant Parameters for Viscosity Determination in Model 2

Parameter	Value	Description
visc1	1 mPa-s	viscosity of 1 mPa-s
visc10	10 mPa-s	viscosity of 10 mPa-s
visc30	30 mPa-s	viscosity of 30 mPa-s
visc50	50 mPa-s	viscosity of 50 mPa-s
visc_water	0.7 mPa-s	viscosity of water at 310 K

$$visc_{drug} = (case == 1) * (visc1) + (case == 2) * (visc1) + (case == 3) * (visc10) + (case == 14) * (visc30) + (case == 5) * (visc50) \quad (41)$$

In this equation, $visc_{drug}$ describes the viscosity of the drug product for each case that is run within the model (see

Table 7-18 for case definitions). For example, when the Boolean operator $(case == 1)$ reads true, the operator in front of visc1 is equal to 1 and the rest of the Boolean operators take on a value of 0. Therefore, the equation takes on the value of visc1 or 1mPa-s.

The value for $visc_{drug}$ is then tied into the equation below, which describes the viscosity of *any* fluid in the simulation based on the volume fraction of the fluid as denoted by the level set method. The equation below demonstrates how the viscosity of any fluid is tied to the level set interface:

$$viscosity = visc_{water} + V_f(visc_{drug} - visc_{water}) \quad (42)$$

Case	Viscosity (mPa-s)	Threshold Pressure (kPa)	Nozzle (µm)	Ejection Time (s)	Max Velocity (mm/s)	Sustained Velocity (mm/s)	Average Velocity (mm/s)	Ejected Volume (mL)
1	1	10	100	50.0	184.4	27.6	90.5	0.016
2	1	50	100	13.0	924.7	125.9	637.3	0.017
3	10	30	100	22.1	496.1	68.7	137.7	0.018
6	10	50	200	11.5	185.1	27.0	58.3	0.018
7	30	30	200	20.5	109.7	15.6	31.3	0.018
5	50	30	100	27.6	376.4	54.0	104.5	0.018
8	50	10	200	50.0	36.2	5.7	10.5	0.016

When in the area of pure drug product, $V_f = 1$, and the equation takes on the value of $visc_{drug}$. When in an area of water, $V_f = 0$, and the equation takes on a value of $visc_{water}$. The variable $viscosity$ is then used as an input in the laminar flow interface, described in section 7.4.2.3.

These set of equations allow for a comprehensive viscosity tracking of the fluid based on the imported velocity profile from Model 1, the volume fraction of fluid determined in the level set module, for use in the laminar flow module to calculate the velocity and pressure field. Recall from section 7.4.2.4 describing the level set method that the velocity used to calculate the location of the boundary interface is imported

from the laminar flow interface. This means that there is an interactive feedback loop between the level set and laminar flow modules that is continuously solved as the model is computed. This feedback is likely also a factor in the long computation times of the model, but allow for an accurate representation of the boundary between the liquid drug product and the water.

7.4.2.4.3 Mesh

A fine, free triangular mesh was generated for use, with the parameters indicated in Table 7-23. Corner refinement was used for the boundaries surrounding the nozzle jet and circling around into the lamina propria and around the first wall into the luminal space (Figure 7-28 a). The mesh was purposefully made to be very fine, so that the interface boundary would be as smooth and realistic as possible (Figure 7-28 b). However, the fine mesh also added to the computational cost of the model.

Table 7-23 Mesh Element Parameters for Model 2

Parameter	Value
Maximum Element Size	7.5x10^-6 m
Minimum Element Size	6.75x10^-8
Maximum Element Growth Rate	1.05
Curvature Factor	0.2
Resoltuion of Narrow Regions	1

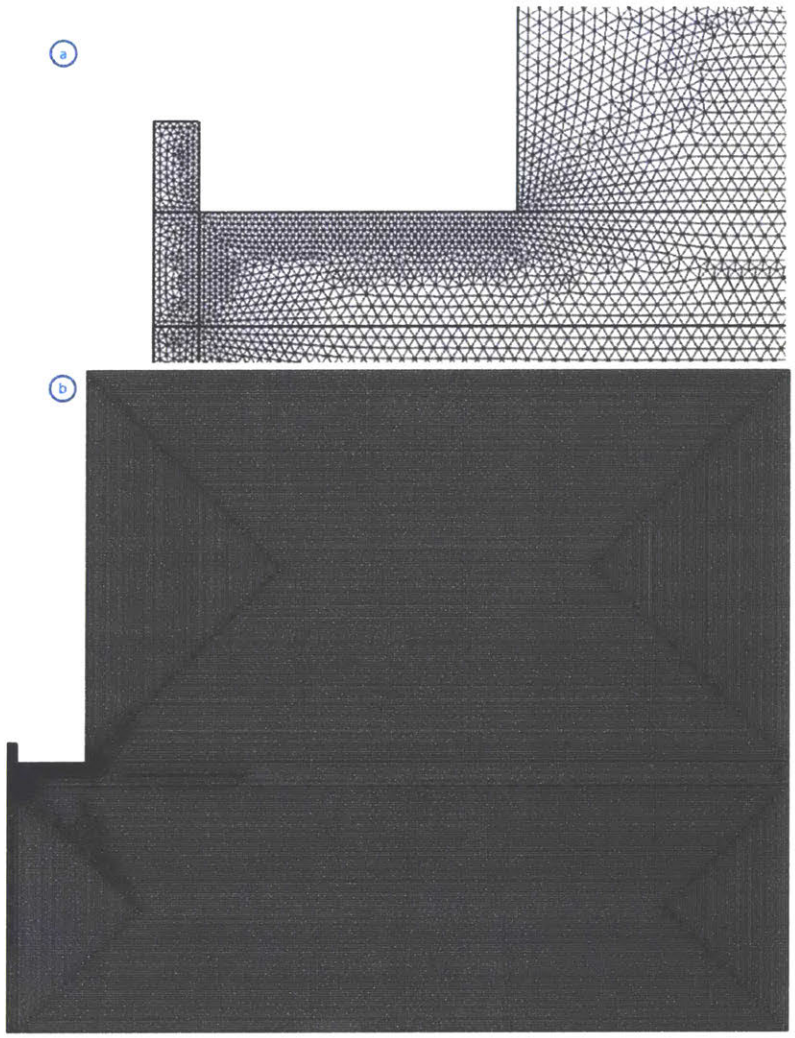

Figure 7-28 (a) corner refinement was used to generate a finer mesh around the sharp corners near the nozzle of Technology A (b) a fine mesh was used throughout the model to ensure good interface tracking

7.4.2.5 Assumptions

7.4.2.5.1 Technology A Jet can Disrupt Epithelial Barrier

The assumption is made that Technology A can disrupt the epithelial barrier, regardless of the exit velocity of the fluid from the nozzle of the device. This assumption is partially validated by the pressure calculations performed in section 7.3.3.4, as the exit pressure from various exit velocity profiles are within or above the cell adhesion forces cited from literature. However, these cell adhesion forces do not include the forces required to disrupt the mucus barrier as well, which sits on top of the epithelial barrier. This assumption was made for simplicity, and can be further validated from future empirical work performed with Technology A deployment into *ex vivo* porcine tissue that includes an intact mucus and epithelial barrier for disruption.

7.4.2.5.2 Localization to small intestine wall

The assumption is made that the nozzle is parallel and adjacent to the wall of the small intestine. The assumption was made for simplicity, as Technology A can be deployed in various locations within the diameter of the small intestinal lumen. Technology A is 4.5mm in outer diameter and the inner lumen of the small intestine can have an inner diameter between 1.5-3.0cm (Duro & Kamin, 2007), nearly 3-6 times larger than the outer diameter of Technology A with its current design. Therefore, the assumption is made that the nozzle is localized to the wall for simplicity.

7.4.2.6 Study Design

A parametric sweep through the different inlet velocity profiles and their associated drug product viscosities was performed by sweeping through the 8 cases defined in

Table 7-18. Sections 7.4.2.4.2 and 7.4.2.1 describe how the case number is connected to the inlet velocity interpolation function and viscosity within the model setup.

A phase initialization step is used to initialize the level set module, followed by a time dependent study to track the fluid movement throughout the layers of the small intestine. The solver used finer time steps in the first two seconds of the study due to the large changes in the velocity profile that occur over this time frame. Between 2 and 50 seconds, the solver uses a step of 0.5 seconds for computation.

A stop condition is implemented to allow the shorter velocity profiles to cease computation before the time limit of 50 seconds has been reached. The equation below describes this interpolation function as:

$$inlet_{velocity} < 0.001[m/s]) * (t > .01[s]) \quad (43)$$

This means that when the inlet velocity is less than 1 mm/s and the time is greater than 0.01 seconds, the solver will cease computation and move onto the next parameter in the parametric sweep.

Recall from earlier (Figure 7-21 below), there are four separate sub-models for computation described below to reflect the different inlet nozzle sizes and to understand the differences of volume dispersion with and without an intact epithelial surface.

Case	Viscosity (mPa-s)	Threshold Pressure (kPa)	Nozzle (μm)	Ejection Time (s)	Max Velocity (mm/s)	Sustained Velocity (mm/s)	Average Velocity (mm/s)	Ejected Volume (mL)
1	1	10	100	50.0	184.4	27.6	90.5	0.016
2	1	50	100	13.0	924.7	125.9	637.3	0.017
3	10	30	100	22.1	496.1	68.7	137.7	0.018
6	10	50	200	11.5	185.1	27.0	58.3	0.018
7	30	30	200	20.5	109.7	15.6	31.3	0.018
5	50	30	100	27.6	376.4	54.0	104.5	0.018
8	50	10	200	50.0	36.2	5.7	10.5	0.016

		Epithelium	
		With	Without
Nozzle Diameter (µm)	100	**a** *(Cases 1,2,3,5)*	**c** *(Cases 1,2,3,5)*
	200	**b** *(Cases 6,7,8)*	**d** *(Cases 6,7,8)*

Figure 7-23 (adapted) Sub-models for Analysis in Model 2

As mentioned multiple times in the sections above, the model was computationally costly due to the feedback loop between the level set and laminar flow modules, the level set tracking method, and the fine mesh. Table 7-24 details the computation times for models (a)-(d) above, with a total computation time of 20.1 hours. Of note, this was the computation time when the model was run on a specialized COMSOL server, equipped with 28 core processors.

Table 7-24 Model 2 Computation Times

Model	Computation Time (hr)
a	5.8
b	6.6
c	2.9
d	4.8
Total	20.1

After computation, the volumetric percentage of drug product in the sub-epithelial space and the pressure under the epithelial barrier is analyzed. Relationships are drawn between the volumetric percentage and the input parameters from Model 1, to determine which factors have the greatest impact on the dispersion of drug product.

7.4.3 Outputs and Analysis

7.4.3.1 Model Validation

7.4.3.1.1 Interface Boundaries

In models without the epithelial barrier, the interface boundary between the drug product and the water tends to be smoother than in models with the epithelial barrier. Figure 7-29 shows the differences between the interfaces generated by (a) models without an epithelial boundary and (b) with the epithelial boundary.

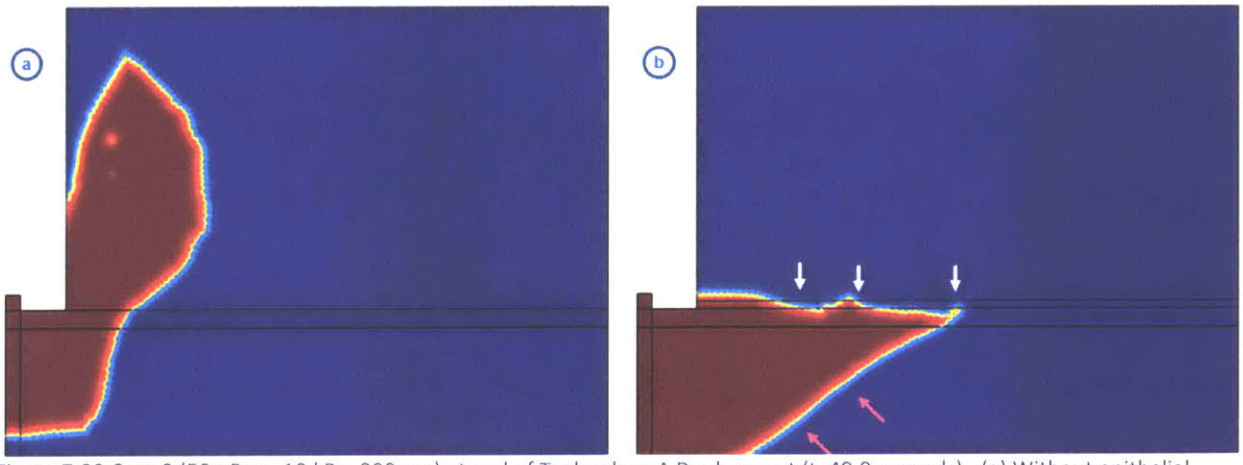

Figure 7-29 Case 8 (50mPa-s, 10 kPa, 200 µm) at end of Technology A Deployment (t=49.9 seconds). (a) Without epithelial barrier, interface between the drug product (red) and water (blue) is relatively smooth and linear in nature. (b) With the epithelial barrier, the interface between the drug product and water is very wavy and irregular in the region of the epithelial barrier (indicated with white arrows), while smooth in other regions (indicated by pink arrows).

In both (a) and (b), Case 8 with a viscosity of 50 mPa-s, a threshold pressure of 10 kPa, and a 200 µm nozzle is represented at the end of the Technology A deployment (t=49.9 seconds). In (a), the interface between the drug product (red) and water (blue) is relatively smooth and linear in nature. In (b), inclusive of the epithelial barrier, the interface between the drug product and water is very wavy and irregular in the region of the epithelial barrier (indicated with white arrows), while smooth in other regions (indicated by pink arrows).

The wavy regions in the region of the epithelial barrier could be due to the low pore size within the epithelial barrier. The pore size of the epithelial barrier, in Table 7-19, is 10 Å, nearly two orders of magnitude lower than the minimum element size for the mesh of 6.75×10^{-8} m, indicated in Table 7-23. This could possible account for the waviness of the interface in this region, as the mesh size is not small enough to account for the pore diameter of the epithelial barrier.

However, because the mesh is already so small and the computational efficiency so low, the decision was made not to re-run the models with a smaller mesh for optimization.

7.4.3.1.2 Expected Volumes

On average, the volume of liquid drug product that exited from Model 1 was measured within the layers of Model 2, with any liquid drug product that had flowed through the outlet accounted for. For the seven

cases considered in Model 2, the average volume ejected was 0.0173 ± 0.0012 mL. Using the surface integral method to measure the volume of the drug product within the layers of the small intestine in model 2 at the end of the Technology A deployment, the average volume across the 7 cases for analysis was 0.0175 ± 0.0019 mL for the 7 cases analyzed in the models inclusive of the epithelial barrier and 0.0180 ± 0.0021 mL for the 7 cases analyzed in models exclusive of the epithelial barrier. The parameters are summarized in Table 7-25.

Table 7-25 Model 2 Validation - Volume analysis

Intended Volume Output from Model 1 (mL)	Volume Output from Technology A Model (mL)	Volume in Models with Epithelial Barrier (mL)	Volumes in Model w/o Epithelial Barrier (mL)
0.018	0.0173 ± 0.0012	0.0175 ± 0.0019	0.0180 ± 0.0021 mL

Interestingly, the volumes measured in Model 2 are greater on average than the output volume measured from Model 1, but closer to the intended volume output of 0.018 mL due to the geometric considerations in Model 1 (see section 7.3.3.1.2 for more context). This is likely due to the different methods used to calculate the volume. For the output from Model 1, a global variable probe that computed as the model solves was used to determine the volume output through integration of the normal velocity over the surface of the outlet boundary. For the volume analysis in Model 2, a volume integral of the computer volume fraction of drug product was utilized. Additionally, due to the fact that the centerline velocity profile, and not the mass flow profile, is imported into Model 2 from Model 1, differences in the volume can occur.

Of note, the average volume of drug product measured in the models exclusive of the epithelial barrier is higher than that of the models inclusive of the epithelial barrier. This may be due to the nonlinear effects in the interface boundary due to the mesh in the region of the epithelial barrier.

Given the small differences between the output from the Technology A model and volume measured in Model 2, the conclusion is made that Model 2 is working as expected.

7.4.3.1.3 Epithelial Barrier Integrity

All seven cases were run on models with and without inclusion of the epithelial barrier. In the models with the epithelial barrier, the pressure was analyzed to determine whether the pressure underneath the epithelial barrier could compromise the integrity of the epithelial barrier.

Originally discussed in section 7.3.3.4 regarding the impact pressure imparted by the fluid jet, the literature suggests that the epithelial cell adhesion strength ranges from 17-50 Pa (Gallant, Michael, & Garcia, 2005) (Hagerman, Chao, Dunn, & Wu, 2005) (Garcia & Boettiger, 1999). In light of this information, the pressure underneath the epithelial barrier was analyzed at different time points to understand whether the epithelial barrier could be compromised during fluid flow into the small intestinal layers. As

seen in Figure 7-30, the pressure was analyzed at time points of 0 seconds (a), at a ¼ (b), ½ (c), and ¾ (d) of the way through deployment, and at the end of deployment (e).

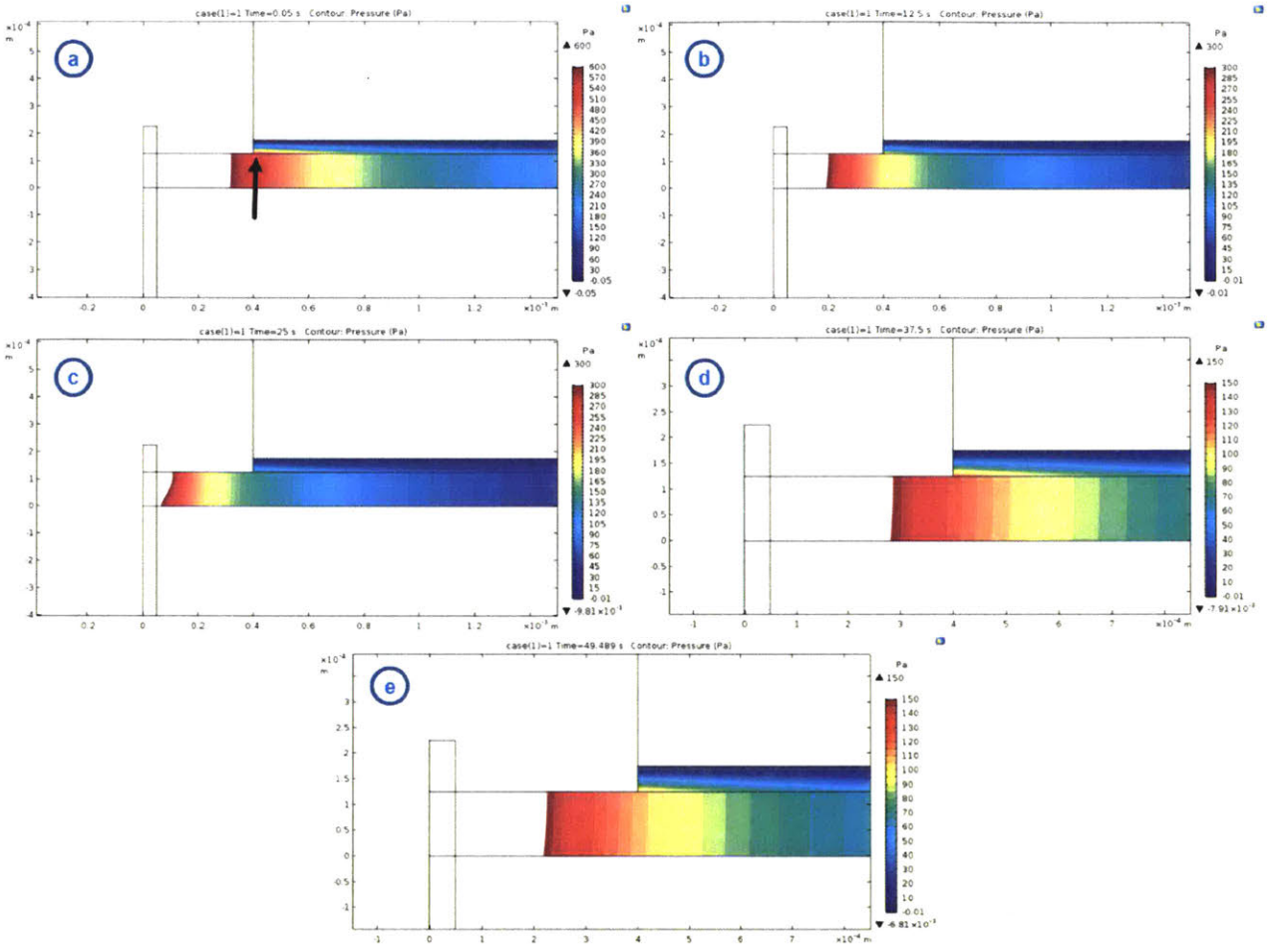

Figure 7-30 Analysis of pressure differential across epithelial barrier

Table 7-26 Pressure under epithelial barrier

Case	Maximum Pressure (Pa)	Minimum Pressure (Pa)
1	450	95
2	2400	450
3	3000	1250
5	12800	1000
6	5100	3000
7	8500	1120
8	4800	390

Although the scale changes in (a)-(e) to improve the granularity for the pressure measurements, the maximal pressure in the epithelial barrier always occurs in the far left corner of the epithelial barrier, indicated with a black arrow in (a). The color in this corner is then correlated to the scale, and the pressure is then recorded. For all seven cases, the maximum and minimum pressures under the epithelial barrier is detailed in Table 7-26.

Given that the minimum pressures for each case are above the cell adhesion force of 50 Pa, there is some likelihood that the epithelial barrier may be compromised during Technology A deployment. However, the cell adhesion strength may not be the only force keeping the epithelial barrier intact – other forces may include the cell-cell adhesions forces formed by the tight junctions between intestinal epithelial cells and the weight of the mucus lining the epithelial barrier.

Furthermore, recall that this model assumes that Technology A disrupts the barrier of the epithelial lining allowing drug product to flow into the lamina propria directly and that Technology A is localized to the wall of the small intestine. Given that energy will be dissipated to penetrate through the mucus and epithelial lining by the exit jet from the device, resulting in jet momentum lost to the environment, the pressures may not be as high as indicated in Table 7-26. These pressures may be further hindered by the fact that the jet may not be localized and immobilized against the intestinal wall during deployment. However, empirical testing needs to be done to validate the pressures and understand whether or not the flow within the sub-epithelial space induced by Technology A can actually compromise the integrity of the epithelial boundary.

7.4.3.2 Two Outputs for Analysis

The volumetric percentage of drug product remaining in the sub-epithelial space (SES) was analyzed in both models – with and without the epithelial barrier. The volumetric percentage was then correlated back to input parameters in Model 1 to see which design parameters into Technology A have the greatest effect on the dispersion of drug product.

The volumetric percentage is defined as :

$$\%V_{SES} = \frac{V_{LP+MM}}{V_{total}} \quad (44)$$

$$\%V_{LP} = \frac{V_{LP}}{V_{total}} \quad (45)$$

Where $\%V_{SES}$ is the volumetric percentage of drug product in the sub-epithelial space (SES), $\%V_{LP}$ is the volumetric percentage of drug product in the lamina propria, V_{LP+MM} is the total volume of drug product in the lamina propria (LP) and muscularis mucosa (MM), V_{LP} is the total volume of drug product in the lamina propria only, and V_{total} is the total drug product injected into the small intestinal wall. The volumentric percentage of drug product in the sub-epithelial space is considered to be a measure of

delivery efficiency and performance, as hypothesized in section 7.2.1, the drug product needs to enter into this space in order to achieve relevant levels of bioavailability.

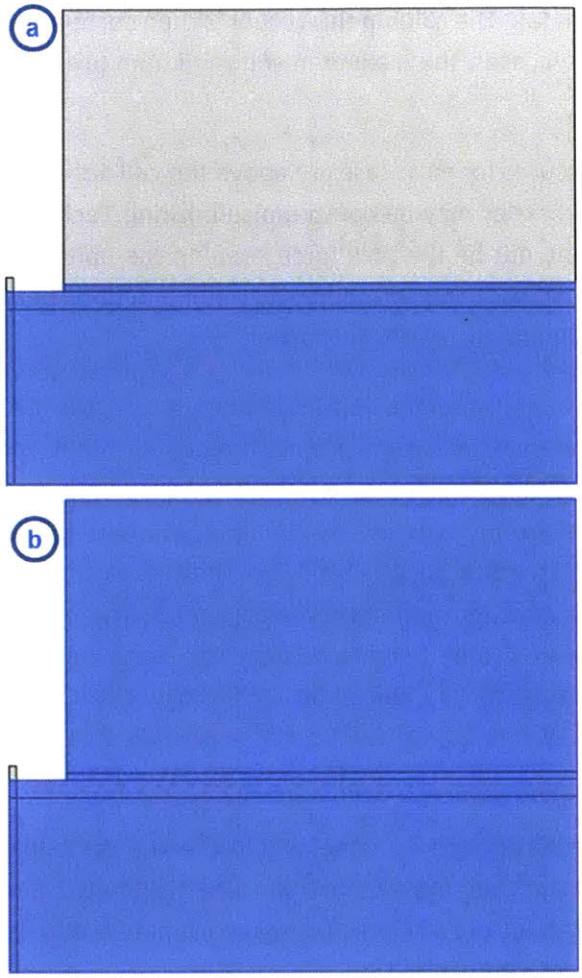

Figure 7-31 (a) The epithelial barrier, lamina propria, and muscularis mucosa domains selected for drug product volume calculation. (b) all domains with the exception of the nozzle domain chosen for calculation of the total volume

7.4.3.2.1 With Epithelial Barrier

The epithelial barrier acts as a firm stop to the flow of liquid into the lumen – performing, as it was intended to, as a barrier. With the EB intact, up to 97.7-98.7% of the drug product remains in the sub-epithelial space in all cases.

The volume of drug product was computed through a volume integral, as mentioned in section 7.4.3.1.2 and graphically depicted in Figure 7-31. In Figure 7-31 (a), the epithelial barrier (EB), lamina propria (LP), and muscularis mucosa (MM) domains were selected for computation of V_{LP+MM}. The epithelial barrier was included for computation since the drug product trapped in the barrier is not yet lost to the luminal space, and can still gain access to the lymph and blood vessels in the lamina propria. In Figure 7-31 (b), all domains with the exception of the nozzle were selected for the volume integral computation to

determine V_{total}. The Technology A nozzle domain was not selected for the volume calculations as the drug product in this domain has not yet entered into the small intestinal wall.

Table 7-27 Volumetric Percentage of Drug Product In Layers of Interest With Epithelial Barrier

Case	Volumetric Percentage of Drug Product in LP ($\%V_{LP}$)	Volumetric Percentage of Drug Product in LP, MM, EB ($\%V_{SES}$)
1	41.4%	97.68%
2	41.6%	98.40%
3	25.7%	98.49%
6	27.0%	98.67%
7	25.2%	98.30%
5	24.2%	98.04%
8	25.5%	97.65%

For all cases, Figure 7-27 (a) is a representative depiction of how the drug product spread when the epithelial barrier is present, although there were slight differences in the spread of drug product for the different cases. Table 7-27 tabulates some of the differences in the dispersion of drug product between the different layers. The percentage of drug product in the lamina propria is analyzed separately from the entire percentage of DP in the SES, to understand how the differences in permeability between the LP and MM affect volume dispersion.

Immediately evident in Table 7-27, cases 1 and 2 yield a value of ~41% for the percentage of drug product (DP) in the lamina propria, while the remaining cases only yield between 24-27%. Recall from

Table 7-18, cases 1 and 2 were the only velocity profiles that had a liquid viscosity of 1mPa-s. To determine the significance of relationships like this, and to uncover other significant parameters, a total of 36 regression analyses were run in Minitab 16 (Minitab, Inc., 2010), tabulated in Table 7-28.

Case	Viscosity (mPa-s)	Threshold Pressure (kPa)	Nozzle (μm)	Ejection Time (s)	Max Velocity (mm/s)	Sustained Velocity (mm/s)	Average Velocity (mm/s)	Ejected Volume (mL)
1	1	10	100	50.0	184.4	27.6	90.5	0.016
2	1	50	100	13.0	924.7	125.9	637.3	0.017
3	10	30	100	22.1	496.1	68.7	137.7	0.018
6	10	50	200	11.5	185.1	27.0	58.3	0.018
7	30	30	200	20.5	109.7	15.6	31.3	0.018
5	50	30	100	27.6	376.4	54.0	104.5	0.018
8	50	10	200	50.0	36.2	5.7	10.5	0.016

The regressions analyzed the volumetric percentage of drug product, both in the lamina propria ($\%V_{LP}$), and in the entirety of the sub-epithelial space, inclusive of the lamina propria, epithelial barrier, and muscularis mucosa ($\%V_{SES}$). The model parameter included the maximum velocity, sustained velocity, viscosity, threshold pressure, and nozzle diameter. The maximum velocity and sustained velocity were analyzed against the volumetric percentages singularly, since the maximum and sustained velocities are functions of the input parameters (viscosity, threshold pressure, and nozzle diameter), as was analyzed in section 7.1. The viscosity, threshold pressure, and nozzle diameter were analyzed in various combinations against the volumetric percentages, to see where there may be interesting relationships to uncover.

Cases 1-18 in Table 7-28 focus on regressions conducted from data sourced from the models with the epithelium, while cases 19-36 focus on analysis of data from the models without the epithelial barrier, as indicated in the column titled "EB included?". The column titled "LP or SES analyzed?" indicates whether the regression analysis used the percentage of drug product in the lamina propria only ($\%V_{LP}$)., or whether it analyzed the volumetric percentage of drug product in the entire sub-epithelial space ($\%V_{SES}$).

Table 7-28 Regression Analyses run On Volumetric Drug Percentages in LP or SES against various input parameters.

			P-Values of Parameters Analyzed					
Case	EB Included?	LP or SES Analyzed?	Max Vel.	Sus. Vel.	Viscosity	Threshold Pressure	Nozzle Diameter	R-Squared Value
1	Yes	LP	0.263	-	-	-	-	24.15%
2	Yes	SES	0.347	-	-	-	-	17.69%
3	Yes	LP	-	0.261	-	-	-	24.29%
4	Yes	SES	-	0.352	-	-	-	17.42%
5	Yes	LP	-	-	0.192	0.609	0.573	61.33%
6	Yes	SES	-	-	0.653	0.052	0.671	81.91%
7	Yes	LP	-	-	0.074	-	-	50.31%
8	Yes	SES	-	-	0.354	-	-	17.28%
9	Yes	LP	-	-	-	0.927	-	0.19%
10	Yes	SES	-	-	-	**0.007**	-	79.87%
11	Yes	LP	-	-	-	-	0.255	24.87%
12	Yes	SES	-	-	-	-	0.875	0.54%
13	Yes	LP	-	-	0.087	0.504	-	56.20%
14	Yes	SES	-	-	0.722	**0.023**	-	80.58%
15	Yes	LP	-	-	0.158	-	0.469	57.15%
16	Yes	SES	-	-	0.341	-	0.615	22.98%
17	Yes	LP	-	-	-	0.925	0.313	25.06%
18	Yes	SES	-	-	-	**0.016**	0.756	80.41%
19	No	LP	**0.032**	-	-	-	-	63.45%
20	No	SES	0.084	-	-	-	-	48.04%
21	No	LP	-	**0.029**	-	-	-	64.57%
22	No	SES	-	0.082	-	-	-	48.60%
23	No	LP	-	-	0.114	0.707	**0.023**	92.76%
24	No	SES	-	-	0.149	0.913	0.179	79.44%
25	No	LP	-	-	0.086	-	-	47.68%
26	No	SES	-	-	**0.048**	-	-	57.46%
27	No	LP	-	-	-	0.632	-	4.95%
28	No	SES	-	-	-	0.683	-	3.61%
29	No	LP	-	-	-	-	**0.011**	75.96%
30	No	SES	-	-	-	-	0.075	50.21%
31	No	LP	-	-	0.144	0.914	-	47.85%
32	No	SES	-	-	0.083	0.763	-	58.54%
33	No	LP	-	-	**0.043**	-	**0.008**	92.35%
34	No	SES	-	-	0.076	-	0.109	79.34%
35	No	LP	-	-	-	0.366	**0.016**	80.91%
36	No	SES	-	-	-	0.606	0.105	53.82%

In the columns named for the different input parameters, the output p-value relating the significance of the variable to the volumetric percentage analyzed is tabulated. Those p-values that are significant

($p<0.05$) at a 95% confidence level are red and bolded. The column to the right indicates the R-Squared value for the regression, indicating how well the data fit into the fitted equation. The full analyses for the included regressions can be seen in 02.

7.4.3.2.1.1 Threshold Pressure with Epithelial Barrier

Evident in Table 7-28, the threshold pressure has a significant effect on the $\%V_{SES}$ when data from the models with the epithelial barrier is analyzed. The regression analysis yield the following correlation for case 10 from Table 7-28, and depicted in Figure 7-32:

$$\%V_{SES} = 0.975 + 0.00022 * P_{threshold} \quad (46)$$

With a p-value of 0.007 for the threshold pressure and an R-squared value of 79.9%. This specific case was chosen for further analysis because the rest of the parameters the threshold pressure was analyzed in combination with were not significant. The relationship between the threshold pressure and the volumetric percentage is direct, indicated by the positive coefficient in front of $P_{threshold}$.

Figure 7-33 shows the dispersion of drug product for (a) Case 1 and (b) Case 2, both of which have a viscosity of 1mPa-s and a 100µm nozzle, but differ in threshold pressure. Case 1 was computed with a 10 kPa threshold pressure and case 2 with 50 kPa. The red indicates pure drug product, with (Vf=1) and the blue indicates pure water (Vf=0). The green contour lines indicate different levels of pressure, indicated by the legend to the right. At a glance, the two subfigures look very similar, and from Table 7-27, we know the two cases have approximately the same volume contained in the lamina propria. However, the two exhibit different interface textures, with case 1 having a wavier boundary between drug product and water than case 2.

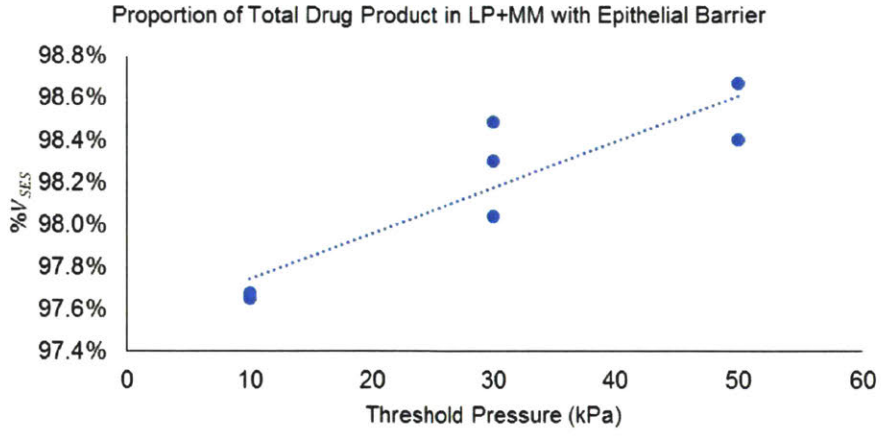

Figure 7-32 $\%V_{SES}$ as a function of Threshold Pressure with Epithelial Barrier

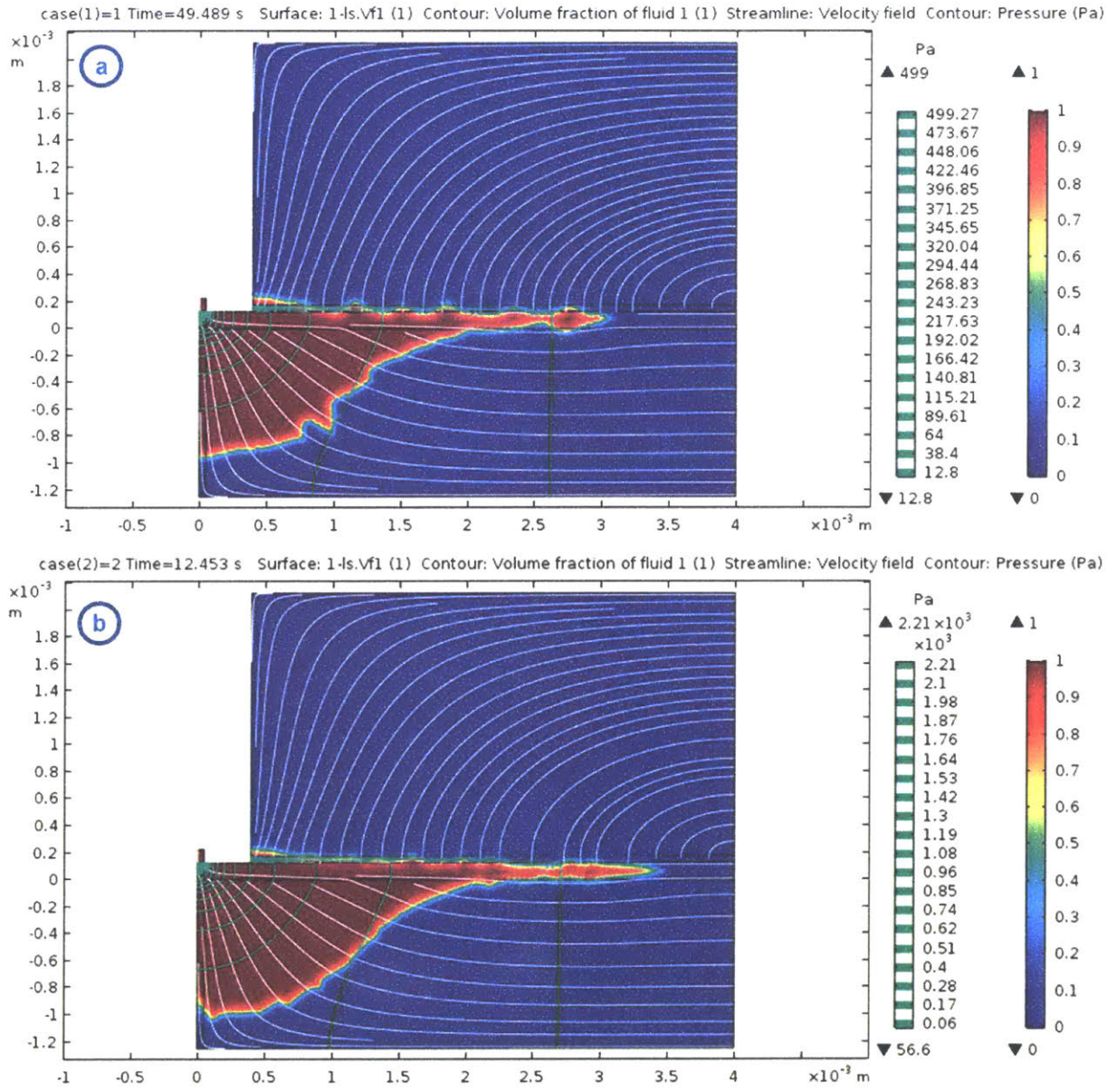

Figure 7-33 Drug Dispersion at End of Technology A Deployment for (a) Case 1 and (b) Case 2

One possible explanation of the above phenomena is that as the threshold pressure increases, drug product is forced to flow into the less permeable muscularis mucosa layer. However, due the small range over which the $\%V_{SES}$ changes, and the fact that at the lower pressures there is more error in the interface between drug product and water, the significance of threshold pressure may just be due to noise in the model.

7.4.3.2.1.2 Viscosity

As indicated Table 7-27, Case 1 and Case 2 have a higher volume of drug product ending up in the lamina propria (41%) than the other cases (~27%). Because Case 1 and Case 2 both have a viscosity of 1mPa-s,

the significance of the viscosity to the percent of volumetric drug product in the lamina propria was analyzed. In Table 7-28, the p-value for this relationship came back as 0.074, which is insignificant for a 95% confidence level.

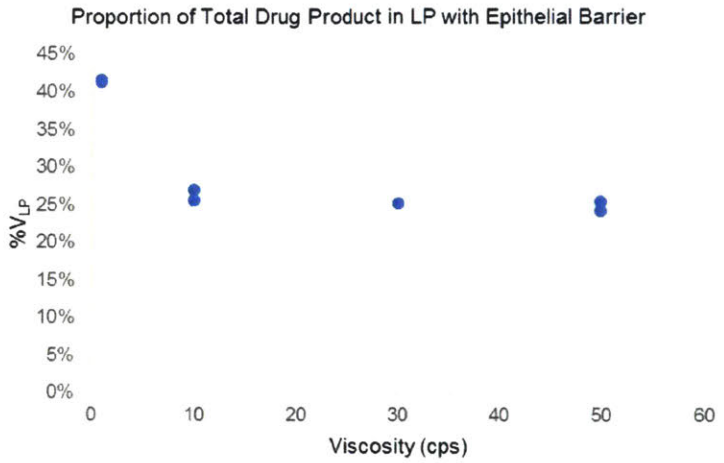

Figure 7-34 %VLP as a function of viscosity with epithelial barrier

However, looking at Figure 7-34, there seems to be an anomaly associated with 1mPa-s. This may be due to the fact that when the drug product has a value of 1mPa-s, it is very close to the viscosity of water at 310 K. This may lead to easier flow radially through the lamina propria, as opposed to vertical movement through the less permeable muscularis mucosa layer.

Although the 1 mPa-s anomaly is enticing, this may also just be due to model noise and the viscosity may not be significant at all. More combinations of velocity profiles will need to be run to determine the relationship

7.4.3.2.1.3 Velocity

In section 7.4.1, the hypothesis was made that the input velocity should have an effect on the dispersion volume within the sub-epithelial space. However, evident in Table 7-28, both the maximum and sustained velocity output from Technology A did not have a significant effect on the volume dispersion. However, due to the small range of percentage of DP in the sub-epithelial space, there may not have been enough granularity in the data to draw a correlation.

7.4.3.2.2 Without Epithelial Barrier

The same regressions were run with data sourced from the models without the epithelial barrier. Figure 7-27 (b) is representative of the volume dispersion within the different layers of the small intestinal wall and the lumen in the velocity profiles run without an epithelial barrier. As expected, when the epithelial barrier is removed, more drug product escapes into the lumen of the small intestine, where it no longer has a chance for uptake into systemic circulation.

In Table 7-29, the $\%V_{LP}$ ranges from 2.3-3.4% and the $\%V_{SES}$ ranges from 11.6-16.5%. As expected, the total volume in the subsepithelial space is much lower without the inclusion of the epithelial barrier; during the simulation, fluid is free to flow from the lamina propria into the lumen of the small intestine. Of note,

none of the analyzed parameters in Table 7-28 had a significant effect on the volume capture within the overall subepithelial space ($\%V_{SES}$), with the exception of the viscosity in Case 26.

Table 7-29 Volumetric Percentage of Drug Product In Layers of Interest Without Epithelial Barrier

Case	Volumetric Percentage of Drug Product in LP ($\%V_{LP}$)	Volumetric Percentage of Drug Product in LP, MM, EB ($\%V_{SES}$)
1	2.5%	12.32%
2	2.3%	11.62%
3	2.7%	14.67%
6	3.2%	15.44%
7	3.3%	15.80%
5	2.9%	15.28%
8	3.4%	16.45%

7.4.3.2.2.1 Velocity

In the models without the epithelial barrier, the maximum velocity and sustained velocity are considered significant in consideration of the percent of drug volume in the lamina propria, but not in consideration of all of the drug product within the sub-epithelial space (cases 19 and 21 in Table 7-28).

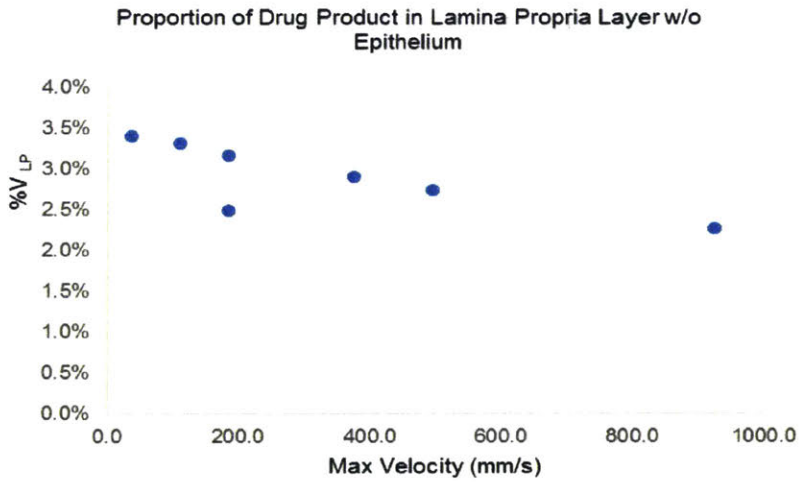

Figure 7-35 $\%V_{LP}$ as a function of maximum velocity without epithelial barrier

As indicated in the correlations below, where v_{max} is the maximum velocisty and $v_{sustained}$ is the sustained velocity, the relationship between velocity and $\%V_{LP}$ is indirect.

$$\%V_{LP} = 0.0325755 - 1.10735x10^{-5} * v_{max} \quad (47)$$

$$\%V_{LP} = 0.032756 - 8.28086x10^{-5} * v_{sustained} \quad (48)$$

This means that as the velocity increases, the percentage of drug product within the lamina propria decreases. This is graphically depicted in Figure 7-35. Although not deemed significant by the regression

analyses (cases 20 and 22 in Table 7-28), the same relationship is present when analyzing the $\%V_{SES}$ as a function of the maximum and sustained velocities.

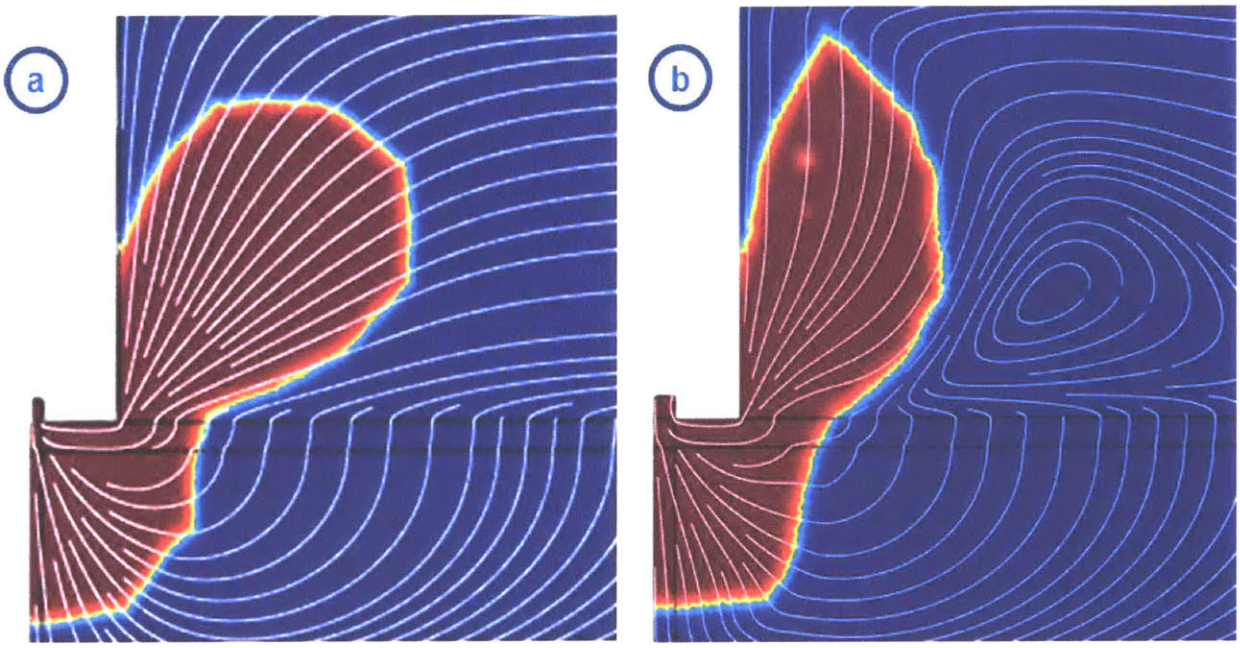

Figure 7-36 (a) Volume dispersion of Case 2 with a maximum velocity of 924 mm/s. (b) Case 8 with a maximum velocity of 36 mm/s

Figure 7-36 shows the differences in drug product (red) dispersion through the water (blue) within the different small intestinal layers for (a) Case 2 and (b) Case 8. Recall that Case 2 has a maximum velocity of 924 mm/s as opposed to case 8 with a maximum velocity of 36 mm/s, representing opposite ends of the spectrum. The white lines in the figure are the velocity streamlines depicting the direction of flow in both models. At a glance, there is not a huge difference in the overall shape of the drug dispersion in (a) and (b), however, case 8 holds ~1.1% more DP in the LP and ~4.8% more DP in the entire sub-epithelial space in comparison to case 2 (calculated from Table 7-29). Both cases have relatively smooth interfaces between the drug product and water, although some sharp corners are present in both depictions, leading me to the conclusion that the relationship between velocity and drug dispersion is not necessarily a product from model error.

One possible explanation for this relationship is that with a higher fluid velocity, the drug product has more energy to travel through the initial lamina propria level, and follow the path of least resistance into the lumen, because the epithelial barrier is not in place to contain the drug product. Therefore, as the velocity increases, there is less drug product within the sub-epithelial space.

7.4.3.2.2.2 Nozzle Diameter & Viscosity

Evidenced by Table 7-28, there is a significant relationship between nozzle diameter and viscosity and the $\%V_{LP}$. In Case 23 in the table, where viscosity, nozzle diameter, and threshold pressure are analyzed against $\%V_{LP}$, only the nozzle diameter is deemed significant. The nozzle diameter is also deemed

significant when analyzed alone (Case 29), in combination with the threshold pressure (Case 35), and in combination with the viscosity (Case 33) against $\%V_{LP}$. The viscosity is deemed significant when analyzed alone (Case 26) against $\%V_{SES}$, and when analyzed in combination with the nozzle diameter (Case 33) against $\%V_{LP}$.

Interestingly, the R-squared value for the equation fit was greatest when all three parameters were analyzed together in Case 23, even though the viscosity and threshold pressure were deemed insignificant. The second highest R-squared value was present in Case 33, where the nozzle diameter and threshold pressure were analyzed in combination against $\%V_{LP}$.

The regression fit in Case 33 (shown below), indicates that as the viscosity of the drug product ($visc_{drug}$) and the nozzle diameter increase (d_{nozzle}), the percentage of drug product in the lamina propia increases.

$$\%V_{LP} = 0.0189358 + 8.527e-005 * visc_{drug} + 0.0569086\, d_{nozzle} \quad (49)$$

Although not deemed significant to the output velocity from the analysis of Model 1, the viscosity is still related to the velocity of the fluid flow when the threshold pressure and nozzle diameter is fixed. The higher the viscosity of the fluid, the higher shear force experienced when moving through a nozzle or through a porous media, and therefore the lower the viscosity. Similarly, the nozzle diameter is also indirectly related to fluid velocity, as demonstrated in the analysis of Model 1.

Because both the nozzle diameter and the viscosity (to a lesser extent) have an indirect relationship to velocity, it physically makes sense that these two parameters would have a direct relationship to the percentage of drug product in the lamina propria. Furthermore, as the viscosity increases, the drug product will encounter greater friction with the porous lamina propria and muscularis mucosa, and lose momentum and settle within those layers prior to escape into the lumen.

7.4.4 Conclusions from Model 2

Model 2 was designed to simulate the effect of drug product velocity, and the coupled factors that affect velocity, to the dispersion of drug product within the desired layers of the wall of the small intestine. There are a couple of pertinent learnings to glean from simulation of Model 2 in COMSOL Multiphysics®.

The initial hypothesis made in section 7.4.1 regarding velocity as related to drug dispersion was partially confirmed, as the velocity had an effect on the drug dispersion in the models without an epithelial barrier, but no significant effect when an epithelial barrier was in place. However, the factor that has the largest effect on the drug dispersion is not related to the inlet velocity of drug product, but instead the integrity of the epithelial barrier. The largest difference between volume of drug product within the sub-epithelial space was due to the inclusion of the epithelial barrier, rather than due to the drug product velocity, drug viscosity, Technology A nozzle diameter, or threshold pressure.

Given a cell adhesion force of 50 Pa, all seven velocity profiles are in danger of compromising the integrity of the epithelial boundary due to the pressure underneath the epithelial lining analyzed in section 7.4.3.1.3. This indicates that the models computed without the epithelial barrier in place may be a better representation of reality, where the drug product that remains in the sub-epithelial space is only between

11.6-16.5% of the total drug product injected into the sub-epithelial space. This indicates that Technology A may not be a suitable option for the delivery of large molecules through the GI tract, since the drug product does not remain in the sub-epithelial space where it has a chance of entering into systemic circulation. Without a high probability of entering into systemic circulation, the large molecules will not be able to achieve bioavailability analogous to that achieved by subcutaneous injection.

However, given the number of assumptions made regarding the structure and properties of the small intestinal wall, the simplifications made within the model itself, and the lack of literature regarding the adhesion strength of the epithelial barrier and adjacent mucus lining, further study is required to fully understand the ability of Technology A to deliver drug through the GI tract.

7.5 Summary and Further Modeling

7.5.1 Summary

Technology A was simulated through the two models presented above to understand the ability of the device to deliver drug product effectively and enable high bioavailability.

In Model 1, focused on the internal mechanics of Technology A, threshold pressure, nozzle diameter, and drug viscosity were simulated in order to determine which factors had the greatest effect on the output velocity profile. The results of this model indicated that nozzle diameter and threshold pressure had a much more significant effect than the drug viscosity, which is a trend generally consistent with the hypotheses made. These initial results indicate that Technology A can be used as a platform technology, able to deliver multiple viscosities of drug with one product design. However, it should be noted that the friction between the plunger and body of the device likely plays a role in the resulting velocity profiles. Given the friction input used for the model, neither inertial nor viscous effects dominate flow. However, if the friction were to decrease, inertial forces may come to dominate. The frictional force should be used as an input parameter in further iterations of the model.

In Model 2, the flow of drug product through the layers of the small intestinal wall were simulated by importing the output velocity profiles from Model 1. There were four sub-models analyzed, using two different nozzle geometries (to match the output flow from Model 1) and the option for inclusion of the epithelial barrier. The results from these simulations indicate that the largest determinant of whether drug product escapes to the lumen is the presence of an epithelial barrier. If the epithelial barrier is compromised during drug delivery, the likelihood that drug product escapes into the lumen is much higher, likely resulting in low bioavailability of the drug product. All velocity profiles simulated in Model 2 had the potential to compromise the epithelial barrier, as the pressure exerted by the movement of fluid under the epithelial cells was greater than the cell adhesion force to the lamina propria. The current version of the simulations indicate that Technology A may not be the best suited for delivery of large molecules via the GI tract, since it may compromise the integrity of the epithelial barrier and result in low bioavailability of drug product.

7.5.2 Further Modeling

Further validation of Technology A is required to determine its ability to deliver large molecules into systemic circulation via the GI tract. The exit jet from the device needs to be able to disrupt the mucus

lining and epithelial barrier of the small intestine in order to reach the sub-epithelial space, but it must not increase the pressure to such an extent in this space that it compromises the epithelial barrier in the surrounding regions.

The models presented above need further refinement so that they can further investigate whether or not Technology A can increase bioavailability. If further refinement is completed, the models can potentially be used as a design tool to create the optimal device for the desired drug product viscosity and volume as specified by Amgen.

Activities for further refinement could include, but are not limited to, the following (in no particular order):

a. Measure the friction between the plunger and outer capsule of Technology A
b. Empirical testing to understand the forces and pressures needed to disrupt the epithelial barrier via a jet, and to compromise the integrity of the epithelial barrier via bellowed pressure.
c. Use particle tracking methods to simulate the flow of the drug product into the porous media with the actual sizes of the large molecules in question
d. Model more layers of the small intestine (e.g. the submucosa) with inclusion of the actual geometry and elastic properties of the small intestine.
e. Validation of the results from this model with empirical testing.

Chapter 8 Next Steps and Recommendations

This chapter summarizes the Novel Oral Drug Delivery project undertaken by the LGO student, and summarizes next steps for the oral drug delivery project. Additionally, this chapter takes a broader perspective on the methods used by large companies to evaluate new technologies and discusses the knowledge transfer of the novel oral project to the wider ADT&I group.

8.1 Project Summary

This thesis intended to evaluate the field of novel oral drug delivery for large molecules, as applicable to Amgen's product portfolio. The project followed three phases: (1) plan technical approach, (2) technology convergence, and (3) proof-of-concept. In phase 1, the value proposition for novel orals was specified, a literature review into historical barriers of novel orals was completed, and a technology landscape was performed. In phase 2 of the project, the technology landscape was down-selected to 2 high-priority candidates (Technology A & C), a technical risk assessment was performed on Technology A, and the testing strategy was determined. In phase 3, the LGO intern modeled Technology A in COMSOL Multiphysics®, while the wider ADT&I group continued to investigate Technology A and others to source the ideal option for Amgen's portfolio.

The results of the technical assessment performed by the LGO intern suggest that Technology A may not be able to successfully achieve a high bioavailability of drug delivered via this method. However, the results of the literature review into historical barriers has provided the means by which to continue looking for technology solutions for Amgen's needs. The challenges of low bioavailability, clinical relevance, and safety need to be met by any technology considered by Amgen. Furthermore, the

technology landscape provides a source for other technologies to be re-visited, and should be continually renewed to ensure Amgen remains up to date in this field.

8.2 Next Steps

For the continuation of work on Technology A, model refinement is recommended to be completed as listed in the conclusion section of Chapter 7. Empirical testing with Technology A prototypes will allow for model refinement and the continued design optimization of the device. Upon further validation, the models presented above may be used as design tools, to optimize the design parameters for the most efficient drug delivery of any drug in question.

As for the novel oral program as a whole, sourcing of technologies that allow for active absorption of drug product across the intestinal epithelium is recommended. Technologies enabling active absorption will allow for drug product to have a high probability of relevant bioavailability, and present an alternative delivery method that could revolutionize the biotech industry.

Continued surveillance of the field is recommended, with small, exploratory investments in promising technologies for proof of concept testing prior to larger investments for design and validation with the delivery of an Amgen product. The Novel Oral Delivery project was moved into the first phase of the stage-gated milestone process ADT&I uses for device technology evaluation at Amgen.

8.3 Technology Evaluation in Large Companies

Innovation is often thought to stem from academic labs and startup companies, rather than companies with a market cap of $185 billion. However, the group of engineers comprising the Advanced Device Technology & Innovation (ADT&I) work to bring the two together, by establishing relationships with external providers and translating them to the needs of the company. A side project of the author was to analyze the current process this group has in place to evaluate different technologies from the perspective of Amgen's needs.

The process the group currently follows involves technology surveillance, establishment of the value proposition of any technology as it relates to the needs of Amgen, initiation of proof of concept testing, and, once that is successful, moving the technology into a more rigorous stage-gated process with defined milestones and goals to validate the technology as a delivery mode.

Given the group's relative youth in comparison to the establishment of Amgen as a company, it is difficult to judge the success of this process by the ease of which technologies are adapted for commercial use after the vetting process completed by ADT&I – the process is too young to allow for that. Alternatively, a literature review into different methods of technology evaluation was completed.

The literature review revealed that industry best practices do not paint a clear picture for the optimal management of innovation sourcing. There are a couple of different models found in the literature. This includes the concept of innovation tournaments, which applies process management methodology to innovation sourcing, emphasizing the need to consider technologies in iterative tournaments for the fulfillment of the highest potential options (Terwiesch & Ulrich, 2009).

Additionally, discovery driven planning, initially conceptualized by Rita McGrath and expanded upon by Clayton Christensen, takes a very different approach. In discovery driven planning, the required profit generation needed to engage in any new venture is determined, and working backwards, the revenue and cost structure necessary to get to the require profit is calculated (McGrath & MacMillan, 1995). With the knowledge of the cost and revenue structure, the activities necessary to get there are then planned. During this entire process, the assumptions that go into the necessary profit, revenue, cost, and planned activities are tracked and milestones based on the confirmation of assumptions are built (McGrath & MacMillan, 1995). Using this type of process, investments aren't made on an expected return on investment (ROI) or net present value (NPV) figure that are based on assumptions that are made, and then never validated (Christensen, Kaufman, & Shih, 2008). By clearly tracking and confirming the assumptions made to get to the required-profit, the venture cannot be completely dismantled by a single-assumption that was made, forgotten, and turned out to be wrong.

Steve Eppinger at MIT Sloan has also proposed a project planning tool, called the Design Structure Matrix (DSM) that maps activities that need to occur prior to decision-making on crucial factors relating to the project's success (MIT, 2018). This allows for a rigorous assessment of technology readiness in a structured way that can be adapted and scaled to a multitude of different types of technologies from different sources.

There are other models that are pursued by other companies within the pharmaceutical industry. Johnson & Johnson (J&J) is known for setting up incubators, such as LabCentral in Cambridge, MA and M2D2 in Lowell, MA, where startups in the life science and medical device fields have access to relatively inexpensive lab space and access to the vast resources at J&J's disposal. In turn, this allows J&J to keep an eye on the newest medical innovations, and invest or partner with those they believe can add value to their business. In fact, Amgen is a member of M2D2, allowing them access to innovative startups in the pharmaceutical and drug delivery spaces.

While Amgen does not explicitly follow any of the aforementioned processes, with the exception of M2D2, their process includes aspects of all of these. They consider technologies at different stages, and place them through their own adaptation of an innovation tournament, create structured activities and milestones based on the needs of the organization in relation to the considered technology, and avoid making financial assumptions about the success of a technology until a verified knowledge-base has been established. Evidenced by the work done on the Novel Oral project, the process is working well, and will allow Amgen to continue as dominant player in the commercialization of innovative device platforms to improve the patient experience and outcome.

8.4 Knowledge Transfer

Shortly prior to the internship end-date, the Novel Oral Delivery project was moved into the first phase of the stage-gated milestone process used by ADT&I for technology evaluation. In order to aid the ongoing project progress, the work completed by the LGO intern was documented and organized for transfer to the full-time employee leading the project.

The author's notes regarding main challenges, historical barriers, and the technology landscape were preserved and organized. Similarly, the down-selection process, risk mitigation, testing strategy analysis, and COMSOL® models were documented and transferred to the full-time owner. Meetings regarding the strategy for continuation of the Novel Oral program were conducted prior to the end of the LGO internship, with an emphasis on small-scale investment into technologies that enable active absorption of large molecule drug product.

The project will continue at Amgen through collaborations with the startup and academic community, and remains an area of priority for innovation at Amgen. If a solution can be found to oral delivery of large molecules, Amgen will revolutionize the way patients interact with their products and disrupt the biotech industry.

References

Adamo, A. (2013). Microfluidic Jet Injection for Delivering Macromolecules into Cells. *ournal of micromechanics and microengineering : structures, devices, and systems*. Retrieved from https://www.ncbi.nlm.nih.gov/pubmed/23956498

Aegis Therapeutics, LLC. (n.d.). *Intravail(R) Technology*. Retrieved from Aegis Therapeutics: http://aegisthera.com/technology/#hydrogel

Altman, L. (1982, October 30). A New Insulin Given Approval for Use in U.S. *New York Times*. Retrieved from http://www.nytimes.com/1982/10/30/us/a-new-insuin-given-approva-for-use-in-us.html.

Amgen Canada Inc. (2017). *Product Monograph.* Retrieved from https://www.amgen.ca/products/~/media/8fda69c1d32b42d5a0347263c22ab22f.ashx

Amgen, Inc. (2013). *Aranesp Safety Data Sheet.* Amgen, Inc. Retrieved from http://msds.amgen.com/~/media/amgen/repositorysites/msds-amgen-com/aranesp_safety_data_sheet_20130213_rev_3.ashx

Amgen, Inc. (2013). *Epogen Safety Data Sheet.* Amgen, Inc. Retrieved from http://msds.amgen.com/~/media/amgen/repositorysites/msds-amgen-com/epogen_safety_data_sheet_20130213_rev_4.ashx

Amgen, Inc. (2013). *Neupogen Safety Data Sheet.* Amgen, Inc. Retrieved from http://msds.amgen.com/~/media/amgen/repositorysites/msds-amgen-com/neupogen_safety_data_sheet_20130218_rev_3.ashx

Amgen, Inc. (2014). *Nplate Safety Data Sheet.* Amgen, Inc. Retrieved from http://msds.amgen.com/nplate-safety-datasheet/

Amgen, Inc. (2015). *Corlanor Safety Data Sheet.* Amgen, Inc. Retrieved from http://msds.amgen.com/~/media/amgen/repositorysites/msds-amgen-com/corlanorsds.ashx

Amgen, Inc. (2015). *Highlights of Prescribing Information - Kyprolis.* Amgen, Inc. Retrieved from http://www.kyprolis.com/static/kyprolis/pdf/kyprolis_pi.pdf

Amgen, Inc. (2017). *Amgen Reports Third Quarter 2017 Financial Results*. Retrieved from Amgen: http://wwwext.amgen.com/media/news-releases/2017/10/amgen-reports-third-quarter-2017-financial-results/

Amgen, Inc. (2017). *Amgen Unlocking the Potential of Biology for Patients.* Retrieved from Amgen: http://wwwext.amgen.com/~/media/amgen/full/www-amgen-com/downloads/amgen_corporate_brochure.ashx

Amgen, Inc. (2017). *Enbrel Safety Data Sheet.* Amgen, Inc. Retrieved from http://msds.amgen.com/~/media/amgen/repositorysites/msds-amgen-com/enbrel_safety_data_sheet_20130213_rev_3.ashx

Amgen, Inc. (2017). *Highights of Prescribing Information - Vectibix.* Amgen, Inc. Retrieved from http://pi.amgen.com/~/media/amgen/repositorysites/pi-amgen-com/vectibix/vectibix_pi.pdf

Amgen, Inc. (2017). *Highlights of Prescribing Information - Blincyto.* Amgen, Inc. Retrieved from http://pi.amgen.com/~/media/amgen/repositorysites/pi-amgen-com/blincyto/blincyto_pi_hcp_english.pdf

Amgen, Inc. (2017). *Highlights of Prescribing Information - Prolia.* Amgen, Inc. Retrieved from http://pi.amgen.com/~/media/amgen/repositorysites/pi-amgen-com/prolia/prolia_pi.pdf

Amgen, Inc. (2017). *Highlights of Prescribing Information - Sensipar.* Amgen, Inc. Retrieved from http://pi.amgen.com/~/media/amgen/repositorysites/pi-amgen-com/sensipar/sensipar_pi_hcp_english.pdf

Amgen, Inc. (2017). *Parsabix(TM) Safety Data Sheet.* Amgen, Inc. Retrieved from http://msds.amgen.com/~/media/amgen/repositorysites/msds-amgen-com/parsabiv-safety-datasheet.ashx

Amgen, Inc. (2017). *Quick Facts*. Retrieved from Amgen: http://wwwext.amgen.com/about/quick-facts/

Amgen, Inc. (2017). *Repatha Safety Data Sheet.* Amgen, Inc. Retrieved from http://msds.amgen.com/~/media/amgen/repositorysites/msds-amgen-com/repathasds.ashx

Amgen, Inc. (2018). *Highlights of Prescribing Information - Xgeva.* Amgen, Inc. Retrieved from http://pi.amgen.com/~/media/amgen/repositorysites/pi-amgen-com/xgeva/xgeva_pi.pdf

Amgen, Inc. (2018). *How to take Repatha*. Retrieved from https://www.repatha.com/how-to-start-injection/

Amgen, Inc. (2018). *Pipeline*. Retrieved from http://www.amgenpipeline.com/pipeline/

Amgen, Inc. (n.d.). *Enbrel(R) Label.* Retrieved from https://www.accessdata.fda.gov/drugsatfda_docs/label/2008/enbrel_pi.pdf

Amgen, Inc. (n.d.). *Highlights of Prescribing Information.* Retrieved from http://pi.amgen.com/~/media/amgen/repositorysites/pi-amgen-com/prolia/prolia_pi.pdf

Amgen, Inc. (n.d.). *Highlights of Prescribing Information - Repatha.* Retrieved from https://www.accessdata.fda.gov/drugsatfda_docs/label/2017/125522s013lbl.pdf

Amgen, Inc. (n.d.). *Storing and Traveling with ENBREL*. Retrieved from Enbrel etanercept: https://www.enbrel.com/support/storage-and-travel

AMT. (n.d.). *Transint(TM) Platform*. Retrieved from Applied Molecular Transport: http://www.appliedmt.com/transint-platform.html

Aran, K., Chooljian, M., Parades, J., Rafi, M., & Liepmann, D. (2017). An oral microjet vaccination system elicits antibody production in rabbits. *Science Translational Medicine*.

Atuma, C., Strugala, V., Allen, A., & Holm, L. (2001). The adherent gastrointestinal mucus gel layer: thickness and physical state in vivo. *American Journal of Physiology, 280*(5), 922-29. doi:https://doi.org/10.1152/ajpgi.2001.280.5.G922

Banerjee, A., Lee, J., & Mitragotri, S. (2016). Intestinal mucoadhesive devices for oral delivery of insulin. *Bioengineering & Translational Medicine*, 338-346. doi:10.1002/btm2.10015

Benedetto, P. D. (2016). Patient compliance with new oral anticoagulants after major orthopaedic surgery: rivaroxaban and dabigatran compared with subcutaneous injection of fondaparinux. *Joints*. doi:doi:10.11138/jts/2016.4.4.214

Benjamin, D. (2017). *What Supplements Should One Take to Build Muscle & Lose Weight?* Retrieved from Livestrong.com: https://www.livestrong.com/article/259493-what-supplements-should-one-take-to-build-muscle-lose-weight/

Blum, M., Koo, D., & Doshi, J. (2011). Measurement and Rates of Persistence With and Adherence to Biologics for Rheumatoid Arthritis: A Systematic Review. *Clinical Therapeutics, 33*(7), 901-913. doi:https://doi.org/10.1016/j.clinthera.2011.06.001

Carillo-Conde, B., Brewer, E., Lowman, A., & Peppas, N. (2015). Complexation Hydrogels as Oral Delivery Vehicles of Therapeutic Antibodies: An in Vitro and ex Vivo Evaluation of Antibody Stability and Bioactivity. *Industrial & Engineering Chemistry Research, 54*(42), 10197-101205. doi: doi:10.1021/acs.iecr.5b01193

Chirra, H., & Desai, T. (2012). Multi-Reservoir Bioadhesive Microdevices for Independent Rate-Controlled Delivery of Multiple Drugs. *Small, 8*(24), 3839-3846. doi:10.1002/smll.201201367

Christensen, C., Kaufman, S., & Shih, W. (2008). Innovation Killers: How Financial Tools Destroy Your Capacity to Do New Things. *Harvard Business Review*. Retrieved from https://www.hbs.edu/faculty/Pages/item.aspx?num=31559

Chum, H. I. (1995). Impact of the change from an injectable to a fully oral regimen on patient adherence to ambulatory tuberculosis treatment in Dar es Salaam, Tanzania. *Tubercle and Lung Disease*, 286-289. doi:doi:10.1016/s0962-8479(05)80025-5

COMSOL AB. (n.d.). COMSOL Multiphysics(R) v. 5.3. Stockholm, Sweden: www.comsol.com.

COMSOL AB. (n.d.). User's Guide. Stockholm, Sweden: COMSOL Multiphysics(R) v. 5.3.

Curran, J. (2017). *IBISWorld Industry Report NN001: Biotechnology in the US.* IbisWorld. Retrieved from www.ibisworld.com

Dahlöf, C. G. (2005). Non-oral formulations of triptans and their use in acute migraine. *Current Pain and Headache Reports,, 9*(3), 206-212. doi:doi:10.1007/s11916-005-0064-x

Dangi, R. (2015). *Needle-Free Devices, Technologies and Global Markets HLC178A.* BCC Research.

Degen, L., & Phillips, S. (1996). Variability of gastrointestinal transit in healthy women and men. *Gut., 39*(2), 299-305. Retrieved from https://www.ncbi.nlm.nih.gov/pubmed/8977347#

Diabetes.co.uk. (2018). *History of Insulin*. Retrieved from https://www.diabetes.co.uk/insulin/history-of-insulin.html

Dibonaventura, M. W. (2010). Multinational Internet-based survey of patient preference for newer oral or injectable Type 2 diabetes medication. *Patient Preference and Adherence*, 397. doi:doi:10.2147/ppa.s14477

Drugbank. (n.d.). *Pegfilgrastim*. Retrieved from https://www.drugbank.ca/drugs/DB00019

Duro, D., & Kamin, D. (2007). Overview of short bowel syndrome and intestinal transplantation. *Colombia Medica, 38*(1). Retrieved from http://colombiamedica.univalle.edu.co/index.php/comedica/article/view/490/1022

Emadi, S. A. (2017). An assessment of the current treatment landscape for rheumatology patients in Qatar: Recognising unmet needs and moving towards solutions. *Journal of International Medical Research, 45*(2), 733-743. doi:doi:10.1177/0300060516686872

Emaze. (n.d.). *Emaze*. Retrieved from https://www.emaze.com/@AWITTLLZ/Untitled

EnteraBio. (n.d.). *Oral Delivery of Large Molecules*. Retrieved from EnteraBio: http://www.enterabio.com/

Esposti, L., Sangiorgi, D., Perrone, V., Radice, S., Clementi, E., Perone, F., & Buda, S. (2014). Adherence and resource use among patients treated with biologic drugs: findings from BEETLE study.

ClinicoEconomics and Outcomes Research, 401-407. doi:https://dx.doi.org/10.2147%2FCEOR.S66338

EvaluatePharma. (n.d.). Market Research.

Fallowfield, L. (2005). Patients preference for administration of endocrine treatments by injection or tablets: results from a study of women with breast cancer. *Annals of Oncology, 17*(2), 205-210. doi:doi:10.1093/annonc/mdj044

Fields, J., Go, J., & Schulze, K. (2015). Pill Properties that Cause Dysphagia and Treatment Failure. *Current Therapeutic Research, 77*, 79-82. doi:10.1016/j.curtheres.2015.08.002

Fox, C., Cao, Y., Nemeth, C., Chirra, H., Chevalier, R., Xu, A., . . . Desai, T. (2016). Fabrication of Sealed Nanostraw Microdevices for Oral Drug Delivery. *ACS Nano, 10*(6), 5873-5881. doi:10.1021/acsnano.6b00809

Fox, C., Kim, J., Le, L., Nemeth, C., Chirra, H., & Desai, T. (2015). Micro/nanofabricated Platforms for Oral Drug Delivery. *Journal of Controlled Release*. doi:10.1016/j.drudis.2006.08.005

Gallant, N. D., Michael, K. E., & Garcia, A. J. (2005, September). Cell Adhesion Strengthening: Contributions of Adhesive Area, Integrin Binding, and Gocal Adhesion Assembly. *Molecular Biology of the Cell, 16*, 4329-4340. Retrieved from http://www.molbiolcell.org/content/16/9/4329.full.pdf+html

Garcia, A., & Boettiger, D. (1999). Integrin–fibronectin interactions at the cell-material interface: initial integrin binding and signaling. *Biomaterials, 20*(23-24), 2427-2433. doi:https://doi.org/10.1016/S0142-9612(99)00170-2

Gleason, C., Yee, C., Masatani, P., Middaugh, C., & Vance, A. (2016). Probing Shear Thinning Behaviors of IgG Molecules at the Air–Water Interface via Rheological Methods. *Langmuir (ACS Society), 32*(2), 496-504. doi:10.1021/acs.langmuir.5b03806

Goswami, T., Jasti, B., & Li, X. (2008). Sublingual Drug Delivery. *Critical Reviews in Therapeutic Drug Carrier Systems, 25*(5), 449-484. doi:10.1615/CritRevTherDrugCarrierSyst.v25.i5.20

Gupta, V., Hwang, B., Doshi, N., & Mitragotri, S. (2013). A permeation enhancer for increasing transport of therapeutic macromolecules across the intestine. *Journal of Controlled Release*, 541-549. doi:10.1016/j.jconrel.2013.05.002

Hagerman, E. M., Chao, S., Dunn, J., & Wu, B. (2005). Surface modification and initial adhesion events for intestinal epithelial cells. *Journal of Biomedical Materials Research, 76A*(2), 272-278. doi:10.1002/jbm.a.30562

Hamman, J., Enslin, G., & Kotze, A. (2005). Oral Delivery of Peptide Drugs. *Biodrugs, 19*(3), 165-177.

Hawe, A., Hulse, W., Jiskoot, W., & Forbes, R. (2011). Taylor Dispersion Analysis Compared to Dynamic Light Scattering for the Size Analysis of Therapeutic Peptides and Proteins and Their Aggregates. *Pharmaceutical Research, 28*(9), 2302-2310. doi:10.1007/s11095-011-0460-3

Hay, M., Thomas, D., Craighead, J., Economides, C., & Rosentahl, J. (2014). Clinical development success rates for investigational drugs. *Nature Biotechnology, 32*(1), 40-51. doi:10.1038/nbt.2786.

He, H., Guan, J., Lee, L., & Hansford, D. (n.d.). *An Oral Delivery Device Based on Self-Folding Hydrogels.* Thesis, Ohio State University. doi:http://citeseerx.ist.psu.edu/viewdoc/download;jsessionid=D9749EA551C3A2C89910F2947A4820D3?doi=10.1.1.665.8961&rep=rep1&type=pdf

Healthline. (n.d.). *Uses of IV Medication*. Retrieved from Healthline: https://www.healthline.com/health/intravenous-medication-administration#uses

Healthline. (n.d.). *What Are Intramuscular Injections?* Retrieved from HealthLine: https://www.healthline.com/health/intramuscular-injection

HealthLine. (n.d.). *What is a subcutaneous injection?* Retrieved from HealthLine: https://www.healthline.com/health/subcutaneous-injection

Hearnden, V., Sankar, V., Hull, K., Juras, D., Greenberg, M., Kerr, A., . . . Thornhill, M. (2012). New developments and opportunities in oral mucosal drug delivery for local and systemic disease. *Advanced Drug Delivery Reviews*, 16-28. doi:http://dx.doi.org/10.1016/j.addr.2011.02.008

Imran, M. (2014). *United States Patent No. US 8.846,040 B2.*

Imran, M. (2016). A Novel Approach to the Oral Delivery of Biologics, Peptides, and Antibodies. *On Drug Delivery*, 18-19.

Into to Anatomy 6: Tissues, Membranes, Organs. (2007). Retrieved from http://www.freethought-forum.com/forum/showthread.php?t=11577

IntractPharma. (n.d.). *Pholoral(R)*. Retrieved from IntractPharma: https://www.intractpharma.com/phloral

Intravenous (IV) Infusion Therapy. (n.d.). Retrieved from Ainsworth Institute of Pain Management: http://ainsworthinstitute.com/intravenous-infusion-therapy/

IPEC Europe. (2013). *IPEC Europe*. Retrieved from http://ipec-europe.org/newsletter_print.asp?nlid=36&nlaid=

Kale, T., & Momin, M. (2014). Needle free injection technology - An overview. *Inov Pharm*. Retrieved from http://pubs.lib.umn.edu/ innovations/vol5/iss1/10

Kendler, D. L. (2009). Preference and satisfaction with a 6-month subcutaneous injection versus a weekly tablet for treatment of low bone mass. *Osteoporosis International, 21*(5), 837-846. doi:doi:10.1007/s00198-009-1023-x

Kristensen, M., & Nielsen, H. (2015). Cell-Penetrating Peptides as Carriers for Oral Delivery of Biopharmaceuticals. *Basic & Clinical Pharmacology & Toxicology, 118*(2), 99-106. doi:10.1111/bcpt.12515

Krohe, M. E. (2016). Patient-reported preferences for oral versus intravenous administration for the treatment of cancer: a review of the literature. *Patient Preference and Adherence, 10*, 1609-1621. doi:doi:10.2147/ppa.s106629

Langer, R., & Traverso, G. (2017). Oral delivery of biologics using drug-device combinations. *Current Opinion in Pharmacology, 36*, 8-13.

Leader, B., Baca, Q., & Golan, D. (2008). Protein therapeutics: a summary and pharmacological classification. *Nature Reviews Drug Discovery*, 21-39. doi:doi:10.1038/nrd2399

Liepmann, D. (2017). Hybrid plasic-based MEMS devices. *Medical MEMs and Sensors 2017 Conference*, 25-35.

Linnankoski, J., Mäkelä, J., Palmgren, J., Mauriala, T., Vedin, C., Ungell, A., . . . Yliperttula, M. (2010). Paracellular porosity and pore size of the human intestinal epithelium in tissue and cell culture models. *J. Pham. Sci.*, 2166-2175. doi:10.1002/jps.21961

Liu, J., Pang, Y., Zhang, S., Cleveland, C., Yin, X., Booth, L., . . . Traverso, G. (2017). Tiggerable tough hydrogels for gastric resident dosage forms. *Nature Communications, 8*(24). doi:10.1038/s41467-017-00144-z

Loh, Q., & Choong, C. (2013). Three-Dimensional Scaffolds for Tissue Engineering Applications: Role of Porosity and Pore Size. *Tissue Engineering*, 485-502.

Lybecker, K. (2016). *The Biologics Revolution in the Production of Drugs.* Fraser Institute. Retrieved from https://www.fraserinstitute.org/sites/default/files/biologics-revolution-in-the-production-of-drugs.pdf

Mapara, S., & Patravale, V. (2017). Medical capsule robots: A renaissance for diagnostics, drug delivery and surgical treatment. *Journal of Controlled Release*, 337-351. doi:10.1016/j.jconrel.2017.07.005

McGrath, R., & MacMillan, I. (1995). Discovery-Driven Planning. *Harvard Business Review*. doi:https://hbr.org/1995/07/discovery-driven-planning

McKenzie, S., & Evers, B. (2016). *Small Intestine*. Retrieved from Thoracic Key: https://thoracickey.com/small-intestine/

MDBR. (n.d.). *Amgen gets FDA approval for Repatha Pushtronex system*. Retrieved from MDBR Specialty Devices: http://drugdeliverydevices.medicaldevices-business-review.com/news/amgen-gets-fda-approval-for-repatha-pushtronex-system-120716-4946611

Mestre-Ferrandiz, J., Sussex, J., & Towse, A. (2012). *The R&D Cost of a New Medicine.* London: Office of Health Economics.

MIMS. (n.d.). *Enbrel Vial/Enbrel Pre-filled Pen/Enbrel Pre-filled Syringe*. Retrieved from MIMS: https://www.mims.com/hongkong/image/info/enbrel%20pre-filled%20syringe%20inj%2050%20mg/50%20mg

Minitab, Inc. (2010). Minitab 16 Statistical Software. State College, PA. Retrieved from www.minitab.com

MIT. (2018). *Research*. Retrieved from http://web.mit.edu/eppinger/www/SDE-MIT/Research.html

Mitragotri, S. (2005). et-induced skin puncture and its impact on needle-free jet injections: Experimental studies and a predictive model. *Journal of Controlled Release, 106*(3), 361-73. doi:10.1016/j.jconrel.2005.05.023.

Mitragotri, S., Burke, P., & Langer, R. (2014). Overcoming the challenges in administering biopharmaceuticals: formulation and delivery strategies. *Nature Reviews - Drug Discovery, 13*, 655-672. doi:10.1038/nrd4363

Montenegro-Nicolini, M., & Morales, J. (2017). Overview and Future Potential of Buccal Mucoadhesive Films as Drug Delivery Systems for Biologics. *AAPS PharmSciTech, 18*(1). doi:10.1208/s12249-016-0525-z

Morales, J., Fathe, K., Brunaugh, A., Ferrati, S., Li, S., Montenegro, M., . . . Smyth, H. (2017). Challenges and Future Prospects for the Delivery of Biologics: Oral Mucosal, Pulmonary, and Transdermal Routes. *The AAPS Journal*. doi:10.1208/s12248-017-0054-z

Morishita, M., & Peppas, N. (2006). Is the oral route possible for peptide and protein drug delivery? *Drug Discovery Today*, 905-910. doi:10.1016/j.drudis.2006.08.005

Muheem, A., Shakeel, F., Jahangir, M., Anwar, M., Mallick, N., Jain, G., . . . Ahmad, F. (2016). A review on the strategies for oral delivery of proteins and peptides and their clinical perspectives. *Saudi Pharmaceutical Journal, 24*(4), 413-428. doi:10.1016/j.jsps.2014.06.004

Munsell, M. F. (2016). An evaluation of adherence in patients with multiple sclerosis newly initiating treatment with a self-injectable or an oral disease-modifying drug. *Patient Preference and Adherence, 11*, 55-62. doi:doi:10.2147/ppa.s118107

Muntz, S. (2008). *Fluid structure interaction for fluid flow normal to deformable porous media.* Doctoral Thesis, Technische Universität Kaiserslautern. Retrieved from https://kluedo.ub.uni-kl.de/frontdoor/index/index/docId/2054

Negreanu, L., Pepescu, B., Babiuc, R., Ene, A., Bajenaru, O., & Smarandache, G. (2011). Duodopa infusion treatment: a point of view from the gastroenterologist. *J Gastointestin Liver Dis*, 325-7. Retrieved from https://www.ncbi.nlm.nih.gov/pubmed/21961105

O'Brien, F., Harley, B., Waller, M., Yannas, I., Gibson, L., & Prendergast, P. (2007). The effect of pore size on permeability and cell attachment in collagen. *Technology and Health Care, 15*(1), 3-17. Retrieved from http://epubs.rcsi.ie/anatart/5

On Drug Delivery. (2015). *INTERVIEW: MIR IMRAN, RANI THERAPEUTICS.* Retrieved from On Drug Delivery: https://www.ranitherapeutics.com/assets/Rani_HR.pdf

Opportunities for biosimilar development. (2011, June 5). Retrieved from Generics and Biosimilars Initiative: http://www.gabionline.net/Biosimilars/Research/Opportunities-for-biosimilar-development

Osterberg, L., & Blaschke, T. (2005). Adherence to Medication. *The New England Journal of Medicine*, 487-497.

Ovensa. (n.d.). *Triozan(TM) Nanomedicine Delivery Platform*. Retrieved from Ovensa: ovensa.com

Philippidis, A. (2017, March 6). *The Top 15 Best-Selling Drugs of 2016*. Retrieved from Leading the Eay in Life Science Technologies: https://www.genengnews.com/the-lists/the-top-15-best-selling-drugs-of-2016/77900868

Proxima. (n.d.). *ProximaConcepts*. Retrieved from http://www.proximaconcepts.com/

PubChem. (n.d.). *Insulin Recombinant*. Retrieved from Open Chemistry Database: https://pubchem.ncbi.nlm.nih.gov/compound/70678557#section=Top

Rani Therapeutics. (2017). *Technology*. Retrieved from Rani Therapeutics: https://www.ranitherapeutics.com/technology/

Rani Therapeutics. (2017, January). The Holy Grail of Drug Delivery. *Rani Therapeutics - Non-Confidential Introduction*.

Rani Therapeutics. (n.d.). *Oral Biotherapeutics Drug Delivery.* Retrieved from Rani Therapeutics: https://www.ranitherapeutics.com/assets/rani_pre-clinical_data.pdf

Rasband, W. S. (1997-2017). ImageJ. Bethesda, MA, USA: U.S. National Institutes of Health. Retrieved from https://imagej.nih.gov/ij/

Reuters. (2017, December 5). *Shire in deal to develop a new way to administer hemophilia drug*. Retrieved from Reuters: https://www.reuters.com/article/us-shire-rani-therapeutics/shire-in-deal-to-develop-a-new-way-to-administer-hemophilia-drug-idUSKBN1DZ1Z1

Richter, W. F., Bhansali, S. G., & Morris, M. E. (2012). Mechanistic Determinants of Biotherapeutics Absorption Following SC Administration. *AAPS J.*, 559–570.

Rieux, A., Fievez, V., Garinot, M., Schneider, Y., & Preat, V. (2006). Nanoparticles as potential oral delivery systems of proteins and vaccines: A mechanistic approach. *Journal of Controlled Release*, 1-27. doi:10.1016/j.jconrel.2006.08.013

Robbins, J., Langmore, S., Hind, J., & Erlichman, M. (2002). Dysphagia research in the 21st century and beyond: Proceedings from Dysphagia Experts Meeting, August 21, 2001. *Journal of Rehabilitation Research & Development, 39*(4), 543-548. Retrieved from https://www.rehab.research.va.gov/jour/02/39/4/robbins.html

Schlegel, F. (2015, January 27). *Which Multiphase Flow Interface Should I Use?* Retrieved from COMSOL Blog: https://www.comsol.com/blogs/which-multiphase-flow-interface-should-i-use/

Schoellhammer, C., & Traverso, G. (2016). Low-frequency ultrasound for drug delivery in the gastrointestinal tract. *Expert Opin Drug Deliv*, 1045-1048. doi:10.1517/17425247.2016.1171841.

Schoellhammer, C., Lauwers, G., Goettel, J., Oberli, M., Cleveland, C., Park, J., . . . Traverso, G. (2017). Ultrasound-Mediated Delivery of RNA to Colonica Mucosa of Live Mice. *Gastroenterology*, 1151-1160. doi:10.1053/j.gastro.2017.01.002

Schoellhammer, C., Schroeder, A., Maa, R., Lauwers, G., Swiston, A., Zervas, M., . . . Traverso, G. (2015). Ultrasound-mediated gastrointestinal drug delivery. *Sci Tranl Med*. doi:10.1126/scitranslmed.aaa5937.

Schull, D., & Sackowitz, K. (n.d.). *Pharmaceutical Companies Lose $637 Billion in Revenue Annually Due to Medication Nonadherence*. Retrieved from https://www.prnewswire.com/news-releases/pharmaceutical-companies-lose-637-billion-in-revenue-annually-due-to-medication-nonadherence-300363979.html

Shergold, O. A., Fleck, N., & King, T. (2006). The penetration of a soft solid by a liquid jet, with application to the administration of a needle-free injection. *Journal of Biomechanics, 39*(14), 2593-2602. Retrieved from https://doi.org/10.1016/j.jbiomech.2005.08.028

Sigma Aldrich. (2017). *Acetylsalicylic Acid*. Retrieved from Sigma-Aldrich: https://www.sigmaaldrich.com/catalog/product/sigma/a5376?lang=en&region=US

Stelray, Inc. (n.d.). *Reference Tables*. Retrieved from Stelray {;astic Products, Inc.: http://stelray.com/reference-tables.html

Stone, K. (2017, October 12). *Top 10 Biologic Drugs in the United States*. Retrieved from The Balance: https://www.thebalance.com/top-biologic-drugs-2663233

Tagawa, Y., Oudalov, N., Ghalbzouri, A., Sun, C., & Lohse, D. (2013). Needle-free injection into skin and soft matter with highly focused microjets. *Lab on a Chip*. doi:doi:10.1039/c2lc41204g

Takahashi-Iwanaga, H., Iwanaga, T., & Isayama, H. (1999). Porosity of the epithelial basement membrane as an indicator of macrophage-enterocyte interaction in the intestinal mucosa.

Archives of Histology and Cytology, 62(5), 471-81. Retrieved from https://www.ncbi.nlm.nih.gov/pubmed/10678576

Tarsa Therapeutics. (n.d.). *Tarsa Therapeutics and Unigene Present Preclinical Data Suggesting Calcitonin May Have Utility in Combination Therapy for the Treatment Of Osteoarthritis*. Retrieved from Tarsa Therapeutics: http://tarsatherapeutics.com/tarsa-therapeutics-and-unigene-present-preclinical-data-suggesting-calcitonin-may-have-utility-in-combination-therapy-for-the-treatment-of-osteoarthritis/

Terwiesch, C., & Ulrich, K. (2009). *Innovation Tournaments.* Boston: Harvard Business Press.

The Composites Store. (n.d.). *Viscosity Comparison Chart*. Retrieved from http://www.cstsales.com/viscosity.html

The Engineering Toolbox. (n.d.). *Specific Heat of Solids*. Retrieved from https://www.engineeringtoolbox.com/specific-heat-solids-d_154.html

The Engineering Toolbox. (n.d.). *Thermal Conductivity of Common Materials and Gases*. Retrieved from https://www.engineeringtoolbox.com/thermal-conductivity-d_429.html

ThermoFisher Scientific. (n.d.). *Immunoglobulin Structure and Classes*. Retrieved from ThermoFisher Scientific: https://www.thermofisher.com/us/en/home/life-science/antibodies/antibodies-learning-center/antibodies-resource-library/antibody-methods/immunoglobulin-structure-classes.html

ThioMatrix. (n.d.). *Thiomer Technology*. Retrieved from ThioMatrix: http://www.thiomatrix.com/Technology/Technology.html

Tibbitt, M., Dahlman, J., & Langer, R. (2016). Emerging Frontiers in Drug Delivery. *Journal of the American Chemical Society*, 704-717. doi:10.1021/jacs.5b09974

Traverso, G., Schoellhammer, C., Schroeder, A., Maa, R., Lauwers, G., Polat, B., . . . Langer, R. (2015). Microneedles for Drug Delivery via the Gastrointestinal Tract. *Journal of Pharmaceutical Sciences, 104*, 362-267. doi:10.1002/jps.24182

UCI. (n.d.). *Epithelial Stem Cells*. (University of California, Irvine) Retrieved from Small Intestine Engineering: http://bme240.eng.uci.edu/students/06s/mfarnia/Untitled-4.html

University of Colorado. (2018). *First-Order System: Transient Response of a Thermocouple to a Step Temperature Change.* Retrieved from https://www.colorado.edu/MCEN/Measlab/background1storder.pdf

Utz, K. S. (2014). Patient preferences for disease-modifying drugs in multiple sclerosis therapy: a choice-based conjoint analysis. *Therapeutic Advances in Neurological Disorders, 7*(6), 263-275. doi:doi:10.2147/ppa.s14477

Vangeli, E., Bakhshi, S., Baker, A., Fisher, A., Bucknor, D., Mrowietz, U., . . . Weinman, J. (2015). A Systematic Review of Factors Associated with Non-Adherence to Treatment for Immune-Mediated Inflammatory Diseases. *Advances in Therapy*, 983-1028. doi:https://dx.doi.org/10.1007%2Fs12325-015-0256-7

Walsh, L., Ryu, J., Bock, S., Koval, M., Mauro, T., Ross, R., & Desai, T. (2015). Nanotopography Facilitates in Vivo Transdermal Delivery of HIgh Molecular Weight Therapeutics through an Integrin-Dependent Mechanism. *Nano Letters*, 2434-2441. doi:10.1021/nl504829f

WHO. (2003). *Adherence to Long-Term Therapies.* World Health Organization. Retrieved from http://www.who.int/chp/knowledge/publications/adherence_full_report.pdf

Yahoo Finance. (2017). *Amgen Inc. (AMGN).* Retrieved from Yahoo! Finance: https://finance.yahoo.com/quote/amgn?ltr=1

Zelikin, A., Ehrhardt, C., & Healy, A. (2016). Materials and methods for delivery of biological drugs. *Nature Chemistry, 8*, 991-1007. doi:10.1038/NCHEM.2629

Appendices

Appendix 1– Weighting and scores from down-selection

Table 0-1 Weighting for criteria among 4 evaluators

	Criteria	Weighting			
1	**Technical Performance**	Intern	Pr. Eng 1	Pr. Eng 2	Dir. Form
	Delivery Abilities (Loading Capacity, Location)				
1.1	Compatible with proteins (50kDa and above)	10	10	10	4
1.2	Compatible with small proteins (6.5kDa to 50kDa)	7	7	5	5
1.3	Compatible with peptides (1kDa to 6.5kDa)	5	5	1	7
1.4	Compatible with small molecules (less than 1kDa)	1	5	1	10
1.5	Volume of delivery / Payload capability	7	7	10	8
1.6	Reduce side effects & increase efficacy of therapy via GI localization	5	7	5	3
1.7	Likelihood of high protein integrity from device MOA	7	10	7	9
1.8	Enables systemic delivery	10	10	10	5
	Safety				
1.9	Retention Time (i.e. risk of retention beyond average digestive cycle, OROS size 9mmx15mm)	7	5	3	8
1.1	Likelihood of long-term health effects	7	7	5	7
1.11	Biocompatible	10	10	10	8
1.12	Risk of infection or immune response	10	10	10	8
	Bioavailability, Protection, Absorption				
1.13	Efficacy on par with Sub-Q	7	7	5	4
1.14	Ability to protect from gut enzymes in stomach and GI (or buccal)	10	10	7	10
1.15	Ability to protect from pH changes in stomach and GI	10	10	7	10
1.16	Likelihood of reliable and predictable dose delivery based on mechanism	10	10	10	10
	Device Characteristics				
1.17	Extent of Reformulation Required*	8	10	1	10
1.18	Inclusion of Visible Sharps	5		8	10
1.19	Ability to deliver highly viscous fluids within size constraint	5	10	5	5
1.2	Pill Size (i.e. Ease of Swallowing)	7	7	5	8
1.21	Large animal in vivo studies performed?	7	7	1	7
1.22	Requires external activation?	7	10	10	5
1.23	Confirmation of dosing event?	4	3	1	3
1.24	Potential for significant pain	7		10	8
2	**Operational Considerations**	Intern	Pr. Eng 1	Pr. Eng 2	Dir. Form
2.1	Potential COGM Impact	4	5	3	7
2.2	Manufacturability Rating (Sterility in GMP setting possible?)	6	10	3	7
2.3	Ease of Fit of Regulatory Pathway with current combo. Products	4	5	7	8
2.4	Protein Stability in Final Form	7	10	5	8

2.5	Device Reliability	5	10	7	7
3	**Value to Business**	Intern	Pr. Eng 1	Pr. Eng 2	Dir. Form
3.1	Maturity of Technology	5	3	1	5
3.2	IP - Ability to Extend Molecule Patent	10	10	7	10
3.3	Ownership by a Corporation	5	0	3	7
3.4	Patient Preference	10	7	10	10

Device	H	A	B	c	D	F	I	E	G
Total Value (TV_j)	407	499	406	492	432	410	335	422	347
Total Possible	702	702	630	687	702	702	702	702	630
Percentage	58%	71%	64%	72%	62%	58%	48%	60%	55%
Rank	7	2	3	1	4	6	9	5	8

Criteria		Weighting Factor (W_i)	Scores for Individual Technologies ($S_{i,j}$)								
1.1	Compatible with proteins (50kDa and above)	10	1	3	3	3	3	1	2	3	3
1.2	Compatible with small proteins (6.5kDa to 50kDa)	7	1	3	3	3	3	2	3	3	3
1.3	Compatible with peptides (1kDa to 6.5kDa)	5	3	3	3	3	3	3	3	3	3
1.4	Compatible with small molecules (less than 1kDa)	1	3	3	3	3	3	3	3	3	3
1.5	Volume of delivery / Payload capability	7	1	3	3	2	3	2	0	1	3
1.6	Reduce side effects & increase efficacy of therapy via GI localization	5	3	3	0	3	3	2	3	3	0
1.7	Likelihood of high protein integrity from device MOA	7	1	1	1	2	1	1	1	2	2
1.8	Enables systemic delivery	10	1	3	3	3	3	1	2	1	2
1.9	Retention Time (i.e. risk of retention beyond average digestive cycle, OROS size 9mmx15mm)	7	3	3	N/A	2	1	3	1	3	N/A
1.10	Likelihood of long-term health effects	7	3	2	1	2	1	2	3	3	2
1.11	Biocompatible	10	3	3	3	3	1	3	2	3	2
1.12	Risk of infection or immune response	10	3	2	2	1	1	2	2	1	1
1.13	Efficacy on par with Sub-Q	7	0	1	2	3	3	1	1	1	1
1.14	Ability to protect from gut enzymes in stomach and GI (or buccal)	10	1	2	2	3	3	2	1	2	1
1.15	Ability to protect from pH changes in stomach and GI	10	3	3	N/A	3	3	3	2	3	N/A
1.16	Likelihood of reliable and predictable dose delivery based on mechanism**	10	0	1	3	1	2	1	1	0	2
1.18	Extent of Reformulation Required*	8	0	2	2	1	2	1	2	1	2
1.19	Inclusion of Visible Sharps	5	3	3	3	2	0	2	3	3	1
1.20	Ability to deliver highly viscous fluids within size constraint	5	0	1	3	N/A	1	1	1	1	1
1.21	Pill Size (i.e. Ease of Swallowing)	7	3	3	N/A	1	1	3	1	3	N/A
1.22	Large animal in vivo studies performed?	7	0	0	0	3	1	0	2	0	1
1.23	Requires external activation?	7	3	3	1	3	3	3	0	3	1
1.24	Confirmation of dosing event?	4	0	0	3	0	0	0	0	0	2
1.25	Potential for significant pain	7	3	3	1	2	1	1	0	2	1
2.1	Potential COGM Impact	4	1	3	3	1	1	1	0	1	1
2.2	Manufacturability Rating (Sterility in GMP setting possible?)	6	3	2	2	1	1	1	1	1	1
2.3	Ease of Fit of Regulatory Pathway with current combo. Products	4	1	2	2	1	2	1	1	0	2
2.4	Protein Stability in Final Form	7	1	2	2	3	2	2	1	2	2
2.5	Device Reliability	10	3	1	1	1	2	2	1	1	2
3.1	Maturity of Technology	5	1	1	1	2	1	0	0	1	0
3.2	IP - Ability to Extend Molecule Patent	10	0	1	1	1	1	2	2	2	2
3.3	Ownership by a Corporation	5	3	1	1	3	1	1	1	1	1
3.4	Patient Preference	10	3	3	1	3	2	3	1	2	1

Figure 0-1 Intern Technology Scores

		Device	H	A	B	c	D	F	I	E	G
		Total Value	359	445	358	411	366	353	370	264	360
		Total Possible	579	579	534	564	579	579	579	579	579
		Percentage	62%	77%	67%	73%	63%	61%	64%	46%	62%
		Rank	7	1	3	2	5	8	4	10	6
1	Technical Performance										
	Delivery Abilities (Loading Capacity, Location)	Importance									
1.1	Compatible with proteins (50kDa and above)	10	1	3	3	3	3	1	1	2	3
1.2	Compatible with small proteins (6.5kDa to 50kDa)	5	1	3	3	3	3	2	3	3	3
1.3	Compatible with peptides (1kDa to 6.5kDa)	1	3	3	3	3	3	3	3	3	3
1.4	Compatible with small molecules (less than 1kDa)	1	3	3	3	3	3	3	3	3	3
1.5	Volume of delivery / Payload capability	10	1	3	3	2	3	2	2	0	1
1.6	Reduce side effects & increase efficacy of therapy via GI localization	5	3	3	0	3	3	2	3	3	3
1.7	Likelihood of high protein integrity from device MOA	7	1	1	1	2	1	1	1	1	2
1.8	Enables systemic delivery	10	1	3	3	3	3	1	1	2	1
	Safety										
1.9	Retention Time (i.e. risk of retention beyond average digestive cycle, OROS size 9	3	3	3	N/A	2	1	3	3	1	3
1.10	Likelihood of long-term health effects	5	3	2	1	2	1	2	3	3	3
1.11	Biocompatible	10	3	3	3	3	1	3	3	2	3
1.12	Risk of infection or immune response	10	3	2	2	1	1	2	2	2	1
	Bioavailability, Protection, Absorption										
1.13	Efficacy on par with Sub-Q	5	0	1	2	3	3	1	0	1	1
1.14	Ability to protect from gut enzymes in stomach and GI (or buccal)	7	1	2	2	3	3	2	1	1	2
1.15	Ability to protect from pH changes in stomach and GI	7	3	3	N/A	3	3	3	3	2	3
1.16	Likelihood of reliable and predictable dose delivery based on mechanism**	10	0	1	3	1	2	1	0	1	0
	Device Characteristics										
1.18	Extent of Reformulation Required*	1	0	2	2	1	2	1	2	2	1
1.19	Inclusion of Visible Sharps	8	3	3	3	2	0	2	3	3	3
1.20	Ability to deliver highly viscous fluids within size constraint	5	0	1	3	N/A	1	1	1	1	1
1.21	Pill Size (i.e. Ease of Swallowing)	5	3	3	N/A	1	1	3	3	1	3
1.22	Large animal in vivo studies performed?	1	0	0	0	3	1	0	0	2	0
1.23	Requires external activation?	10	3	3	1	3	3	3	3	0	3
1.24	Confirmation of dosing event?	1	0	0	3	0	0	0	0	0	0
1.25	Potential for significant pain	10	3	3	1	2	1	1	3	0	2
0	0	0									
2	Operational Considerations										
	Detail Requirements	Importance									
2.1	Potential COGM Impact	3	1	3	3	1	1	1	1	0	1
2.2	Manufacturability Rating (Sterility in GMP setting possible?)	3	3	2	2	1	1	1	1	1	1
2.3	Ease of Fit of Regulatory Pathway with current combo. Products	7	1	2	2	1	2	1	1	1	0
2.4	Protein Stability in Final Form	5	1	2	2	3	2	2	1	1	2
2.5	Device Reliability	7	3	1	1	1	2	2	2	1	1
3	Value to Business										
	Detail Requirements	Importance									
3.1	Maturity of Technology	1	1	1	1	2	1	0	0	0	1
3.2	IP - Ability to Extend Molecule Patent	7	0	1	1	1	1	2	2	2	2
3.3	Ownership by a Corporation	3	3	1	1	3	1	1	1	1	1
3.4	Patient Preference	10	3	3	1	3	2	3	3	1	2
3.5	0	0									

Figure 0-2 Principal Engineer #1 Technology Scores

		Device	H	A	B	c	D	F	I	E	G
		Total Value	386	529	427	474	462	420	414	348	425
		Total Possible	711	711	645	681	711	711	711	711	711
		Percentage	54%	74%	66%	70%	65%	59%	58%	49%	60%
		Rank	9	1	3	2	4	6	7	10	5
1	Technical Performance										
	Delivery Abilities (Loading Capacity, Location)	Importance									
1.1	Compatible with proteins (50kDa and above)	10	1	3	3	3	3	1	1	2	3
1.2	Compatible with small proteins (6.5kDa to 50kDa)	7	1	3	3	3	3	2	3	3	3
1.3	Compatible with peptides (1kDa to 6.5kDa)	5	3	3	3	3	3	3	3	3	3
1.4	Compatible with small molecules (less than 1kDa)	5	3	3	3	3	3	3	3	3	3
1.5	Volume of delivery / Payload capability	7	1	3	3	2	3	2	2	0	1
1.6	Reduce side effects & increase efficacy of therapy via GI localization	7	3	3	0	3	3	2	3	3	3
1.7	Likelihood of high protein integrity from device MOA	10	1	1	1	2	1	1	1	1	2
1.8	Enables systemic delivery	10	1	3	3	3	3	1	1	2	1
	Safety										
1.9	Retention Time (i.e. risk of retention beyond average digestive cycle, OROS size 9	5	3	3	N/A	1	1	3	3	1	3
1.10	Likelihood of long-term health effects	7	3	2	1	1	1	2	3	3	3
1.11	Biocompatible	10	3	3	3	3	1	3	3	2	3
1.12	Risk of infection or immune response	10	3	2	2	1	1	2	2	2	1
	Bioavailability, Protection, Absorption										
1.13	Efficacy on par with Sub-Q	7	0	1	2	3	3	1	0	1	1
1.14	Ability to protect from gut enzymes in stomach and GI (or buccal)	10	1	2	2	3	3	2	1	1	2
1.15	Ability to protect from pH changes in stomach and GI	10	3	3	N/A	3	3	3	3	2	3
1.16	Likelihood of reliable and predictable dose delivery based on mechanism**	10	0	1	3	1	2	1	0	1	0
	Device Characteristics										
1.18	Extent of Reformulation Required*	10	0	3	2	1	2	1	2	2	1
1.19	Inclusion of Visible Sharps	0	3	3	3	2	0	2	3	3	3
1.20	Ability to deliver highly viscous fluids within size constraint	10	0	2	3	N/A	1	1	1	1	1
1.21	Pill Size (i.e. Ease of Swallowing)	7	3	3	N/A	1	1	3	3	1	3
1.22	Large animal in vivo studies performed?	7	0	0	0	3	1	0	0	2	0
1.23	Requires external activation?	10	3	3	1	3	3	3	3	0	3
1.24	Confirmation of dosing event?	3	0	0	3	0	0	0	0	0	0
1.25	Potential for significant pain	0	3	3	1	2	1	1	3	0	2
0	0	0									
2	Operational Considerations										
	Detail Requirements	Importance									
2.1	Potential COGM Impact	5	1	3	3	1	1	1	1	0	1
2.2	Manufacturability Rating (Sterility in GMP setting possible?)	10	3	2	2	1	1	1	1	1	1
2.3	Ease of Fit of Regulatory Pathway with current combo. Products	5	1	2	2	1	2	1	1	1	0
2.4	Protein Stability in Final Form	10	1	2	2	3	2	2	1	1	2
2.5	Device Reliability	10	3	2	1	1	2	2	2	1	1

Figure 0-3 Principal Engineer #2 Technology Scores

		Device	H	A	B	c	D	F	I	E	G
		Total Value	500	414	418	425	419	402	369	437	319
		Total Possible	723	645	708	723	723	723	723	723	645
		Percentage	69%	64%	59%	59%	58%	56%	51%	60%	49%
		Rank	1	2	4	5	6	7	9	3	10
1	Technical Performance										
	Delivery Abilities (Loading Capacity, Location)	Importance									
1.1	Compatible with proteins (50kDa and above)	4	3	3	1	3	1	1	2	2	2
1.2	Compatible with small proteins (6.5kDa to 50kDa)	5	3	3	1	3	2	2	3	2	2
1.3	Compatible with peptides (1kDa to 6.5kDa)	7	3	3	3	3	3	3	3	3	3
1.4	Compatible with small molecules (less than 1kDa)	10	3	3	3	3	3	3	3	3	3
1.5	Volume of delivery / Payload capability	8	3	3	1	3	2	2	0	1	3
1.6	Reduce side effects & increase efficacy of therapy via GI localization	3	3	0	3	3	2	3	3	3	0
1.7	Likelihood of high protein integrity from device MOA	9	2	2	2	2	1	1	1	2	2
1.8	Enables systemic delivery	5	2	3	2	2	1	1	2	1	2
	Safety										
1.9	Retention Time (i.e. risk of retention beyond average digestive cycle, OROS size 9	8	3	N/A	2	1	3	3	1	3	N/A
1.10	Likelihood of long-term health effects	7	2	1	2	1	2	3	3	3	2
1.11	Biocompatible	8	3	3	3	1	3	3	2	3	2
1.12	Risk of infection or immune response	8	2	2	1	1	2	2	2	2	1
	Bioavailability, Protection, Absorption										
1.13	Efficacy on par with Sub-Q	4	1	2	3	3	1	0	1	1	1
1.14	Ability to protect from gut enzymes in stomach and GI (or buccal)	10	2	2	3	3	2	1	1	2	1
1.15	Ability to protect from pH changes in stomach and GI	10	3	N/A	3	3	3	3	2	3	N/A
1.16	Likelihood of reliable and predictable dose delivery based on mechanism**	10	1	2	1	2	1	0	2	0	1
	Device Characteristics										
1.18	Extent of Reformulation Required*	10	2	2	1	2	1	2	2	1	2
1.19	Inclusion of Visible Sharps	10	3	3	1	0	2	3	3	3	1
1.20	Ability to deliver highly viscous fluids within size constraint	5	1	3	N/A	1	1	1	1	1	1
1.21	Pill Size (i.e. Ease of Swallowing)	8	3	N/A	1	1	3	3	1	3	N/A
1.22	Large animal in vivo studies performed?	7	0	0	3	1	0	0	2	0	1
1.23	Requires external activation?	5	3	1	3	3	3	0	0	3	1
1.24	Confirmation of dosing event?	3	0	3	1	1	0	0	0	0	2
1.25	Potential for significant pain	8									
0	0	0									
2	Operational Considerations										
	Detail Requirements	Importance									
2.1	Potential CGM Impact	7	3	3	1	1	1	1	0	1	1
2.2	Manufacturability Rating (Sterility in GMP setting possible?)	7	1	1	2	1	1	1	1	1	1
2.3	Ease of Fit of Regulatory Pathway with current combo. Products	8	1	1	1	2	1	1	2	2	2
2.4	Protein Stability in Final Form	8	2	2	2	2	2	1	1	2	2
2.5	Device Reliability	7	1	1							
3	Value to Business										
	Detail Requirements	Importance									
3.1	Maturity of Technology	5	1	1	2	1	0	0	0	1	0
3.2	IP - Ability to Extend Molecule Patent	10	1	1	1	2	2	2	2	2	2
3.3	Ownership by a Corporation	7	3	3	1	2	2	2	2	2	1
3.4	Patient Preference	10	3	1	3	2	3	3	1	2	1
3.5	0	0									

Figure 0-4 Director of Formulation Technology Scores

Appendix 2

Minitab 16 General Regression Analyses. The numbers correlate to those in Table 7-28.

1) Max velocity vs LP

General Regression Analysis: %LP - EPI versus Max Velocity (mm/s)

```
Regression Equation

%LP - EPI  =  0.259114 + 0.000125937 Max Velocity (mm/s)


Coefficients

Term                    Coef    SE Coef        T      P
Constant            0.259114  0.0434170  5.96804  0.002
Max Velocity (mm/s) 0.000126  0.0000998  1.26168  0.263


Summary of Model

S = 0.0747209      R-Sq = 24.15%         R-Sq(adj) = 8.98%
PRESS = 0.0704607  R-Sq(pred) = -91.45%


Analysis of Variance

Source                DF     Seq SS     Adj SS     Adj MS        F         P
Regression             1  0.0088876  0.0088876  0.0088876  1.59184  0.262720
  Max Velocity (mm/s)  1  0.0088876  0.0088876  0.0088876  1.59184  0.262720
Error                  5  0.0279161  0.0279161  0.0055832
Total                  6  0.0368036


Fits and Diagnostics for Unusual Observations
```

2) Max velocity vs SES

General Regression Analysis: %SES - EPI versus Max Velocity (mm/s)

Regression Equation

%SES - EPI = 0.979952 + 5.46239e-006 Max Velocity (mm/s)

Coefficients

Term	Coef	SE Coef	T	P
Constant	0.979952	0.0022917	427.617	0.000
Max Velocity (mm/s)	0.000005	0.0000053	1.037	0.347

Summary of Model

S = 0.00394395 R-Sq = 17.69% R-Sq(adj) = 1.23%
PRESS = 0.000142071 R-Sq(pred) = -50.35%

Analysis of Variance

Source	DF	Seq SS	Adj SS	Adj MS	F	P
Regression	1	0.0000167	0.0000167	0.0000167	1.07492	0.347352
Max Velocity (mm/s)	1	0.0000167	0.0000167	0.0000167	1.07492	0.347352
Error	5	0.0000778	0.0000778	0.0000156		
Total	6	0.0000945				

Fits and Diagnostics for Unusual Observations

No unusual observations

3) Sus. Velocity vs LP

General Regression Analysis: %LP - EPI versus Sustained Velocity (mm/s)

Regression Equation

%LP - EPI = 0.257321 + 0.000936199 Sustained Velocity (mm/s)

Coefficients

Term	Coef	SE Coef	T	P
Constant	0.257321	0.0443907	5.79672	0.002
Sustained Velocity (mm/s)	0.000936	0.0007392	1.26642	0.261

Summary of Model

S = 0.0746530 R-Sq = 24.29% R-Sq(adj) = 9.14%
PRESS = 0.0680244 R-Sq(pred) = -84.83%

Analysis of Variance

Source	DF	Seq SS	Adj SS	Adj MS	F	P
Regression	1	0.0089383	0.0089383	0.0089383	1.60383	0.261153
Sustained Velocity (mm/s)	1	0.0089383	0.0089383	0.0089383	1.60383	0.261153
Error	5	0.0278654	0.0278654	0.0055731		
Total	6	0.0368036				

Fits and Diagnostics for Unusual Observations

No unusual observations

4) Sus Velocity vs SES

General Regression Analysis: %SES - EPI versus Sustained Velocity (mm/s)

Regression Equation

%SES - EPI = 0.979894 + 4.01738e-005 Sustained Velocity (mm/s)

Coefficients

Term	Coef	SE Coef	T	P
Constant	0.979894	0.0023491	417.133	0.000
Sustained Velocity (mm/s)	0.000040	0.0000391	1.027	0.352

Summary of Model

S = 0.00395057 R-Sq = 17.42% R-Sq(adj) = 0.90%
PRESS = 0.000139465 R-Sq(pred) = -47.59%

Analysis of Variance

Source	DF	Seq SS	Adj SS	Adj MS	F
Regression	1	0.0000165	0.0000165	0.0000165	1.05459
Sustained Velocity (mm/s)	1	0.0000165	0.0000165	0.0000165	1.05459
Error	5	0.0000780	0.0000780	0.0000156	
Total	6	0.0000945			

Source	P
Regression	0.351544
Sustained Velocity (mm/s)	0.351544
Error	
Total	

Fits and Diagnostics for Unusual Observations

No unusual observations

5) All input parameters vs LP

General Regression Analysis: %LP - EPI versus Viscosity (c, Threshold Pr, ...

Regression Equation

%LP - EPI = 0.439809 - 0.00255744 Viscosity (cps) - 0.00107152 Threshold Pressure (kPa) - 0.35987 Nozzle (mm)

Coefficients

Term	Coef	SE Coef	T	P
Constant	0.439809	0.097926	4.49125	0.021
Viscosity (cps)	-0.002557	0.001525	-1.67742	0.192
Threshold Pressure (kPa)	-0.001072	0.001883	-0.56900	0.609
Nozzle (mm)	-0.359870	0.570633	-0.63065	0.573

Summary of Model

S = 0.0688787 R-Sq = 61.33% R-Sq(adj) = 22.66%
PRESS = 0.0545902 R-Sq(pred) = -48.33%

Analysis of Variance

Source	DF	Seq SS	Adj SS	Adj MS	F
Regression	3	0.0225708	0.0225708	0.0075236	1.58583
Viscosity (cps)	1	0.0185141	0.0133492	0.0133492	2.81375
Threshold Pressure (kPa)	1	0.0021698	0.0015360	0.0015360	0.32376
Nozzle (mm)	1	0.0018869	0.0018869	0.0018869	0.39772
Error	3	0.0142328	0.0142328	0.0047443	
Total	6	0.0368036			

Source	P
Regression	0.357015
Viscosity (cps)	0.192053
Threshold Pressure (kPa)	0.609167
Nozzle (mm)	0.573037
Error	
Total	

Fits and Diagnostics for Unusual Observations

No unusual observations

6) All input paramerters vs SES

General Regression Analysis: %SES - EPI versus Viscosity (c, Threshold Pr, ...

Regression Equation

%SES - EPI = 0.97488 - 2.63285e-005 Viscosity (cps) + 0.00020402 Threshold Pressure (kPa) + 0.00928907 Nozzle (mm)

Coefficients

Term	Coef	SE Coef	T	P
Constant	0.974880	0.0033939	287.249	0.000
Viscosity (cps)	-0.000026	0.0000528	-0.498	0.653
Threshold Pressure (kPa)	0.000204	0.0000653	3.126	0.052
Nozzle (mm)	0.009289	0.0197767	0.470	0.671

Summary of Model

S = 0.00238716 R-Sq = 81.91% R-Sq(adj) = 63.82%
PRESS = 0.0000702019 R-Sq(pred) = 25.71%

Analysis of Variance

Source	DF	Seq SS	Adj SS	Adj MS	F
Regression	3	0.0000774	0.0000774	0.0000258	4.52736
Viscosity (cps)	1	0.0000163	0.0000014	0.0000014	0.24827
Threshold Pressure (kPa)	1	0.0000598	0.0000557	0.0000557	9.77181
Nozzle (mm)	1	0.0000013	0.0000013	0.0000013	0.22062
Error	3	0.0000171	0.0000171	0.0000057	
Total	6	0.0000945			

Source	P
Regression	0.123301
Viscosity (cps)	0.652531
Threshold Pressure (kPa)	0.052228
Nozzle (mm)	0.670603
Error	
Total	

Fits and Diagnostics for Unusual Observations

No unusual observations

7) Viscosity vs LP

General Regression Analysis: %LP - EPI versus Viscosity (cps)

Regression Equation

%LP - EPI = 0.356542 - 0.00257076 Viscosity (cps)

Coefficients

Term	Coef	SE Coef	T	P
Constant	0.356542	0.0337375	10.5681	0.000
Viscosity (cps)	-0.002571	0.0011427	-2.2498	**0.074**

Summary of Model

S = 0.0604805 R-Sq = 50.31% R-Sq(adj) = 40.37%
PRESS = 0.0329532 R-Sq(pred) = 10.46%

Analysis of Variance

Source	DF	Seq SS	Adj SS	Adj MS	F	P
Regression	1	0.0185141	0.0185141	0.0185141	5.061	0.0742994
Viscosity (cps)	1	0.0185141	0.0185141	0.0185141	5.061	0.0742994
Error	5	0.0182895	0.0182895	0.0036579		
Lack-of-Fit	2	0.0181172	0.0181172	0.0090586	157.729	0.0009143
Pure Error	3	0.0001723	0.0001723	0.0000574		
Total	6	0.0368036				

Fits and Diagnostics for Unusual Observations

No unusual observations

8) Viscosity vs SES

General Regression Analysis: %SES - EPI versus Viscosity (cps)

Regression Equation

%SES - EPI = 0.983414 - 7.63479e-005 Viscosity (cps)

Coefficients

Term	Coef	SE Coef	T	P
Constant	0.983414	0.0022055	445.882	0.000
Viscosity (cps)	-0.000076	0.0000747	-1.022	0.354

Summary of Model

S = 0.00395384 R-Sq = 17.28% R-Sq(adj) = 0.74%
PRESS = 0.000156051 R-Sq(pred) = -65.14%

Analysis of Variance

Source	DF	Seq SS	Adj SS	Adj MS	F	P
Regression	1	0.0000163	0.0000163	0.0000163	1.04457	0.353640
Viscosity (cps)	1	0.0000163	0.0000163	0.0000163	1.04457	0.353640
Error	5	0.0000782	0.0000782	0.0000156		
Lack-of-Fit	2	0.0000429	0.0000429	0.0000215	1.82863	0.302509
Pure Error	3	0.0000352	0.0000352	0.0000117		
Total	6	0.0000945				

Fits and Diagnostics for Unusual Observations

No unusual observations

9) Pressure vs LP

General Regression Analysis: %LP - EPI versus Threshold Pressure (kPa)

Regression Equation

%LP - EPI = 0.294504 + 0.0002072 Threshold Pressure (kPa)

Coefficients

Term	Coef	SE Coef	T	P
Constant	0.294504	0.0719878	4.09102	0.009
Threshold Pressure (kPa)	0.000207	0.0021429	0.09669	0.927

Summary of Model

S = 0.0857146 R-Sq = 0.19% R-Sq(adj) = -19.78%
PRESS = 0.0891767 R-Sq(pred) = -142.30%

Analysis of Variance

Source	DF	Seq SS	Adj SS	Adj MS	F
Regression	1	0.0000687	0.0000687	0.0000687	0.00935
Threshold Pressure (kPa)	1	0.0000687	0.0000687	0.0000687	0.00935
Error	5	0.0367349	0.0367349	0.0073470	
Lack-of-Fit	1	0.0133600	0.0133600	0.0133600	2.28621
Pure Error	4	0.0233749	0.0233749	0.0058437	
Total	6	0.0368036			

Source	P
Regression	0.926726
Threshold Pressure (kPa)	0.926726
Error	
Lack-of-Fit	0.205066
Pure Error	
Total	

Fits and Diagnostics for Unusual Observations

No unusual observations

10) Pressure vs SES

General Regression Analysis: %SES - EPI versus Threshold Pressure (kPa)

Regression Equation

%SES - EPI = 0.975241 + 0.000217184 Threshold Pressure (kPa)

Coefficients

Term	Coef	SE Coef	T	P
Constant	0.975241	0.0016382	595.313	0.000
Threshold Pressure (kPa)	0.000217	0.0000488	4.454	0.007

Summary of Model

S = 0.00195057 R-Sq = 79.87% R-Sq(adj) = 75.84%
PRESS = 0.0000339236 R-Sq(pred) = 64.10%

Analysis of Variance

Source	DF	Seq SS	Adj SS	Adj MS	F
Regression	1	0.0000755	0.0000755	0.0000755	19.8359
Threshold Pressure (kPa)	1	0.0000755	0.0000755	0.0000755	19.8359
Error	5	0.0000190	0.0000190	0.0000038	
Lack-of-Fit	1	0.0000054	0.0000054	0.0000054	1.5869
Pure Error	4	0.0000136	0.0000136	0.0000034	
Total	6	0.0000945			

Source	P
Regression	0.006679
Threshold Pressure (kPa)	0.006679
Error	
Lack-of-Fit	0.276261
Pure Error	
Total	

Fits and Diagnostics for Unusual Observations

No unusual observations

11) Nozzle Diameter vs LP

General Regression Analysis: %LP - EPI versus Nozzle (mm)

Regression Equation

%LP - EPI = 0.405106 - 0.730699 Nozzle (mm)

Coefficients

Term	Coef	SE Coef	T	P
Constant	0.405106	0.085869	4.71771	0.005
Nozzle (mm)	-0.730699	0.567971	-1.28651	0.255

Summary of Model

S = 0.0743649 R-Sq = 24.87% R-Sq(adj) = 9.84%
PRESS = 0.0492388 R-Sq(pred) = -33.79%

Analysis of Variance

Source	DF	Seq SS	Adj SS	Adj MS	F	P
Regression	1	0.0091529	0.0091529	0.0091529	1.65510	0.254611
Nozzle (mm)	1	0.0091529	0.0091529	0.0091529	1.65510	0.254611
Error	5	0.0276507	0.0276507	0.0055301		
Total	6	0.0368036				

Fits and Diagnostics for Unusual Observations

No unusual observations

12) Nozzle Diameter vs SES

General Regression Analysis: %SES - EPI versus Nozzle (mm)

Regression Equation

%SES - EPI = 0.980975 + 0.00547143 Nozzle (mm)

Coefficients

```
Term             Coef    SE Coef        T      P
Constant     0.980975  0.0050061  195.954  0.000
Nozzle (mm)  0.005471  0.0331125    0.165  0.875


Summary of Model

S = 0.00433545       R-Sq = 0.54%           R-Sq(adj) = -19.35%
PRESS = 0.000192172  R-Sq(pred) = -103.37%


Analysis of Variance

Source          DF     Seq SS     Adj SS     Adj MS          F         P
Regression       1  0.0000005  0.0000005  0.0000005  0.0273034  0.875230
  Nozzle (mm)    1  0.0000005  0.0000005  0.0000005  0.0273034  0.875230
Error            5  0.0000940  0.0000940  0.0000188
Total            6  0.0000945


Fits and Diagnostics for Unusual Observations


No unusual observations
```

13) Visc, P vs LP

General Regression Analysis: %LP - EPI versus Viscosity (cps), Threshold Pressu

```
Regression Equation

%LP - EPI  =  0.402075 - 0.00292994 Viscosity (cps) - 0.00125777 Threshold
              Pressure (kPa)


Coefficients

Term                          Coef    SE Coef         T      P
Constant                  0.402075  0.0714462   5.62765  0.005
Viscosity (cps)          -0.002930  0.0012954  -2.26175  0.087
Threshold Pressure (kPa) -0.001258  0.0017141  -0.73377  0.504


Summary of Model

S = 0.0634817      R-Sq = 56.20%         R-Sq(adj) = 34.30%
PRESS = 0.0538488  R-Sq(pred) = -46.31%


Analysis of Variance

Source                      DF     Seq SS     Adj SS     Adj MS        F
Regression                   2  0.0206839  0.0206839  0.0103420  2.56629
  Viscosity (cps)            1  0.0185141  0.0206152  0.0206152  5.11553
  Threshold Pressure (kPa)   1  0.0021698  0.0021698  0.0021698  0.53841
Error                        4  0.0161197  0.0161197  0.0040299
Total                        6  0.0368036

Source                         P
Regression              0.191837
  Viscosity (cps)       0.086513
  Threshold Pressure (kPa) 0.503780
Error
Total


Fits and Diagnostics for Unusual Observations


No unusual observations
```

14) Visc, P vs SES

General Regression Analysis: %SES - EPI versus Viscosity (c, Threshold Pr

```
Regression Equation

%SES - EPI  =  0.975854 - 1.67134e-005 Viscosity (cps) + 0.000208827 Threshold
               Pressure (kPa)


Coefficients

Term                          Coef    SE Coef        T      P
Constant                  0.975854  0.0024108  404.793  0.000
Viscosity (cps)          -0.000017  0.0000437   -0.382  0.722
```

```
Threshold Pressure (kPa)   0.000209  0.0000578    3.611  0.023


Summary of Model

S = 0.00214201        R-Sq = 80.58%        R-Sq(adj) = 70.87%
PRESS = 0.0000655114  R-Sq(pred) = 30.67%


Analysis of Variance

Source                      DF     Seq SS     Adj SS     Adj MS        F
Regression                   2  0.0000761  0.0000761  0.0000381   8.2975
  Viscosity (cps)            1  0.0000163  0.0000007  0.0000007   0.1462
  Threshold Pressure (kPa)   1  0.0000598  0.0000598  0.0000598  13.0359
Error                        4  0.0000184  0.0000184  0.0000046
Total                        6  0.0000945

Source                          P
Regression                0.037722
  Viscosity (cps)         0.721638
  Threshold Pressure (kPa)  0.022546
Error
Total


Fits and Diagnostics for Unusual Observations


No unusual observations
```

15) Visc, ND vs LP

General Regression Analysis: %LP - EPI versus Viscosity (cps), Nozzle (mm)

```
Regression Equation

%LP - EPI  =  0.407312 - 0.00220627 Viscosity (cps) - 0.41079 Nozzle (mm)


Coefficients

Term                  Coef   SE Coef         T      P
Constant          0.407312  0.072511   5.61721  0.005
Viscosity (cps)  -0.002206  0.001271  -1.73609  0.158
Nozzle (mm)      -0.410790  0.513729  -0.79962  0.469


Summary of Model

S = 0.0627870      R-Sq = 57.15%        R-Sq(adj) = 35.73%
PRESS = 0.0395503  R-Sq(pred) = -7.46%


Analysis of Variance

Source             DF     Seq SS     Adj SS     Adj MS        F         P
Regression          2  0.0210348  0.0210348  0.0105174     2.67  0.183577
  Viscosity (cps)   1  0.0185141  0.0118819  0.0118819     3.01  0.157557
  Nozzle (mm)       1  0.0025206  0.0025206  0.0025206     0.64  0.468722
Error               4  0.0157688  0.0157688  0.0039422
  Lack-of-Fit       3  0.0157666  0.0157666  0.0052555  2326.53  0.015239
  Pure Error        1  0.0000023  0.0000023  0.0000023
Total               6  0.0368036


Fits and Diagnostics for Unusual Observations


No unusual observations
```

16) Visc, ND vs SES

General Regression Analysis: %SES - EPI versus Viscosity (cps), Nozzle (mm)

```
Regression Equation

%SES - EPI  =  0.981068 - 9.31928e-005 Viscosity (cps) + 0.0189844 Nozzle (mm)


Coefficients

Term                  Coef    SE Coef         T      P
Constant          0.981068  0.0049262   199.152  0.000
Viscosity (cps)  -0.000093  0.0000863    -1.079  0.341
Nozzle (mm)       0.018984  0.0349014     0.544  0.615
```

Summary of Model

S = 0.00426558 R-Sq = 22.98% R-Sq(adj) = -15.53%
PRESS = 0.000252123 R-Sq(pred) = -166.81%

Analysis of Variance

Source	DF	Seq SS	Adj SS	Adj MS	F	P
Regression	2	0.0000217	0.0000217	0.0000109	0.59667	0.593235
Viscosity (cps)	1	0.0000163	0.0000212	0.0000212	1.16513	0.341145
Nozzle (mm)	1	0.0000054	0.0000054	0.0000054	0.29587	0.615379
Error	4	0.0000728	0.0000728	0.0000182		
Lack-of-Fit	3	0.0000469	0.0000469	0.0000156	0.60270	0.711929
Pure Error	1	0.0000259	0.0000259	0.0000259		
Total	6	0.0000945				

Fits and Diagnostics for Unusual Observations

No unusual observations

17) NC, P vs LP

General Regression Analysis: %LP - EPI versus Threshold Pressu, Nozzle (mm)

Regression Equation

%LP - EPI = 0.39889 + 0.0002072 Threshold Pressure (kPa) - 0.730699 Nozzle (mm)

Coefficients

Term	Coef	SE Coef	T	P
Constant	0.398890	0.114336	3.48875	0.025
Threshold Pressure (kPa)	0.000207	0.002076	0.09981	0.925
Nozzle (mm)	-0.730699	0.634222	-1.15212	0.313

Summary of Model

S = 0.0830392 R-Sq = 25.06% R-Sq(adj) = -12.42%
PRESS = 0.0796693 R-Sq(pred) = -116.47%

Analysis of Variance

Source	DF	Seq SS	Adj SS	Adj MS	F	P
Regression	2	0.0092216	0.0092216	0.0046108	0.6687	0.561656
Threshold Pressure (kPa)	1	0.0000687	0.0000687	0.0000687	0.0100	0.925299
Nozzle (mm)	1	0.0091529	0.0091529	0.0091529	1.3274	0.313445
Error	4	0.0275820	0.0275820	0.0068955		
Lack-of-Fit	3	0.0274699	0.0274699	0.0091566	81.7145	0.081100
Pure Error	1	0.0001121	0.0001121	0.0001121		
Total	6	0.0368036				

Fits and Diagnostics for Unusual Observations

No unusual observations

18) NC, P vs SES

General Regression Analysis: %SES - EPI versus Threshold Pressu, Nozzle (mm)

Regression Equation

%SES - EPI = 0.974459 + 0.000217184 Threshold Pressure (kPa) + 0.00547143 Nozzle (mm)

Coefficients

Term	Coef	SE Coef	T	P
Constant	0.974459	0.0029620	328.992	0.000
Threshold Pressure (kPa)	0.000217	0.0000538	4.038	0.016

```
Nozzle (mm)               0.005471  0.0164300     0.333  0.756


Summary of Model

S = 0.00215119        R-Sq = 80.41%        R-Sq(adj) = 70.62%
PRESS = 0.0000476176  R-Sq(pred) = 49.61%


Analysis of Variance

Source                       DF     Seq SS     Adj SS     Adj MS        F
Regression                    2  0.0000760  0.0000760  0.0000380   8.2098
  Threshold Pressure (kPa)    1  0.0000755  0.0000755  0.0000755  16.3087
  Nozzle (mm)                 1  0.0000005  0.0000005  0.0000005   0.1109
Error                         4  0.0000185  0.0000185  0.0000046
  Lack-of-Fit                 3  0.0000086  0.0000086  0.0000029   0.2902
  Pure Error                  1  0.0000099  0.0000099  0.0000099
Total                         6  0.0000945

Source                            P
Regression                 0.038373
  Threshold Pressure (kPa) 0.015625
  Nozzle (mm)              0.755846
Error
  Lack-of-Fit              0.839603
  Pure Error
Total


Fits and Diagnostics for Unusual Observations


No unusual observations
```

19) Max velocity vs LP

General Regression Analysis: %LP - NEPI versus Max Velocity (mm/s)

```
Regression Equation

%LP - NEPI  =  0.0325755 - 1.10735e-005 Max Velocity (mm/s)


Coefficients

Term                      Coef    SE Coef         T      P
Constant             0.0325755  0.0016350   19.9242  0.000
Max Velocity (mm/s) -0.0000111  0.0000038   -2.9460  0.032


Summary of Model

S = 0.00281379        R-Sq = 63.45%        R-Sq(adj) = 56.14%
PRESS = 0.0000627563  R-Sq(pred) = 42.05%


Analysis of Variance

Source                  DF     Seq SS     Adj SS     Adj MS        F          P
Regression               1  0.0000687  0.0000687  0.0000687  8.67878  0.0320342
  Max Velocity (mm/s)    1  0.0000687  0.0000687  0.0000687  8.67878  0.0320342
Error                    5  0.0000396  0.0000396  0.0000079
Total                    6  0.0001083


Fits and Diagnostics for Unusual Observations

Obs  %LP - NEPI        Fit     SE Fit    Residual  St Resid
  1   0.0248871  0.0305331  0.0011966  -0.0056460  -2.21700  R

R denotes an observation with a large standardized residual.
```

20) Max velocity vs SES

General Regression Analysis: %SES - NEPI versus Max Velocity (mm/s)

```
Regression Equation

%SES - NEPI  =  0.158794 - 4.14577e-005 Max Velocity (mm/s)


Coefficients
```

```
Term                      Coef    SE Coef        T      P
Constant              0.158794  0.0083869  18.9335  0.000
Max Velocity (mm/s)  -0.000041  0.0000193  -2.1501  0.084


Summary of Model

S = 0.0144339       R-Sq = 48.04%       R-Sq(adj) = 37.65%
PRESS = 0.00189876  R-Sq(pred) = 5.29%


Analysis of Variance

Source                 DF     Seq SS     Adj SS     Adj MS        F          P
Regression              1  0.0009631  0.0009631  0.0009631  4.62289  0.0842354
  Max Velocity (mm/s)   1  0.0009631  0.0009631  0.0009631  4.62289  0.0842354
Error                   5  0.0010417  0.0010417  0.0002083
Total                   6  0.0020048


Fits and Diagnostics for Unusual Observations

Obs  %SES - NEPI       Fit     SE Fit    Residual  St Resid
  1     0.123152  0.151147  0.0061384  -0.0279945  -2.14293  R

R denotes an observation with a large standardized residual.
```

21) Sus. Velocity vs LP

General Regression Analysis: %LP - NEPI versus Sustained Velocity (mm/s)

```
Regression Equation

%LP - NEPI  =  0.032756 - 8.28086e-005 Sustained Velocity (mm/s)


Coefficients

Term                          Coef    SE Coef        T      P
Constant                 0.0327560  0.0016472  19.8855  0.000
Sustained Velocity (mm/s) -0.0000828  0.0000274  -3.0187  0.029


Summary of Model

S = 0.00277019        R-Sq = 64.57%        R-Sq(adj) = 57.49%
PRESS = 0.0000603509  R-Sq(pred) = 44.27%


Analysis of Variance

Source                     DF     Seq SS     Adj SS     Adj MS        F
Regression                  1  0.0000699  0.0000699  0.0000699  9.11270
  Sustained Velocity (mm/s) 1  0.0000699  0.0000699  0.0000699  9.11270
Error                       5  0.0000384  0.0000384  0.0000077
Total                       6  0.0001083

Source                        P
Regression            0.0294594
  Sustained Velocity (mm/s)  0.0294594
Error
Total


Fits and Diagnostics for Unusual Observations

Obs  %LP - NEPI        Fit     SE Fit    Residual  St Resid
  1    0.0248871  0.0304712  0.0011667  -0.0055841  -2.22253  R

R denotes an observation with a large standardized residual.
```

22) Sus Velocity vs SES

General Regression Analysis: %SES - NEPI versus Sustained Velocity (mm/s)

```
Regression Equation

%SES - NEPI  =  0.159427 - 0.000309106 Sustained Velocity (mm/s)


Coefficients

Term                          Coef    SE Coef        T      P
Constant                  0.159427  0.0085363  18.6763  0.000
Sustained Velocity (mm/s) -0.000309  0.0001422  -2.1744  0.082
```

Summary of Model

S = 0.0143557 R-Sq = 48.60% R-Sq(adj) = 38.32%
PRESS = 0.00184946 R-Sq(pred) = 7.75%

Analysis of Variance

Source	DF	Seq SS	Adj SS	Adj MS	F
Regression	1	0.0009744	0.0009744	0.0009744	4.72806
Sustained Velocity (mm/s)	1	0.0009744	0.0009744	0.0009744	4.72806
Error	5	0.0010304	0.0010304	0.0002061	
Total	6	0.0020048			

Source	P
Regression	0.0816871
Sustained Velocity (mm/s)	0.0816871
Error	
Total	

Fits and Diagnostics for Unusual Observations

Obs	%SES - NEPI	Fit	SE Fit	Residual	St Resid	
1	0.123152	0.150898	0.0060463	-0.0277458	-2.13096	R

R denotes an observation with a large standardized residual.

23) All input parameters vs LP

General Regression Analysis: %LP - NEPI versus Viscosity (c, Threshold Pr, ...

Regression Equation

%LP - NEPI = 0.0194893 + 7.92889e-005 Viscosity (cps) - 1.82498e-005 Threshold Pressure (kPa) + 0.0577758 Nozzle (mm)

Coefficients

Term	Coef	SE Coef	T	P
Constant	0.0194893	0.0022987	8.47825	0.003
Viscosity (cps)	0.0000793	0.0000358	2.21542	0.114
Threshold Pressure (kPa)	-0.0000182	0.0000442	-0.41284	0.707
Nozzle (mm)	0.0577758	0.0133952	4.31316	0.023

Summary of Model

S = 0.00161688 R-Sq = 92.76% R-Sq(adj) = 85.52%
PRESS = 0.0000333232 R-Sq(pred) = 69.23%

Analysis of Variance

Source	DF	Seq SS	Adj SS	Adj MS	F
Regression	3	0.0001005	0.0001005	0.0000335	12.8087
Viscosity (cps)	1	0.0000516	0.0000128	0.0000128	4.9081
Threshold Pressure (kPa)	1	0.0000002	0.0000004	0.0000004	0.1704
Nozzle (mm)	1	0.0000486	0.0000486	0.0000486	18.6033
Error	3	0.0000078	0.0000078	0.0000026	
Total	6	0.0001083			

Source	P
Regression	0.032356
Viscosity (cps)	0.113527
Threshold Pressure (kPa)	0.707459
Nozzle (mm)	0.022953
Error	
Total	

Fits and Diagnostics for Unusual Observations

No unusual observations

24) All input paramerters vs SES

General Regression Analysis: %SES - NEPI versus Viscosity (c, Threshold Pr, ...

Regression Equation

%SES - NEPI = 0.108835 + 0.000501654 Viscosity (cps) + 3.81381e-005 Threshold Pressure (kPa) + 0.169577 Nozzle (mm)

Coefficients

```
Term                          Coef    SE Coef        T      P
Constant                  0.108835  0.0166654  6.53058  0.007
Viscosity (cps)           0.000502  0.0002595  1.93340  0.149
Threshold Pressure (kPa)  0.000038  0.0003205  0.11900  0.913
Nozzle (mm)               0.169577  0.0971128  1.74619  0.179


Summary of Model

S = 0.0117221       R-Sq = 79.44%        R-Sq(adj) = 58.88%
PRESS = 0.00158588  R-Sq(pred) = 20.90%


Analysis of Variance

Source                       DF     Seq SS     Adj SS     Adj MS        F
Regression                    3  0.0015926  0.0015926  0.0005309  3.86344
  Viscosity (cps)             1  0.0011519  0.0005136  0.0005136  3.73803
  Threshold Pressure (kPa)    1  0.0000217  0.0000019  0.0000019  0.01416
  Nozzle (mm)                 1  0.0004190  0.0004190  0.0004190  3.04916
Error                         3  0.0004122  0.0004122  0.0001374
Total                         6  0.0020048

Source                           P
Regression                0.148128
  Viscosity (cps)         0.148670
  Threshold Pressure (kPa)0.912796
  Nozzle (mm)             0.179114
Error
Total


Fits and Diagnostics for Unusual Observations


No unusual observations
```

25) Viscosity vs LP

General Regression Analysis: %LP - NEPI versus Viscosity (cps)

```
Regression Equation

%LP - NEPI  =  0.0259692 + 0.000135765 Viscosity (cps)


Coefficients

Term                  Coef    SE Coef        T      P
Constant         0.0259692  0.0018779  13.8290  0.000
Viscosity (cps)  0.0001358  0.0000636   2.1346  0.086


Summary of Model

S = 0.00336643       R-Sq = 47.68%        R-Sq(adj) = 37.21%
PRESS = 0.000116666  R-Sq(pred) = -7.72%


Analysis of Variance

Source              DF     Seq SS     Adj SS     Adj MS        F        P
Regression           1  0.0000516  0.0000516  0.0000516  4.55636  0.085906
  Viscosity (cps)    1  0.0000516  0.0000516  0.0000516  4.55636  0.085906
Error                5  0.0000567  0.0000567  0.0000113
  Lack-of-Fit        2  0.0000324  0.0000324  0.0000162  1.99902  0.280684
  Pure Error         3  0.0000243  0.0000243  0.0000081
Total                6  0.0001083


Fits and Diagnostics for Unusual Observations


No unusual observations
```

26) Viscosity vs SES

General Regression Analysis: %SES - NEPI versus Viscosity (cps)

```
Regression Equation

%SES - NEPI  =  0.131173 + 0.000641229 Viscosity (cps)
```

Coefficients

Term	Coef	SE Coef	T	P
Constant	0.131173	0.0072857	18.0042	0.000
Viscosity (cps)	0.000641	0.0002468	2.5985	0.048

Summary of Model

S = 0.0130609 R-Sq = 57.46% R-Sq(adj) = 48.95%
PRESS = 0.00162609 R-Sq(pred) = 18.89%

Analysis of Variance

Source	DF	Seq SS	Adj SS	Adj MS	F	P
Regression	1	0.0011519	0.0011519	0.0011519	6.75239	0.0483349
Viscosity (cps)	1	0.0011519	0.0011519	0.0011519	6.75239	0.0483349
Error	5	0.0008529	0.0008529	0.0001706		
Lack-of-Fit	2	0.0007308	0.0007308	0.0003654	8.97417	0.0541948
Pure Error	3	0.0001221	0.0001221	0.0000407		
Total	6	0.0020048				

Fits and Diagnostics for Unusual Observations

No unusual observations

27) Pressure vs LP

General Regression Analysis: %LP - NEPI versus Threshold Pressure (kPa)

Regression Equation

%LP - NEPI = 0.030654 - 5.78943e-005 Threshold Pressure (kPa)

Coefficients

Term	Coef	SE Coef	T	P
Constant	0.0306540	0.0038107	8.04416	0.000
Threshold Pressure (kPa)	-0.0000579	0.0001134	-0.51038	0.632

Summary of Model

S = 0.00453735 R-Sq = 4.95% R-Sq(adj) = -14.06%
PRESS = 0.000252643 R-Sq(pred) = -133.28%

Analysis of Variance

Source	DF	Seq SS	Adj SS	Adj MS	F	P
Regression	1	0.0000054	0.0000054	0.0000054	0.260487	0.631512
Threshold Pressure (kPa)	1	0.0000054	0.0000054	0.0000054	0.260487	0.631512
Error	5	0.0001029	0.0001029	0.0000206		
Lack-of-Fit	1	0.0000039	0.0000039	0.0000039	0.156370	0.712704
Pure Error	4	0.0000991	0.0000991	0.0000248		
Total	6	0.0001083				

Fits and Diagnostics for Unusual Observations

No unusual observations

28) Pressure vs SES

General Regression Analysis: %SES - NEPI versus Threshold Pressure (kPa)

Regression Equation

%SES - NEPI = 0.151478 - 0.000212689 Threshold Pressure (kPa)

Coefficients

Term	Coef	SE Coef	T	P
Constant	0.151478	0.0165110	9.17438	0.000
Threshold Pressure (kPa)	-0.000213	0.0004915	-0.43275	0.683

Summary of Model

S = 0.0196593 R-Sq = 3.61% R-Sq(adj) = -15.67%
PRESS = 0.00493582 R-Sq(pred) = -146.20%

Analysis of Variance

Source	DF	Seq SS	Adj SS	Adj MS	F
Regression	1	0.0000724	0.0000724	0.0000724	0.187273
Threshold Pressure (kPa)	1	0.0000724	0.0000724	0.0000724	0.187273
Error	5	0.0019324	0.0019324	0.0003865	
Lack-of-Fit	1	0.0002862	0.0002862	0.0002862	0.695460
Pure Error	4	0.0016462	0.0016462	0.0004116	
Total	6	0.0020048			

Source	P
Regression	0.683227
Threshold Pressure (kPa)	0.683227
Error	
Lack-of-Fit	0.451219
Pure Error	
Total	

Fits and Diagnostics for Unusual Observations

No unusual observations

29) Nozzle Diameter vs LP

General Regression Analysis: %LP - NEPI versus Nozzle (mm)

Regression Equation

%LP - NEPI = 0.0190211 + 0.0692727 Nozzle (mm)

Coefficients

Term	Coef	SE Coef	T	P
Constant	0.0190211	0.0026350	7.21866	0.001
Nozzle (mm)	0.0692727	0.0174288	3.97460	**0.011**

Summary of Model

S = 0.00228197 R-Sq = 75.96% R-Sq(adj) = 71.15%
PRESS = 0.0000476359 R-Sq(pred) = 56.02%

Analysis of Variance

Source	DF	Seq SS	Adj SS	Adj MS	F	P
Regression	1	0.0000823	0.0000823	0.0000823	15.7975	0.0105875
Nozzle (mm)	1	0.0000823	0.0000823	0.0000823	15.7975	0.0105875
Error	5	0.0000260	0.0000260	0.0000052		
Total	6	0.0001083				

Fits and Diagnostics for Unusual Observations

No unusual observations

30) Nozzle Diameter vs SES

General Regression Analysis: %SES - NEPI versus Nozzle (mm)

Regression Equation

%SES - NEPI = 0.110481 + 0.242317 Nozzle (mm)

Coefficients

Term	Coef	SE Coef	T	P
Constant	0.110481	0.016315	6.77151	0.001
Nozzle (mm)	0.242317	0.107917	2.24540	0.075

Summary of Model

S = 0.0141296 R-Sq = 50.21% R-Sq(adj) = 40.25%
PRESS = 0.00179928 R-Sq(pred) = 10.25%

Analysis of Variance

Source	DF	Seq SS	Adj SS	Adj MS	F	P
Regression	1	0.0010066	0.0010066	0.0010066	5.04184	0.0747064
Nozzle (mm)	1	0.0010066	0.0010066	0.0010066	5.04184	0.0747064
Error	5	0.0009982	0.0009982	0.0001996		
Total	6	0.0020048				

Fits and Diagnostics for Unusual Observations

No unusual observations

31) Visc, P vs LP

General Regression Analysis: %LP - NEPI versus Viscosity (c, Threshold Pr

Regression Equation

%LP - NEPI = 0.0255474 + 0.000139093 Viscosity (cps) + 1.1652e-005 Threshold Pressure (kPa)

Coefficients

Term	Coef	SE Coef	T	P
Constant	0.0255474	0.0042290	6.04096	0.004
Viscosity (cps)	0.0001391	0.0000767	1.81397	0.144
Threshold Pressure (kPa)	0.0000117	0.0001015	0.11484	0.914

Summary of Model

S = 0.00375759 R-Sq = 47.85% R-Sq(adj) = 21.78%
PRESS = 0.000181998 R-Sq(pred) = -68.05%

Analysis of Variance

Source	DF	Seq SS	Adj SS	Adj MS	F
Regression	2	0.0000518	0.0000518	0.0000259	1.83515
Viscosity (cps)	1	0.0000516	0.0000465	0.0000465	3.29048
Threshold Pressure (kPa)	1	0.0000002	0.0000002	0.0000002	0.01319
Error	4	0.0000565	0.0000565	0.0000141	
Total	6	0.0001083			

Source	P
Regression	0.271954
Viscosity (cps)	0.143882
Threshold Pressure (kPa)	0.914105
Error	
Total	

Fits and Diagnostics for Unusual Observations

No unusual observations

32) Visc, P vs SES

General Regression Analysis: %SES - NEPI versus Viscosity (c, Threshold Pr

Regression Equation

%SES - NEPI = 0.126616 + 0.000677183 Viscosity (cps) + 0.000125903 Threshold Pressure (kPa)

Coefficients

Term	Coef	SE Coef	T	P
Constant	0.126616	0.0162238	7.80430	0.001
Viscosity (cps)	0.000677	0.0002942	2.30207	0.083
Threshold Pressure (kPa)	0.000126	0.0003892	0.32346	0.763

Summary of Model

S = 0.0144153 R-Sq = 58.54% R-Sq(adj) = 37.81%
PRESS = 0.00292449 R-Sq(pred) = -45.87%

Analysis of Variance

Source	DF	Seq SS	Adj SS	Adj MS	F
Regression	2	0.0011736	0.0011736	0.0005868	2.82392
Viscosity (cps)	1	0.0011519	0.0011012	0.0011012	5.29952
Threshold Pressure (kPa)	1	0.0000217	0.0000217	0.0000217	0.10462
Error	4	0.0008312	0.0008312	0.0002078	
Total	6	0.0020048			

Source	P
Regression	0.171894
Viscosity (cps)	0.082750
Threshold Pressure (kPa)	0.762553
Error	
Total	

Fits and Diagnostics for Unusual Observations

No unusual observations

33) Visc, ND vs LP

General Regression Analysis: %LP - NEPI versus Viscosity (cps), Nozzle (mm)

Regression Equation

%LP - NEPI = 0.0189358 + 8.527e-005 Viscosity (cps) + 0.0569086 Nozzle (mm)

Coefficients

Term	Coef	SE Coef	T	P
Constant	0.0189358	0.0016624	11.3904	0.000
Viscosity (cps)	**0.0000853**	**0.0000291**	**2.9267**	**0.043**
Nozzle (mm)	**0.0569086**	**0.0117780**	**4.8318**	**0.008**

Summary of Model

S = 0.00143949 R-Sq = 92.35% R-Sq(adj) = 88.52%
PRESS = 0.0000184151 R-Sq(pred) = 83.00%

Analysis of Variance

Source	DF	Seq SS	Adj SS	Adj MS	F	P
Regression	2	0.0001000	0.0001000	0.0000500	24.1327	0.005857
Viscosity (cps)	1	0.0000516	0.0000177	0.0000177	8.5653	0.042957
Nozzle (mm)	1	0.0000484	0.0000484	0.0000484	23.3459	0.008450
Error	4	0.0000083	0.0000083	0.0000021		
Lack-of-Fit	3	0.0000057	0.0000057	0.0000019	0.7476	0.668798
Pure Error	1	0.0000026	0.0000026	0.0000026		
Total	6	0.0001083				

Fits and Diagnostics for Unusual Observations

No unusual observations

34) Visc, ND vs SES

General Regression Analysis: %SES - NEPI versus Viscosity (cps), Nozzle (mm)

Regression Equation

%SES - NEPI = 0.109991 + 0.000489155 Viscosity (cps) + 0.171389 Nozzle (mm)

Coefficients

Term	Coef	SE Coef	T	P
Constant	0.109991	0.0117515	9.35976	0.001
Viscosity (cps)	0.000489	0.0002060	2.37505	0.076
Nozzle (mm)	0.171389	0.0832573	2.05855	0.109

Summary of Model

S = 0.0101756 R-Sq = 79.34% R-Sq(adj) = 69.01%

PRESS = 0.000940295 R-Sq(pred) = 53.10%

Analysis of Variance

Source	DF	Seq SS	Adj SS	Adj MS	F	P
Regression	2	0.0015907	0.0015907	0.0007953	7.68119	0.042678
Viscosity (cps)	1	0.0011519	0.0005841	0.0005841	5.64085	0.076400
Nozzle (mm)	1	0.0004388	0.0004388	0.0004388	4.23763	0.108631
Error	4	0.0004142	0.0004142	0.0001035		
Lack-of-Fit	3	0.0003901	0.0003901	0.0001300	5.39625	0.304101
Pure Error	1	0.0000241	0.0000241	0.0000241		
Total	6	0.0020048				

Fits and Diagnostics for Unusual Observations

No unusual observations

35) NC, P vs LP

General Regression Analysis: %LP - NEPI versus Threshold Pressu, Nozzle (mm)

Regression Equation

%LP - NEPI = 0.0207579 - 5.78943e-005 Threshold Pressure (kPa) + 0.0692727 Nozzle (mm)

Coefficients

Term	Coef	SE Coef	T	P
Constant	0.0207579	0.0031303	6.63132	0.003
Threshold Pressure (kPa)	-0.0000579	0.0000568	-1.01862	0.366
Nozzle (mm)	0.0692727	0.0173637	3.98951	**0.016**

Summary of Model

S = 0.00227344 R-Sq = 80.91% R-Sq(adj) = 71.37%
PRESS = 0.0000581859 R-Sq(pred) = 46.27%

Analysis of Variance

Source	DF	Seq SS	Adj SS	Adj MS	F	P
Regression	2	0.0000876	0.0000876	0.0000438	8.4769	0.036441
Threshold Pressure (kPa)	1	0.0000054	0.0000054	0.0000054	1.0376	0.365982
Nozzle (mm)	1	0.0000823	0.0000823	0.0000823	15.9162	0.016272
Error	4	0.0000207	0.0000207	0.0000052		
Lack-of-Fit	3	0.0000193	0.0000193	0.0000064	4.5464	0.328948
Pure Error	1	0.0000014	0.0000014	0.0000014		
Total	6	0.0001083				

Fits and Diagnostics for Unusual Observations

No unusual observations

36) NC, P vs SES

General Regression Analysis: %SES - NEPI versus Threshold Pressu, Nozzle (mm)

Regression Equation

%SES - NEPI = 0.116861 - 0.000212689 Threshold Pressure (kPa) + 0.242317 Nozzle (mm)

Coefficients

Term	Coef	SE Coef	T	P
Constant	0.116861	0.020948	5.57865	0.005
Threshold Pressure (kPa)	-0.000213	0.000380	-0.55920	0.606
Nozzle (mm)	0.242317	0.116198	2.08537	**0.105**

Summary of Model

S = 0.0152139 R-Sq = 53.82% R-Sq(adj) = 30.73%
PRESS = 0.00266009 R-Sq(pred) = -32.68%

Analysis of Variance

Source	DF	Seq SS	Adj SS	Adj MS	F
Regression	2	0.0010790	0.0010790	0.0005395	2.3307
Threshold Pressure (kPa)	1	0.0000724	0.0000724	0.0000724	0.3127
Nozzle (mm)	1	0.0010066	0.0010066	0.0010066	4.3488
Error	4	0.0009259	0.0009259	0.0002315	
Lack-of-Fit	3	0.0009076	0.0009076	0.0003025	16.5930
Pure Error	1	0.0000182	0.0000182	0.0000182	
Total	6	0.0020048			

Source	P
Regression	0.213273
Threshold Pressure (kPa)	0.605856
Nozzle (mm)	0.105380
Error	
Lack-of-Fit	0.178088
Pure Error	
Total	

Fits and Diagnostics for Unusual Observations

No unusual observations